2001

Continuous flow system for combined chemical and enzyme-catalyzed removal of nitroaromatics from synthetic wastewater.

Ramkrishna. Mantha
University of Windsor

INFORMATION TO USERS

This manuscript has been reproduced from the microfilm master. UMI films the text directly from the original or copy submitted. Thus, some thesis and dissertation copies are in typewriter face, while others may be from any type of computer printer.

The quality of this reproduction is dependent upon the quality of the copy submitted. Broken or indistinct print, colored or poor quality illustrations and photographs, print bleedthrough, substandard margins, and improper alignment can adversely affect reproduction.

In the unlikely event that the author did not send UMI a complete manuscript and there are missing pages, these will be noted. Also, if unauthorized copyright material had to be removed, a note will indicate the deletion.

Oversize materials (e.g., maps, drawings, charts) are reproduced by sectioning the original, beginning at the upper left-hand corner and continuing from left to right in equal sections with small overlaps.

Photographs included in the original manuscript have been reproduced xerographically in this copy. Higher quality 6" x 9" black and white photographic prints are available for any photographs or illustrations appearing in this copy for an additional charge. Contact UMI directly to order.

ProQuest Information and Learning
300 North Zeeb Road, Ann Arbor, MI 48106-1346 USA
800-521-0600

UMI®

CONTINUOUS FLOW SYSTEM FOR COMBINED CHEMICAL AND ENZYME-CATALYZED REMOVAL OF NITROAROMATICS FROM SYNTHETIC WASTEWATER

by

Ramkrishna Mantha

A Dissertation
submitted to the Faculty of Graduate Studies and Research
through Civil and Environmental Engineering
in Partial Fulfillment of the Requirements for
the Degree of Doctor of Philosophy at the
University of Windsor

Windsor, Ontario, Canada

2001

ABSTRACT

Nitroaromatic compounds (NACs) are major environmental pollutants and their degradation is difficult to achieve. Using zero-valent iron reduction of the NACs coupled with peroxidase-catalyzed capture of the resulting anilines, a two-step strategy for removal of NACs from waste- and process-water, is investigated here. The concentration range of NACs studied was that which would be present in industrial wastewater streams (millimolar, 123 ppm), a concentration range considerably higher than those studied previously with groundwater by other researchers. Zero-valent iron (Fe^0) has been successfully employed to reduce nitrobenzene, *o*-, *m*- and *p*-nitrotoluenes to corresponding anilines in synthetic wastewater in both batch and continuous flow reactors. Anaerobic conditions were maintained in the reactors by including Na_2SO_3 as an oxygen scavenger in the presence of $CoCl_2.6H_2O$, which acted as a catalyst. Batch reactors exhibited adsorption of aniline on the Fe^0, which could be described by a Langmuir isotherm. A 200 g Fe^0 (particle size: 1-2 mm) bed completely converted 1 mM of NAC flowing upward for about 600 pore volumes before experiencing flow reduction due to clogging by corrosion products. A green-black precipitate was formed at the influent end of the column, an Fe^0 corrosion product identified as maghemite.

The enzymatic treatment following the zero-valent iron reduction was done in a plug-flow reactor (PFR) using a crude preparation of the enzyme soybean peroxidase extracted from soybean hulls. The complete reaction time for the two steps was 5-5½ h. Parameters like pH, peroxide to substrate ratio, enzyme concentration and alum concentration were optimized. At pH 7-7.2, the optimum H_2O_2 to substrate ratio was

found to be 1.5 for the aryl amines, aniline, *o*-, *m*- and *p*-toluidines, investigated in this study. Alum concentrations between 50-100 mg/L were useful in removing the end-color from the treated water. NACs were quantitatively reduced to their corresponding amines, which were completely removed from the wastewater in the enzymatic treatment step.

DEDICATION

Dedicated to all my teachers and to "Jagat Guru" Bhagwan Shree Krishna- teacher and Lord of the whole universe

ACKNOWLEDGEMENTS

The author would like to express his sincere gratefulness and indebtedness to his advisors, Dr N. Biswas and Dr K. E. Taylor for their kindness, guidance, continuous support, valuable suggestions and recommendations throughout the progress of the dissertation. Special thanks are due to Dr Biswas for his financial support, without which the dissertation would have stayed as a dream only. The author wishes to express his sincere gratefulness to Dr. J. K. Bewtra for his advice, patience, encouragement and invaluable discussions.

Sincere thanks are also expressed to Dr. T. C. Young, Clarkson University, Potsdam, NY, for taking out time from his busy schedule and reviewing the dissertation and providing valuable comments. Thanks are due to Dr P. Dutton and Dr. A. Gnyp for providing useful contributions by way of discussions. All their efforts have helped to improve the quality of the work.

The author wishes to thank Mr. Bill Henderson, Civil and Environmental Engineering and Mr. John Robinson, Materials and Mechanical Engineering, for their timely technical support. The author would like to express his gratitude to Ms. JoAnn Grondin, Secretary, Civil and Environmental Engineering for her cooperation in many matters.

I wish to take this opportunity to express gratitude to the faculty of Civil and Environmental engineering for the education they provided to me.

The author is grateful to all his friends and peers in the Civil and Environmental Engineering program for making the ambient most cordial and warm.

Special word of thanks are due to my wife, Smita, and my little loved ones, Keshav and Bhargavi, for their understanding and support, in good times and in bad. Smita sacrificed her own career for mine and never complained about living on student income. I am grateful to my parents, in-laws, other family members and my friends Sanjay and Dr Madan for their 'long-distance' encouragement and prayers that worked wonders for me.

The author gratefully acknowledges the support from the Natural Sciences and Engineering Research Council of Canada, the Ontario Graduate Scholarship program, and the University of Windsor Scholarship program.

TABLE OF CONTENTS

LIST OF NOMENCLATURE

Abbreviations

4-AAB	4-aminoazobenzene
AA	Aromatic amine
AAP	4-aminoantipyrine
ARP	Arthromyces ramosus Peroxidase
CCl_4	Carbon tetrachloride
CMP	*Coprinus macrorhizus* Peroxidase
CSTR	Continuous Stirred Tank Reactor
DCP	Direct Coupling Plasma
EDS	Energy dispersive X-ray spectrometry
HA	Ionizable nitrophenol
HRP	Horseradish Peroxidase
HSDB	Hazardous Substances Data Bank
IR	Infra Red
LHHW	Langmuir-Hinshelwood-Hougen-Watson kinetic model
MCA	Multi-component analysis
NAC	Nitroaromatic compound
NB	Nitrobenzene
OSHA	Occupational Safety and Health Administration
PCE	Perchloroethylene
PEG	Polyethylene glycol

PFR	Plug Flow Reactor
RDX	Hexahydro-1,3,5-trinitro-1,3,5-triazine
SA	Synthetic aniline
SBP	Soybean Peroxidase
SEM	Scanning electron microscopy
TCE	trichloroethylene
TNBS	Trinitrobenzene sulfonic acid
TNT	2,4,6- trinitrotoluene
TRI	Toxics Release Inventory
TWA	Time-Weighted Average
USEPA	United States Environmental Protection Act
UV	Ultra violet
Vis	Visible
XRD	X-ray diffraction

Symbols

$(C_{ads})_{max}$	Maximum saturation concentration of aniline
$[AH_2]$	Aromatic concentration at any time
$[AH_2]_0$	Initial aromatic concentration
$[HRP]_{min}$	Minimum HRP concentration
$AH^{\bullet}$	Aromatic radical
AH_2	Aromatic substrate
$ArNO_2$	Nitroaromatic compound

c	Aqueous phase reactant concentration
c_0	Initial dissolved reactant concentration
C_{ads}	Concentration of aniline on iron surface
C_{aq}	Concentration of aniline in solution
C_{ph}	Aromatic concentration, mM
E	Native enzyme
E_i	Compound I
E_{ii}	Compound II
E_{iii}	Compound III
E_{inact}	Concentration of inactivated enzyme
k	Rate constant
k_0	Zero-order rate constant
K_1	Michaelis constant
$k_{1,obs}$	Rate constant
$K_{1/2}$	Aqueous TCE concentration at half-maximum rate
K_2	Michaelis constant
k_7	Rate constant
k_a	Rate constant
k_{a1}	Second order rate constant
k_{a2}	Second order rate constant
k_{app}	Rate constant
k_{cat}	Enzyme turnover number
k_d	Overall inactivation rate constant

K_d	Ratio of concentrations of the sorbate at the surface and in solution
k_{DS}	First order rate constant for dissociation of TCE
k_{eff}	Rate constant
K_L	Langmuir constant
K_M	Michaelis constant
k_r	Inactivation rate constant of the enzyme due to free radicals
k_{RS}	First order rate constant for sorption of TCE
k_{SA}	Derived specific rate constant
mM	Millimolar
P_{670}	Inactivated form of enzyme E
r	Correlation coefficient
R^2	Regression coefficient
RCl	Chlorinated aliphatic compound
R_{Fe}	Surface area
RH	Dechlorinated aliphatic compound
S	Standard error
t	Time

Greek Letters

Ω_s	*turnovers*
α	Reaction stoichiometry between peroxide and aromatic substrate
α_0	Fraction of nondissociated species
β	Reaction stoichiometry between PEG and aromatic substrate

μ_b	Pseudo first-order degradation rate coefficient
$\mu g/L$	Microgram per litre
μM	Micromolar
ρ_a	Iron surface concentration

LIST OF TABLES

LIST OF FIGURES

CHAPTER 1 INTRODUCTION

1.1 Background

Nitroaromatic compounds (NACs) are produced on a large scale in the manufacture of dyes, pesticides, plastics, and explosives. The impact on the environment is felt by their discharge in wastewater and application as insecticides and herbicides. They are highly toxic and hazardous and some of them have been identified as human carcinogens (McCoy *et al.*, 1981). The remediation of NACs is of interest because they are common environmental contaminants and are among the most characteristic of anthropogenic contaminants. Table 1.1 depicts the Toxics Release Inventory (TRI) data for some industrially important NACs for 1998.

Available conventional physico-chemical processes including activated carbon adsorption process, solvent extraction process, microbial degradation and various chemical oxidation processes developed over the years are capable of removing organic contaminants to very low levels. Most of these processes are not selective in terms of the range of the pollutants removed during treatment. These treatment strategies are more economically suitable for treatment of dilute wastewaters and are invariably used as polishing steps. Thus, the process can become economically prohibitive for high strength wastes, even when the target pollutant is present in low concentrations (Aitken, 1993). They also suffer from such drawbacks as harsh conditions, high cost, incomplete removal, formation of toxic by-products and applicability to a limited concentration range (Klibanov *et al.*, 1980).

Table 1.1 TRI data for important NACs for 1998 (source: www.rtk.net)

NAC	Production related Waste	Incinerated	Released on-site or sent for off-site disposal
nitrobenzene	3453380	1406900	233080
2,4-dinitrophenol	1200220	268460	16780
4,6-dinitro *o*-cresol	748070	669950	61140
4-nitrophenol	633360	268200	
dinitrotoluene (mixed isomers)	478300		28800
2-nitrophenol	235950	37200	
m-dinitrobenzene	235020		
dinitrobutylphenol	171400	140600	
2,4-dinitrotoluene	103110	23060	6400
p-nitroaniline	95400		5700
o-dinitrobenzene	27400		
2,6-dinitrotoluene	22200		
p-dinitrobenzene	8200		

All units are in kg.

1.2 Enzymes as catalysts

The idea of using enzymes to remove toxic pollutants from wastewater was first proposed in the 1930s (Munnecke, 1976). The application of enzymes to wastewater treatment was widely investigated in the 1980s in Europe, North America and Japan (Wu, 1996). A systematic approach for the treatment of wastewaters using enzymes for individual pollutants was first proposed by Klibanov *et al.* (1980). Over 30 different phenols and aromatic amines were tested individually and in conjunction with one another using this method. Most phenols and amines were removed from water with efficiency exceeding 99%. In this treatment strategy, horseradish peroxidase (HRP) catalyzes the oxidation of phenols and amines in the presence of hydrogen peroxide, generating phenoxyl radicals or anilinium cation radicals. These radicals diffuse from the active center of the enzyme, the region that contains the binding and catalytic sites, into solution and then react to form dimers, trimers and higher oligomers which are insoluble and precipitate from the aqueous phase. Higher oligomers and polymers can be easily removed by simple filtration or sedimentation (Klibanov *et al.*, 1983; Nicell *et al.*, 1992). Thus in effect, the peroxidase-catalyzed oxidative polymerization transforms water-soluble organics into water-insoluble compounds without any apparent degradation. Researchers used various other peroxidases for removing the toxic organic pollutants from wastewater: Al-Kassim *et al.* (1994) used *Coprinus macrorhizus* peroxidase (CMP), Caza *et al.* (1999) used soybean peroxidase (SBP), Biswas (1999) used crude SBP, while Ibrahim *et al.* (2001) used *Arthromyces ramosus* peroxidase (ARP). Researchers used additives to protect the enzyme from inactivation during the reaction. Polyethylene glycol (PEG) was found to be the best additive (Wu, J. *et al.*, 1993).

NACs even when they are phenolic or anilino compounds, are outside the scope of peroxidase catalysis (Monsef *et al.*, 2000). The presence of a nitro-group as a substituent deters the enzymatic reaction from taking place. Electron-withdrawing substituents that destabilize carbocations cause the reaction itself to proceed more slowly (Atkins and Carey, 1990). The corresponding anilines are, nevertheless, excellent substrates for enzymes. Thus, once an NAC is reduced, its corresponding amine can be subjected to the enzyme-mediated oxidative polymerization, for example, using crude soybean peroxidase enzyme.

1.3 Use of zero-valent iron for the reduction of NACs

Zero-valent iron (Fe^0) is finding wide-spread applications in groundwater remediation techniques. It is estimated that there are about 300,000 to 400,000 contaminated sites in the USA with a variety of toxic chemicals, indicating a clean up cost of around $500 billion to $1 trillion (Scherer *et al.*, 2000). Use of iron as a means to carry out reductive transformations of organic pollutants was primarily introduced by the research groups of Gillham and of Tratnyek (Chem. & Eng. News, 1995). Reynolds *et al.* (1990) studied the suitability of various materials for construction of ground water monitors. They found that metals like aluminum, stainless steel and galvanized steels apparently transformed compounds like trichloroethylene (TCE), hexachloroethane and other chloro-aliphatics. Gillham recognized that the process responsible for degradation of the chlorinated compounds by zero-valent metal could be applied to the treatment of ground water (Gillham and O'Hannesin, 1994). The properties of metallic iron that make it useful in remediation of chlorinated solvents also allow reduction of other contaminants

such as NACs (Agrawal and Tratnyek, 1996) and azoaromatics (Weber, 1996). The zero-valent iron reduction requires anaerobic conditions. Hence, O_2 has to be scavenged either by degassing or by chemical reaction.

There is substantial literature on the potential for using Fe^0 to treat groundwater contaminated with various compounds, though no reports on the application and potential uses of Fe^0 to treat wastewater. In groundwater, the concentration of contaminant is typically in the range of 20-50 μM; whereas the focus of this study was on industrial wastewater containing organic pollutants in the millimolar range.

1.4 Objectives

The primary objectives for this study were to:

- Develop an efficient Fe^0-based process for the reduction of NACs (in the millimolar range) present in waste- or process-water in a continuous system; and
- Develop the peroxidase-catalyzed oxidative coupling and precipitation of the anilines formed in the Fe^0 reduction reaction.

1.5 Scope

The scope of this study included:

- Investigating the potential of Fe^0 as a reductant for nitrobenzene, *o*-, *m*- and *p*-nitrotoluenes present in millimolar range in wastewater.
- Optimization of the use of an O_2 scavenger so that degassing of solutions is avoided.
- Studying adsorption of aniline on Fe^0 as a function of pH.

- Optimization of the removal of aniline, *o*-, *m*- and *p*-toluidines with crude SBP enzyme with respect to pH, SBP concentration and molar ratio of H_2O_2 to substrate.
- Studying the effect of PEG on optimum enzyme concentration.
- Conducting studies on the two-steps operated together for developing a continuous system.
- Evaluating existing kinetic models to represent the data for future prediction of the removal of aryl amines in the second stage of the treatment process.

CHAPTER 2 LITERATURE REVIEW

2.1 NACs in wastewater and their treatment

Although NACs have been reported to be synthesized by microorganisms (Bush *et al.*, 1951) and from other aromatic contaminants (Kagan *et al.*, 1990), by far the biggest producer of NACs is the chemical industry (Higson, 1992). The production of nitrobenzene (NB) in the USA was close to 0.75 billion kg for the year 1995 (Chem. and Eng. News, 1996). The commercial uses of NB are: the production of aniline; synthesis of metal polishes, shoe-black, perfumes and dye intermediates; as an industrial solvent and as a combustible propellant (United States Environmental Protection Agency (USEPA), 1980). Total production-related waste of NB for 1998 was estimated to be 3.45 million kg of which 233,080 kg was released on-site or was sent for off-site disposal (TRI data, 1998). Nitrobenzene also forms spontaneously in the atmosphere from the photochemical reaction of benzene with oxides of nitrogen (USEPA, 1980).

The insecticides parathion and paraoxon are derived from 4-nitrophenol (Higson, 1992). 2,4,6-Trinitrotoluene (TNT) has been used extensively in explosives and its current world production is estimated to be about 1 million kg (Higson, 1992). Nitrobiphenyls are used as plasticizers and as wood preservatives (Higson, 1992). Nitroanilines and their derivatives exist in wastewater as a result of discharge from dye and pharmaceutical industries. Wastewater from dye manufacturing industries makes a substantial contribution of nitrotoluenes into the environment.

The available data for NB indicate that acute toxicity to saltwater aquatic life occurs at concentrations as low as 6 mg/L (USEPA, 1980). Animal studies have reported methemoglobinemia and effects on the liver, kidney, spleen and central nervous system

from acute inhalation exposure to NB (Hazardous Substances Data Bank (HSDB), 1993). Methemoglobinemia is the conversion of hemoglobin to methemoglobin in the blood, which lowers the oxygen released to the tissues of the blood (HSDB, 1993). The major hazards encountered in the use and handling of *o*-, *m*- and *p*-nitrotoluenes stem from their toxicological properties and explosivity. Toxic by all routes, inhalation, ingestion, and dermal absorption, exposure to nitrotoluenes results in burns to the skin and eyes, headache, weakness, dizziness, nausea, shortness of breath, tachycardia, and methemoglobinemia. The Occupational Safety and Health Administration (OSHA), in 1992, set a time-weighted-average (TWA) exposure limit of 12 mg/m^3 (http:/www.speclab.com). 1,3-dinitrobenzene is toxic to humans, fish and several bacterial and fungal species (Higson, 1992). The U.S. Environmental Protection Agency's list of 129 'priority pollutants' includes the following seven NACs: nitrobenzene, 2,4- and 2,6-dinitrotoluene, 2- and 4-nitrophenol, 2,4-dinitrophenol, and 4,6-dinitro-2-methylphenol (McCoy *et al.*, 1981).

A review (Higson, 1992) and a recent monograph (Haderlein *et al.*, 2000) have discussed the biodegradation of nitroaromatics and have provided insights into the toxicity of nitroaromatics. Microbial degradation of NACs is generally incomplete, leaving behind metabolites that are themselves toxic. Some reports, however, (Boopathy and Manning, 1996, Widrig *et al.*, 1997, Peres *et al.*, 1998) indicate significant progress in this area, with complete mineralization being achieved in some instances.

2.2 Application of Enzymes in Wastewater Treatment

Fundamentally, biological treatment of wastewater is based on the microorganisms, mainly bacteria, which produce enzymes that catalyze decomposition of the pollutants. In enzymatic treatments, enzymes isolated from parent organisms are used instead of the intact organism itself. The two most characteristic features of enzymes are their high activity and specificity. Enzymes are easy to handle and store (Vieth and Venkatasubramanian, 1973). Their concentration is more easily controlled since it is independent of microbial growth (Bailey and Ollis, 1986). The factors that determine the effectiveness of an enzymatic reaction are the enzyme concentration, substrate concentration, pH, temperature, reaction time and the presence of inhibitors or activators (Wynn, 1979).

The inherent advantages of an enzyme-based approach over conventional biological treatment are as follows:

- Application to a broad range of compounds including those that are biorefractory.
- Action on, or in presence of, many substrates which are toxic to microbes.
- Operation over wide temperature, pH and salinity ranges.
- Effectiveness over a wide range of concentrations of contaminants.
- No shock loading effect.
- No delays associated with shutdown/startup (no acclimatization or growth of biomass).
- Reduction in sludge volume (no biomass generation).
- Better defined system with simpler process control.
- Application for the selective removal of single class of contaminant.

- Effectiveness at low hydraulic retention time. (Nicell *et al.*, 1993a).

Similarly, an enzyme-based treatment has potential advantages over physical-chemical processes, which include:

- Operation under milder, less corrosive conditions than chemical oxidation method.
- Operation in a catalytic manner with reduced consumption of oxidants.
- Reduction in solid waste production compared to activated carbon treatment.
- Ability to remove organic material not removed by chemical oxidation methods.
- Highly selective method.
- Effectiveness at high and low concentrations of contaminants. (Nicell *et al.*, 1993a).

2.3 Soybean Peroxidase Enzyme

Plant peroxidases have broad substrate specificity and can oxidize many aromatic compounds in the presence of hydrogen peroxide (Saunders *et al.*, 1964). Peroxidases, such as HRP, have been the most extensively researched enzymes due to their ubiquitous presence in almost all plants and animal kingdom. However, commercial applications of HRP have been ruled out due to limitations in its availability. Although the SBP enzyme has not been researched as much as HRP, it is considered to be a viable alternative to most peroxidases. Previous studies with commercially-purified SBP (Caza *et al.*, 1999) and a crude preparation of SBP (Biswas, 1999) indicate its effectiveness in removing several different phenols from wastewater. Purified SBP was found to be highly stable even at elevated temperatures and under severe acidic conditions (McEldoon and Dordick, 1996). Crude SBP also exhibited high thermal stability (McEldoon and Dordick, 1996; Biswas, 1999). SBP was found to follow a ping-pong, bi-bi catalytic reaction

mechanism with an oxidation potential of 1.42 V during the oxidation of methoxybenzenes (McEldoon *et al.*, 1995). In addition to the vast resource of soybean hulls as a major by-product of the food industry, SBP is easy to isolate and purify (McEldoon *et al.*, 1995).

The results of Caza *et al.* (1999) demonstrated the potential of commercially-purified SBP enzyme for removing different phenolic compounds from wastewater. Reaction parameters like pH, SBP concentration, PEG concentration and $[H_2O_2]$/[Substrate] were optimized to achieve at least 95% removal of phenolic compounds.

Biswas (1999) worked with crude SBP to precipitate cresols from synthetic wastewater. An experimental protocol for extracting the enzyme from the soybean hulls was also established. Pertinent characteristic properties like temperature stability, hydrogen peroxide demand and phenol content in the crude enzyme have been reported. It was reported that tap water was better suited for extraction of enzyme as compared to different buffers.

2.4 Mechanism of Peroxidase-Catalyzed Reaction

One-electron oxidation of an aromatic substrate (AH_2) in presence of peroxidase catalyst is usually represented by the following Chance-George mechanism (Job and Dunford, 1976):

$$E + H_2O_2 \xrightarrow{k_1} E_i + H_2O \qquad (2.4.1)$$

$$E_i + AH_2 \xrightarrow{k_2} E_{ii} + AH^{\bullet} \qquad (2.4.2)$$

$$E_{ii} + AH_2 \xrightarrow{k_3} E + AH^{\bullet} + H_2O \qquad (2.4.3)$$

Native enzyme (E) reacts with peroxide to form "Compound I" (E_i) which is oxidized by two electrons above the native enzyme and carries the peroxidic oxygen. Compound I accepts an aromatic molecule in its active site and carries out its one-electron oxidation.

The oxidized aromatic ($AH^{\bullet}$) is released from the catalytic site as a free radical, while the enzyme is reduced to "Compound II" (E_{ii}). The cycle is completed when Compound II oxidizes a second aromatic molecule releasing another free radical and the enzyme itself returns to its native state. The overall enzymatic reaction is as follows:

$$2AH_2 + H_2O_2 \xrightarrow{E} 2AH^{\bullet} + 2H_2O \qquad (2.4.4)$$

The free radicals thus generated diffuse from the enzyme active center into solution where they spontaneously combine to form dimers. These dimers undergo further enzymatic conversion to radicals that combine to form trimers, tetramers and higher oligomers that are less soluble than their monomeric precursors and tend to precipitate from solution. Any oligomer that fails to precipitate may be further oxidized through the catalytic action of the enzyme resulting in formation of even higher oligomers or polymers with lower solubility, ultimately leading to precipitation.

There are some side reactions that are believed to be responsible for the inactivation and inhibition of the active enzyme (Nicell *et al.*, 1993a). Klibanov *et al.* (1983) suggested that a permanent inactivation could result from the return of an aromatic free radical to the active center of the enzyme resulting in bond formation and blockage of the site upsetting the critical geometric configuration of the enzyme. Nakamoto and Machida (1992) indicated that the apparent enzyme inactivation during phenol polymerization was mainly caused by the end-product polymer that adsorbed enzyme molecule and blocked the pathway of substrate to the enzyme's active center.

The enzyme exhibits another way of inactivation – suicide inactivation. In the absence of reducing substrates and with excess H_2O_2, peroxidase exhibits behavior of suicide inactivation, H_2O_2 being the suicide substrate (Arnao *et al.*, 1990 and Baynton *et al.*, 1994). It was suggested that the enzyme in the Compound II state can get oxidized by excess H_2O_2 to form Compound III (E_{iii}) as follows:

$$E_{ii} + H_2O_2 \xrightarrow{k_{app}} E_{iii} + H_2O \qquad (2.4.5)$$

Compound III is catalytically inactive but its formation does not represent a terminal inhibition of peroxidase. E_{iii} spontaneously decomposes to native peroxidase.

$$E_{iii} \xrightarrow{k_{eff}} E + O_2^- \qquad (2.4.6)$$

The return of the enzyme to its native state is sufficiently slow that, once E_{iii} is formed, the enzyme effectively loses its catalytic power to carry out the oxidation any further. Therefore, any accumulation of enzyme in E_{iii} state represents a loss of its catalytic activity.

Arnao *et al.* (1990) described another way of inactivation of enzyme, whereby an irreversibly inactivated intermediate Compound P_{670} is formed. P_{670} is dominant at H_2O_2 concentration above 1.0 mM. It was concluded that a competition takes place between the two catalytic pathways with the formation of either E_{iii} or P_{670} depending upon which reaction is more prevalent- the catalase forming pathway or the suicide inactivation pathway (Baynton *et al.*, 1994).

Researchers used a variety of additives to circumvent the inactivation of enzyme. Wu, Y. *et al.* (1993, 1997) used additives including polyethylene glycol (PEG), gelatin and some polyelectrolytes to study their effect on enzyme inactivation for removal of phenolic compounds from aqueous solutions by HRP.

Ichinohe *et al.* (1998) carried out oxidative polymerization of *o*-, *m*- and *p*-phenylenediamines in mixed solvents of water and 1,4-dioxane catalyzed by HRP. They found that the enzyme structure was significantly modified when they used high concentrations of 1,4-dioxane, which may be responsible for the decrease of catalytic activity of the enzyme. On the basis of IR and electronic spectra of the polymers, it was suggested that the polymerization proceeded mainly via N-N coupling.

2.5 Enzymatic oxidation of Aromatic Amines (AAs)

Klibanov *et al.* (1980) were the earliest to employ enzymes for treatment of wastewater containing anilines. They used HRP to remove nine different AAs from water effectively. The effect of reaction conditions like pH, concentration of enzyme and concentration of hydrogen peroxide on the removal efficiency were studied. They noted that there were two independent factors affecting the overall efficiency of aniline removal

from water. The first one was its reactivity towards the peroxidase and the second one was solubility of the products of peroxidase oxidation.

Huang and Dunford (1990) studied the oxidation of substituted anilines by HRP Compound II (E_{ii}) and compared the reactivity with Compound I (E_i). They found that the reactivity of anilines with E_{ii} was lower than that when reacted with E_i. The difference in reactivity was explained by the relative complexities of the reaction of compounds I and II.

Hughes *et al.* (1992) studied the oxidation of 4-aminobiphenyl by HRP and concluded that a one-electron oxidation mechanism takes place resulting in the formation of a free radical. This radical reacts with another free radical to form a dimer. Thompson and Eling (1991) had earlier found similar results while investigating the oxidation of anisidine isomers by peroxidase.

Chang & Bumpus (1993) studied the biodegradation of 4-chloroaniline and noted that the intermediates formed were as toxic or more toxic and as environmentally persistent as the parent compound.

Tatsumi *et al.* (1994) developed a model for enzyme-mediated coupling of 3,4-dichloroaniline and ferulic acid. Their study was more of a binding of pollutant to humic substances than removal from wastewater catalyzed by an analogous oxidative enzyme, laccase.

2.6 Reaction kinetics and modeling

2.6.1 Reactor Configurations

Most of the research involving peroxidase-catalyzed oxidation and removal of aromatics has been done using batch reactors and useful information has been obtained. For the process to be economically viable, however, it is desirable to treat wastewater on a continuous flow basis (Nicell, 1991). Early researchers employed immobilized enzymes on a solid medium for treatment in a flow reactor. However, in the case of HRP-based reactors, rapid clogging of the support media occurred while using immobilized enzymes (Siddique, 1992).

To measure the enzyme efficiency, the term "*turnovers*" was introduced by Klibanov *et al.* (1980) and subsequently used in this laboratory (Nicell *et al.*, 1993b) to characterize an enzyme's operating lifetime. It is defined as the number of aromatic molecules removed from solution per enzyme molecule inactivated and is expressed as:

$$turnovers = \frac{[AH_2]_0 - [AH_2]}{E_{inact}} \qquad (2.6.1)$$

in which $[AH_2]_0$ and $[AH_2]$ represent the initial and final aromatic concentrations, and E_{inact} represents the concentration of inactivated enzyme. Thus, high *turnovers* indicates a better enzyme efficiency and usage. There have been various studies to increase the *turnovers*. It was reported that *turnovers* could be increased by adding enzyme over a period of time, rather than all at once, thereby maintaining a low instantaneous active enzyme concentration at any given period of time. Low active enzyme to substrate ratio would reduce the chances of a free radical binding to the enzyme active center due to a

competition for the scant sites. Nakamoto and Machida (1992) also recommended the use of low instantaneous H_2O_2 for limiting the rate.

Lowering of reaction rates has the design effects of favoring selection of continuous stirred tank reactor (CSTR). It was shown by Nicell *et al.* (1993b) that a CSTR was more efficient than either batch or semi-batch reactors. Generally, a CSTR operation is desirable when substrate inhibition is more pronounced; while a plug-flow reactor (PFR) is preferred when product inhibition predominates (Howaldt *et al.*, 1983). In the case of peroxidase reaction, both substrate (H_2O_2) and product (aromatic radical and/ or polymer) seem to have an inhibition effect, thus pointing towards a PFR.

Nicell *et al.* (1993b) made a comparison between batch, semi-batch, single CSTR and multiple CSTRs in series. They concluded that the number of reactor turnovers was extended many times when a low instantaneous enzyme concentration was maintained. Conducting the reaction in a semi-batch mode more than doubled the catalyst turnovers as compared to a batch reactor. Al-Kassim *et al.* (1993) studied the effect of reactor configuration by varying both the peroxide and the enzyme in a semi-batch fashion. They did not find much utility in the semi-batch mode of operation.

Ibrahim *et al.* (1997) used ARP for the removal of phenols from actual industrial wastewater in a continuous flow system. They used a plug flow reactor with a reaction time of 2 hours and achieved 94% removal of 1mM phenol with an ARP concentration of 0.6 U/mL. They got the best result when they divided the treatment scheme into two parts: oligomerization of phenol by enzymatic route, followed by precipitation of products by coagulation and flocculation method.

2.6.2 Existing Models

Kinetic modeling of any reaction is useful in developing a reactor system. The kinetic parameters are the basic building blocks for designing a reactor system. Empirical models were developed to relate the minimum enzyme concentration required for fixed amount of aromatic removed. Saadi (1993) developed the following equation:

$$[HRP]_{min} = 1.431 \bullet [AH_2]_0 \qquad (2.6.2.1)$$

where, $[AH_2]_0$ is the initial aromatic concentration, and $[HRP]_{min}$ is the enzyme concentration required to remove at least 90% of the initial phenol. Wu, J. *et al.* (1993) observed the following relationship:

$$[HRP]_{min} = 0.0435 + 0.0048C_{ph} + 0.0031C^2_{ph} \qquad (2.6.2.2)$$

where, C_{ph} (mM) is aromatic concentration, and $[HRP]_{min}$ (U/mL) is the enzyme concentration required to remove at least 95% of phenol.

Over the last few years, many kinetic models have been proposed to predict the behavior of the enzymatic reactions.

2.6.2.1 Model 1: Oxidation of phenol by HRP was shown to be a pseudo-first order reaction with respect to both the active enzyme and the substrate concentration, while the peroxide concentration was kept at 1:1 ratio with respect to the substrate (Yu *et al.*, 1994). Mathematically:

$$-\frac{d[AH_2]}{dt} = k[E_a][AH_2] \qquad (2.6.2.1.1)$$

$$-\frac{dE_a}{dt} = k_d\sqrt{2k[E_a]^3[AH_2]} \qquad (2.6.2.1.2)$$

where, E_a is the active enzyme and $[AH_2]$ is the molar concentration of substrate, k is the second–order rate constant and k_d is the overall inactivation constant. However, the model does not account for either the enzyme inactivation by end-product polymers or for the formation of Compound III.

2.6.2.2 Model 2: Siddique (1992) devised a simple model combining the one-substrate Michaelis-Menten equation and a first-order depletion equation for enzyme:

$$-\frac{d[AH_2]}{dt} = \frac{k_{cat}[E_a][AH_2]}{K_m + [AH_2]} \qquad (2.6.2.2.1)$$

$$-\frac{dE_a}{dt} = k_a[E_a] \qquad (2.6.2.2.2)$$

where, K_m is the Michaelis constant for phenol, k_{cat} is the turnover number, and k_a is the inactivation constant. At a constant H_2O_2 concentration, the model could predict the reaction quite accurately. However, the constants were a function of the H_2O_2 concentration and, hence, the model is not truly universal in nature.

2.6.2.3 Model 3: Nicell (1994) developed a model based on the assumptions that the amount of enzyme inactivated was directly proportional to the amount of aromatic substrate removed from solution and consumption rate of substrate and H_2O_2 was 1:1. It can be represented as:

$$-\frac{d[AH_2]}{dt} = \frac{E_a}{\frac{k_2 + k_3}{k_2 k_3}\frac{1}{[AH_2]} + \frac{1}{k_1[H_2O_2]}} \qquad (2.6.2.3.1)$$

$$\frac{d[E_{iii}]}{dt} = \frac{k_{app}[E_a]}{\frac{k_2 + k_3}{k_2}\frac{1}{[AH_2]} + \frac{k_3}{k_1[H_2O_2]}}[H_2O_2] - k_7[E_{ii}] \qquad (2.6.2.3.2)$$

$$E_{inact} = \frac{1}{\Omega_s}\{[AH_2]_0 - [AH_2]\} \qquad (2.6.2.3.3)$$

$$E_a = E_0 - E_{iii} - E_{inact} \qquad (2.6.2.3.4)$$

$$E_{ii} + H_2O_2 \xrightarrow{k_{app}} E_{iii} + H_2O \qquad (2.6.2.3.5)$$

$$E_{iii} \xrightarrow{k_7} E + O_2^- \qquad (2.6.2.3.6)$$

where, E_{iii} is the concentration of Compound III and E_{inact} is the inactivated enzyme concentration. Ω_s is the enzyme *turnovers*; k_1, k_2 and k_3 are the rate constants in the Chance-George mechanism (Equations 2.4.1, 2.4.2 and 2.4.3). A major fault in the model was the assumption that Ω_s was a constant, while experiments showed that it was a function of enzyme and substrate concentrations. A modified version of the above model was later developed (Nicell and Buchanan, 1997), which showed a good fit, to their data collected.

2.6.2.4 Model 4: Wu, Y. *et al.* (1999a and 1999b) found the reaction kinetics for peroxidase-catalyzed removal of phenol in a batch-mixed reactor and a plug-flow reactor to be identical. HRP was used as the enzyme. They found that semi-batch operation or step-addition operation of the PFR with respect to H_2O_2 produced very similar results. They developed steady-state differential equations to model HRP-mediated oligomerization of phenol in presence of polyethylene glycol (PEG).

They predicted the results using the model, which matched perfectly with the actual experimental results. Based on the results, they recommended a plug-flow system for both high and low phenol concentrations. It was shown that continuous mixing was not necessary. However, the influent, H_2O_2 and the enzyme had to be mixed uniformly before they entered the PFR. This may be achieved by either having an in-line mixer or a small CSTR just before the PFR. They predicted up to 50% conversion could take place in the mixer itself depending on the detention time.

$$-\frac{d[AH_2]}{dt} = \frac{kE_a[AH_2][H_2O_2]}{K_1[AH_2]+K_2[H_2O_2]+[AH_2][H_2O_2]} \qquad (2.6.2.4.1)$$

$$-\frac{dE_a}{dt} = k_{a1}E_a[AH_2]+k_{a2}E_a[H_2O_2] \qquad (2.6.2.4.2)$$

$$-\frac{d[H_2O_2]}{dt} = -\alpha\frac{d[AH_2]}{dt} \qquad (2.6.2.4.3)$$

$$-\frac{dC_{PEG}}{dt} = -\beta\frac{d[AH_2]}{dt} \qquad (2.6.2.4.4)$$

$$\alpha = \frac{100 - [AH_2]_0}{90} \qquad (2.6.2.4.5)$$

$$\beta = \frac{C_{PEG_{min}}}{[AH_2]_0} \qquad (2.6.2.4.6)$$

$$C_{PEG_{min}} = 0.0064 + 0.024[AH_2]_0 \qquad (2.6.2.4.7)$$

where, k is the overall reaction rate constant, k_{a1} and k_{a2} are the second order inactivation constants for phenol and H_2O_2 respectively. K_1 and K_2 are the Michaelis constants for H_2O_2 and phenol respectively. E_a is the active enzyme concentration. α is the reaction stoichiometry between H_2O_2 and phenol, while β is the reaction stoichiometry between PEG and phenol.

The main drawback in this model is that none of the constants was determined based on experimental data. The model was calibrated using a trial and error curve fitting method. Hence, the optimum values reached may not be the global optima. Also, k_{a1} was assumed to be a function of PEG; however, it was not derived.

2.6.2.5 Model 5: Ibrahim (1998) developed a robust model based on the following assumptions:

- Inactivation of enzyme (by hydrogen peroxide) is a parallel process, taking place simultaneously along with the inhibition by free radicals.
- Total inhibition is additive and is estimated by simply adding the two inactivation pathways.
- Consumption of H_2O_2 is linearly dependent on the consumption of substrate.

- The rate of change of concentration of free radicals is assumed zero.

The set of pseudo-steady-state differential equations used to model were as follows:

$$-\frac{d[AH_2]}{dt} = \frac{k_{cat}E_a[AH_2][H_2O_2]}{K_1[AH_2]+K_2[H_2O_2]+[AH_2][H_2O_2]} \quad (2.6.2.5.1)$$

$$-\frac{dE_a}{dt} = k_r E_a \sqrt{-\frac{d[AH_2]}{dt}} + k_a E_a [H_2O_2] \quad (2.6.2.5.2)$$

$$[H_2O_2] = [H_2O_2]_0 - \alpha\{[AH_2]_0 - [AH_2]\} \quad (2.6.2.5.3)$$

where, k_{cat} is the turnover number for the enzyme, E_a represents all forms of the enzyme which have not been permanently inactivated, K_1 is the Michaelis constant of H_2O_2, K_2 is the Michaelis constant of phenol, k_r is the inactivation rate constant of the enzyme arising due to free radicals, k_a is the inactivation rate constant of the enzyme due to H_2O_2 and α is the molar ratio between H_2O_2 and phenol.

2.7 Fe^0: an effective reductant

Use of zero-valent metals in the processing of organic liquids has been known for a long time. The earliest environmental application of zero-valent iron was reported in the patent literature by Sweeny and Fischer in 1972 (Gillham and O'Hannesin, 1994). However, it was largely due to the work of Gillham and of Tratnyek and their coworkers, that zero-valent iron reduction treatment of contaminated groundwater gained momentum (Chem. & Eng. News, 1995). Early studies of reduction by iron metal focused primarily on halogenated organics (Matheson and Tratnyek, 1994; Gillham and O'Hannesin, 1994; Chuang *et al.*, 1995, Burris *et al.*, 1995; Grittini *et al.*, 1995; Orth and Gillham, 1996; Johnson *et al.*, 1996; Scherer *et al.*, 1997; Wust *et al.*, 1999; Arnold and Roberts, 2000).

Only recently, has the reduction of other compounds such as nitro aromatic compounds (Agrawal and Tratnyek, 1996. Burris *et al.*, 1996, Singh *et al.*, 1998, Devlin *et al.*, 1998), nitrate (Cheng *et al.*, 1997, Chew and Zhang, 1998, Huang *et al.*, 1998), azoaromatics (Weber, 1996; Nam and Tratnyek, 2000) and various metals (Cantrell *et al.*, 1995, Blowes *et al.*, 1997, Pratt *et al.*, 1997, Fiedor *et al.*, 1998, Gu *et al.*, 1998) received significant attention.

In a recent review article (with over 200 references), Scherer *et al.* (2000) presented an overview of the mechanisms and factors controlling different processes like sorption, precipitation, chemical reaction etc. that are involved in the Permeable Reactive Barriers (PRBs) for *in situ* ground water clean up.

2.8 Mechanism of Fe^0 reduction pathways of organic compounds

The major hindrance to designing new iron treatment systems is that the mechanism by which Fe^0 degrades the organics is not totally understood. Reduction of chlorinated organic compounds by iron metal is a well-known process. The transformation process is a redox reaction where the iron metal is oxidized and the organic compound is reduced. Iron metal is a strong reducing agent with a reduction potential of –0.44 *V* (Scherer *et al.*, 2000).

$$Fe^0 \rightarrow Fe^{2+} + 2e^- \qquad (2.8.1)$$

Matheson and Tratnyek (1994) hypothesized three general pathways for the reduction of carbon tetrachloride by zero-valent iron. The first pathway involves direct transfer of electrons from the iron metal to CCl_4:

$$Fe^0 + RCl + H^+ \xrightarrow{2e^-} RH + Cl^- + Fe^{2+} \qquad (2.8.2)$$

The second pathway involves reduction of CCl_4 by dissolved or surface Fe^{2+} ions formed from the anaerobic oxidation of iron metal by water:

$$Fe^0 + 2H_2O \rightarrow H_{2(g)} + 2OH^- + Fe^{2+} \qquad (2.8.3)$$

$$Fe^{2+} + RCl \xrightarrow{H^+} Fe^{3+} + RH + Cl^- \qquad (2.8.4)$$

The third pathway involves reduction of CCl_4 by dissolved or surface H_2 gas generated above as a product of anaerobic corrosion:

$$RCl + H_2 \rightarrow RH + Cl^- + H^+ \qquad (2.8.5)$$

Reduction rates of chlorinated aliphatics are considerably slower as compared to nitroaromatics (Scherer, *et al.*, 2000).

Agrawal and Tratnyek (1996) investigated the reduction of nitroaromatic compounds by Fe^0 in bicarbonate-buffered batch reactors. They found that the nitrobenzene reduction rate increased linearly with the available iron surface area and the effect of solution pH was minimal on the conversion. Mass transfer to the metal surface seemed to be the rate-controlling step in the zero-valent iron reduction of nitroaromatic compounds. They reported first-order reduction rates for nitrobenzene, nitrosobenzene and aniline and concluded that rate of aniline formation was slower than either nitroso- or nitrobenzene. Based on their findings, they concluded that sequential nitro reduction to aniline via intermediate nitroso and hydroxylamine compounds seemed to be the major transformations taking place in the Fe^0-H_2O-CO_2 system. It was represented as:

$$ArNO_2 + Fe^0 + 2H^+ \xrightarrow{k_1} ArNO + Fe^{2+} + H_2O \quad (2.8.6)$$

$$ArNO + Fe^0 + 2H^+ \xrightarrow{k_2} ArNHOH + Fe^{2+} \quad (2.8.7)$$

$$ArNHOH + Fe^0 + 2H^+ \xrightarrow{k_3} ArNH_2 + Fe^{2+} + H_2O \quad (2.8.8)$$

where each k represents the observed pseudo first-order rate constant for the involved reduction step. Formally, the overall reaction can be written as:

$$ArNO_2 + 3Fe^0 + 6H^+ \rightarrow ArNH_2 + 3Fe^{2+} + 2H_2O \quad (2.8.9)$$

Charlet *et al.* (1998) found that during the degradation of TCE, the reduction reaction was not coupled to the oxidation of Fe^0 to Fe(II) but rather to that of Fe^{2+} sorbed on to iron corrosion products such as hematite. Since, Fe(II) is very unstable in aerobic environments, Fe^0 serves as the main source for Fe(II). The reduction kinetic rate was found to be a function of concentrations of OH^-, Fe^{2+} and reactive surface sites.

Weber (1996), in a seminal paper, conclusively proved that the iron-mediated reductive transformations were surface-mediated. He took 4-aminoazobenzene (4-AAB) as his probe molecule and studied its reduction both in the solution phase and bound to a solid support in the presence of Fe^0.

Arnold and Roberts (2000) examined the rates and products of Fe^0 reaction with chlorinated ethylenes in batch reactors. They used a modified Langmuir-Hinshelwood-Hougen-Watson (LHHW) kinetic model to interpret their data in the context of interspecies inhibitory effects. Their results indicated that the pseudo first-order rate constant was linear to the metal loading over a limited range. Comparison of product

distribution observed in their study in batch systems with column and field results elsewhere, revealed that inspite of a variety of factors like reactor types, reaction rates, iron types, and solution conditions controlling the reaction, the product distribution changed relatively little.

2.9 Kinetics of NAC reduction by zero-valent iron

Devlin *et al.* (1998) adopted a recirculating batch reactor with an immobilized solid phase to study the kinetics of NAC reduction. They found that the disappearance of any single NAC did not strictly follow pseudo-first-order kinetics, with rate-constants declining with time, indicating a continuous loss of reactivity of the Fe^0.

Burris *et al.* (1996) studied heterogeneous reaction kinetics of NB with zero-valent iron in both batch and flow-through columns. They studied the effects of solids to liquid ratio, metallic iron concentration, and mass transfer limitations. They also used batch and continuous flow models to interpret their results. Results from batch experiments were consistent with pseudo first-order reaction kinetics:

$$c = c_0 Exp(-\mu_b t) \qquad (2.9.1)$$

where, c is the aqueous-phase reactant concentration at any time, c_0 is the initial dissolved-reactant concentration in the batch reactor, and μ_b is the pseudo first-order degradation-rate coefficient.

Singh *et al.* (1998) studied the remediation of hexahydro-1,3,5-trinitro-1,3,5-triazine (RDX) in both soil and water. They found complete destruction of RDX within 72 h. Nitroso derivatives of RDX accounted for about one-quarter of the RDX transformed, which were ultimately mineralized after 112 days.

Wust *et al.* (1999) successfully employed an enhanced model accounting for both zero- and first-order kinetics for the degradation of TCE over the full concentration range:

$$\frac{d[TCE]}{dt} = \frac{[TCE]R_{Fe}k_{RS}\rho_a}{[TCE] + (k_{DS} + k_{RS})/k_s} = \frac{[TCE]k_0}{[TCE] + K_{1/2}} \qquad (2.9.2)$$

The zero-order rate constant (k_0) is defined as the product of the number of reactive sites per unit surface area (R_{Fe}), the iron surface concentration (ρ_a), and the first-order rate constant for reaction of sorbed TCE (k_{RS}). The parameter $K_{1/2}$ corresponds to the aqueous TCE concentration at half-maximum transformation rate and is defined as the sum of the first-order rate constants for dissociation (k_{DS}) and reaction of sorbed TCE (k_{RS}) divided by the association rate constant for dissolved TCE onto the reactive sites (k_S). Since the model is a one-site model, the estimated parameters represent mean values of the sites on the iron possibly differing in location and reactivity.

2.10 Reduction of other chemicals with Fe^0

Gotpagar *et al.* (1997) studied the reductive dehalogenation of trichloroethylene (TCE) using zero-valent iron. They examined the effect of feed concentration, initial pH, metal loading and particle size of Fe^0 on the degradation. They found that the conversion was independent of the initial TCE concentration; however, TCE degraded at any given time was directly proportional to the dissolved iron in solution. They also found the pseudo first-order rate constant doubled when the particle size was decreased by a factor of 2.5. Initial solution pH had no significant effect on the degradation process. Pseudo first-order kinetics were given as:

$$\frac{d[TCE]}{dt} = -k_{1,obs}[TCE] \qquad (2.10.1)$$

Johnson *et al.* (1996) analyzed kinetic data relating to dehalogenation by Fe^0 obtained from different sources. They normalized these data to iron surface area concentration and derived specific rate constants (k_{SA}) that varied only by 1 order of magnitude for individual halocarbons. They found that dechlorination was generally more rapid at saturated carbon centers compared to unsaturated carbons. The k_{SA} depended on area available for reaction which was affected by reagent grade iron used, grain size distribution, acid-washing etc. Variability of k_{SA} was also due to the different techniques employed to measure the surface area.

Cantrell *et al* (1995) tried to remove various metals in groundwater using Fe^0 as permeable reactive barrier. They found through a series of kinetic-batch studies that the rate of removal of CrO_4^{2-} and UO_2^{2+} from groundwater permitted an inexpensive barrier to be used for *in situ* cleanup purposes.

Scherer *et al.* (1997) addressed some of the fundamental questions regarding the kinetics of reduction of contaminants by zero-valent iron. They studied the kinetics of CCl_4 in pH 8.8 borate buffer, so that oxide film would not form on the iron electrode. They found that the rate of reduction of CCl_4 by oxide-free Fe^0 appeared to be dominated by reaction at the metal-water interface rather than by transport to the metal surface and that the overall rates were limited by reaction kinetics.

Farrell *et al.* (2000) investigated the long-term performance of zero-valent iron column for reduction of TCE. They measured rates of TCE dechlorination over a period of 2 years in simulated groundwater containing different electrolytes as background

substances. The TCE reaction rates were found to be pseudo first-order and were independent of solution pH at early reaction periods. However, with passage of time, reaction rates were found to diverge from pseudo first-order behavior due to reactive site saturation and augmented iron surface dormancy toward the influent end of column. The extent of dormancy was found to depend both on the TCE concentration and the background electrolyte solution.

2.11 Sorption property of zero-valent iron

Haderlein and Schwarzenbach (1993) studied the adsorption of a large number of nitroaromatic compounds on mineral surfaces. They found that NACs may adsorb reversibly on the mineral surfaces, the strength of adsorption depending on the structure of the compound and the type of the surface. The sorption isotherms were modeled by the Langmuir equation. They studied the effect of pH on the distribution coefficient, K_d (defined as the ratio of concentrations of the sorbate at the surface and in solution). They found that the nonionizable NACs did not show any dependence of K_d between pH 4 and 8, while the ionizable nitrophenols (HA) exhibited a strong pH dependence of the apparent K_d value in the region corresponding to the pK_a of the compound. They proposed the following model to explain this behavior:

$$K_d(pH) = \alpha_0 K_d^{HA} \qquad (2.11.1)$$

where, K_d^{HA} is the K_d value of nondissociated species and is assumed constant over the whole pH range considered, while α_0 is the fraction of the nondissociated species and is given by:

$$\alpha_0 = 1 / (1 + 10^{(pH - pKa)}) \qquad (2.11.2)$$

Devlin *et al.* (1998), in their recirculating batch experiments, found that the NACs were reduced very rapidly to anilines, which sorbed irreversibly and strongly to the solid surfaces, interfering with the reduction reaction. They found that the zero-valent iron lost reactivity very rapidly in the initial stages of the reaction. The reactivity was somewhat regained on back-washing with background electrolyte. However, they could not definitely conclude if the passivation process was indeed due to the accumulation of aniline on the solid surface, or due to build-up of Fe^0 corrosion products.

Orth and Gillham (1996) found in a flow-through column study of dechlorination of TCE by Fe^0 that only 73% of carbon could be accounted for in the identified products, while the rest was sorbed on the iron surface until complete dechlorination was achieved.

Burris *et al.* (1995) found that both TCE and PCE exhibited nonlinear sorption behavior. They fitted the data by the generalized Langmuir isotherm expression. Once the mass sorbed on the iron was accounted for, they found the reduction rates to be first-order. For heterogeneous reactions to take place, it is required that the reactant molecules reach the solid surface. They then combine with either 'reactive' or 'non-reactive' surface sites. Reactive sites are those where the breaking of bonds in the reactant molecule takes place, while on non-reactive sites only sorption interactions occur where the solute molecule remains intact. They also speculated that the bulk of sorption was to the non-reactive sites.

2.12 Other materials in use for reduction of organic pollutants

Besides, zero-valent iron, there has been active research to find other suitable materials to reduce the aromatics suitably.

Klausen *et al.* (1995) studied the reduction of a class of substituted nitrobenzenes (NBs) by Fe(II) in aqueous suspensions of minerals that are commonly present in soils like magnetite (Fe_3O_4), lepidocrocite (γ-FeOOH), goethite (α-FeOOH), aluminum oxide (γ-Al_2O_3) etc. They found that aqueous solutions of Fe(II) by themselves were unreactive, while it readily reduced the NBs in suspensions of Fe(III) containing minerals.

Butler and Hayes (2000) studied the kinetics of transformation of halogenated aliphatic compounds by iron sulfide. Most of the compounds they studied seemed to be transformed with short half-lives of hours to days. However, no correlation could be established suggesting distinctions among the mechanisms for reductive dehalogenation of these compounds by FeS.

Chromate ion reduction has been achieved by Fe(II)-Fe(III) hydroxysalt green rusts more recently in soils (Lawniczak *et al.*, 2000). The interactions between Cr(VI) and hydroxysulfate and hydroxychloride were thoroughly investigated.

Warren *et al.* (1995) studied the possibility of using elemental zinc alongside iron to reduce CCl_4 to chloroform. They found that process kinetics were dependent on solution pH, surface area of the elemental metal, concentration of the substrate and even buffer selection. Experiments with Zn^0 conclusively proved that the reaction rate was directly proportional to the surface area of the suspended metal.

The research group of Arnold (Roberts *et al.*, 1996 and Arnold and Roberts, 1998) studied various zero-valent metals besides iron for reduction of chlorinated aliphatics. They used zero-valent zinc, copper and aluminum in their study. Their focus of study was on determining the various pathways for dehalogenation of aliphatics.

Korte and coworkers investigated reduction of chloroaliphatics and polychlorinated biphenyls by zero-valent iron and palladized iron and compared their respective reductive efficiencies. They concluded that the reduction with palladized iron was greater by an order of magnitude as compared to zero-valent iron (Muftkian *et al.*, 1995; Grittini *et al.*, 1995; Liang *et al.*, 1997).

2.13 Fe^0 corrosion products

Cornell and Schwertmann (1996) discussed various forms of the iron oxides formed under different conditions like pH, presence of O_2, temperature and background electrolyte. Many factors may dictate the speciation and morphology of the metallic iron corrosion products. They stated that under anaerobic conditions, the first corrosion product formed was the amorphous ferrous hydroxide, $Fe(OH)_2$ which subsequently got oxidized to form magnetite (Fe_3O_4). Under neutral pH conditions, prior to the formation of magnetite, mixed-valent salts {Fe(II) and Fe(III)} may form. These are generally referred to as "Green Rusts" (Cornell and Schwertmann, 1996). They found the "Green Rusts" to be stable only at low redox potentials. The "Green Rusts" easily oxidized to form maghemite (γ-Fe_2O_3). Maghemite formed via oxidation of magnetite is nonporous (Cornell and Schwertmann, 1996 and Farrell *et al.*, 2000). Aged iron surfaces have been found to be coated with an inner layer of magnetite and an outer layer of maghemite (Farrell *et al.*, 2000). Even though magnetite is a semiconductor, it has electric conductive properties close to that of metals. Therefore, magnetite is not considered to be a passivating oxide, in contrast to maghemite (Farrell *et al.*, 2000).

CHAPTER 3 MATERIALS AND METHODS

The present work was divided into three sections, A, B and C. Section A involved the optimization of the first step of the two-stage reaction, *viz.*, Fe^0 reduction of the NACs. Section B was devoted to the optimization of the enzymatic reaction of the anilines formed in the first stage and their precipitation and removal. Section C was the integration of the two stages of treatment into a continuous flow process.

3A Zero-valent iron reduction of NACs

3A.1 Materials

Analytical grade aniline and nitrobenzene, ACS grade $NaHPO_4$, Na_2HPO_4, Na_2CO_3 and $NaHCO_3$ were purchased from BDH, Toronto, ON. ACS grade sodium sulfite and cobaltous chloride were obtained from Fisher Scientific, Pittsburgh, PA. Analytical grade *p*-toluidine and trinitrobenzenesulfonic acid (TNBS) (as picrylsulfonic acid 5% (w/v) aqueous solution) were obtained from Sigma Chemicals, St. Louis, MO. 2-, 3-, 4-nitrotoluenes, *o*- and *m*-toluidines were obtained from Aldrich Chemicals, Milwaukee, WI.

Two preparations of iron metal were used in this study. The first was purchased from Fisher Chemicals, Fair Lawn, NJ (I57-500: lot no. 976195), as iron filings of about 40 mesh size. The second one was purchased from Alfa Aesar, Ward Hill, MA, as iron granules (lot no.: D03I24) with the nominal size between 1-2 mm. The purity of the metal was 99.98% (on metal basis) with the major impurities being phosphorous (16ppm), cobalt (14 ppm), nickel and manganese (each 10ppm).

Disposable polystyrene semi-micro cuvettes were used to measure the absorbance of the samples. They were purchased from Bio-Rad Laboratories, Hercules, CA. Quartz cuvettes with 10 mm path length were purchased from Hellma (Canada) Limited, Concord, ON.

3A.2 Experimental and Analytical Equipment

Solution absorbance was measured using a Hewlett-Packard Diode Array Spectrophotometer, Models 8451A and 8452A. UV-vis spectra measurements and Multi-component analysis (MCA) software was used with authentic standards to determine nitrobenzene and aniline concentrations in reaction solutions.

Dissolved oxygen measurements were done with an oxygen meter (Model 57) supplied by YSI Inc., Yellow Springs, OH. An Expandable Ion Analyzer EA 940, manufactured by Orion Research, Cambridge, MA, was used to measure the pH of the samples. Standard buffer solutions of pH 4, 7 and 10 were purchased from BDH, Toronto, ON.

The batch reactor vials were shaken at maximum setting on a Burrell Model 75 wrist-shaker supplied by Burrell, Pittsburgh, PA. Peristaltic pump (Auto Analyzer) was supplied by Technicon Corp., Tarrytown, NY. Another peristaltic pump (Autoclude-VL) was supplied by Cole Parmer Instrument Company, Chicago, IL. The continuous flow columns were purchased from Bio-Rad, Mississauga, ON.

Scanning electron microscopy (SEM) model JEOL 5800-LV with energy-dispersive X-ray spectrometry (EDS) analysis (Kevex) was used for surface morphology and elemental composition of iron particles. X-ray diffraction (XRD) analysis was employed to characterize the iron filings with model Rigaku DMAX/1200. SpectraSpan

V System supplied by SpectraMetrics Inc., Andover, MA, was employed to analyze the effluent samples by the Direct Coupling Plasma (DCP) technique.

3A.3 Experimental Procedure

3A.3.1 General Reaction Conditions

All reactions were carried out at room temperature, 18-22 °C, except where noted. Buffers, whenever used, were prepared following the recommendations of Gomori (1955).

3A.3.2 Optimization of Oxygen Scavenger

Anaerobic conditions were necessary for the reduction of NAC to aromatic amine by zero-valent iron to take place. 5 mM Na_2SO_3 along with 0.1% (of Na_2SO_3) by mass of $CoCl_2$, as catalyst, was used in the preliminary experiments. It was decided to optimize the amount of Na_2SO_3 required for the reaction to proceed under anaerobic conditions. Replicate, open feed reservoirs of the type to be used in continuous operation were set up that contained 1mM of nitrobenzene and Na_2SO_3 in various amounts at room temperature. An oxygen meter was used to measure the amount of residual O_2 left in the feed reservoirs after the addition of Na_2SO_3. Concentration of O_2 in the reservoir due to re-absorption from atmosphere was also followed as a function of time.

3A.3.3 Iron Pretreatment

Initially, the iron metal from Fisher was used as received (about 40 mesh). However, the proportion of finer particles was comparatively much higher with particles

passing through 40 mesh being greater than 70%. Hence, prior to use, the Fe^0 was hand-sieved to obtain a size range of 30-40 mesh. This is called Iron-I throughout this report. The other iron sample was from Alfa Aesar and is henceforth called Iron-II. This was of 1-2 mm size and was used as received.

Iron was always pretreated with HCl acid as recommended by Agrawal and Tratnyek (1996). The purpose of the pretreatment was to clean the surface of the iron to remove any (hydr)oxide. A measured quantity of Fe^0 particles was taken in a glass vial and washed with 10% HCl. This was followed with 15 mM carbonate buffer wash (pH 9.5) for 4 times, to ensure the removal of all chlorides from the iron surface. The buffer was previously made anaerobic by the addition of Na_2SO_3. This was followed by rinsing with and maintaining it in Na_2SO_3 solution to remove carbonates and bicarbonates. This also ensured that the Fe^0 surface did not come in contact with atmospheric O_2.

In the column operations, Fe^0 was pretreated *in situ*. After the wash, the column was kept soaked in Na_2SO_3 solution to ensure anaerobic conditions.

3A.3.4 Batch Reactors

Before performing the continuous column experiments to study the reduction process of NAC by Fe^0, batch reactor experiments were designed with a view to collect useful information about the various parameters of the process. Batch reactor runs were carried out typically in 30 mL vials sealed by screw-cap and ensuring that there was no head-space. The vials were shaken on a shaker at maximum setting for 3 h. This provided a wrist-like action to the vials for proper mixing. Solutions were made anaerobic by adding appropriate amounts of Na_2SO_3 and $CoCl_2$, except where noted otherwise. In general, all the vials received 1g of Iron-I and 1mM NB, unless noted otherwise.

Standing the vial on a magnet for a few minutes facilitated settling of iron particles after the reaction. The contents were later analyzed. Batch experiments were carried out on nitrobenzene only.

3A.3.4.1 Experiments to Study effects of pH

Studies were carried out to explore the effects of pH on the reduction process. In a typical batch reactor, initial solution pH was varied by using HCl or NaOH, usually 1 M. The pH was measured by an ion analyzer. At the end of the reaction, after 1 h, the pH was measured again and the contents analyzed.

3A.3.4.2 Adsorption Experiments

Batch reactor experiments were designed with a view to study the phenomenon of adsorption of the aniline, formed from reduction of the NB, on to the surface of zero-valent iron. A typical batch sample was prepared as follows: about 1 g of granular iron and 30 mL of solution containing various concentrations between 0 and 2 mM of authentic aniline. All other conditions remaining the same, pH of the solution was varied and the sorption data were recorded after a period of 3 h. pH range studied was from 2 to 8.5. Concentrations of aniline in the solution, before and after the experiment, were measured.

3A.3.5 Packed-bed porosity

Tests were done to estimate the bulk porosity of a packed-bed column. A known mass of the iron granules (Iron-II) was taken in test tubes and a measured amount of water was added to it until all the pores were saturated with water. Knowing the volume

of the test tube and the amount of water added, pore bed-space and bed volumes were calculated for future use.

3A.3.6 Continuous Column Operations

Column operation of the Fe^0 reduction step was initially investigated with 50 g of Iron-I in a 15x150 mm column with the Fe^0 bed depth of 110 mm. After pretreatment, iron was kept immersed in Na_2SO_3 solution to maintain anaerobic conditions. During the experiments upward flow of the nitrobenzene solution was executed through the column by using a peristaltic pump. A continuous flow of 3.0 ± 0.1 mL/min was maintained. The effluent from the column was analyzed at regular intervals for aniline. However, most of the column operations were subsequently studied with 200 g Fe^0 (Iron-II) in a 15x300 mm size column under similar flow conditions. Fe^0 bed depth, in this case, was about 280 mm.

3A.3.7 Analytical Methods

The concentration of the reduction product, aniline, was determined by TNBS test (Monsef *et al*, 2000). In a final volume of 1.0 mL, 100 µL of 10 mM TNBS, 100 µL of 0.5 M phosphate buffer of pH 6.4 and 800 µL of sample plus water were added. Samples were allowed to stand for 30 min and then absorbance was measured at 384 nm against a reagent blank. The calibration curves had shown that there was a linear relationship between the absorbance and the concentration. Concentrations were calculated using an experimentally-determined extinction coefficient (molar absorptivity) of 13200 $M^{-1}.cm^{-1}$. It is known that TNBS readily forms an adduct with SO_3^{2-} that affects the analysis (Means *et al.*, 1972). This complication was overcome by preparing a calibration curve

for authentic aniline solution doped with Na_2SO_3 and measuring the peak at 398 nm at a slightly higher extinction coefficient (14000 $M^{-1}.cm^{-1}$) than for pure aniline. Details of the procedure are relegated to the Appendix B.3.

UV-Vis spectra measurements and Multi-component analysis (MCA) software was used with authentic standards to determine nitrobenzene and aniline concentration in reaction solutions.

3B Enzymatic Reaction of the Aromatic Amine

3B.1 Extraction of crude soybean peroxidase enzyme

3B.1.1 Materials

Soybean hulls were obtained from ADM-Agri Industries Limited, Windsor, ON. Enzyme extracted from the hulls was characterized on the basis of enzyme activity. Details of the activity test are given in subsequent analytical section. A unit of activity is defined as the number of micromoles of hydrogen peroxide converted per minute at pH 7.4 and temperature 25°C. The SBP hulls were stored at room temperature and the enzyme extract was stored at 4°C.

Catalase (EC 1.11.1.6) with an activity of 15000 units/mg solid and polyethylene glycol 3350 (PEG 3350) were purchased from Sigma Chemical Co., St. Louis, MO. One unit of catalase decomposes 1 micromole of hydrogen peroxide per minute at pH 7 and temperature 25°C. An aqueous stock solution of catalase was stored at 4°C and used when needed.

Hydrogen peroxide (30% w/v) was purchased from BDH Inc., Toronto, ON and was stored at 4°C. The diluted H_2O_2 solutions were prepared every day. Glass microfiber

filters of 42.5 mm diameter (934-AH) were purchased from Whatman Inc., Clifton, NJ. Non-sterile syringe filters with 25-mm membrane diameter and pore size of 0.2 μm were purchased from Nalge Nuno International Corp., Rochester, NY. These were used in conjunction with Luer Lock syringe with needles purchased from Sherwood Medical, St. Louis, MO. Other chemicals and equipment have been discussed previously in Section 3A.1.

3B.1.2 Analytical Equipment

Suspended particles in the enzyme extract were settled by using an IEC Centra-8 Centrifuge, supplied by International Equipment Company, Needham Hts., MA. It was operated at 4000 rpm for 5 min (Biswas, 1999).

3B.1.3 Extraction Procedure

The experiments were conducted at room temperature, 18-22°C. The study was based on the findings and protocol developed by Biswas (1999). 10 g of soybean hulls was added to 200 mL water and mixed thoroughly with magnetic stirrer for 1 h. After mixing, the hulls were separated from the solution, first by centrifugation at 4000 rpm for 5 min and then by vacuum filtration using glass microfiber filter. Regardless of the amount of water used, about 50 mL of it was lost in the extraction process. The enzyme extracted was termed "crude soybean peroxidase". Activity of the filtrate, containing crude SBP enzyme, was determined and the filtrate was stored at 4°C for future use. The enzyme was prepared on a weekly basis. Further details about the experiment can be found elsewhere (Biswas, 1999).

3B.1.4 Stability of the Crude SBP enzyme

Final experiments were conceived to be conducted on a continuous flow basis. Hence, it was necessary to know the stability of the enzyme at room temperature over a period of time as compared to storing at 4°C. The experiments were conducted to determine the changes in activity of the crude SBP enzyme while standing at room temperature. A known volume, 5 mL, of the enzyme solution with known activity, previously measured, was taken in a test tube and left in the room. The activity of the sample was measured periodically over a period of one week and the change in activity with time was recorded. Similarly, enzyme stored in the refrigerator at 4°C, was also tested at regular intervals for changes in activity.

3B.2 Oxidative polymerization and removal of substrates

3B.2.1 Experimental Procedure

3B.2.1.1 Batch Reactors

3B.2.1.1.i. Experiments with pure aniline

Batch experiments were set up to study the various parameters, *viz.* pH, $[H_2O_2]$/[aniline], SBP concentration and alum concentration, affecting the oxidative polymerization of aniline. Typically, batch experiments were conducted in glass vials of 30 mL volume, closed by rubber stoppers. Each batch received 1mM aniline and various concentrations of H_2O_2 and enzyme. For studies that involved step-wise addition of either H_2O_2 or SBP, appropriate amounts were added at the beginning of the reaction and after 1 h. In the present study, only two-steps addition was investigated. Initial pH of the solutions was adjusted by the addition of either HCl or NaOH, usually 1 M. The contents of the vials were mixed thoroughly and continuously with Teflon-coated magnetic stir

bars placed within the glass vials. The reaction was stopped after 3 h by the addition of catalase such that the final concentration of catalase in the solution came to 125 U/mL. At the end of the reaction, the pH of the solution was measured again. Alum was added to each batch to reach a final concentration of 50 mg/L, unless noted otherwise. After mixing the contents uniformly, 5 mL of that solution was taken for centrifuging for 30 min at 3500 rpm. The clear supernatant was either analyzed directly for residual aniline or subjected to filtration. Filtration was done using syringe filters with a nominal cut-off of 0.45 microns, so that errors could be eliminated from the analysis.

3B.2.1.1.ii. Experiments with "synthetic" aniline (SA)

Batch experiments, similar to section 3B.2.1.1.i, were set up to study the various parameters, *viz.* pH, $[H_2O_2]$/[aniline], SBP concentration and alum concentration, effecting the oxidative polymerization of "synthetic" aniline, SA, formed from reduction of NB by Fe^0. The SA contained unreacted Na_2SO_3 and product Fe^{2+} from the zero-valent iron column. Hence, the effects of these two variations from pure aniline were studied in batch reactors. First, the unreacted Na_2SO_3 and product Fe^{2+} were converted to Na_2SO_4 and product Fe^{3+} respectively and then the enzymatic treatment was carried out and the parameters were optimized just as in the previous section.

3B.2.1.2 Continuous flow system

The design of a continuous flow system for the enzymatic treatment stage was based on the findings of Ibrahim *et al.* (2001), which consisted of:

- A pre-mixer, where H_2O_2, aerated aniline from the first stage and crude SBP enzyme were mixed. The mixing time was 5 min.
- A plug-flow reactor, 15x1100 mm, where the enzymatic reaction took place for 1 h.
- A flocculation tank where alum was added to the effluent from the second stage column. Mixing and coagulation time was about 30 min.
- A sedimentation tank with a retention time of 3 h, where the settled solids were removed from the bottom of the tank.

Samples from the reactor at various sampling ports were mixed with a concentrated aliquot of catalase solution immediately upon collection to quench the reaction by quickly converting residual H_2O_2 into water and O_2 (Nicell, 1994).

3B.3 Analytical Methods

3B.3.1 SBP Activity Assay

Although, it is theoretically possible to measure the amount of enzyme, it is practically impossible to do so. Instead, enzymes are measured by their catalytic activity. This is done by measuring the rate of reaction at which they are catalyzing and comparing the same with the rate of uncatalyzed reaction.

An assay containing phenol, 4-aminoantipyrine (AAP) and hydrogen peroxide was employed to measure the SBP enzyme activity. The approach was to provide all components except enzyme in excess, so that the initial rate of reaction became directly proportional to the amount of enzyme present. The rate of reaction was measured by monitoring the rate of formation of products that absorbed light at a peak wavelength of 510 nm. One unit of activity used in this study is defined as the number of micromoles of

H_2O_2 converted per minute at pH 7.4 and 25°C. A detailed description of the assay procedure is given in Appendix B.1 (Wu *et al.*, 1997).

3B.3.2 Hydrogen Peroxide Assay

A colorimetric assay was employed for the measurement of H_2O_2 concentration using *Arthromyces ramosus* peroxidase (ARP) as catalyst and AAP and phenol as color generating substances. This assay procedure was set up so that H_2O_2 was the only limiting substrate in an endpoint determination. Therefore, the intensity of color developed at 510 nm was directly proportional to the amount of peroxide present in the sample. The assay sample volume was kept at 1 mL. The peroxide concentration was never allowed to exceed 50 μM. A detailed explanation on the preparation of assay reagents and the description of assay procedure is given in Appendix B.2 (Wu *et al.*, 1997).

3C. Continuous flow system integrating the two steps of reduction and oxidative polymerization

The two-stage continuous process is schematically shown in Figure 3.1. The effluent from the Fe^0 column was collected and aerated for 30 min so that unreacted Na_2SO_3 and Fe^{2+} were fully oxidized, before the stream was subjected to peroxidase treatment. The effluent from the first stage became influent to the second stage of the 2-stage reaction.

3D. Sources of Error and Error Analysis

During any experimental work, two kind of errors can occur: systematic errors and random errors. The former errors are due to the measuring or analytical methodologies and the in-built errors of the instruments. The latter are due to the personal factors. As an example, systematic errors can occur in both direct spectrophotometric method and colorimetric method when very low concentrations are required to be measured. Also, the products of the enzymatic treatment of anilines are expected to be higher oligomers of anilines. Hence, it is possible that those higher order oligomers that did not precipitate would actually take part in the TNBS test and interfere with the interpretation of the result. Although errors may not be completely eliminated, they can be reduced to minimum by following standard protocol and careful experimentation. Calibration curves were prepared many times so that reproducibility could be achieved. The protocol of analysis procedure was followed strictly and the order of steps was never changed. Reproducibility of the experiments was determined by including duplicate batch reactors and blank batch reactors; while for the analytical tests, duplicate and triplicate samples were analyzed. Standard deviations from Table 3D, Appendix C, indicate that the analytical tests at higher concentrations were accurate within 1%, while at the lower concentrations the accuracy was within 5%.

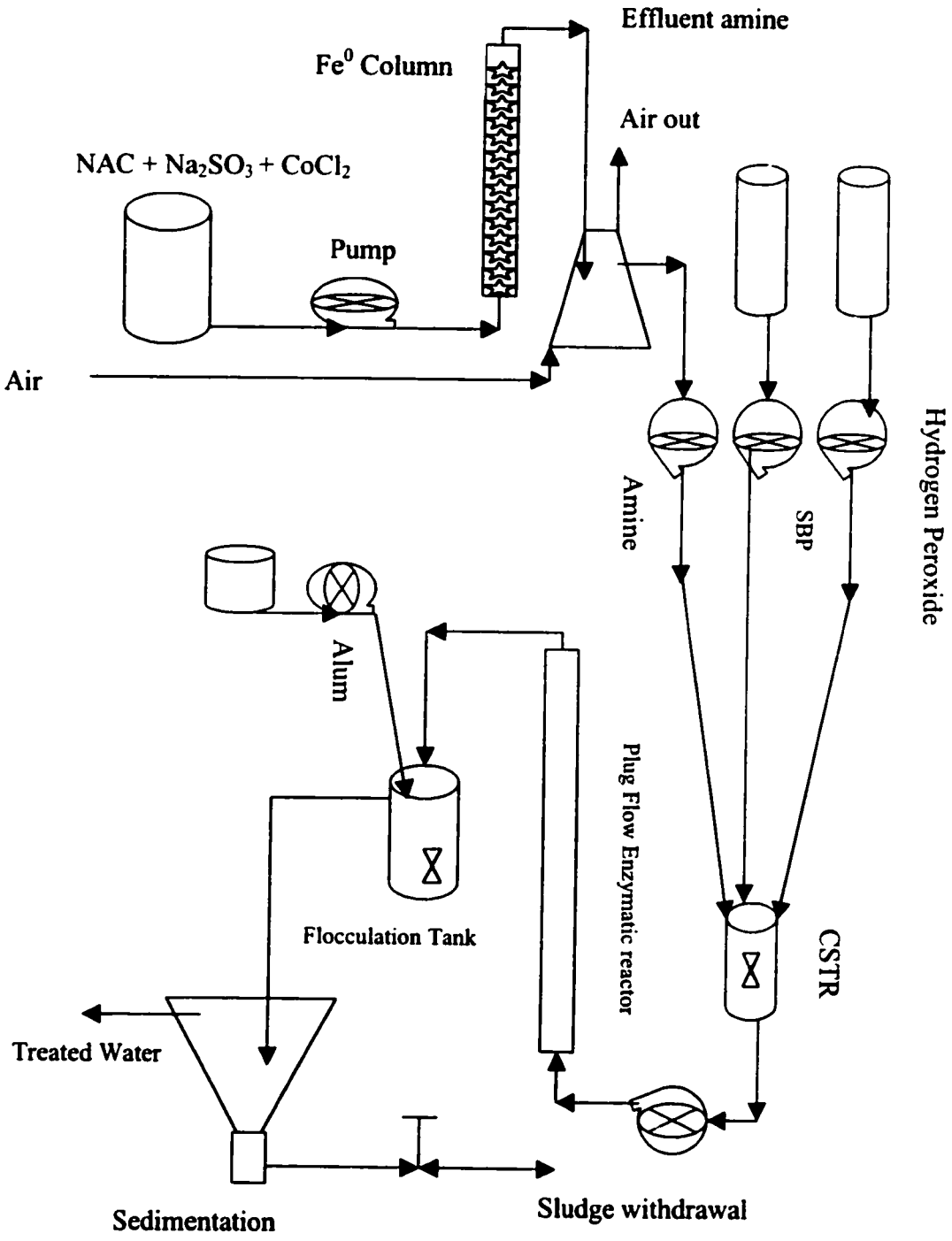

Fig. 3.1 Schematic of the Continuous-flow system using single CSTR as pre-mixer and Plug flow enzymatic reactor

CHAPTER 4 RESULTS AND DISCUSSION

STAGE 1 Fe^0 reduction of nitroaromatic compounds (NACs)

Four different nitroaromatic compounds, NACs, were used in this study: nitrobenzene, *o*-, *m*- and *p*-nitrotoluenes. Preliminary studies were, however, done with NB alone and the parameters optimized.

The zero-valent iron reduction of nitrobenzene yields aniline via nitrosobenzene and phenylhydroxylamine as intermediates (Agrawal and Tratnyek, 1996) according to the following reactions:

$$C_6H_5NO_2 + Fe^0 + 2H^+ \rightarrow C_6H_5NO + Fe^{2+} + H_2O \quad (4.1)$$

$$C_6H_5NO + Fe^0 + 2H^+ \rightarrow C_6H_5NHOH + Fe^{2+} \quad (4.2)$$

$$C_6H_5NHOH + Fe^0 + 2H^+ \rightarrow C_6H_5NH_2 + Fe^{2+} + H_2O \quad (4.3)$$

The overall reaction can be written as:

$$C_6H_5NO_2 + 3Fe^0 + 6H^+ \rightarrow C_6H_5NH_2 + 3Fe^{2+} + 2H_2O \quad (4.4)$$

Similar equations can be written for other NACs also.

4.1 Use of Na_2SO_3 as O_2 scavenger

In groundwater treatment with zero-valent iron, anaerobic conditions generally exist. However, in industrial- or process- water streams, anaerobic conditions have to be achieved either by degassing or by chemical scavenging of O_2. Previous researchers achieved the anaerobic condition by using degassing as an option. Monsef *et al.* (2000) suggested the use of oxygen scavenger to scavenge O_2 chemically. They used $FeSO_4$ as scavenger and were successful in removing O_2. However, high concentrations of $FeSO_4$

were required and its role was not clearly understood. It seemed that $FeSO_4$ did more than just scavenge O_2 in that residual nitrobenzene was converted to aniline upon raising the pH in the effluent. It was surmised (Monsef *et al.*, 2000) that this conversion was due to Fe^{2+} species deposited on the Fe^{3+} particles that had formed, a phenomenon reported by Klausen *et al.* (1995). Gotpagar *et al.* (1997) dehalogenated trichloroethylene using zero-valent iron in presence of sodium bisulfite as the O_2 scavenger. However, a detailed study of the effects and concentrations of the O_2 scavenger has not been reported.

Literature (Babbitt *et al.*, 1975 and Brandvold, 1975) shows that Na_2SO_3 is capable of scavenging O_2 effectively. From stoichiometric considerations, the amount of Na_2SO_3 needed to scavenge O_2 from tap water at room temp. (20-22°C) is about 0.5 mM. However, Brandvold (1975) suggested a much higher ratio of Na_2SO_3 to O_2 for complete removal of oxygen, along with $CoCl_2$ as catalyst at 0.1% of Na_2SO_3 by mass. Therefore, all Na_2SO_3 solutions used in this study contained $CoCl_2$ in this proportion. In the absence of the catalyst, scavenging of O_2 was very slow. The reaction of Na_2SO_3 with O_2 can be represented as follows:

$$Na_2SO_3 + \tfrac{1}{2}O_2 \xrightarrow{CoCl_2} Na_2SO_4 \qquad (4.1.1)$$

In the present study anaerobic condition had to be simulated in the laboratory. Batch reactor studies had shown that anaerobic conditions were necessary to achieve complete reduction of NAC. Figure 4.1.1 shows the reduction of NB in batch reactors under three different conditions, without anaerobic conditions, with previously degassed solutions and with 5 mM Na_2SO_3. Figure 4.1.2 shows the reduction process in a continuous column with different initial concentrations of Na_2SO_3 (0-5 mM) in the feed.

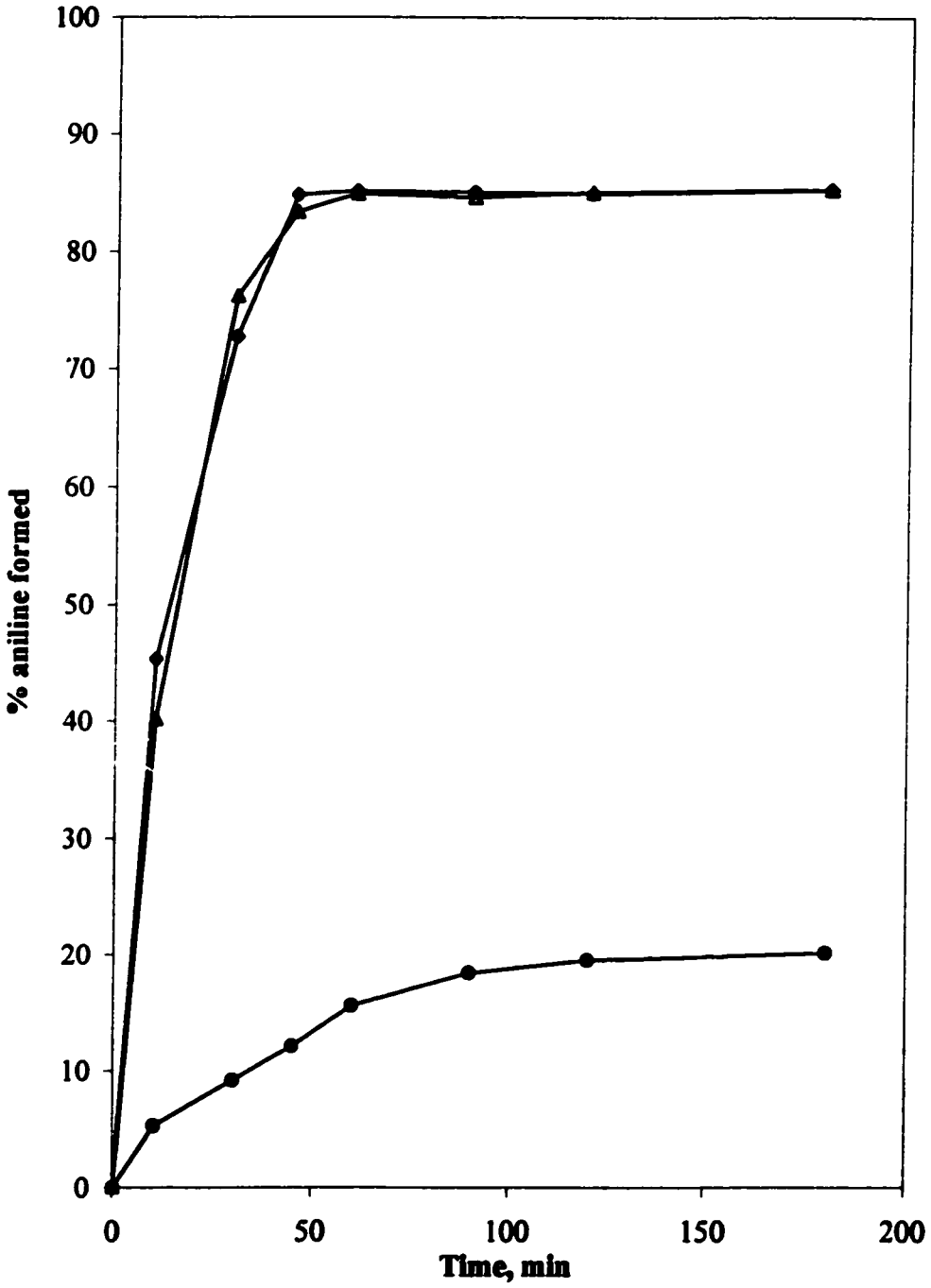

Fig. 4.1.1 Nitrobenzene reduction under different solution conditions Batch reactions of 30 mL volume, initially contained 1.0 mM of nitrobenzene at pH 8.5 in the presence of 1.0 g Iron-I, under the following conditions: oxygen saturated, •; degassed, Δ; sodium sulfite present at 5 mM, ◇

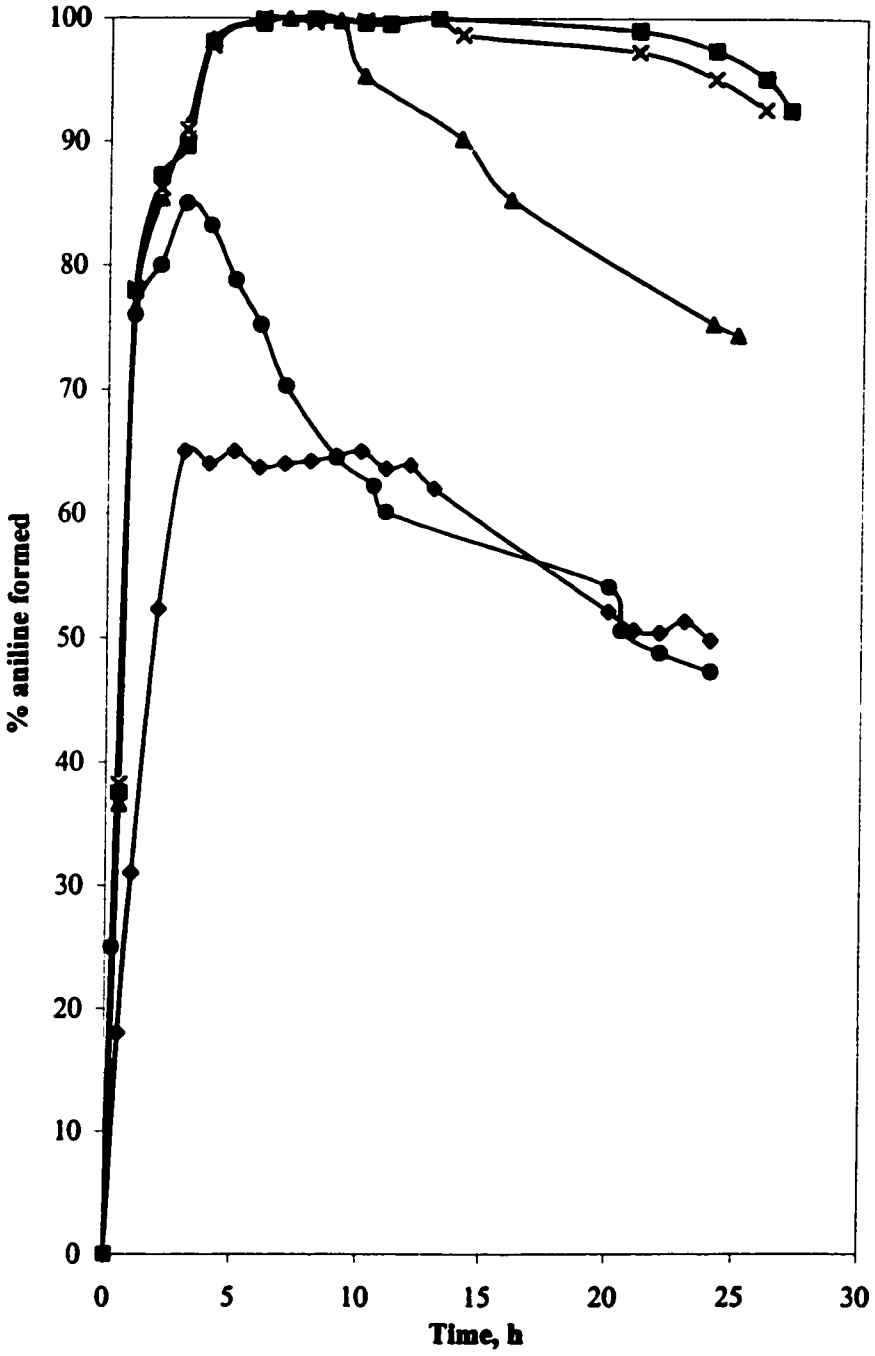

Fig. 4.1.2 Conversion of nitrobenzene to aniline in a continuous-flow column

Continuous-flow system in a 15x150 mm column with 50 g of Iron-I, influent nitrobenzene concentration of 1 mM at a flow rate of 2.8 mL/min, pH 7.2-7.4 and effluent pH 7.3-7.6. Concentration of Na_2SO_3 in the influent solution was varied as follows: 0 mM, ◆; 0.5 mM, ●; 1 mM, ▲; 2 mM, ×; 5 mM, ■.

Aniline concentrations were not corrected for loss due to adsorption on the metal surface. It can be seen from both batch reactions and continuous-flow reactions that anaerobic conditions have to be established, either by chemical scavenging of O_2 or by degassing of solutions, before zero-valent metal reduction can take place.

The concentration of O_2 in the open feed reservoirs, of the type used in continuous operations, due to re-absorption from the atmosphere was followed as a function of time, Figure 4.1.3. pH obtained under these conditions was 7.3-8.0. It is apparent from the plot that the stoichiometric amount of Na_2SO_3, 0.5 mM, could not scavenge dissolved O_2 completely. Based on these observations, 1 mM Na_2SO_3 was used for the continuous-column operations and the feed from an open reservoir was changed after every 7 hours. This was followed as a standard protocol for all subsequent runs. UV-vis spectral measurements of the influent solution containing nitrobenzene and Na_2SO_3 confirmed that the aromatic was not transformed by Na_2SO_3. Also, the presence of Na_2SO_3 did not shift the λ_{max} or change the molar extinction coefficient, ε, for nitrobenzene.

4.2 Zero-valent iron pre-treatment

Zero-valent iron as received from Fisher Inc. contained a high amount of fine particles, with more than 70% of the particles passing through a 40 mesh sieve, Table 4.2.1. This was also reflected in the efficiency of washing cycles, where 25-30% of fine particles were washed away. Loss of Fe^0 (as received) due to washing is reported in Table 4.2.2. Also, in preliminary column studies wash-off of fine iron particles was a concern. A single wash-cycle, for a batch reactor of 1 g of Fe^0 involved washing with 10% HCl,

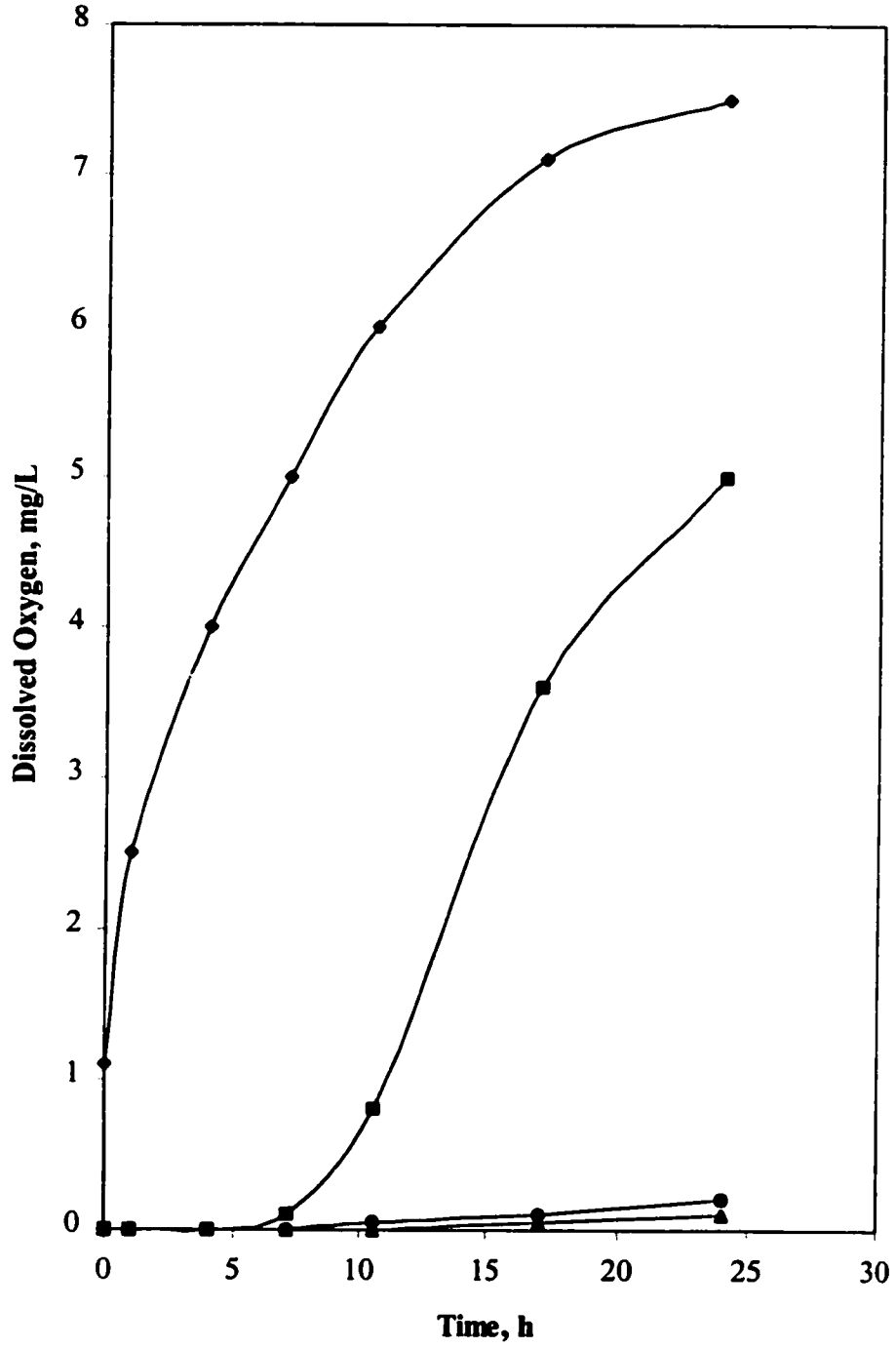

Fig. 4.1.3 Amount of O_2 absorbed into the solution
Concentration of oxygen due to re-absorption in the open feed reservoirs, of the type used in continuous column operations under different conditions of sodium sulfite present in the solution initially: 0.5 mM, ◆; 1.0 mM, ■; 2.0 mM, ●; 5.0 mM, ▲. pH obtained under these conditions was 7.3-8.0.

Table 4.2.1 Sieving Results of Fe^0

Iron-I was hand-sieved to constrain to a size 30-40 mesh.

Amount of iron sieved, g	-40 mesh g	-30+40 mesh g	+30 mesh g
25.0	17.8	3.52	3.73
25.2	17.7	3.74	3.54
50.3	35.9	7.0	7.1
50.1	35.8	7.43	6.83
100	72.4	14.1	13.6
100	71.7	15.1	13.3

Table 4.2.2 Washing results of Fe^0 (as received)

A single wash-cycle, for a batch reactor of 1 g of Fe^0 involved washing with 10% HCl, four times 15 mM carbonate buffer wash (pH 9.5) and then rinsed and maintained in Na_2SO_3 solution to remove carbonates and bicarbonates.

Fe^0 before pre-treatment g	Fe^0 after acid pre-treatment g	% loss
1	0.751	24.9
1	0.741	25.9
2.01	1.44	27.5
2	1.51	24.5
5.02	3.51	30.1
5	3.55	29

15 mM carbonate buffer wash (pH 9.5) for 4 times and then rinsing with and maintaining it in Na_2SO_3 solution to remove carbonates and bicarbonates. Hence, prior to use, the iron particles were hand-sieved to constrain to a constant size between 30-40 mesh. Loss of material during the wash-cycles of 30-40 mesh was 4 ± 0.2 %, Table 4.2.3. Loss of Fe^0 particles during washing cycles was speculated to be only due to washing and not due to Fe^0 dissolving in acid (Agrawal and Tratnyek, 1996).

The concentration of organic pollutants in groundwater is extremely low as compared to wastewater. This provides a very high surface area/mass of pollutants removed in groundwater as compared to the conditions in this study. Processes limited by mass transport do not reflect influence of surface conditions, whereas processes controlled by chemical reaction are often sensitive to even small surface alterations. Acid pre-treatment of iron was recommended (Agrawal and Tratnyek, 1996) to enhance the reactivity of iron by cleaning the metal surface of hydr(oxides) and it was surmised that acid washing caused pitting of the metal and imparted surface area enhancement. Pre-treatment of oxide-covered iron particles tends to increase the reaction rate. The impact of acid treatment on the rate of reaction was quite remarkable in some preliminary investigations done during a study at this laboratory previously (Monsef *et al.*, 2000). Scherer *et al.* (1997) also experienced rate enhancement with surface cleaning. Devlin *et al.* (1998), on the other hand, did not pre-treat iron particles by HCl, yet found that the hydroxide/oxide layer present on their Master Builders iron had no effect on the relative reaction rates.

Table 4.2.3 Washing results of Iron-I (30-40 mesh)

A single wash-cycle, for a batch reactor of 1 g of Fe^0 involved washing with 10% HCl, 15 mM carbonate buffer wash (pH 9.5) for 4 times and then rinsing with and maintaining it in Na_2SO_3 solution to remove carbonates and bicarbonates.

Fe^0 before pre-treatment g	Fe^0 after acid pre-treatment g	% loss
1	0.961	3.9
1.03	0.99	4
1.99	1.91	4
2.04	1.96	3.9
5.01	4.8	4.2
5.1	4.9	3.9

4.3 Batch Reactor Experiments

Batch reactor data are useful in predicting and estimating parameters in an easy and fast way. They can be readily set up and data collected conveniently. The study was initially focused upon batch reactor performance and the information collected was used to develop a continuous flow system. Preliminary studies on NB reduction were done with Iron-I.

4.3.1 Effect of pH

Owing to direct involvement of H^+ in the reduction of nitrobenzene, it was thought that changes in pH might affect the nitrobenzene reduction. The pH range studied was from 2.5 to 8.5. In a 30 mL vial, 1 g of Fe^0 had completely reduced 1 mM nitrobenzene. However, depending on the prevailing pH, product recovery varied widely (Figure 4.3.1). Product recovery, here, was defined as the concentration of aniline detected in the reaction solution at the end of the reaction. Since no nitrobenzene was detected in the final analysis of the batch reactor, it was thought that protonation of the aniline formed (pK_a = 4.6) prevented its desorption from the iron surface completely. Ionizable nitrophenols exhibited a strong pH dependence of the distribution coefficient value in the pH region corresponding to the pK_a of the compound (Haderlein and Schwarzenbach, 1993). This is similar to what was observed for aniline. It is also possible that the amino group of aniline (in the neutral, free-base form) acts as a ligand in complex formation with the metal as indicated by Vasudevan and Stone (1996). No analysis was done to ascertain the presence of any intermediates, phenylhydroxylamine

or nitrosobenzene, since it is known from the literature (Agrawal and Tratnyek, 1996 and Monsef *et al.*, 2000) that their presence was negligible in the final stages of conversion.

4.3.2 Adsorption Isotherm

Results obtained in the batch experiments conducted to study the effects of pH indicated that adsorption could play a major role in desorption of products from the metal surface and eventually, in controlling the rate of the reaction. Separate batch experiments were conducted as described in Section 3A.3.4.2 to evaluate the sorptive properties of aniline on Fe^0. Figure 4.3.2 depicts the isotherm at a solution pH of 7.3. Different plots were generated at different pH values. The isotherms plotted are non-linear over the range tested (0-2 mM) and are described by the Langmuir Equation (Langmuir, 1918):

$$C_{ads} = \frac{K_L.C_{aq}}{1+K_L.C_{aq}}(C_{ads})_{max} \qquad (4.3.2)$$

Here C_{ads} and C_{aq} are the concentrations of aniline on Fe^0 and in solution respectively. K_L is the Langmuir constant and $(C_{ads})_{max}$ is the maximum saturation concentration.

A non-linear regression yielded the coefficients, K_L and $(C_{ads})_{max}$, under different conditions of solution pH. In general, at different pH values and under different C_{aq} ranges, the values of K_L and $(C_{ads})_{max}$ were different (data are presented in Table 4.3.2.2) indicating that the behavior was not truly Langmuir in nature. Once the product loss due to adsorption was accounted for, a complete mass balance for nitrobenzene reduction was obtained. The nature of the Langmuir isotherm is consistent with the past literature

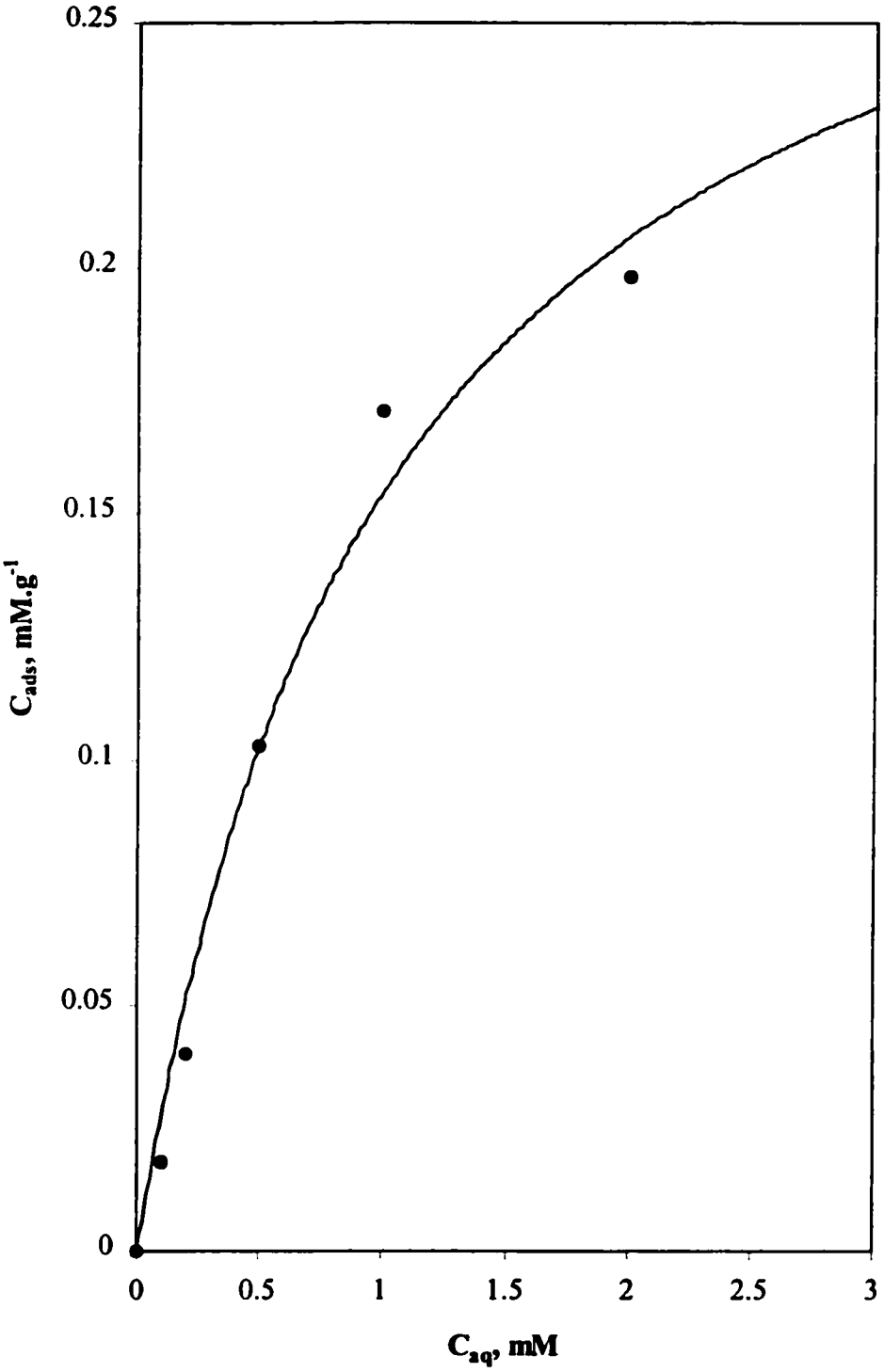

Fig. 4.3.2 Adsorption isotherm for aniline on Iron-I
Batch reactors of 30 mL volume at pH 7.3. 5 mM of Na_2SO_3 was used to make the solutions anoxic. Each batch received 1 g of Iron-I and 0-2 mM authentic aniline. Curve is fit to Eq. 4.3.2 with parameters used in the text.

Table 4.3.2.2 Langmuir isotherm parameters determined from sorption experiments under different solution pH and concentration range

Non-linear regression was performed on the data from Table 4.3.2.1, Appendix C. Constants obtained pertain to the Eq. 4.3.2 for aniline.

pH	K_L $10^4\ M^{-1}$	$(C_{ads})_{max}$ $10^5 mol.g^{-1}$	S	r
6.8	10.000	1.245	0.020	0.996
7.2	13.301	0.564	0.005	0.993
7.3	9.800	0.936	0.012	0.992
8.5	2.500	2.244	0.007	0.988

where,

K_L	Langmuir constant
$(C_{ads})_{max}$	Maximum saturation concentration
S	Standard error
r	Correlation coefficient

(Arnold and Roberts, 2000; Scherer *et al.*, 2000; Wust *et al.*, 1999; Devlin *et al.*, 1998; Agrawal and Tratnyek, 1996; Burris *et al.*, 1995). Agrawal and Tratnyek (1996) did not detect any aniline in the solution, below pH 5, leading them to conclude that the product was adsorbed on to the metal surface. However, sorption constants differ sharply from the results presented by Devlin *et al.* (1998) who reported their sorption constants for a solution pH of 10 (K_L=1.4x10^{-8} M^{-1} and $(C_{ads})_{max}$=0.9 $\mu mol.g^{-1}$). It is expected that at such a high pH, aniline adsorption would be quite low, especially since the pK_a of aniline is around 4.6 and it exists above this pH. Thus, as pH increases beyond its pK_a value, sorption on the metal surface is expected to diminish. Also, the type of iron in their study was different, with particle size of about 0.3 mm, and it was not acid pre-treated. It has been shown (Agrawal and Tratnyek, 1996) that acid wash increased the surface area by a factor of 7.6. Thus, it is expected that the iron used in this study had a lot more sites amenable for aniline adsorption.

4.4 Continuous Column Studies

Preliminary studies with column operations were carried out with NB involving both Iron-I and Iron-II and the parameters optimized. Based on the observations for NB, continuous column studies were later designed and performed for other NACs with Iron-II only.

4.4.1 Volatilization of the aromatic from wastewater

Continuous column operations were run under atmospheric pressure and the feed to the column was pumped from reservoirs open to the atmosphere as per the

experimental protocol developed in Section 4.4. Since NACs are volatile compounds, it was expected that their solutions, over a period of time, would lose the aromatic due to volatilization under normal room temperature and pressure conditions. Hence, the volatilization data for NB were recorded starting with different initial concentrations. The data roughly indicate that the volatilization process could be of first-order. To verify this and to find the rate constant of volatilization, the data were plotted as $\ln(C_0/C)$ *vs.* time as shown in Figure 4.4.1, where C_0 is the initial concentration of nitrobenzene in an open reservoir and C is the concentration measured at any time. The plot is a straight line indicating that the volatilization phenomenon was a first-order process. The slope of the line, which was found by least-squares technique, gave the rate constant of 0.0034 h^{-1} with an $R^2 = 0.9998$. This is equivalent to a loss of about 8% of nitrobenzene over a 24-hour period due to volatilization from the feed reservoir. This was accounted for while calculating the rates of formation of aniline in the reduction step.

4.4.2 Packed bed porosity

It is necessary to estimate the bulk porosity of the packed bed before the continuous column experiments are performed, so that number of pore volumes over the operating lifetime of a column can be estimated. The bulk of the work was done using Iron-II in the columns. Hence, data were collected for this type of iron only. Porosity data are relegated to Appendix C, Table 4.4.2. These were utilized in calculation of pore volume, which was 22.3 mL.

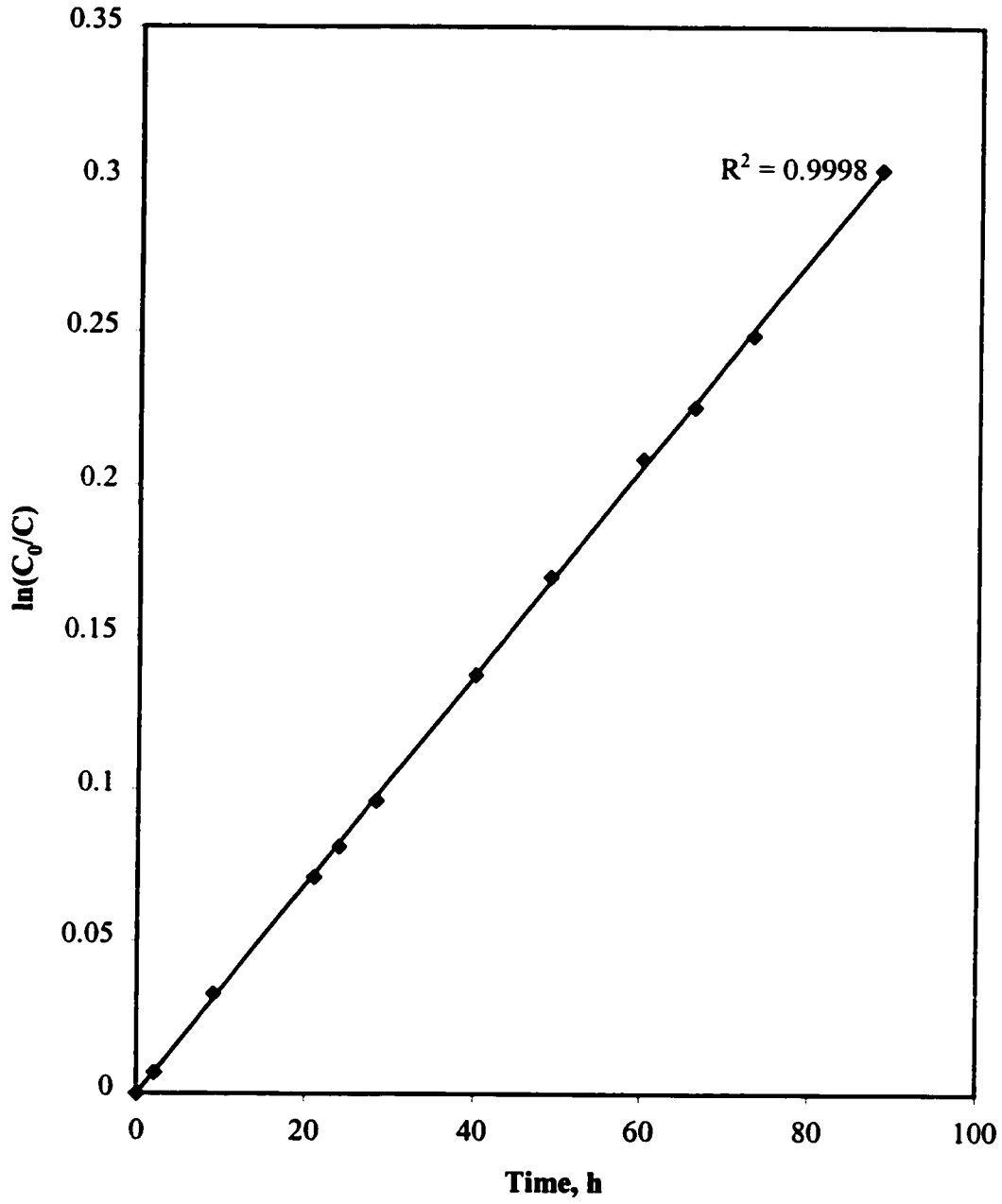

Fig. 4.4.1 Rate of volatilization of nitrobenzene from aqueous solution
The change in concentration of nitrobenzene in the open feed reservoirs, of the type used in continuous operations, due to volatilization to atmosphere was followed as a function of time, starting with an initial concentration of 2.18 mM of NB.

4.4.3 Effect of pH

The overall process of corrosion in anaerobic Fe^0-H_2O systems may be depicted by the following reactions (Agrawal and Tratnyek, 1996):

$$Fe^0 + 2H^+ \rightarrow Fe^{2+} + H_2 \qquad (4.4.3.1)$$

$$Fe^0 + 2H_2O \rightarrow Fe^{2+} + H_2 + 2OH^- \qquad (4.4.3.2)$$

Early experiments in batch reactors resulted in the expected pH rise of nearly 2 units due to aqueous corrosion of the metal (Eq 4.4.3.2). However, the same effect was not observed in the continuous flow system. Continuous-flow studies were conducted with different influent solution pH. The conversion data are shown in Figures 4.4.3.1-4.4.3.4. The effluent pH was more or less comparable to the inlet solution pH, except when the influent solution pH was less than neutral, in which case the effluent pH got closer to neutral pH. And, for the situation where the influent pH was 8.5, the effluent pH was between 8.5-8.7. Also, there was a general lack of dependency of conversion on pH as found by Agrawal and Tratnyek (1996). Hence, most of the column studies were conducted at pH of about 7-7.5.

4.4.4 Effect of sorption of aniline on Fe^0 bed

It can be seen from the preceding figures that it took several hours to reach the 100% conversion level. This was due both to the time required to flush out the original solution and to saturate the available sites during sorption of aniline on to the Fe^0 bed. However, once the sites were saturated, complete product recovery was obtained and persisted until the column became clogged. It was shown by Burris *et al.* (1996) that in a continuous flow-through system, the extent of reaction was not affected by sorption on

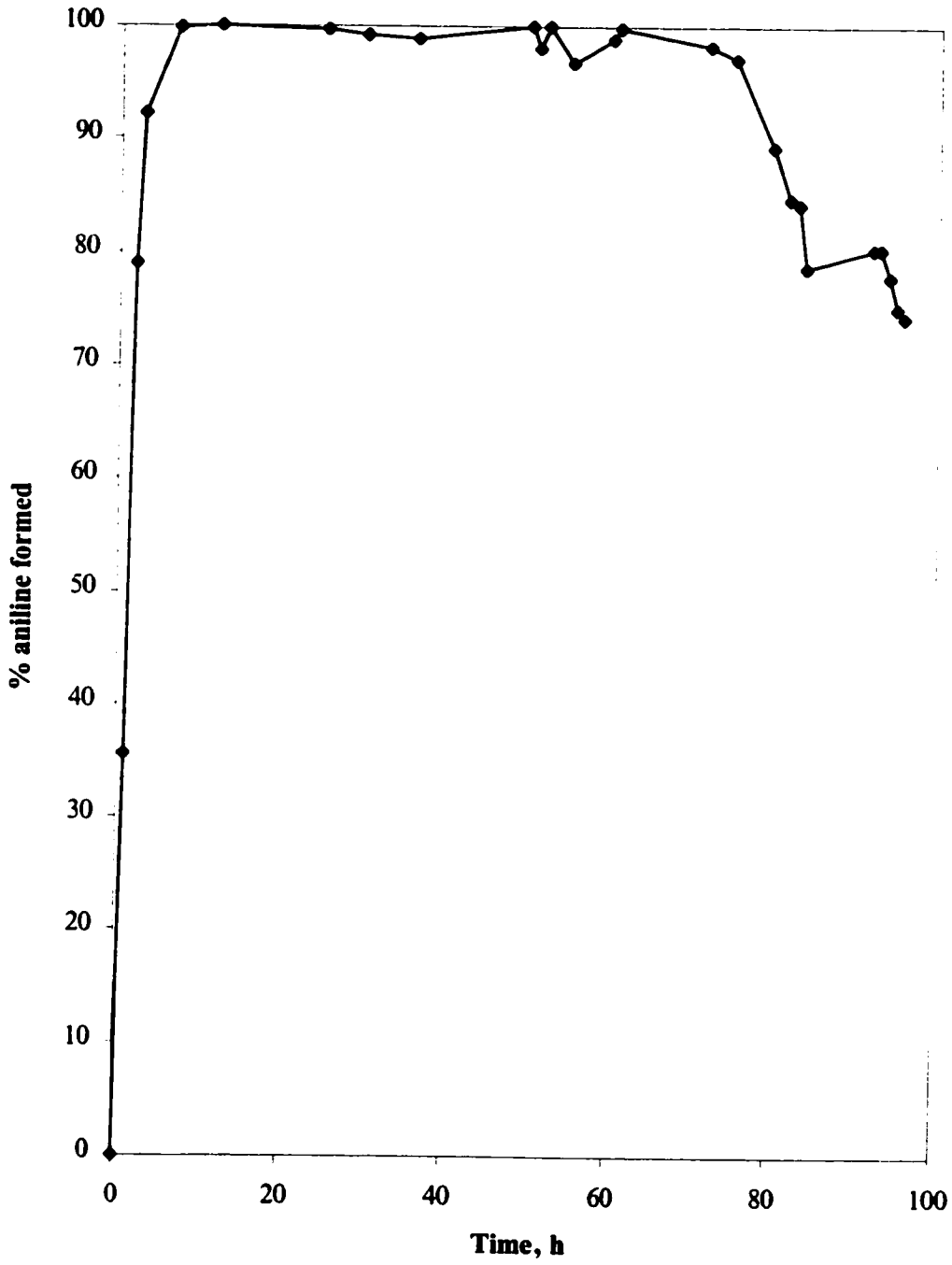

Fig. 4.4.3.1 Reduction of nitrobenzene to aniline at an influent pH of 5.0
Continuous column operations in a 15x300 mm column, with 200 g of Iron-II at a flow rate of 3.1 mL/min. Influent concentration of NB was 1 mM. 1 mM of Na_2SO_3 was included in the solution to make it anoxic. Effluent pH was between 7.1 and 7.3.

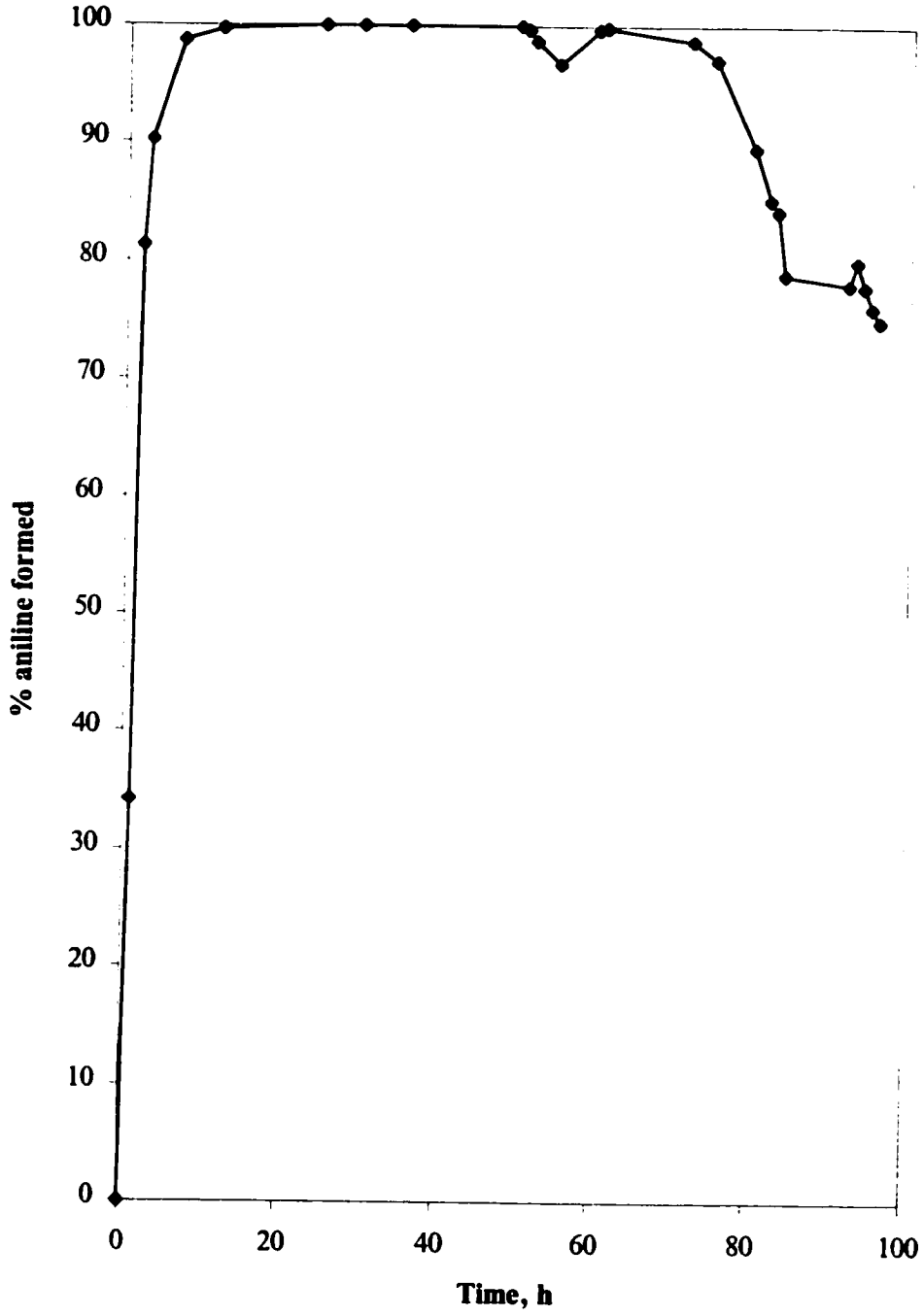

Fig. 4.4.3.2 Reduction of nitrobenzene to aniline at an influent pH of 6.5
Continuous column operations in a 15x300 mm column, with 200 g of Iron-II at a flow rate of 3.1 mL/min. Influent concentration of NB was 1 mM. 1 mM of Na_2SO_3 was included in the solution to make it anoxic. Effluent pH was between 7.4 and 7.6.

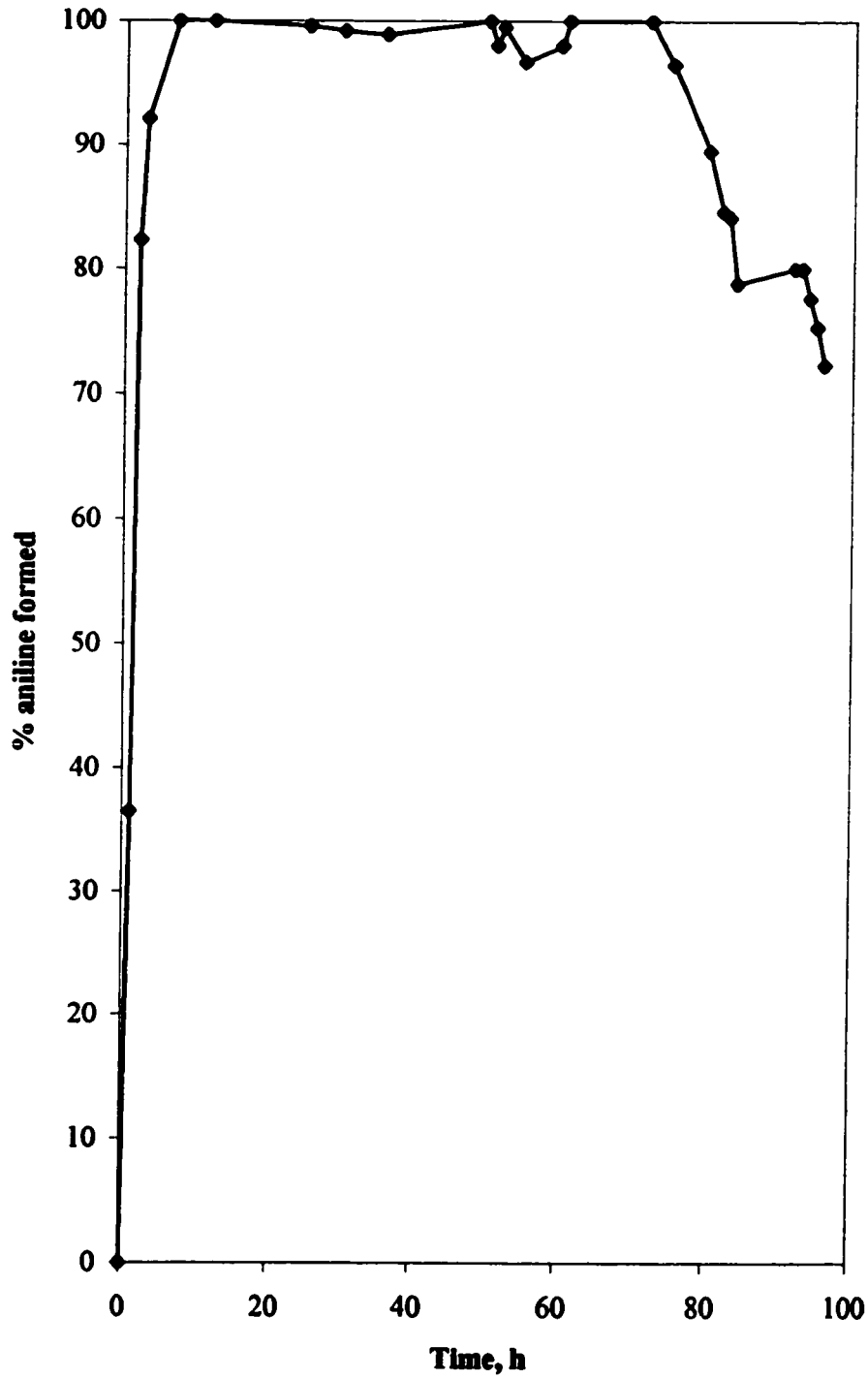

Fig. 4.4.3.3 Reduction of nitrobenzene to aniline at an influent pH of 7.4 Continuous column operations in a 15x300 mm column, with 200 g of Iron-II at a flow rate of 3.1 mL/min. Influent concentration of NB was 1 mM. 1 mM of Na_2SO_3 was included in the solution to make it anoxic. Effluent pH was between 7.4 and 7.6.

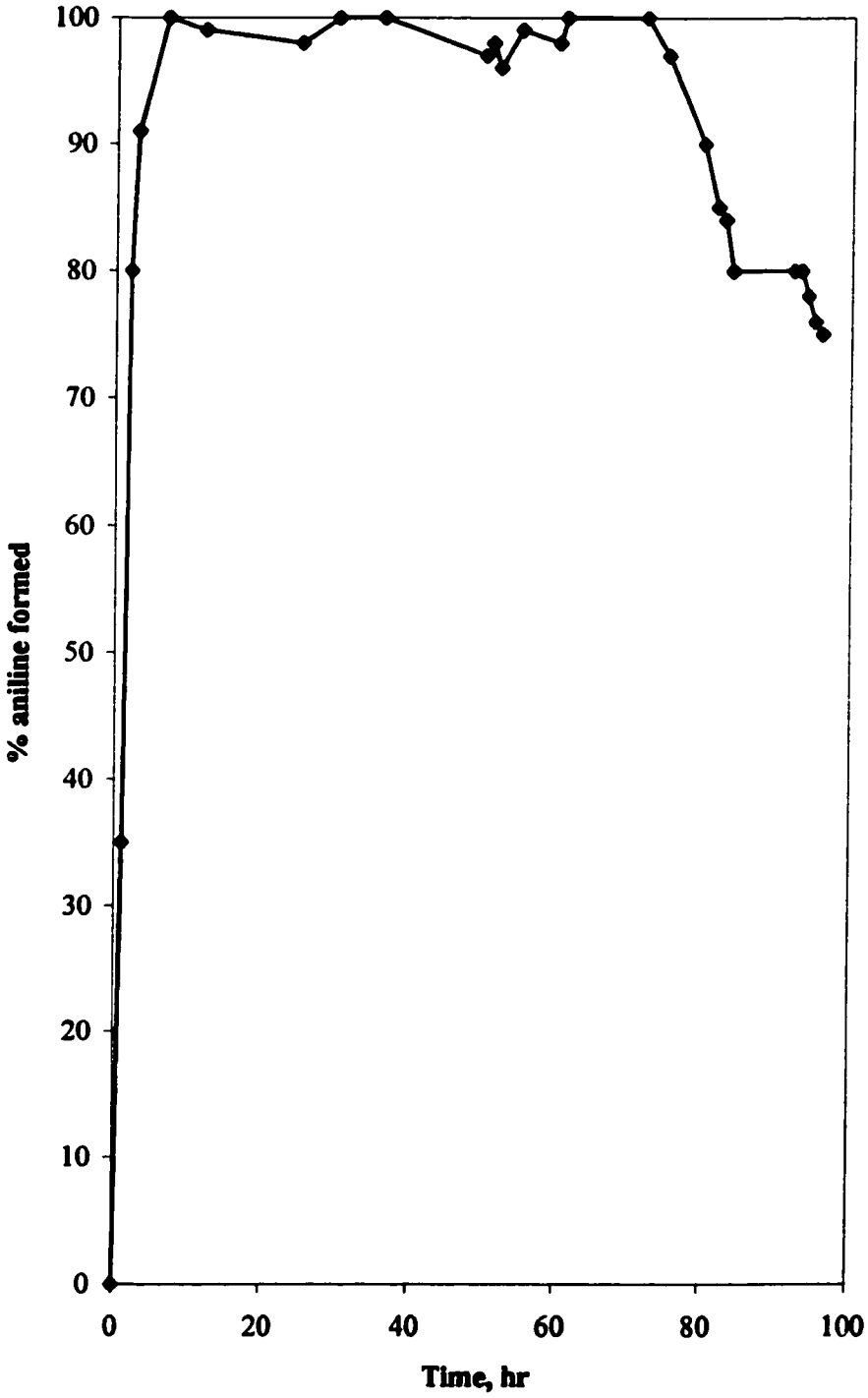

Fig. 4.4.3.4 Reduction of nitrobenzene to aniline at an influent pH of 8.5 Continuous column operations in a 15x300 mm column, with 200 g of Iron-II at a flow rate of 3.1 mL/min. Influent concentration of NB was 1 mM. 1 mM of Na_2SO_3 was included in the solution to make it anoxic. Effluent pH was between 8.5 and 8.7.

non-reactive sites under steady-state conditions. Also, since Iron-II had lower surface area per unit mass as compared to Iron-I (actual surface areas were not measured), the sorption over the former iron was expected to be lower.

4.4.5 Continuous Column Studies with other NACs

Conversion *vs.* time plots for the three nitrotoluenes show a similar trend, Figure 4.4.5, indicating that conversion and adsorption of each of the nitroaromatics was the same, reaching saturation at about the same time. Irrespective of the NAC used, the Fe^0 column completely reduced 1 mM of NAC. The Fe^0 column was operated continuously for more than 18 months and was found to perform exactly the same way after each regeneration.

4.4.6 Iron (Fe^0) corrosion products

A 200 g Fe^0 (Iron-II) bed completely converted 1 mM of nitrobenzene flowing upward at 3.1mL/ min for almost 72 hours on a continuous basis. However, the operation had to be discontinued at this point due to formation of a dark green-black precipitate (corrosion products) at the influent end of the column. The zone of the precipitates had risen to almost one-third of the bed height. Fig. 4.4.6.1 shows the change in height of the precipitate front from the influent end of the column with time. It is a linear relationship suggesting that the rate of formation of corrosion products is directly proportional to the duration of the conversion reaction. Linear regression of the data yielded the following equation for corrosion reaction ($R^2 = 0.997$):

$$\text{Height} = 0.88\text{Time} \qquad (4.4.6.1)$$

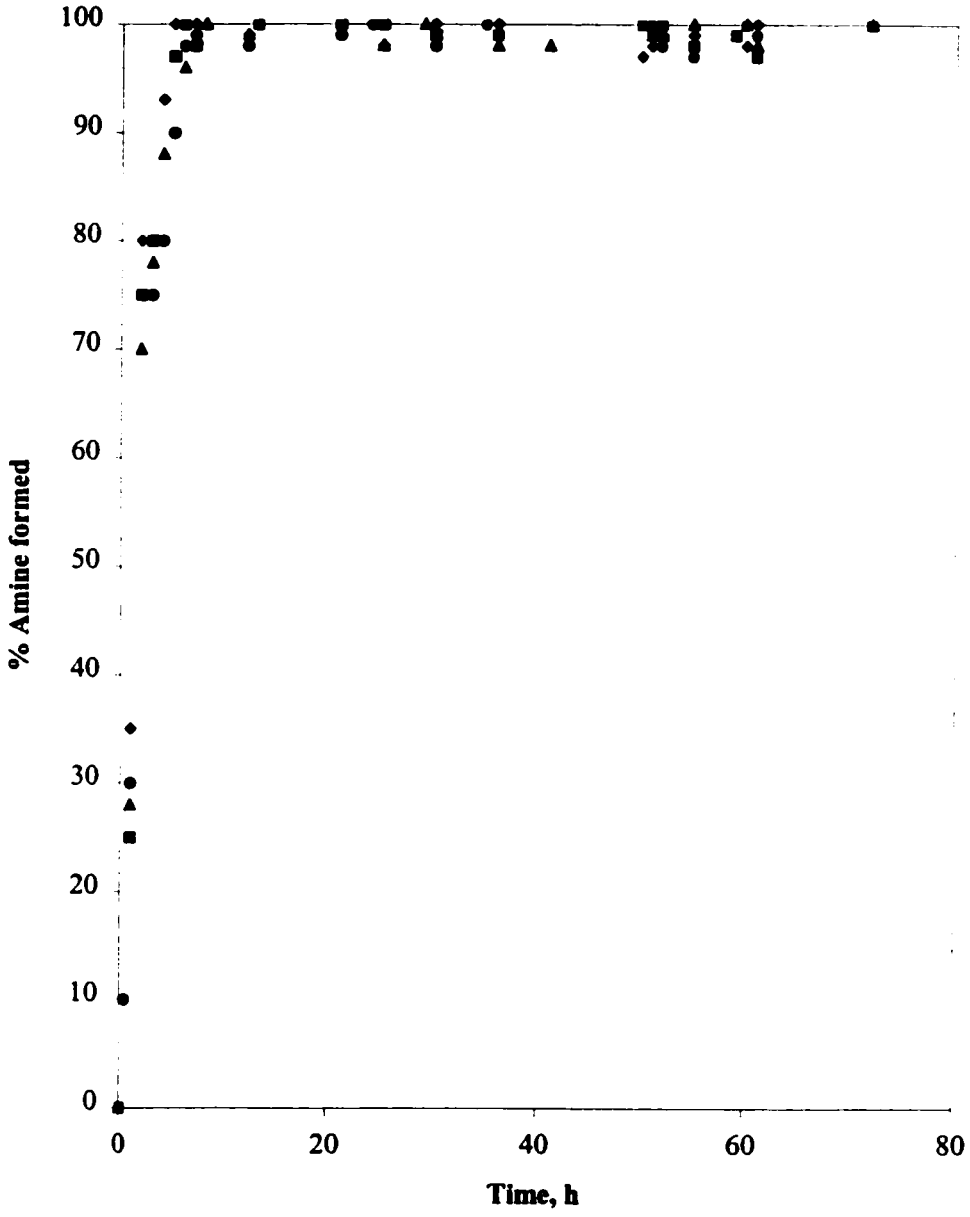

Fig. 4.4.5 Reduction of NAC to the corresponding aniline
Continuous column operations in a 15x300 mm column, with 200 g of Iron-II at a flow rate of 3.1 mL/min. 1 mM of Na_2SO_3 was included in the solution to make it anoxic. Influent pH was 7.2-7.4, while the effluent pH was 7.3-7.5. Influent concentration of each NAC was 1 mM: nitrobenzene, ◆; *o*-nitrotoluene, ■; *m*-nitrotoluene, ▲; *p*-nitrotoluene, ●.

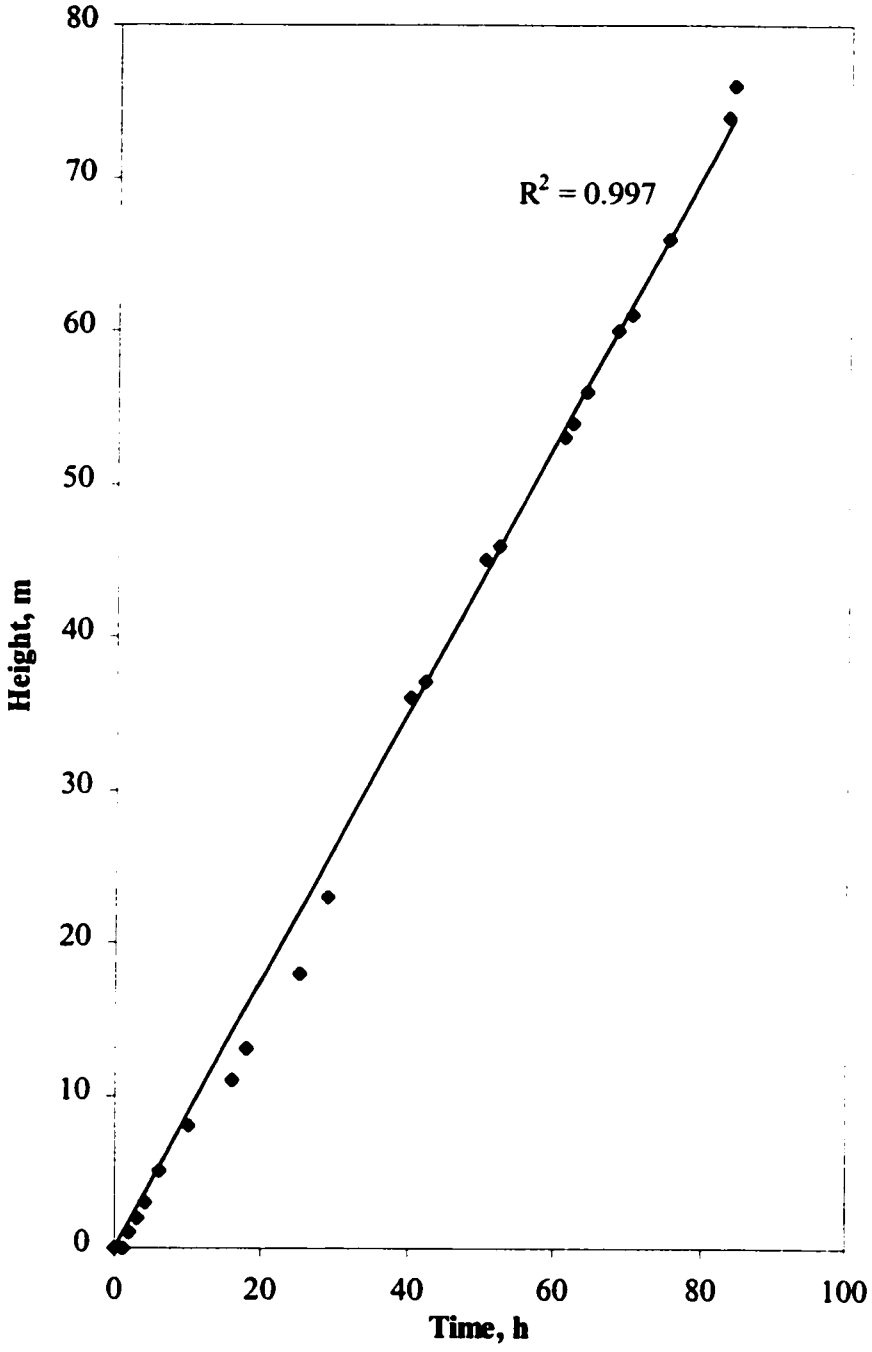

Fig. 4.4.6.1 Change in height of precipitate front from influent end of the column Continuous column operations in a 15x300 mm column, with 200 g of Iron-II at a flow rate of 3.1 mL/min. Influent concentration of NB was 1 mM. Influent pH was 7.4 and effluent pH was 7.5-7.6.

Corrosion of the metal in anaerobic aqueous media, in absence of the nitroaromatic compound, was too slow to be a significant contributor to material damage by corrosion as observed in a control experiment where the feed had no nitrobenzene.

The flow rate also dropped drastically (3-fold) due to clogging by corrosion products. Influent flow rate data are plotted as a function of time in Fig. 4.4.6.2. A third-degree polynomial was fit to the data. The equation is shown below ($R^2 = 0.991$):

$$\text{Flow rate} = -6\text{x}10^{-6}t^3 + 0.0002t^2 - 0.028t + 3.1 \qquad (4.4.6.2)$$

where, t represents time and flow rate is in mL/min.

From the Figure 4.4.6.2 it is obvious that initial formation of corrosion products does not really hinder the flow rate of influent solution. However, with passage of time and further formation of corrosion products, effect of clogging is obvious. After about 50 h of operation, the flow rate dropped to about 2.8 mL/min from an original 3.1 mL/min. However, after 80 h of operation, there was about a 3-fold drop in the flow rate. These results are consistent with previous studies that indicated plugging and porosity reduction as a result of precipitation of corrosion products (Gu *et al.*, 1999).

It is known that the first corrosion product of Fe^0 under anaerobic conditions is $Fe(OH)_2$, which may be further oxidized to magnetite Fe_3O_4 (Cornell and Schwertmann, 1996 and Farrell *et al.*, 2000). Prior to the formation of magnetite, mixed-valent Fe(II)+Fe(III) salts, known as green rusts, may form under neutral pH conditions (Cornell and Schwertmann, 1996, Gu *et al.*, 1999 and Farrell *et al.*, 2000). The oxidation of mixed-valent salts commonly leads to the formation of maghemite (γ-Fe_2O_3) (Cornell and Schwertmann, 1996).

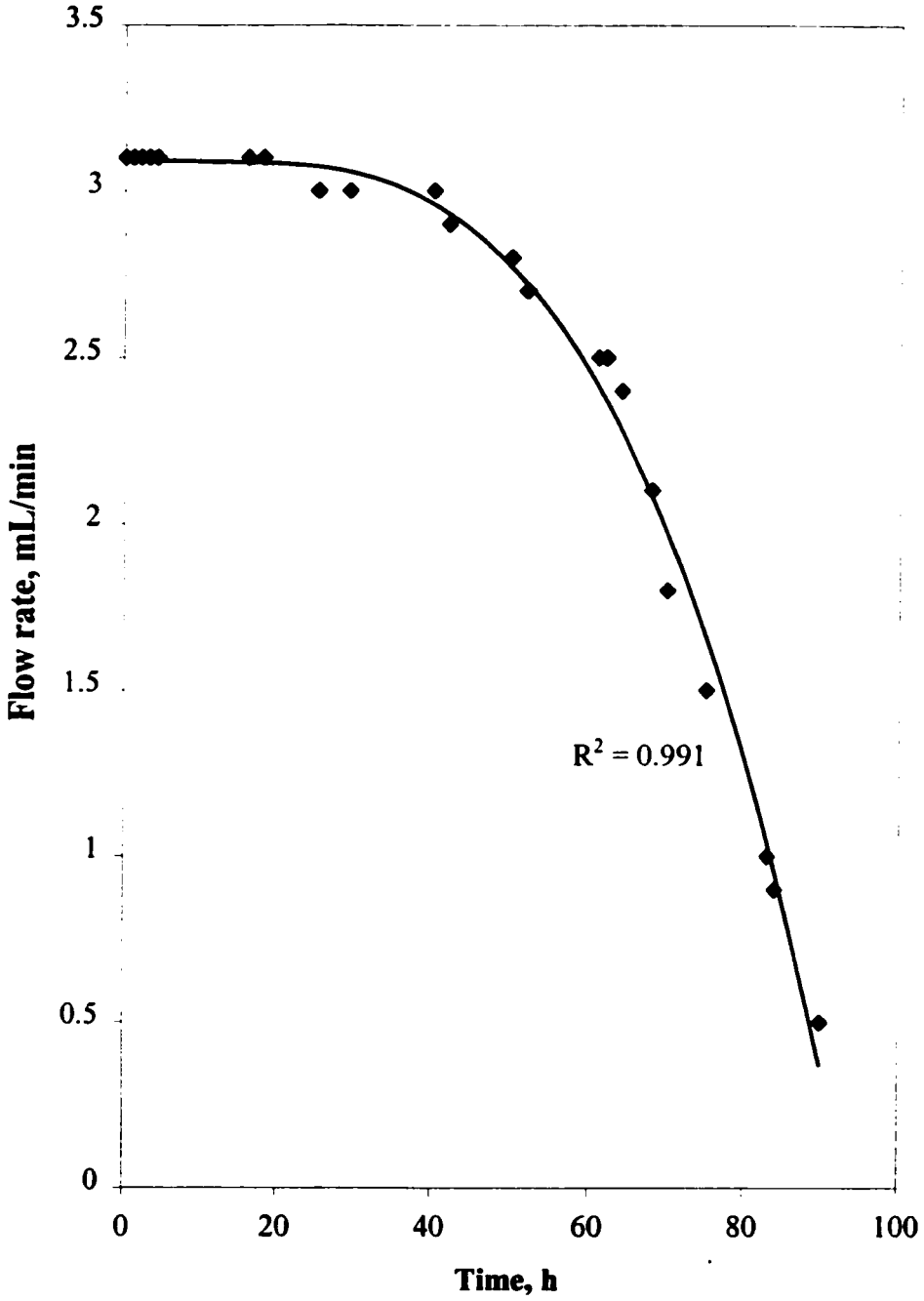

Fig. 4.4.6.2 Change in flow-rate due to clogging
Continuous column operations in a 15x300 mm column, with 200 g of Iron-II at a flow rate of 3.1 mL/min. Influent concentration of NB was 1 mM. 1 mM of Na_2SO_3 was included in the solution to make it anoxic. Influent pH was 7.4 and effluent pH was 7.5-7.6. Curve is fit to a 3rd degree polynomial.

Energy-dispersive X-ray spectrometry (EDS) analysis of N_2-dried iron filings, taken from the inlet end of the column, indicated the presence of only Fe and O (Fig. 4.4.6.3). Also, X-ray diffraction analyses of the same filings confirmed that they were coated with maghemite, which could only have formed by oxidation of the corrosion product magnetite. The corrosion products in this study were similar to those reported in the literature (Gu *et al.*, 1999 and Farrell *et al.*, 2000).

There is a net dissolution of Fe^0 following the reduction reaction (Eq 4.4, page 48). Analysis of the effluent stream and the precipitates was done by the direct coupling plasma (DCP) technique. The analyses showed that Fe was present both in the effluent stream, 0.667 g and in the precipitates, 1.44 g. DCP results indicated that, although 68% of the corrosion products had precipitated in the column itself, the effluent stream still contained corrosion products above the detection limit (concentration of the corrosion products was about 0.05 g/L). From the flow rate equation, Eq. 4.4.6.2, we notice that the total flow of aqueous solution of nitrobenzene can be integrated for a time period of 72 h, which is 8112 mL. Stoichiometric amount of Fe^0 dissolved, based on this total flow of the nitrobenzene aqueous solution, turns out to be 1.36g, which is 35% less than what was found by the DCP analyses of effluent water and precipitates in the column. It is possible that, while physically dislodging precipitates from the column, some of the zero-valent iron itself might have disengaged and fallen into the beaker, thus over-predicting the DCP result. All the above calculations are shown in Appendices A1 and A2.

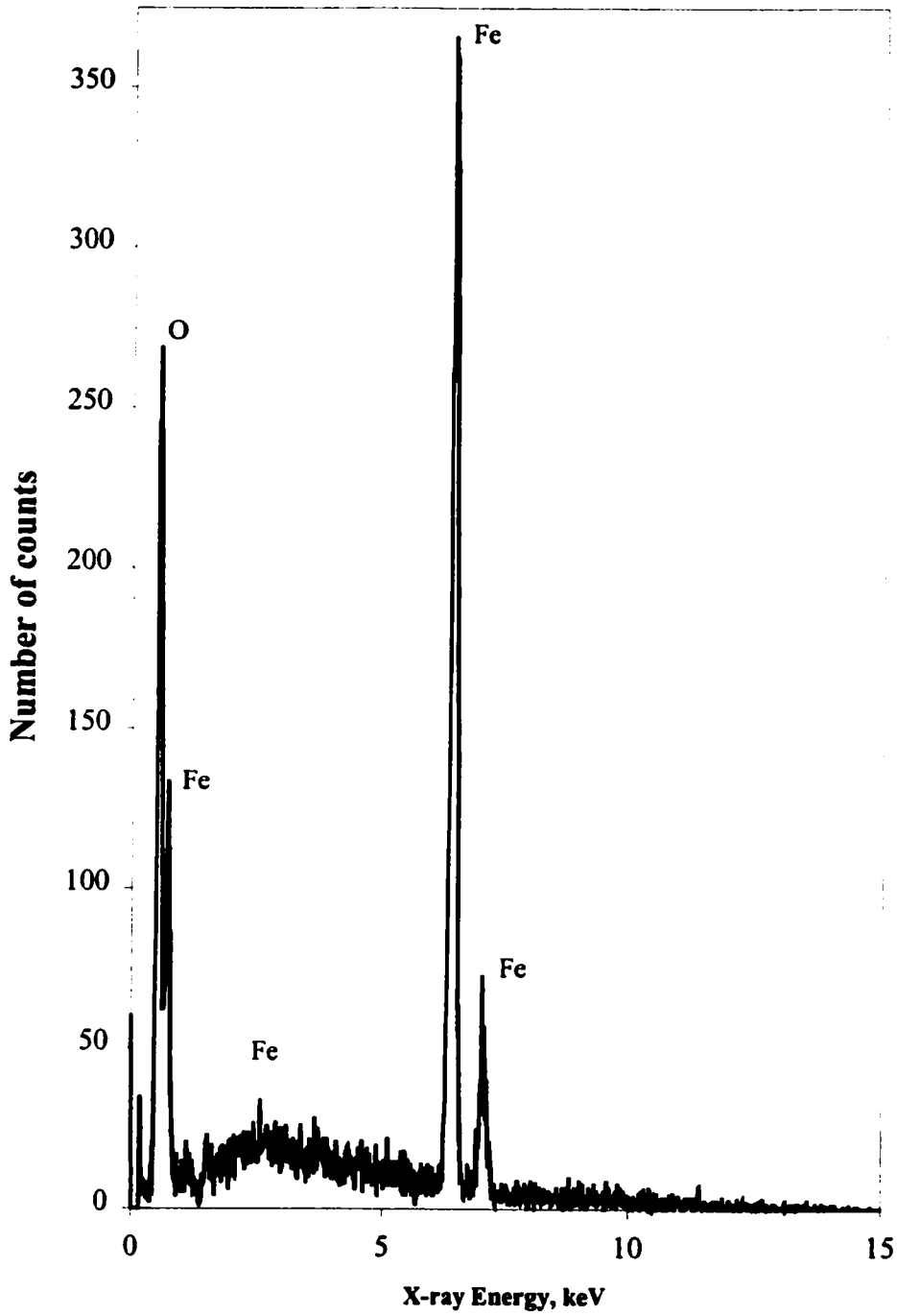

Fig. 4.4.6.3 Energy-dispersive X-ray spectrometry (EDS) analysis of Fe filings
N_2-dried iron filings, taken from the inlet end of the column at the end of operation after 72 h and 600 pore-volumes.

4.4.7 Cleaning of Fe^0 bed

It can be seen that over a reaction period of 72 h, approximately 600 pore-volumes, net Fe^0 dissolved would be 1.36 g based on stoichiometry. Owing to the formation of magnetite and maghemite over the zero-valent iron bed, clogging reduces the efficiency of the reduction reaction considerably. However, the oxides and hydroxides of iron are readily soluble in acid solutions (Cornell and Schwertmann, 1996). Hence, the clogged bed could be back-washed using dilute acid solutions to comprehensively remove the surface hydr(oxides), freeing the metal bed, readying it for another reduction cycle.

These precipitates were removed by using 1.2 M HCl to clean the bed. Similar procedure, as stated in Section 3A.3.3, was followed to remove the precipitates from the metal bed. Preliminary studies indicated that a more dilute acid could not remove the precipitates completely. It was found that the same bed could be used again and again with the same efficiency as before, once it was cleaned.

4.4.8 Fate of $CoCl_2$ and Na_2SO_3

DCP analyses were done on the effluent to ascertain the fate of $CoCl_2.6H_2O$ being added as a catalyst to scavenge O_2 in the feed. Analyses indicated that most of the cobalt (as total Co) was plated out in the Fe^0 column itself. From an initial 126 μg/L of $CoCl_2.6H_2O$ (31.2 μg/L as Co) in the feed, only 1.96 μg/L of Co could be detected in the effluent stream. It might be speculated that in this deposition a bimetallic zero-valent metal phase was created. However, a bimetallic bed of the Co/Fe system was ruled out as the effective agent, since even with 100% Co plating out in the bed it would amount to

only an additional 2 ppm in the Fe^0 bed over the 600 pore-volume operating lifetime. Researchers have used between 200-500 ppm of metal doping to achieve bimetallic systems (Kim and Carraway, 2000 and Liang *et al.*, 1997).

An optimum value of 1mM of Na_2SO_3 as O_2 scavenger has been used in this study. This is equivalent to 126 mg/L. At this level of addition, both Na^{2+} and SO_4^{2-} (since SO_3^{2-} either gets oxidized in the feed or upon elution from the column by atmospheric O_2) are not a problem. They are within the accepted levels of discharge, even from a drinking water point of view.

STAGE 2 Enzymatic reaction of amines

4.5.1 Extraction of enzyme soybean peroxidase

Details of extraction of SBP are reported by Biswas (1999). For a continuous-flow system to be feasible, it is necessary that the enzyme be stable at room temperature and not lose activity. Activity measurements done with SBP, stored in two different bottles at 4°C and at room temperature (18-20°C), are plotted as a function of time in Figure 4.5.1.

It can be seen that at room temperature the loss in activity of the enzyme is faster as compared with the enzyme sample stored at 4°C. Hence, for continuous-flow experiments, the enzyme solution added to the influent was changed periodically, before the drop in activity became significant. It is conjectured that the significant decrease in the activity of enzyme was due to microbial activity. Enzymes are protein molecules and possibly were degraded by microbes prcsent in the enzyme preparation. Attempts to filter the enzyme preparation by syringe filters (0.2 microns) failed due to clogging.

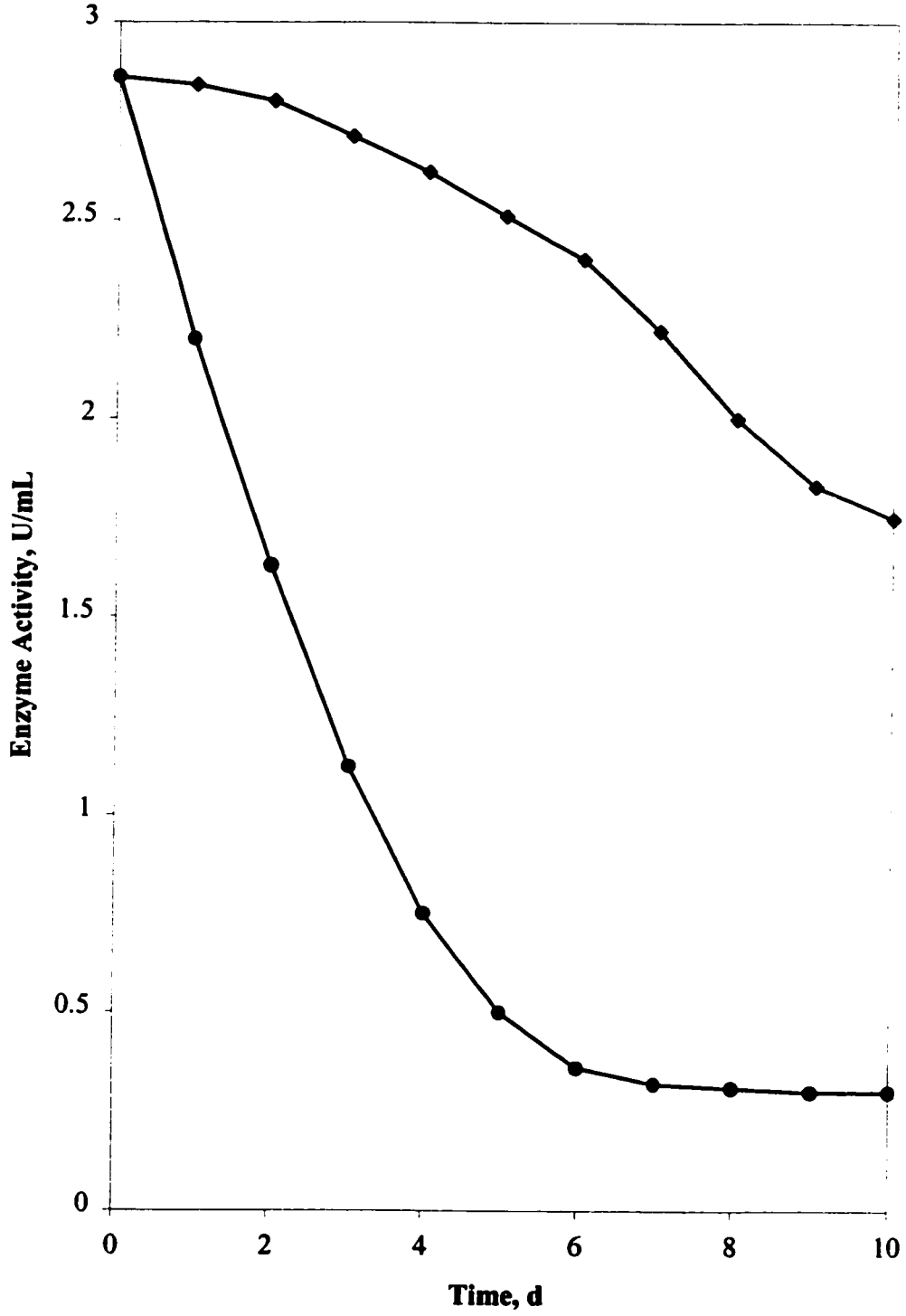

Fig. 4.5.1 Change in enzyme activity with time
Activity measurements done with crude enzyme SBP stored at two different temperatures: 4°C, ◆; 18-20 °C, ●.

4.5.2 Enzymatic treatment of pure anilines in batch reactors

NACs after passing through the zero-valent iron column would be reduced to their corresponding anilines. Four different NACs were used in this study: nitrobenzene, *o*-, *m*- and *p*-nitrotoluenes, which on reduction would yield aniline, *o*-, *m*- and *p*-toluidines respectively. Thus, before running the enzymatic step in conjunction with the zero-valent iron reduction, it was necessary to optimize the various parameters that could affect the enzymatic treatment process. Analytical grade aniline, *o*-, *m*- and *p*-toluidines were utilized to optimize various parameters e.g., PEG, pH, enzyme concentration, hydrogen peroxide to substrate ratio and alum concentration.

4.5.2.1 Effectiveness of PEG as an additive

Previous studies with phenols indicated that PEG had a protective effect on the activity of enzyme (Wu, J *et al.*, 1993 and Wu, Y. *et al.*, 1997). A series of batch experiments were carried out to test the effectiveness of PEG, at 0-800 mg/L concentration, as an additive to protect the enzyme from losing its activity. The data are plotted in Figure 4.5.2.1. It can be seen that PEG, in all concentrations, had no impact either on the removal efficiency or on the savings on enzyme concentration. The variation in removal signifies no trend and is purely statistical. Hence, PEG was not used in further studies.

4.5.2.2 pH effect

The activity of enzyme is dependent on pH, with each enzyme possessing an optimum pH. Enzymes very often function only when certain ionizable side chains are in

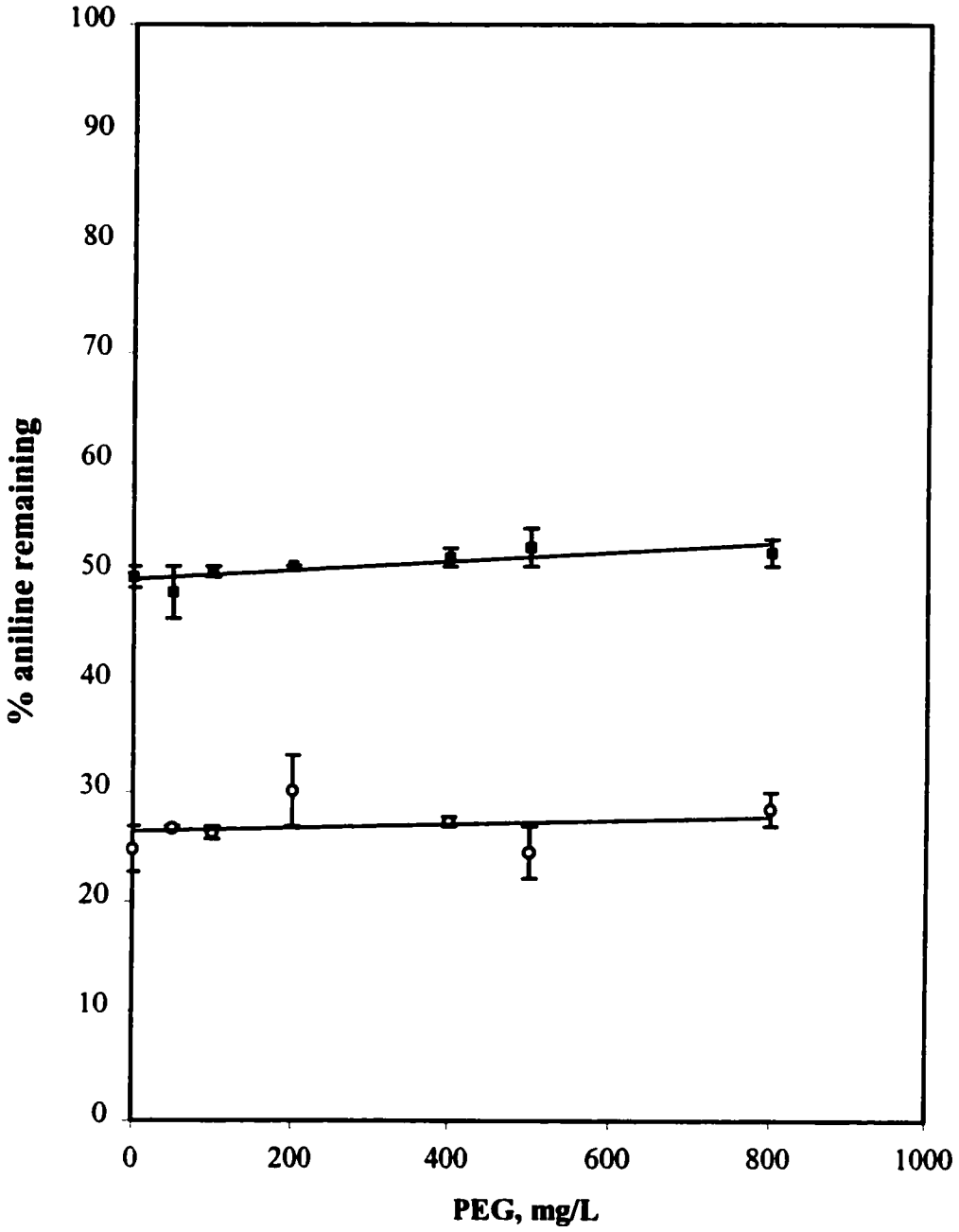

Fig. 4.5.2.1 Effect of PEG on removal of aniline

Batch reactors of 30 mL volume, initially contained 1 mM aniline, 1.5 mM H_2O_2, at a solution pH of 6.9-7.1. At the end of reaction time of 3 h, catalase, at a final concentration of 125 U/mL, was added to stop the reaction. Alum, at a final concentration of 50 mg/L, was added to help settle the contents by gravity under the following conditions of SBP concentration: 0.18 U/mL, o; 0.11 U/mL, .

a specific form. It is known that the characteristics of the ionizable side chains of amino acids depend on pH. Since, enzymes are amino acid polymers, their activity is expected to depend on pH. Usually, the activity of an enzyme is at its peak at a certain pH and any change in pH, to either higher or lower values, causes significant lowering of the activity. Besides, the crude preparation of SBP has other constituents that could interfere with the optimum value of pH. Therefore, exploration into the effect of pH on the activity of crude SBP was required to define the pH range over which it could function optimally.

These experiments were designed so as to have only SBP concentration as the limiting constituent (stringent conditions) in the reaction solution so that the effect of pH would be clearly manifested. The pH range considered in this study was between 4 and 10. A fixed H_2O_2 to substrate ratio of 1.5 was employed. Reaction time of 3 h was considered to be sufficient for the reaction to go to completion (Klibanov *et al.*, 1980). Results for aniline, *o*- *m*- and *p*-toluidines are shown in Figures 4.5.2.2.1-4.5.2.2.4. They all show a broad range of effective pH, with the optimum conditions obtained from pH 4-8. This is useful since treatment of wastewater is commonly carried near the neutral pH.

4.5.2.3 H_2O_2 to Substrate ratio

Peroxidases can exhibit both catalase and peroxidase activities depending on the conditions of the reaction (Ramelmeier and Blanch, 1988). Biswas (1999) indicated that the crude SBP had significant peroxide demand possibly due to catalase activity. Experiments were performed to determine the effect of the initial $[H_2O_2]$/[amine] on the removal efficiency of the amine. The results are presented in Figures 4.5.2.3.1-4.5.2.3.4 for aniline and the three toluidines. The results indicate that the removal efficiency

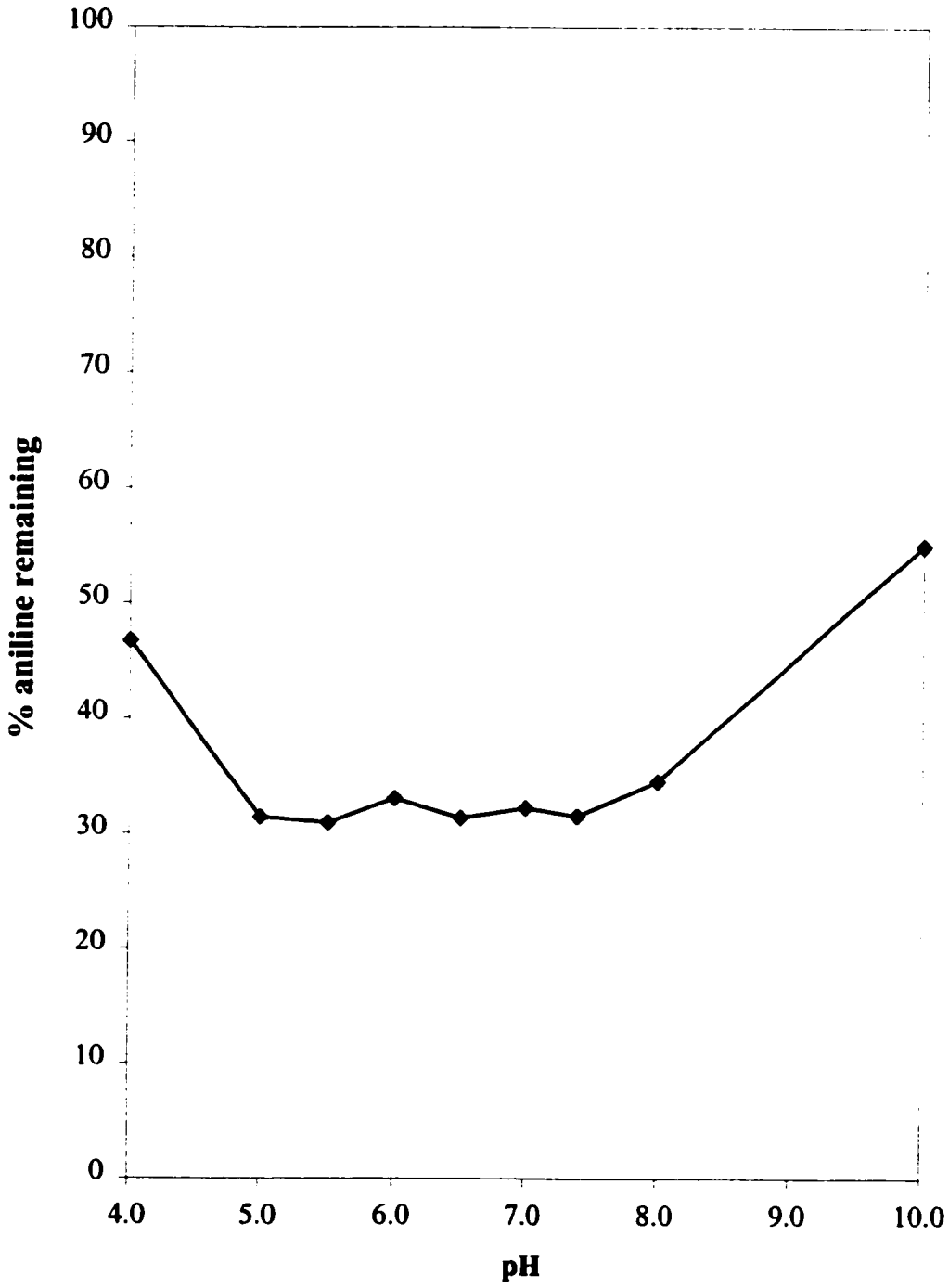

Fig. 4.5.2.2.1 pH optimization for removal of aniline
Batch reactors of 30 mL volume, initially contained 1 mM aniline, 1.5 mM H_2O_2 and 0.17 U/mL of SBP. At the end of reaction time of 3 h, catalase, at a final concentration of 125 U/mL, was added to stop the reaction. Alum, at a final concentration of 50 mg/L, was added to help settle the contents by gravity.

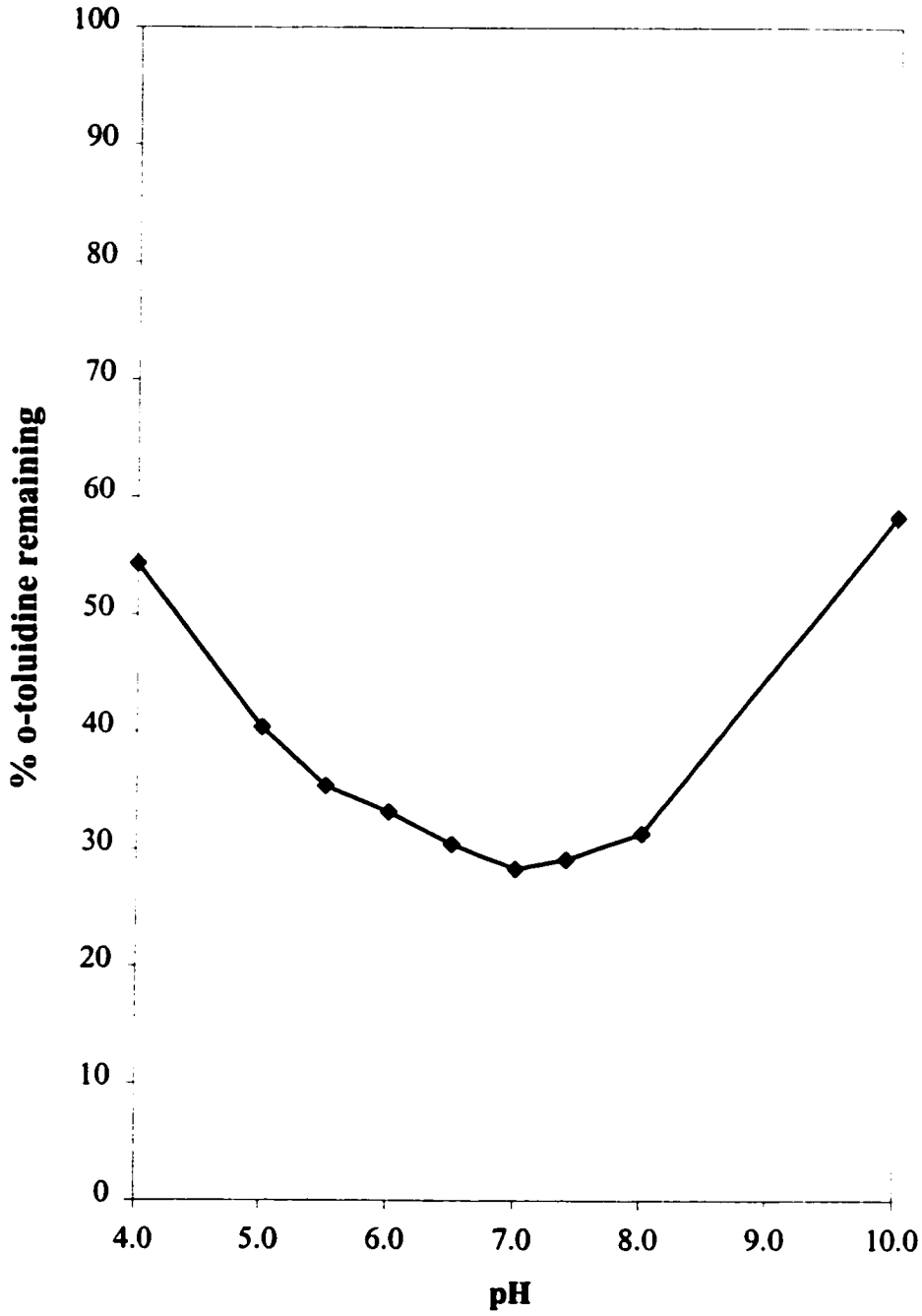

Fig. 4.5.2.2.2 pH optimization for removal of *o*-toluidine
Batch reactors of 30 mL volume, initially contained 1 mM *o*-toluidine, 1.5 mM H_2O_2 and 0.20 U/mL of SBP. At the end of reaction time of 3 h, catalase, at a final concentration of 125 U/mL, was added to stop the reaction. Alum, at a final concentration of 50 mg/L, was added to help settle the contents by gravity.

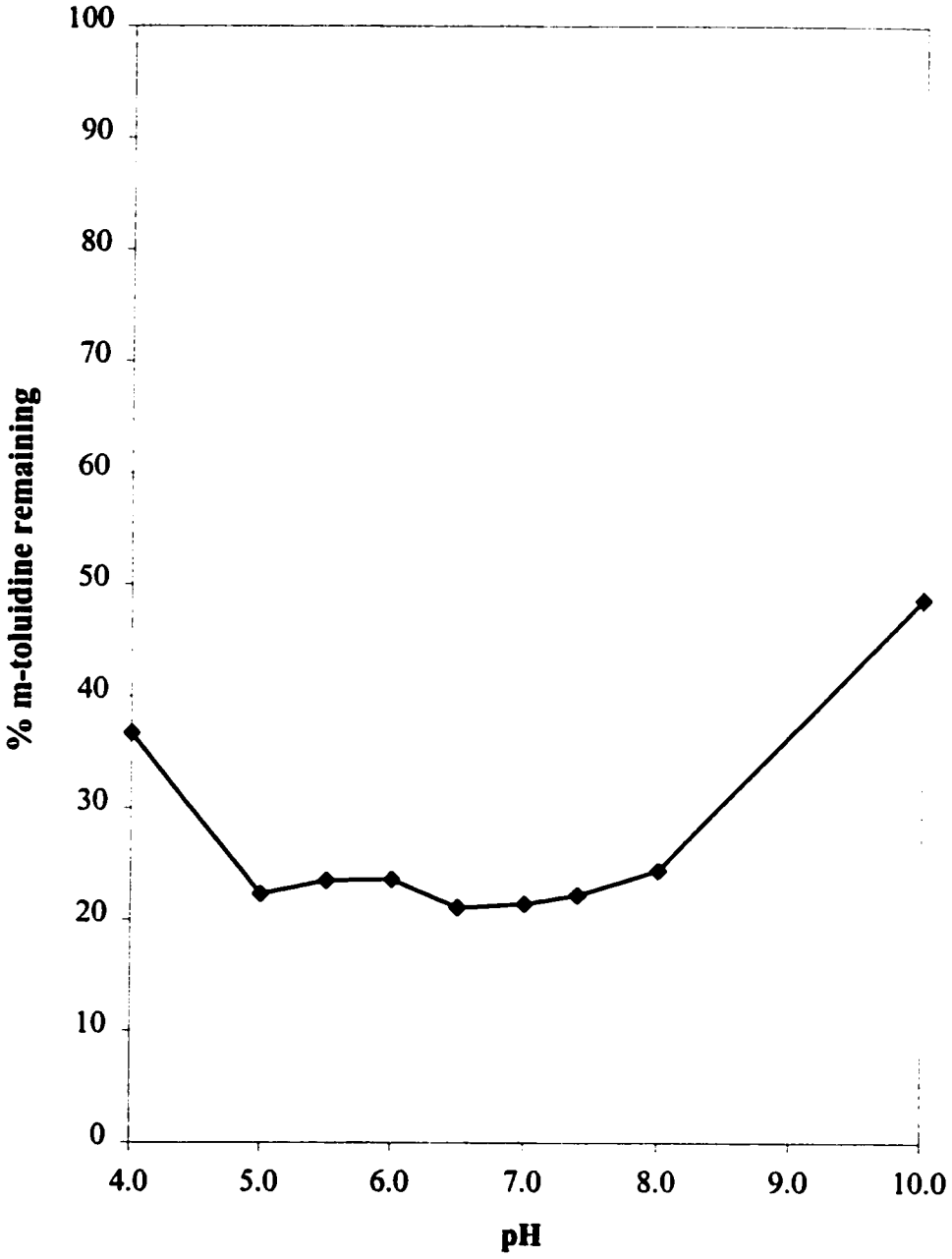

Fig. 4.5.2.2.3 pH optimization for removal of *m*-toluidine
Batch reactors of 30 mL volume, initially contained 1 mM *m*-toluidine, 1.5 mM H_2O_2 and 0.10 U/mL of SBP. At the end of reaction time of 3 h, catalase, at a final concentration of 125 U/mL, was added to stop the reaction. Alum, at a final concentration of 50 mg/L, was added to help settle the contents by gravity.

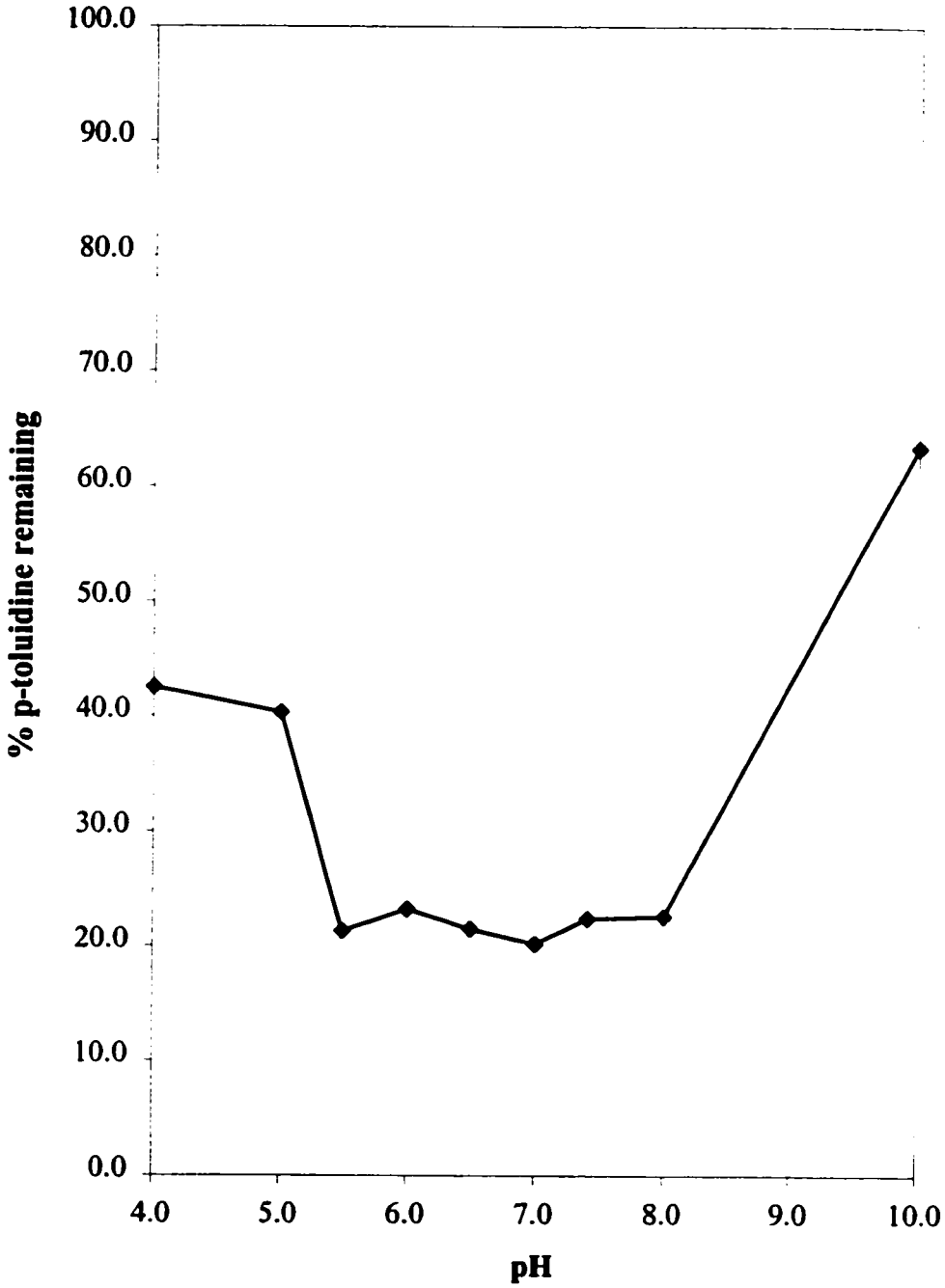

Fig. 4.5.2.2.4 pH optimization for removal of *p*-toluidine
Batch reactors of 30 mL volume, initially contained 1 mM *p*-toluidine, 1.5 mM H_2O_2 and 0.01 U/mL of SBP. At the end of reaction time of 3 h, catalase, at a final concentration of 125 U/mL, was added to stop the reaction. Alum, at a final concentration of 50 mg/L, was added to help settle the contents by gravity.

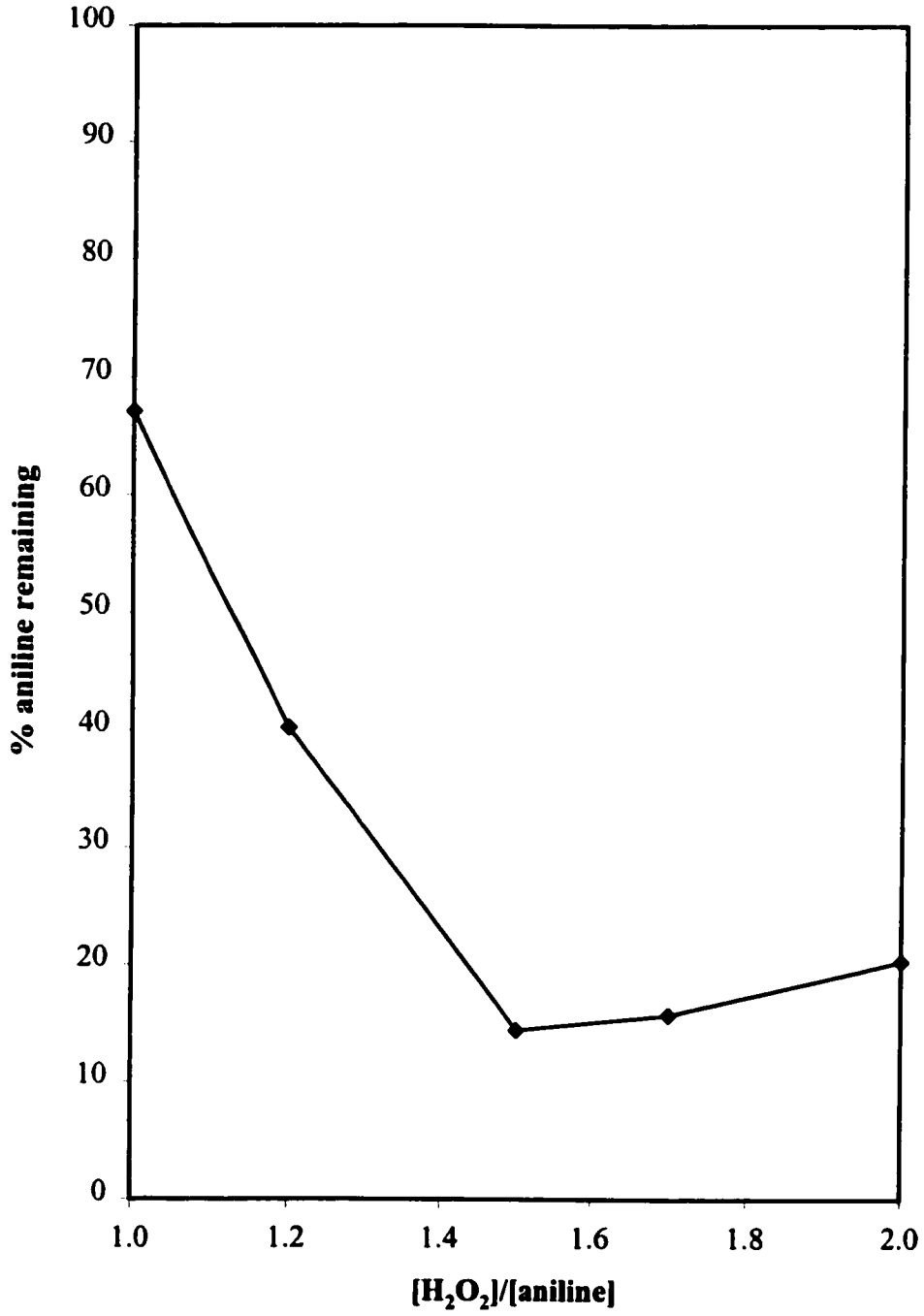

Fig. 4.5.2.3.1 H_2O_2 optimization for removal of aniline
Batch reactors of 30 mL volume, initially contained 1 mM aniline and 0.20 U/mL of SBP at pH 7.3. At the end of reaction time of 3 h, catalase, at a final concentration of 125 U/mL, was added to stop the reaction. Alum, at a final concentration of 50 mg/L, was added to help settle the contents by gravity.

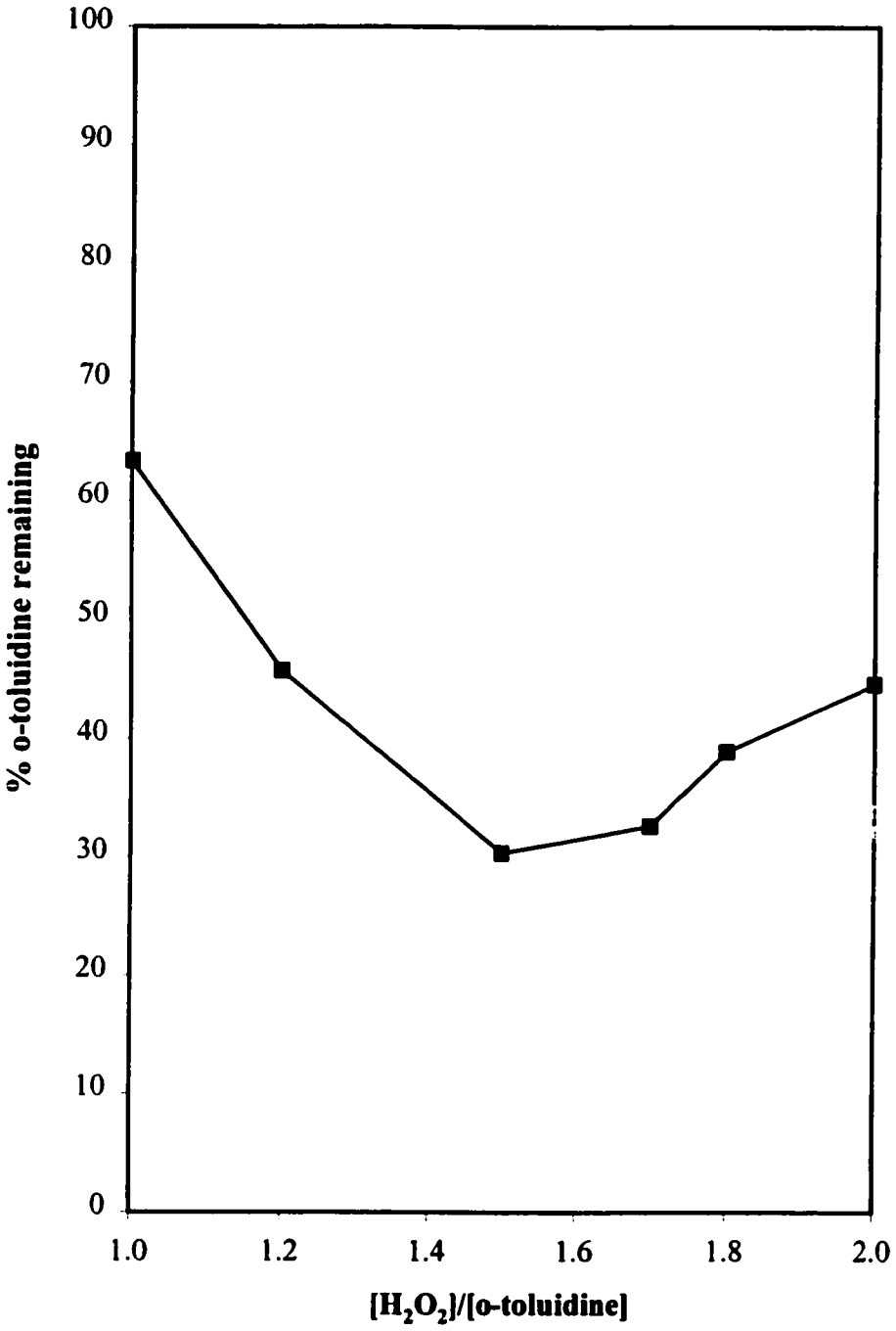

Fig. 4.5.2.3.2 H_2O_2 optimization for removal of *o*-toluidine
Batch reactors of 30 mL volume, initially contained 1 mM *o*-toluidine and 0.20 U/mL of SBP at pH 7.2. At the end of reaction time of 3 h, catalase, at a final concentration of 125 U/mL, was added to stop the reaction. Alum, at a final concentration of 50 mg/L, was added to help settle the contents by gravity.

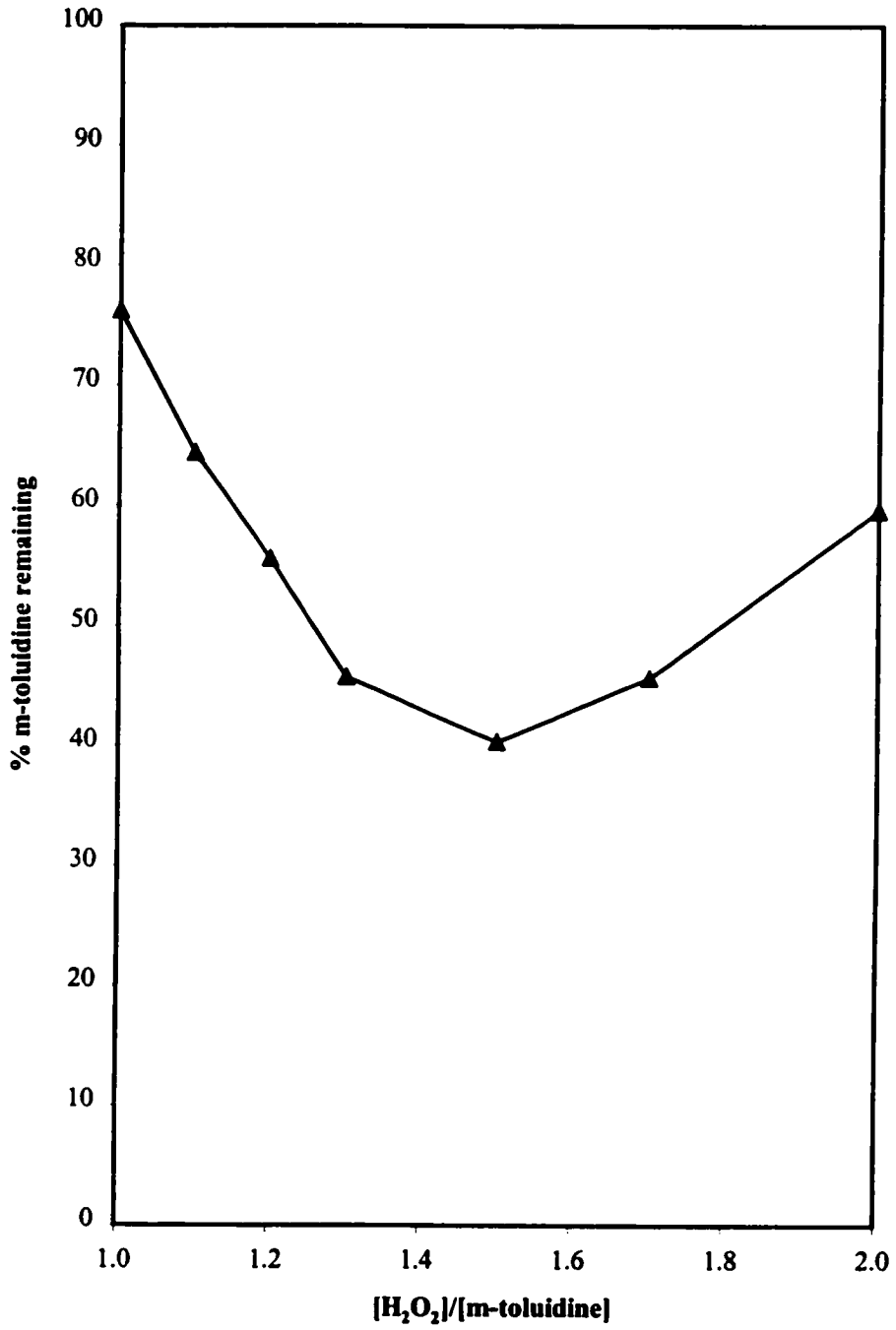

Fig. 4.5.2.3.3 H_2O_2 optimization for removal of *m*-toluidine
Batch reactors of 30 mL volume, initially contained 1 mM *m*-toluidine and 0.07 U/mL of SBP at pH 6.8. At the end of reaction time of 3 h, catalase, at a final concentration of 125 U/mL, was added to stop the reaction. Alum, at a final concentration of 50 mg/L, was added to help settle the contents by gravity.

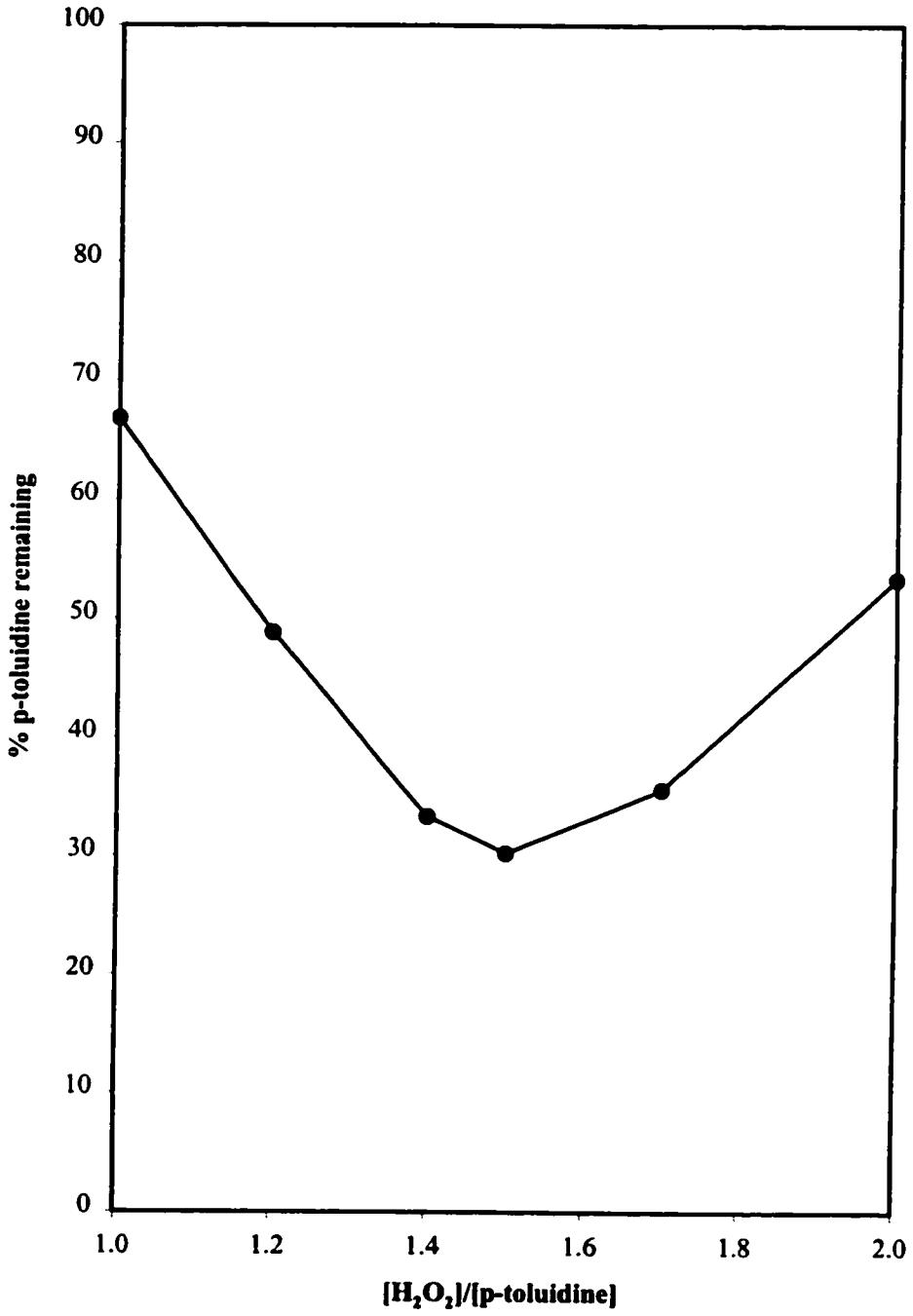

Fig. 4.5.2.3.4 H_2O_2 optimization for removal of *p*-toluidine
Batch reactors of 30 mL volume, initially contained 1 mM *p*-toluidine and 0.008 U/mL of SBP at pH 7.0. At the end of reaction time of 3 h, catalase, at a final concentration of 125 U/mL, was added to stop the reaction. Alum, at a final concentration of 50 mg/L, was added to help settle the contents by gravity.

(lowest remaining concentration of the substrate) increased sharply with an increase in $[H_2O_2]$/[amine] until the ratio reached an optimum. However, beyond this point, the remaining concentration of the substrate increased with an increase in $[H_2O_2]$/[amine]. It was speculated that any excess hydrogen peroxide was not only ineffective in amine removal but also increased the enzyme inactivation by forming Compound III according to Eq. 2.4.5 (page 13) or the irreversible form P_{670}. It is also possible that due to the peroxide-demand exhibited by the other ingredients of the crude enzyme, once the main reaction was satiated, the residual peroxide was used up in the catalase side-reaction. Hence, the excess peroxide was used up without any perceivable increase in the removal efficiency of the amine. It was observed that the optimum molar ratio of H_2O_2 to anilines was 1.5.

The overall reaction for the oxidation of the aromatic substrate by H_2O_2 in the presence of SBP is given by Eq. 2.4.4 (page 12), according to which, two aromatic free radicals are produced for every molecule of peroxide consumed. Therefore, the stoichiometric ratio of peroxide consumed to aromatic precipitated would be 0.5 provided the resulting dimer is completely insoluble in water. The measured stoichiometry was inconsistent with what is predicted by Eq. 2.4.4 (page 12) indicating that the process of polymerization and precipitation was beyond the scope of simple single bond formation between two aromatic molecules. Yu *et al.* (1994) reported that many of the dimers formed during phenol oxidation were substrates of the peroxidase, and thus their reaction increased the consumption of H_2O_2. This had the effect of shifting the stoichiometry away from what is predicted by Eq. 2.4.4 (page 12), to a limit of 1.0. Peroxide consumption stoichiometry beyond this limit is thought to be "peroxide demand" of the

crude SBP preparation, either from catalase activity or from simple chemical reactions (Mantha *et al.*, 2001a)

The concept of "*turnovers*", as defined with Eq. 2.6.1 (page 16), was primarily introduced to measure the enzyme efficiency. There have been various studies to increase the *turnovers*. Nakamoto and Machida (1992) recommended the use of low instantaneous H_2O_2 concentration for limiting the rate. In this study, H_2O_2 was used in step-wise fashion to achieve the above situation. In 30 mL batch reactors, hydrogen peroxide was added in steps of two: 1 mM initially and 0.5 mM after 1 h of reaction. However, this step-wise feeding of H_2O_2 showed no improvement in terms of either reduced enzyme concentration or increased substrate removal. Comparative studies for 'peroxide in single aliquot' and 'peroxide in steps of two' are shown in Figures 4.5.2.3.5-4.5.2.3.8.

4.5.2.4 Optimization of SBP concentration

To determine the optimum SBP concentration, batch reactor studies were performed using various SBP concentrations at the previously obtained optimum pH range of 7.2-7.4 for each substrate. The H_2O_2 to substrate ratio was held constant at 1.5. The results for all four aniline polymerizations are shown in Figures 4.5.2.4.1-4.5.2.4.4. It can be seen that the optimum concentration of SBP in the present study for each of the substrates was a unique one. At any lower concentration of the enzyme, the removal efficiency was lower. It is, however, interesting to note that the removal efficiency did not get better at a higher enzyme concentration either. This was due to the fact that, at higher enzyme concentration and the same peroxide to substrate ratio of 1.5, the catalase activity of the crude enzyme consumed a greater amount of H_2O_2 than during the reaction

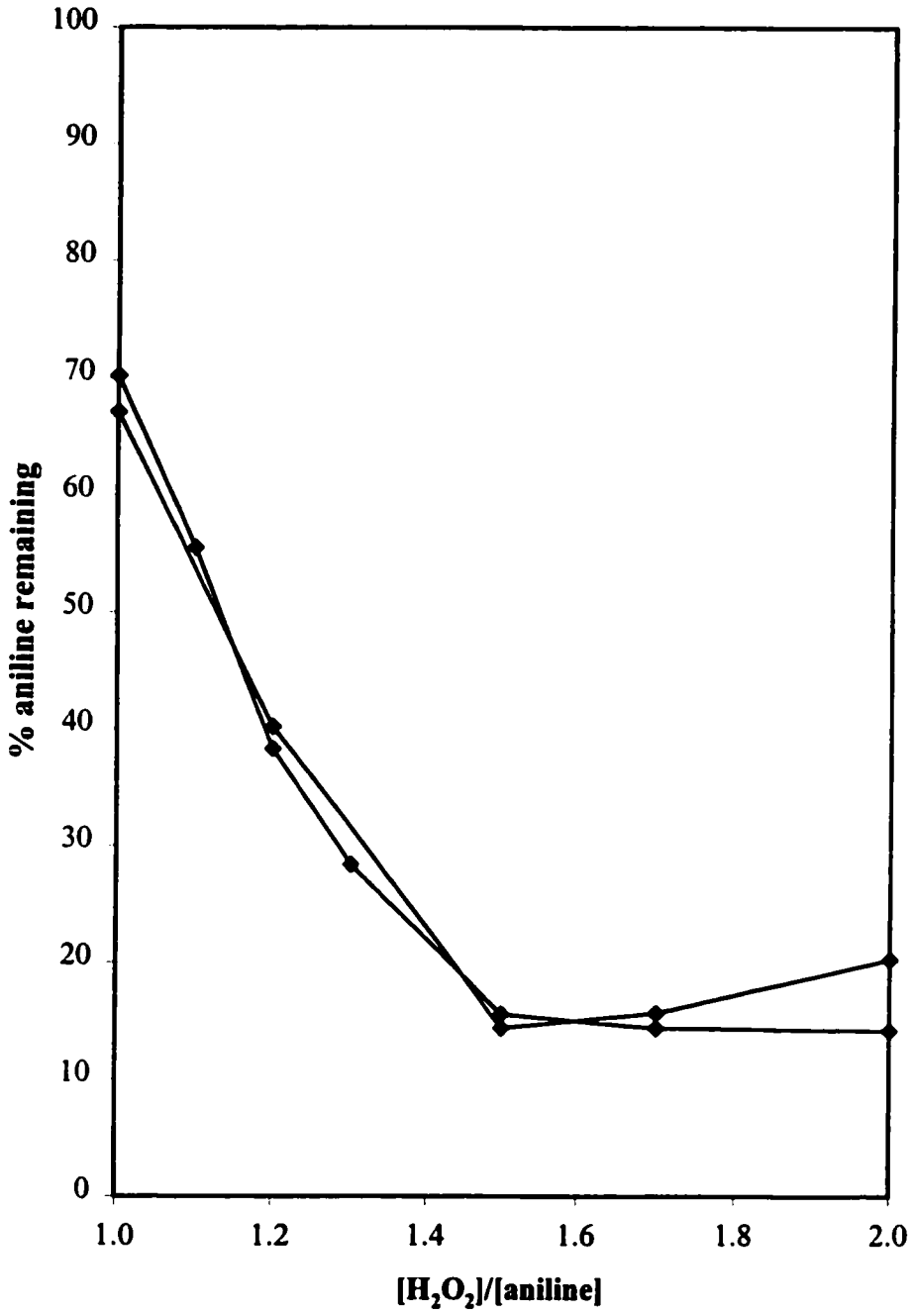

Fig. 4.5.2.3.5 Step-wise H_2O_2 optimization for removal of aniline
Batch reactors of 30 mL volume, initially contained 1 mM aniline and 0.20 U/mL of SBP at pH 7.3. At the end of reaction time of 3 h, catalase, at a final concentration of 125 U/mL, was added to stop the reaction. Alum, at a final concentration of 50 mg/L, was added to help settle the contents by gravity. H_2O_2 was used in the following ways: single aliquot, ♦; in steps of two, ◇.

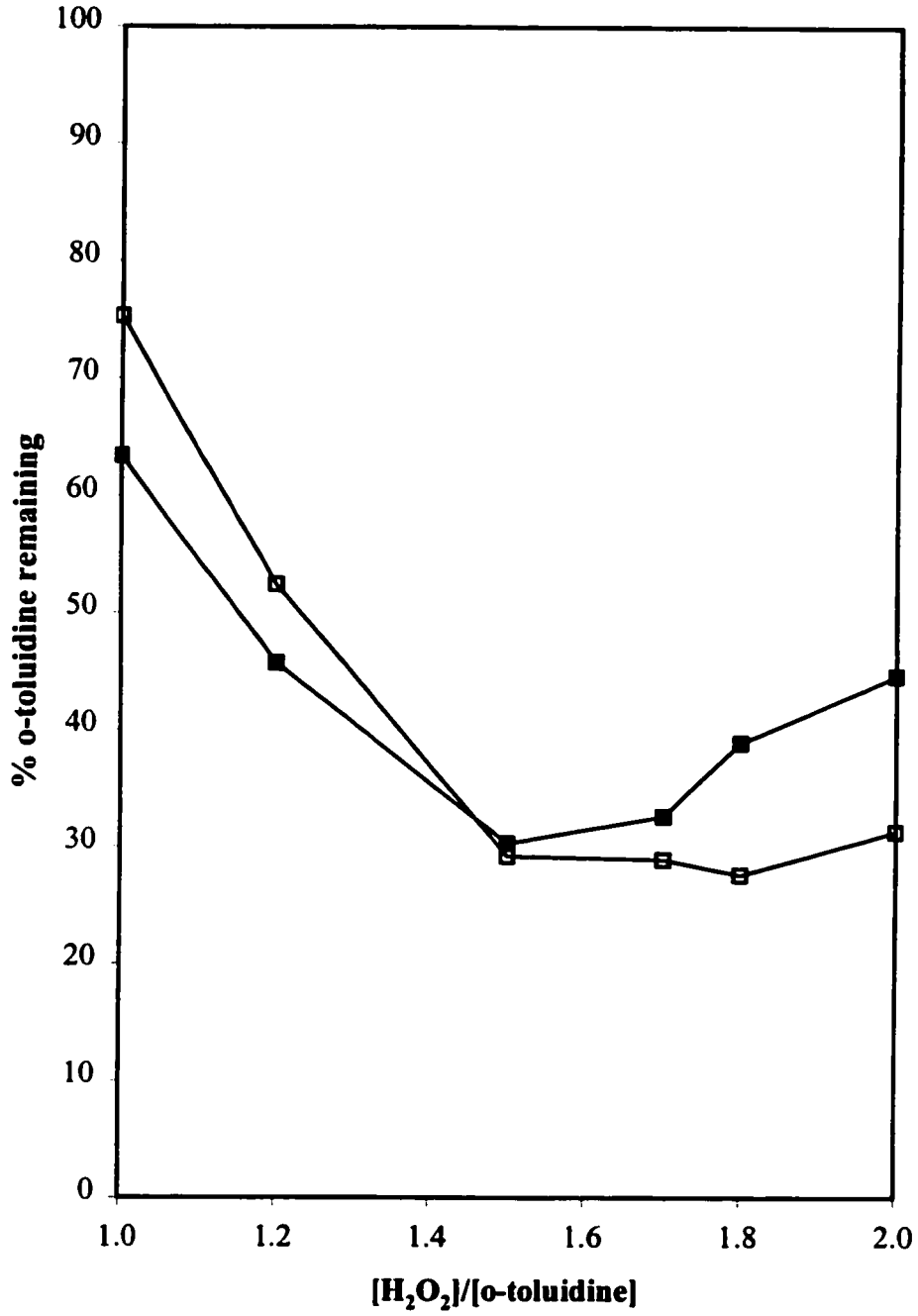

Fig. 4.5.2.3.6 Step-wise H_2O_2 optimization for removal of *o*-toluidine
Batch reactors of 30 mL volume, initially contained 1 mM *o*-toluidine and 0.20 U/mL of SBP at pH 7.2. At the end of reaction time of 3 h, catalase, at a final concentration of 125 U/mL, was added to stop the reaction. Alum, at a final concentration of 50 mg/L, was added to help settle the contents by gravity. H_2O_2 was used in the following ways: single aliquot, ■; in steps of 2, □.

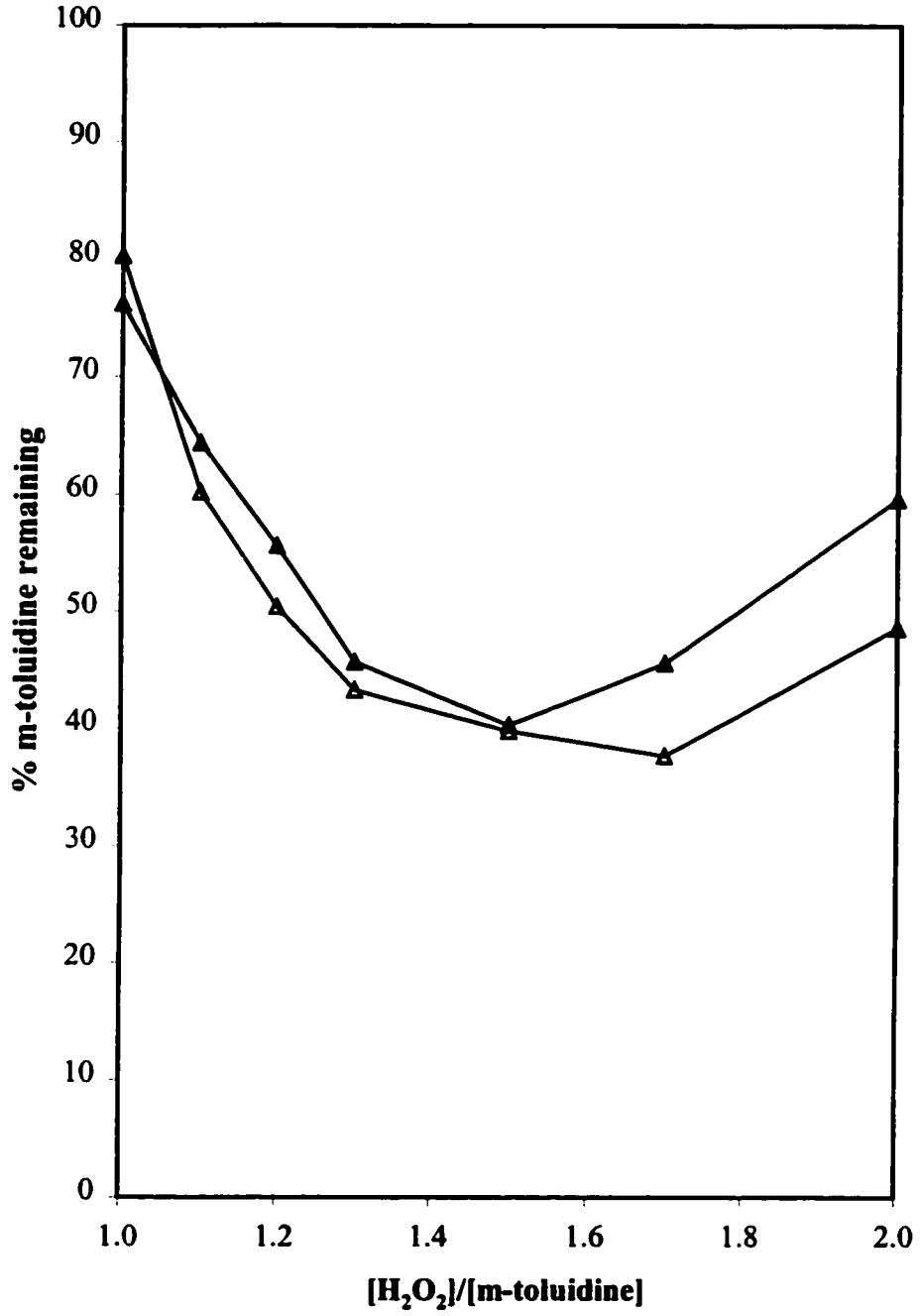

Fig. 4.5.2.3.7 Step-wise H_2O_2 optimization for removal of *m*-toluidine
Batch reactors of 30 mL volume, initially contained 1 mM *m*-toluidine and 0.07 U/mL of SBP at pH 6.8. At the end of reaction time of 3 h, catalase, at a final concentration of 125 U/mL, was added to stop the reaction. Alum, at a final concentration of 50 mg/L, was added to help settle the contents by gravity. H_2O_2 was used in the following ways: single aliquot, ▲; in steps of 2, Δ.

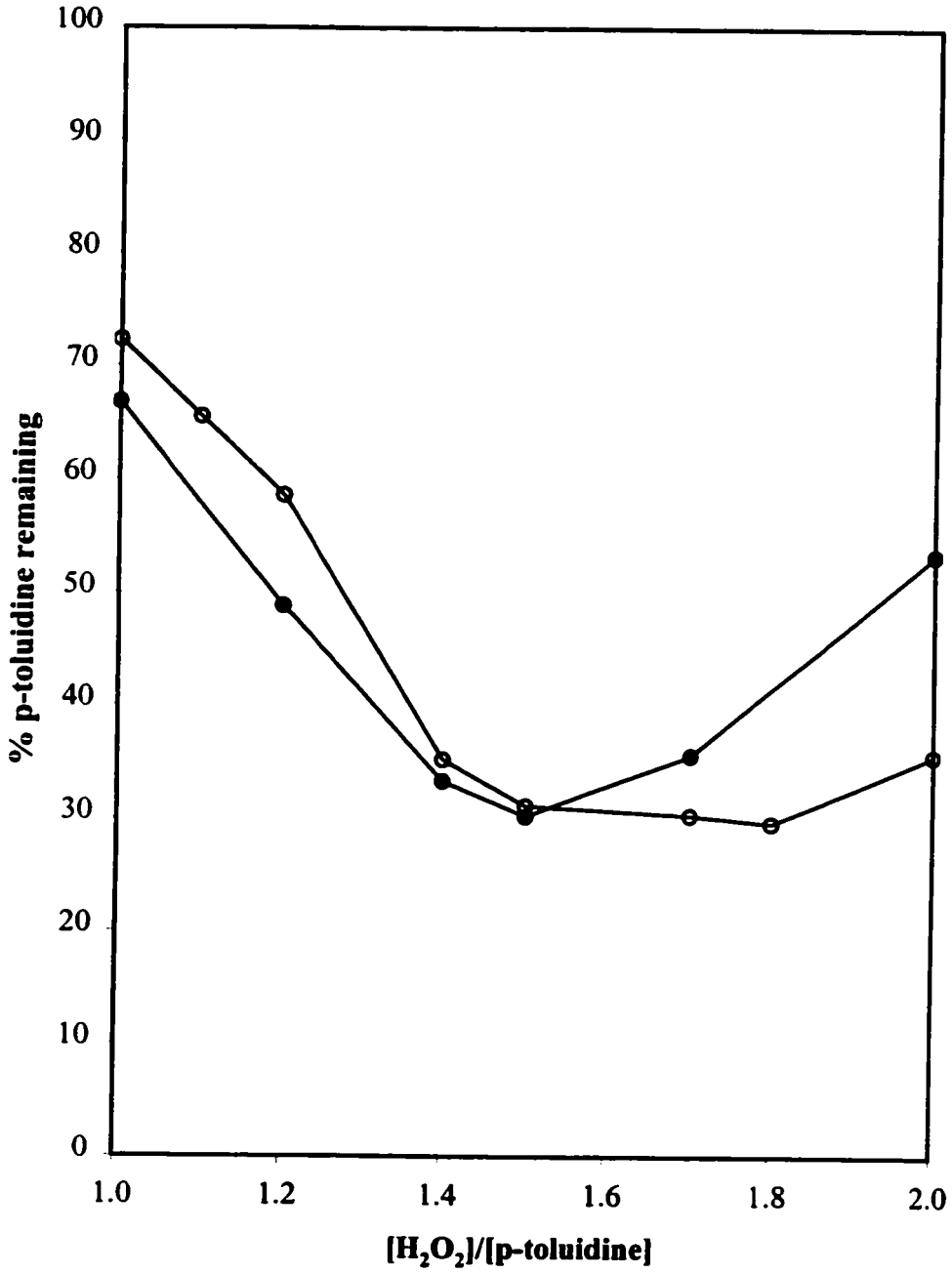

Fig. 4.5.2.3.8 Step-wise H_2O_2 optimization for removal of *p*-toluidine
Batch reactors of 30 mL volume, initially contained 1 mM *p*-toluidine and 0.008 U/mL of SBP at pH 7.0. At the end of reaction time of 3 h, catalase, at a final concentration of 125 U/mL, was added to stop the reaction. Alum, at a final concentration of 50 mg/L, was added to help settle the contents by gravity. H_2O_2 was used in the following ways: single aliquot, •; in steps of 2, o.

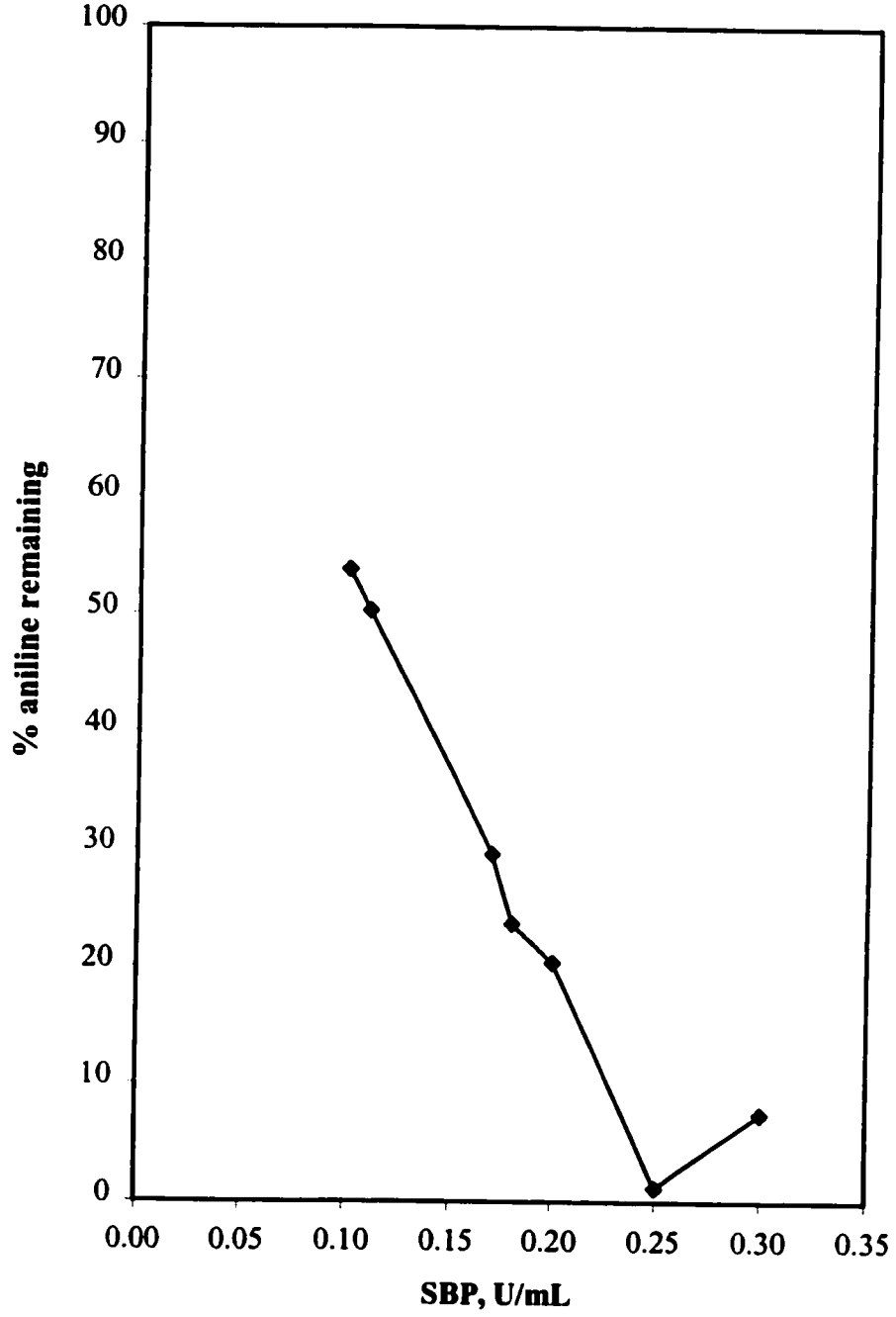

Fig. 4.5.2.4.1 SBP optimization for removal of aniline
Batch reactors of 30 mL volume, initially contained 1 mM aniline and 1.5 mM of H_2O_2 at pH 7.3. At the end of reaction time of 3 h, catalase, at a final concentration of 125 U/mL, was added to stop the reaction. Alum, at a final concentration of 50 mg/L, was added to help settle the contents by gravity.

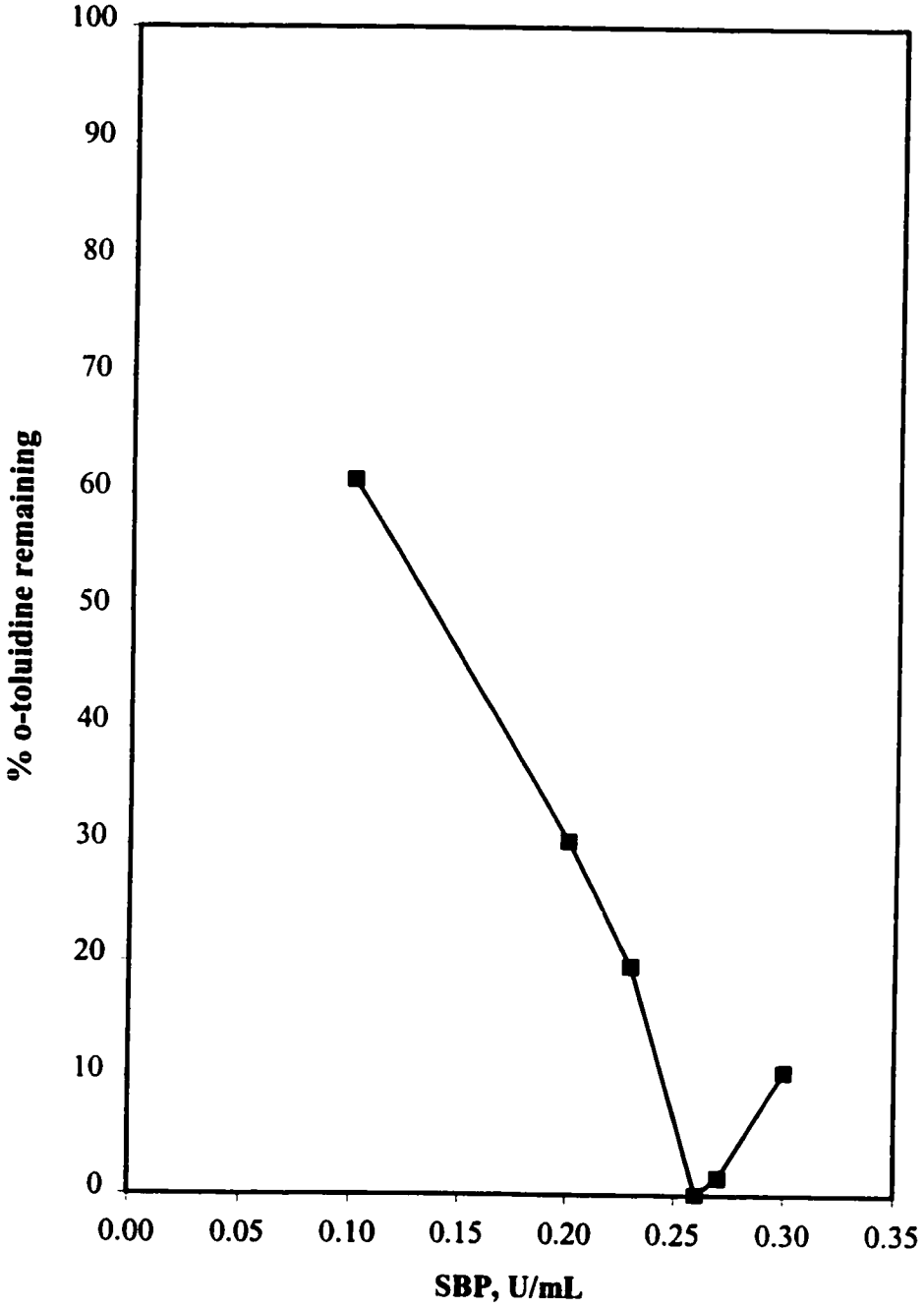

Fig. 4.5.2.4.2 SBP optimization for removal of *o*-toluidine
Batch reactors of 30 mL volume, initially contained 1 mM *o*-toluidine and 1.5 mM of H_2O_2 at pH 6.8. At the end of reaction time of 3 h, catalase, at a final concentration of 125 U/mL, was added to stop the reaction. Alum, at a final concentration of 50 mg/L, was added to help settle the contents by gravity.

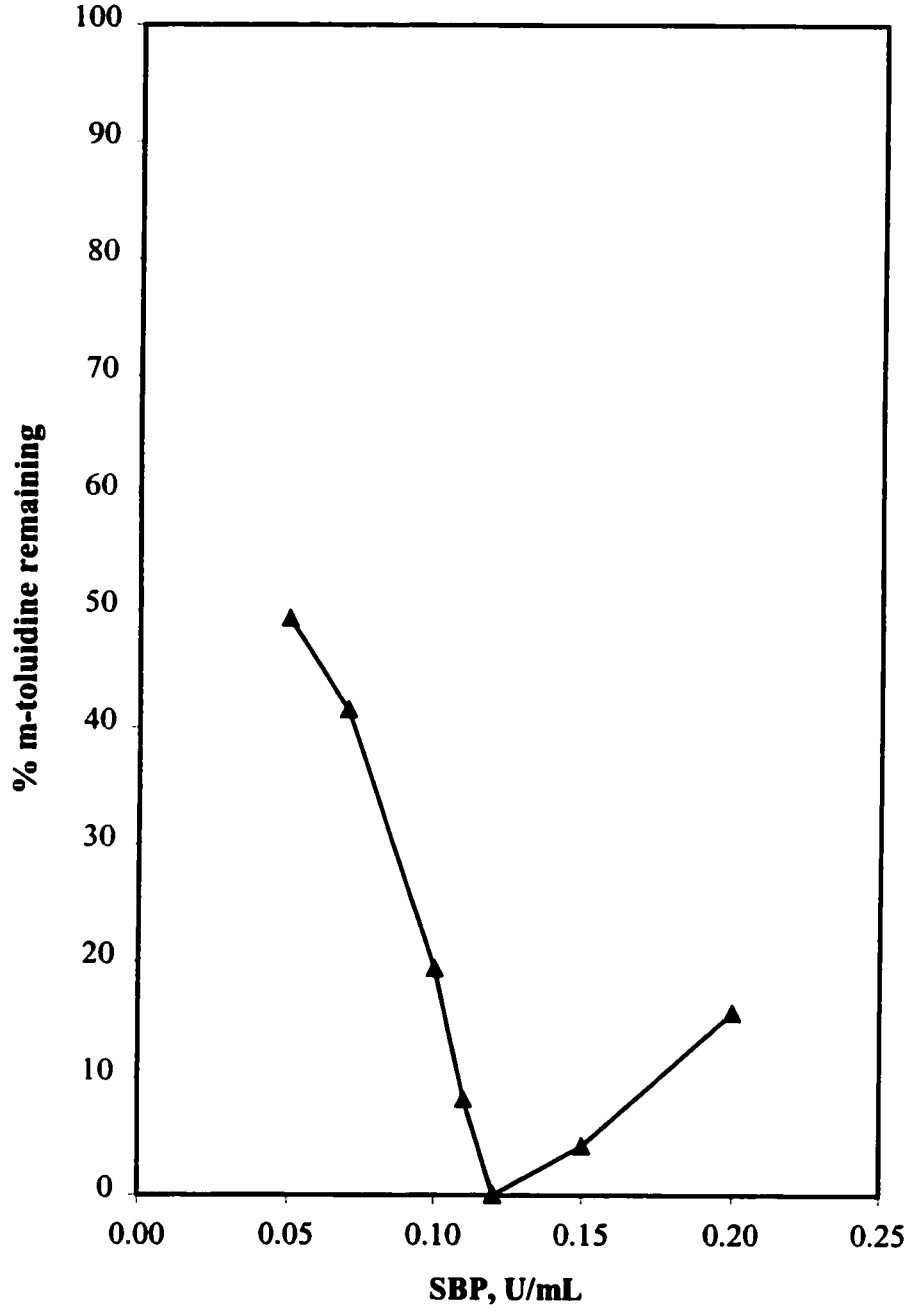

Fig. 4.5.2.4.3 SBP optimization for removal of *m*-toluidine
Batch reactors of 30 mL volume, initially contained 1 mM *m*-toluidine and 1.5 mM of H_2O_2 at pH 7.1. At the end of reaction time of 3 h, catalase, at a final concentration of 125 U/mL, was added to stop the reaction. Alum, at a final concentration of 50 mg/L, was added to help settle the contents by gravity.

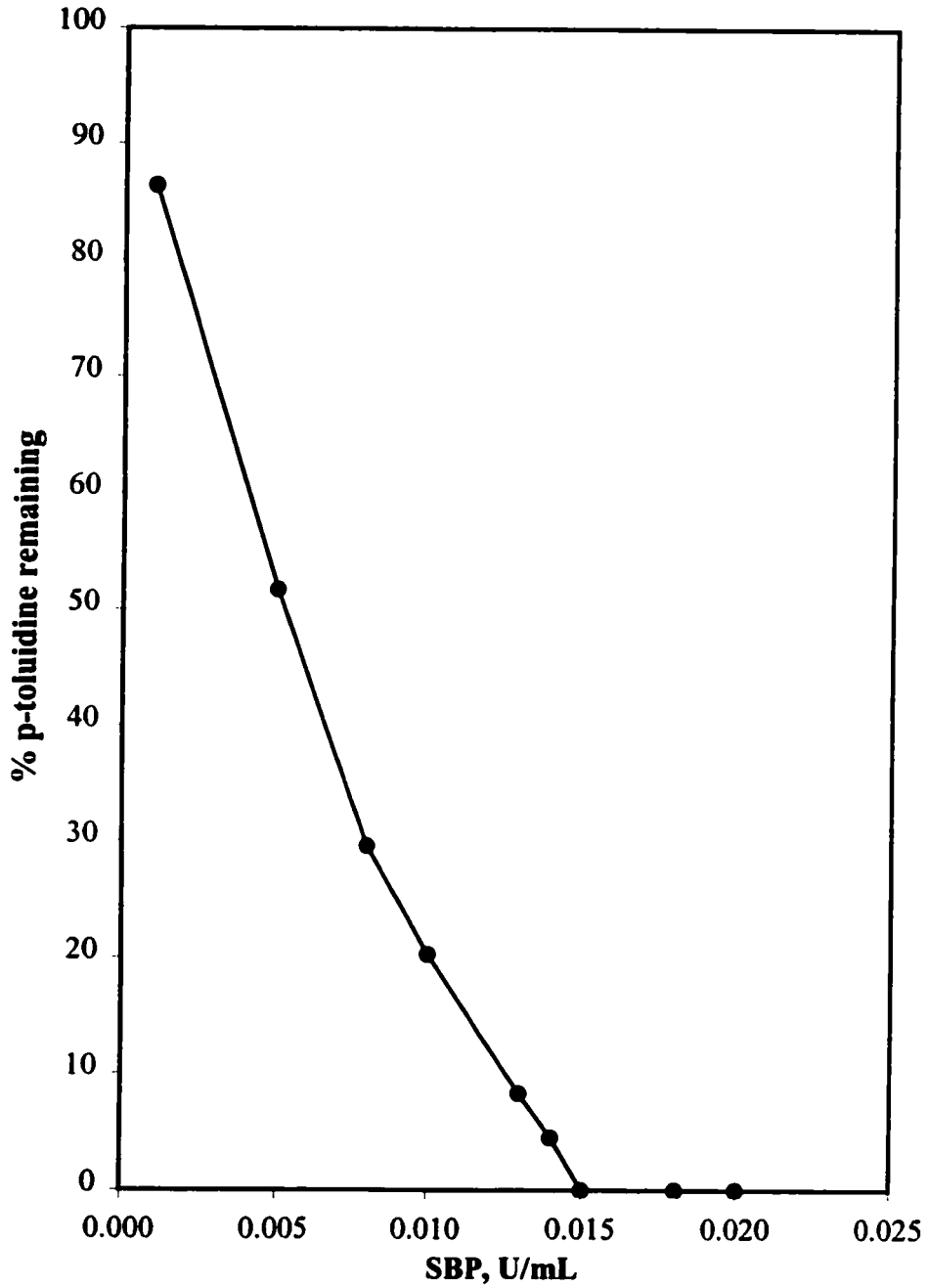

Fig. 4.5.2.4.4 SBP optimization for removal of *p*-toluidine
Batch reactors of 30 mL volume, initially contained 1 mM *p*-toluidine and 1.5 mM of H_2O_2 at pH 7.0. At the end of reaction time of 3 h, catalase, at a final concentration of 125 U/mL, was added to stop the reaction. Alum, at a final concentration of 50 mg/L, was added to help settle the contents by gravity.

when only optimum concentration of enzyme was used. Similar results for all substrates show a particular trend generalizing the generic nature of aryl amines. However, from Fig. 4.5.2.4.4, it is seen that for *p*-toluidine greater than the optimum enzyme concentrations do not pose a problem. This could be due to the fact that there is about 15-fold less crude SBP present for *p*-toluidine as there is for aniline, *o*- and *m*-toluidines. Hence, the catalase action of the enzyme is less significant on *p*-toluidine.

4.5.2.5 Effect of Alum

It was indicated by previous researchers (Ibrahim *et al.*, 1997 and 2001; Caza *et al.*, 1999) that alum was useful in settling of the final flocs, formed during the enzymatic treatment of phenols. They indicated an optimum pH range of 6.5-8.0 for effective treatment with alum. However, it does not increase the removal efficiency of the aromatic substances. These investigators worked with phenolic class of aromatic compounds. Alum, under specific conditions of pH, has been used as an effective coagulant in industries for treatment of water and wastewater. However, the effect of alum during the polymerization of aryl amines has not been well researched. In the current study it was decided to optimize the concentration of alum needed for settling the flocs and removing the residual color.

Alum concentrations in the range of 0-300 mg/L were studied. At the end of the reaction, the contents of the batch reactors were adjusted to a pH of 6.5-8.0, and alum was quickly added to the reactors and the contents were allowed to settle by gravity. The color of the supernatant and time of settling under each condition was noted. Table 4.5.2.5 in Appendix C, shows the time of settling and the absorbance at 500 nm. It is

clear from the table that the batch reactors, which did not receive any alum, took a substantially longer time to clarify. Also, the residual color in the solutions was high. This high color in the effluent solutions is a problem, not only from an analytical point of view, but also from wastewater discharge point of view. Alum concentrations of 50-100 mg/L were most suitable for removing the color and in gravity settling of flocs. Concentrations higher than these did not have any particular advantage.

4.5.3 Enzymatic treatment of "synthetic" anilines (SAs) in batch reactors

The matrix composition of the aniline produced as a result of reduction of NAC in the Fe^0 column was expected to be quite different as compared to wastewater prepared from pure chemicals. The SAs would contain unreacted Na_2SO_3 and product Fe^{2+} from the zero-valent iron column. Hence, the effects of these two were studied in batch reactors. Preliminary studies indicated that the effluent from the Fe^0 column contained sufficient Fe^{2+} and Na_2SO_3, to interfere with the enzymatic treatment. Fe^{2+} in conjunction with H_2O_2 produces OH radicals and this mixture is known as Fenton's reagent (Walling, 1975). Fenton chemistry presents an essentially different scenario as compared to enzymatic treatment. Na_2SO_3 by itself also has stoichiometric (1:1) peroxide demand. Although most of the corrosion products had precipitated in the column itself, the effluent stream still contained detectable corrosion products, Section 4.4.6, page 76, (Mantha *et al.*, 2001b). Hence, the effluent was aerated to oxidize and precipitate out Fe^{2+} as Fe^{3+} and to convert Na_2SO_3 to Na_2SO_4, respectively. Figure 4.5.3 shows the percentage of aniline, formed during the course of reduction of NB in the Fe^0 column, removed under different conditions of H_2O_2 and enzyme concentrations both with and without pre-

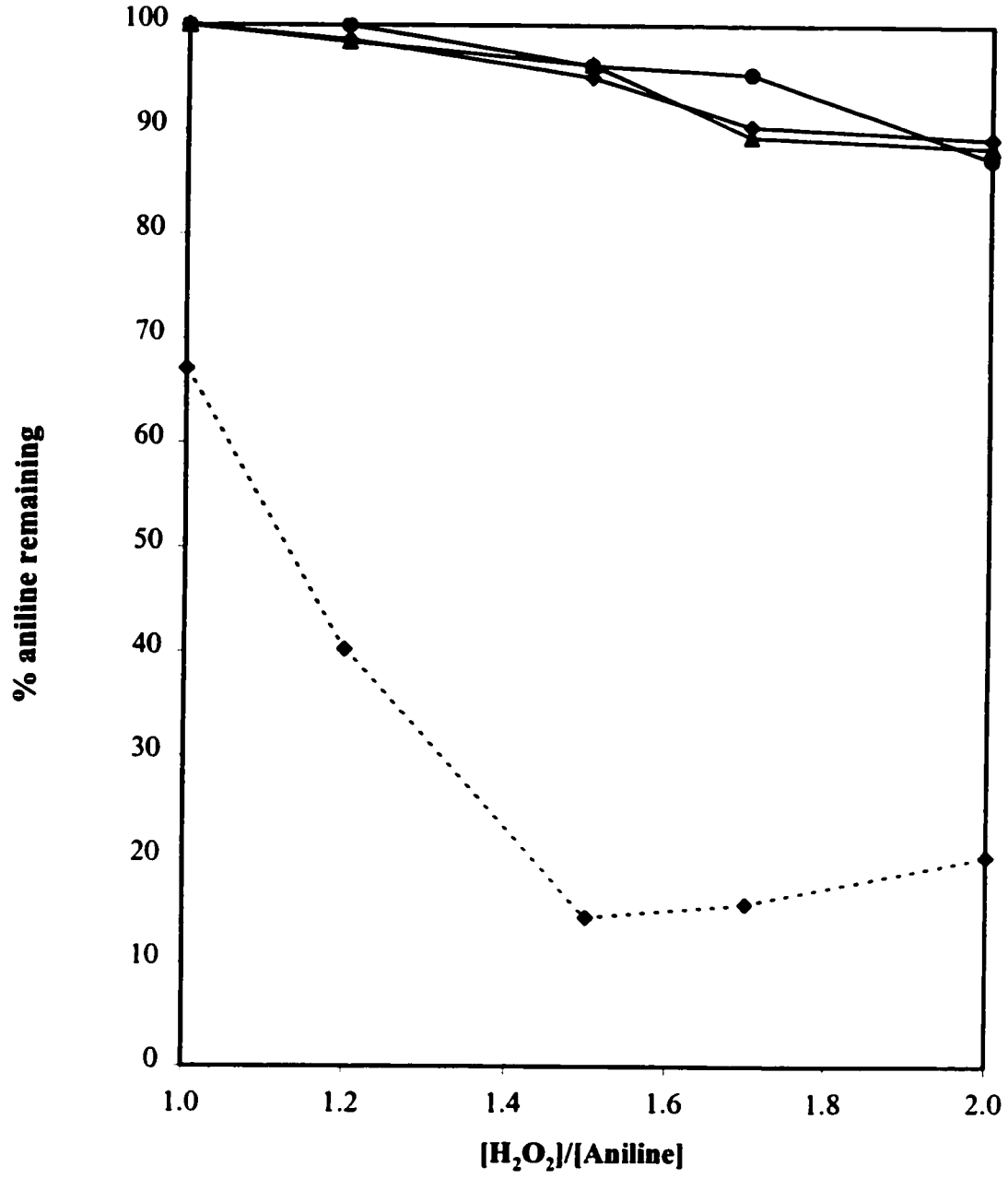

Fig. 4.5.3 Removal efficiency of aniline, formed as a result of reduction of nitrobenzene

30 mL batch reactors were set up with the effluent, containing aniline, from the Fe^0 column. Initial aniline present in the batch, after dilution due to addition of enzyme and hydrogen peroxide, was 0.93 mM at a pH of 7.4. The following conditions of SBP, U/mL, were chosen: 0.2, ◆; 0.3, ▲; 0.4, ●.

aeration. It is apparent from the graph that unless Fe^{2+} and Na_2SO_3 were removed completely, enzymatic oxidation was not efficient. This conclusively proved the necessity for sufficient pre-aeration until all Fe^{2+} and Na_2SO_3 were oxidized completely. However, no optimum air dose was established in this study. Also, it is interesting to note that, once Fe^{2+} and Na_2SO_3 were removed completely, the solution behaved ideally as if it contained pure anilines. Thus, the various parameters optimized earlier for pure anilines could also be utilized to describe the behavior of various SAs.

STAGE 3 Continuous flow system

Based on the information collected from the batch reactors, a continuous flow system was designed, keeping in view the recommendations of Ibrahim *et al.* (2001) for phenol. The zero-valent iron technique was integrated with the peroxidase-catalyzed treatment strategy. This, in effect, was the optimization of the second step *viz.*, the enzymatic treatment step. The influent to the zero-valent iron column was pure, deoxygenated NAC. However, the influent to the enzymatic column, a plug flow reactor (PFR), was the effluent from the Fe^0 column. Hence, the stream entering the PFR for enzymatic treatment was the synthetic wastewater matrix containing Na_2SO_4 and Fe^{3+} and was expected to behave differently as compared to a stream of pure aqueous aromatic amine. The integrated system was operated and optimized and data were collected to establish trends and removal efficiencies of the NACs from wastewater.

4.6.1 pH Effect

Batch reactor studies showed that the enzyme SBP worked best at or around neutral conditions of pH. The effluent from the zero-valent metal column was at a pH 7.2-7.5 in most cases. Hence, its pH was not adjusted for further treatment by enzymatic route.

4.6.2 H_2O_2 to Substrate ratio

Data obtained for optimization of $[H_2O_2]$/[amine] in a PFR is depicted in Figures 4.6.2.1-4.6.2.4. 'Time-on-stream' data showed that under optimum reaction conditions, more than 90% of the polymerization reaction was complete within an hour, while for the reaction to go to completion it took about 2 h. Also, regardless of the $[H_2O_2]$/[amine], the nature of time-on-stream data were comparable for all the aryl amines indicating a generic trend. Comparison of batch reactor data and continuous-flow reactor data had indicated that, irrespective of the type of reactor, the peroxide to aromatic amine ratio was 1.5.

Following the recommendations of Nakamoto and Machida (1992) step-wise feeding of hydrogen peroxide for oxidative polymerization of aniline was studied in the continuous-flow system also, although step-wise feeding of H_2O_2 in the batch-mode of operation had no advantage. Two continuous stirred tank reactors (CSTRs) with detention times of 5 min and 18 min, respectively, were used in series, Figure 4.6.2.5, to determine whether step-wise feeding of H_2O_2 was useful or not. In the first CSTR with 5 min detention time, only two-thirds of the required amount of peroxide was added. The stream after coming out of the first CSTR was directed to the next CSTR with 18 min

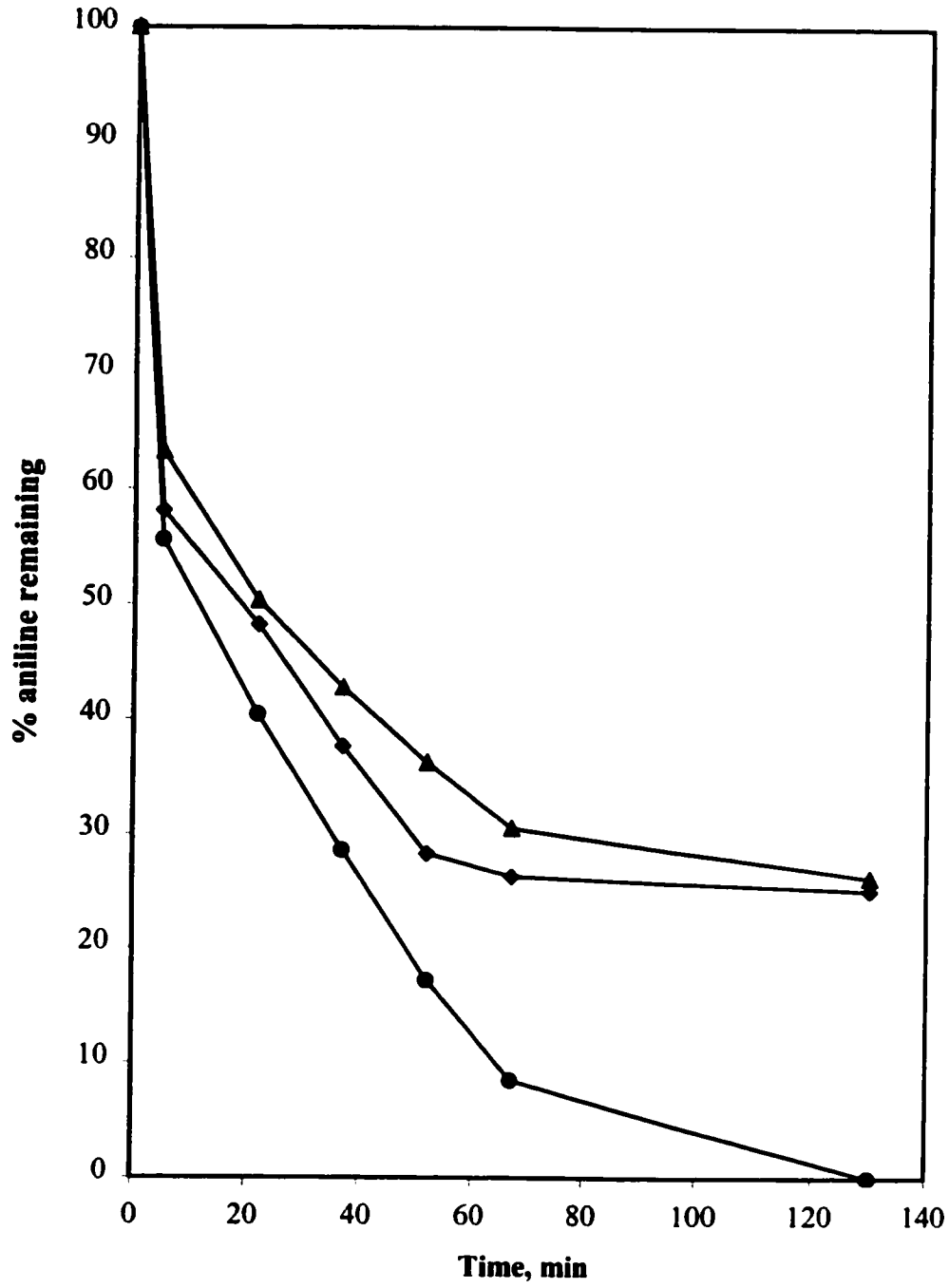

Fig. 4.6.2.1 Optimization of $[H_2O_2]/[aniline]$ in the continuous-flow column
Integrated continuous-flow column studies with initial nitrobenzene, entering the Fe^0 column, of 1 mM. Effective aniline after dilution with peroxide and SBP, 0.2 U/mL, was 0.8 mM. Influent pH was 7.2-7.3, under the following conditions of $[H_2O_2]/[aniline]$: 1.0, ♦; 1.5, •; 2.0, ▲.

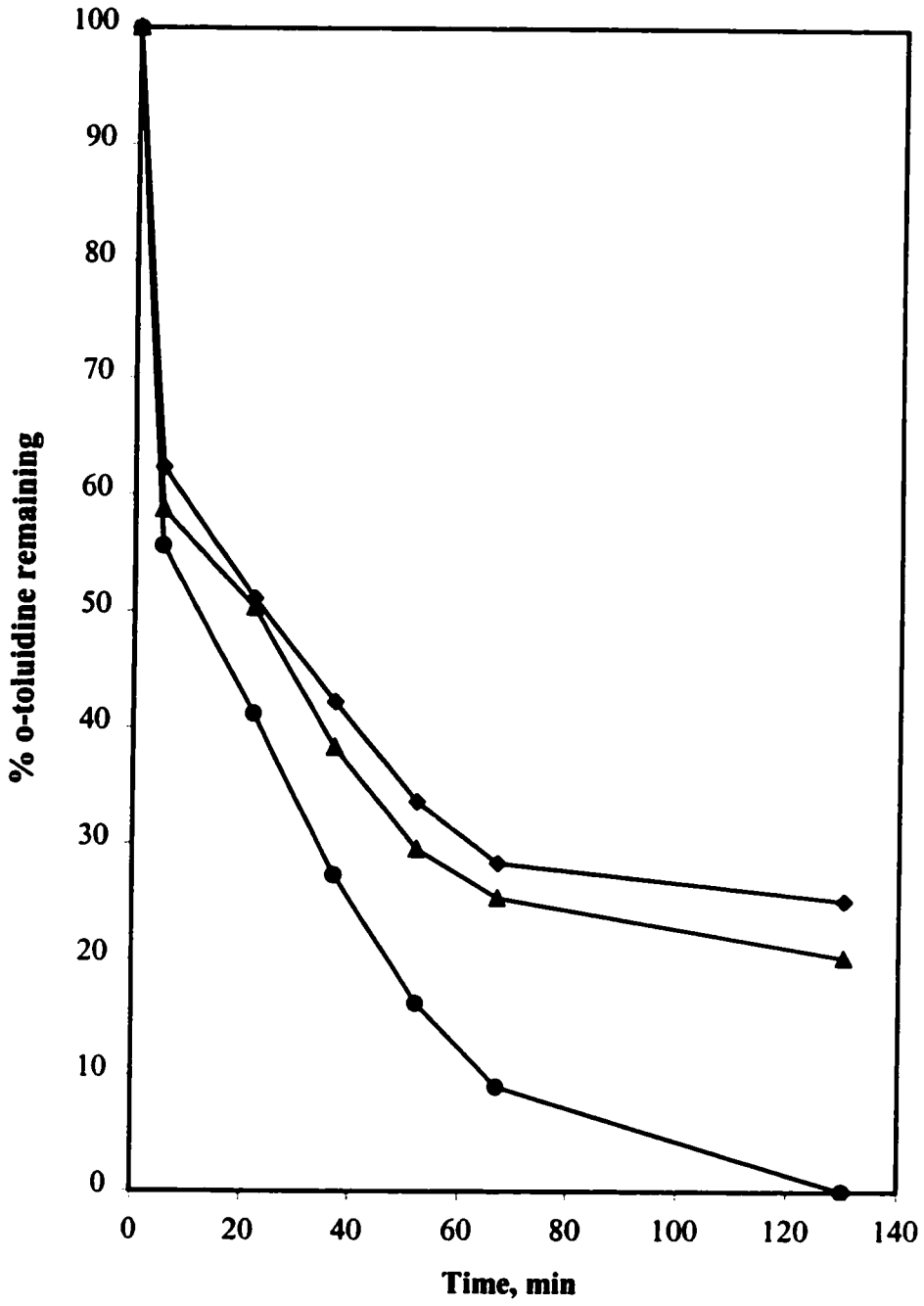

Fig. 4.6.2.2 Optimization of [H_2O_2]/[*o*-toluidine] in the continuous-flow column
Integrated continuous-flow column studies with initial *o*-nitrotoluene, entering the Fe^0 column, of 1 mM. Effective *o*-toluidine after dilution with peroxide and SBP, 0.23 U/mL, was 0.8 mM. Influent pH was 7.2-7.3, under the following conditions of [H_2O_2]/[*o*-toluidine]: 1.0, ♦; 1.5, ●; 2.0, ▲.

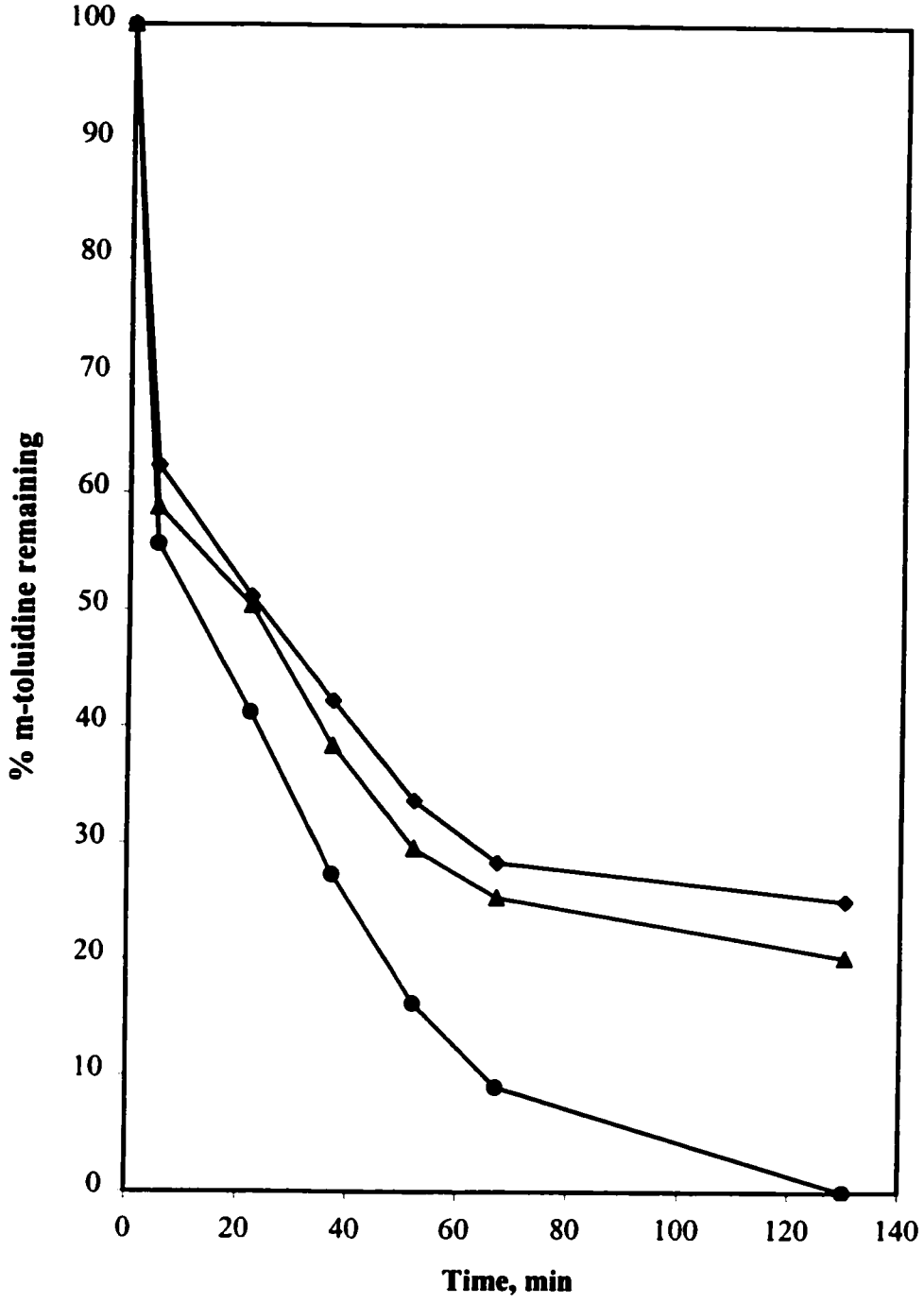

Fig. 4.6.2.3 Optimization of [H_2O_2]/[*m*-toluidine] in the continuous-flow column
Integrated continuous-flow column studies with initial *m*-nitrotoluene, entering the Fe^0 column, of 1 mM. Effective *m*-toluidine after dilution with peroxide and SBP, 0.10 U/mL, was 0.8 mM. Influent pH was 7.2-7.3, under the following conditions of [H_2O_2]/[*m*-toluidine]: 1.0, ♦; 1.5, ●; 2.0, ▲.

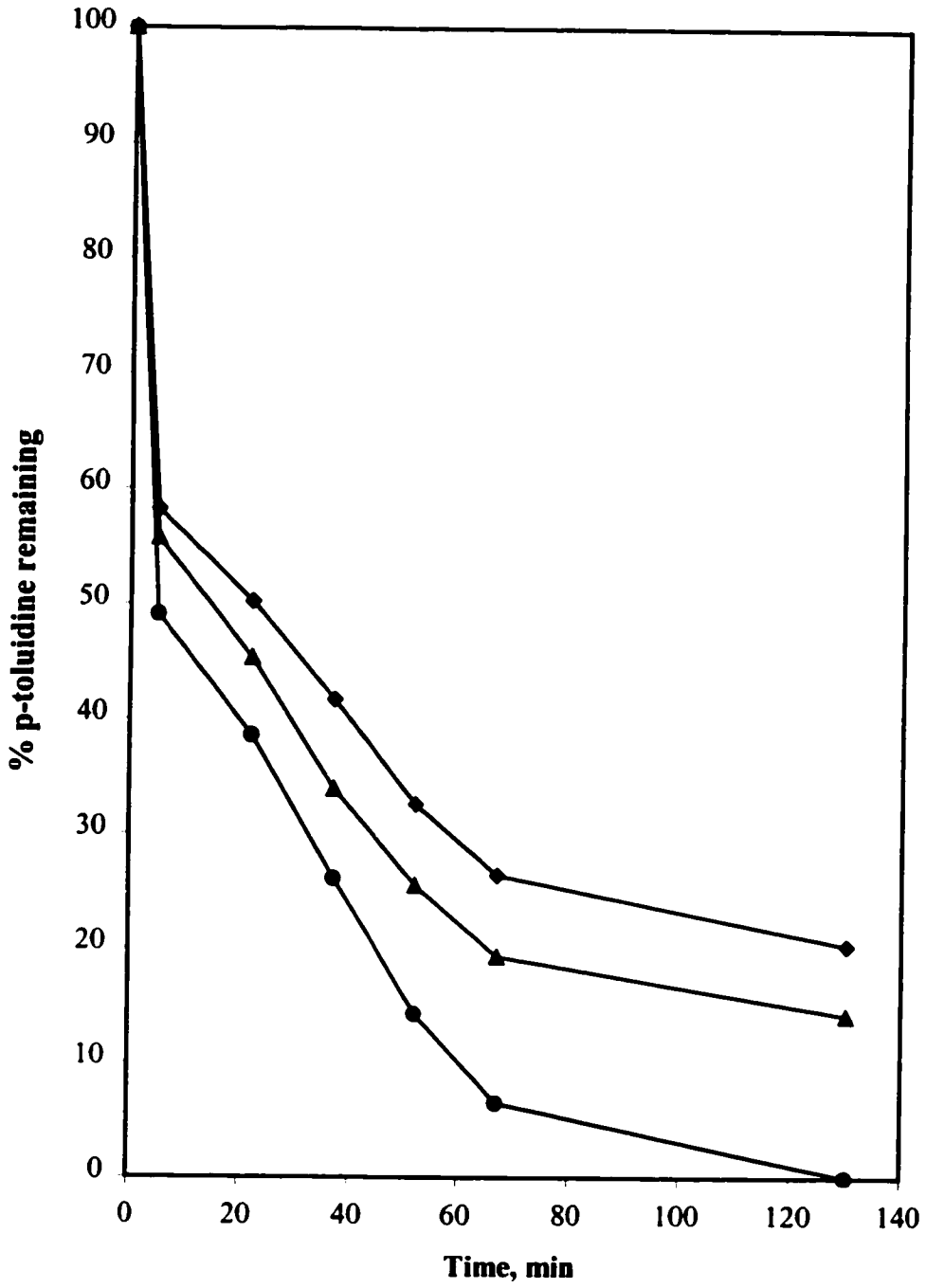

Fig. 4.6.2.4 Optimization of [H_2O_2]/[*p*-toluidine] in the continuous-flow column
Integrated continuous-flow column studies with initial *p*-nitrotoluene, entering the Fe^0 column, of 1 mM. Effective *p*-toluidine after dilution with peroxide and SBP, 0.01 U/mL, was 0.8 mM. Influent pH was 7.2-7.3, under the following conditions of [H_2O_2]/[*p*-toluidine]: 1.0, ♦; 1.5, ●; 2.0, ▲.

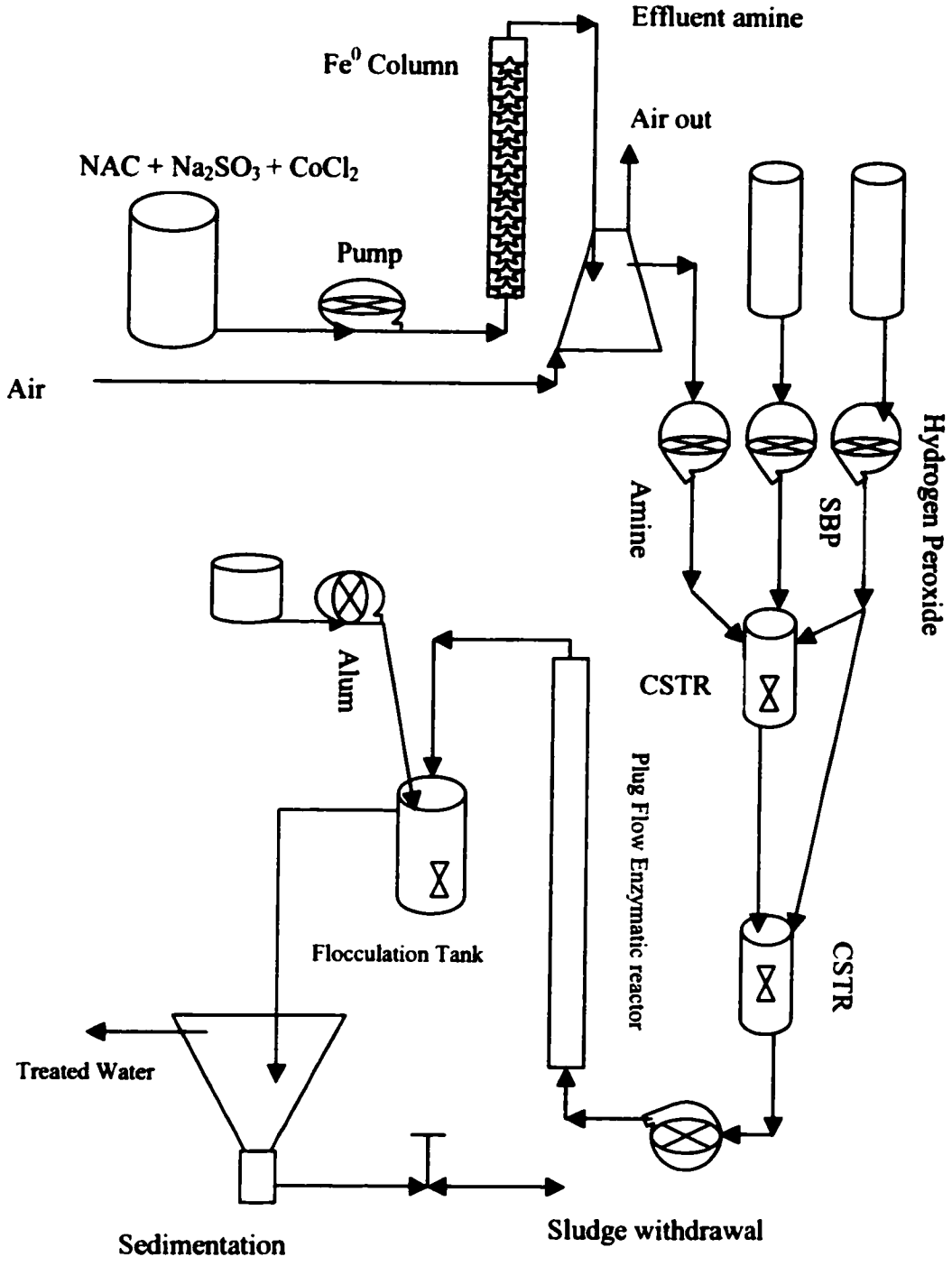

Fig. 4.6.2.5 Schematic of the Continuous-flow system using 2 CSTRs as pre-mixers, where H_2O_2 was added in steps

detention time where remaining one-third of required total peroxide was added to provide the ratio of 1.5 to 1 with the substrate. Then the stream entered the PFR. Samples from the two CSTRs were withdrawn at the exit points after 5 minutes and 23 minutes respectively. This step-wise feeding of H_2O_2 showed some improvement in terms of reduction of reaction time, which may be translated into either reducing the enzyme dose or increasing the substrate removal, Figure 4.6.2.6. However, a better knowledge about the economics of the system is required before justifying the additional cost of CSTR and step-wise feeding operation. Al-Kassim *et al.* (1993), in a similar type of study, varied the peroxide concentration in a semi-batch fashion for treatment of phenols and did not find significant improvement with the semi-batch mode of operation. It is speculated that, in absence of sufficient H_2O_2, the catalase activity of the enzyme dominates and uses up the peroxide. Figures 4.6.2.7 and 4.6.2.8 show the concentration *vs.* time plots of H_2O_2 in single and two CSTRs respectively, used as pre-mixers before the PFR, during the removal of aniline, formed as a result of reduction of NB in the zero-valent metal column.

4.6.3 Optimization of SBP concentration

Column studies were performed using various SBP concentrations at the optimum pH range, 7.0-7.4, to determine the optimum SBP concentration. The H_2O_2 to substrate ratio was held constant at 1.5. The results for aniline, produced as a result of the reduction of NB in the Fe^0 column, are shown in Figure 4.6.3.1. It can be seen that the optimum concentration of SBP in the present study was 0.20 U/mL. At lower enzyme concentration, the removal efficiency was lower.

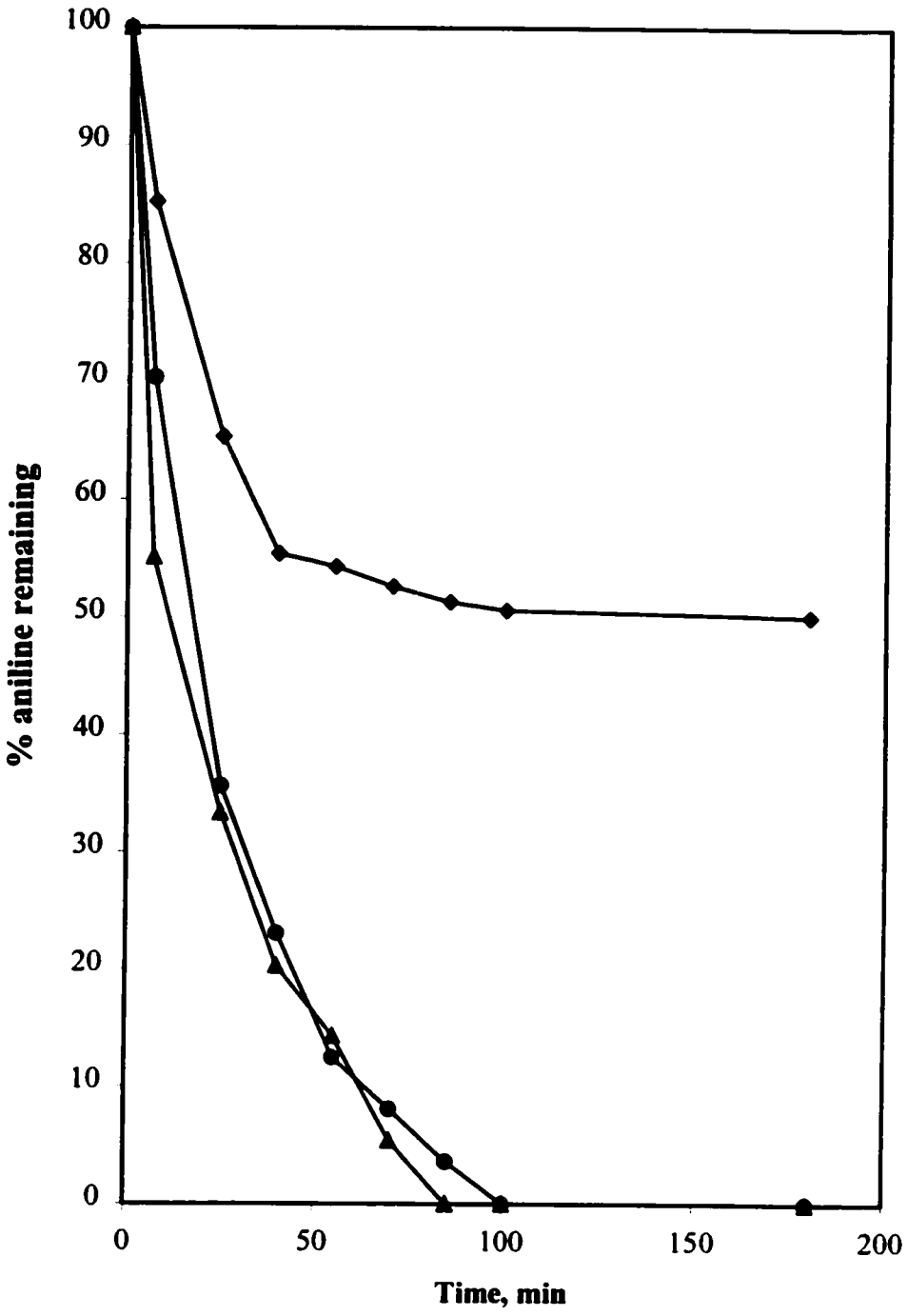

Fig. 4.6.2.6 Step-wise feeding of H_2O_2 in the continuous-flow column
Integrated continuous-flow column studies with initial nitrobenzene, entering the Fe^0 column, of 1 mM. Effective aniline after dilution with peroxide and SBP, 0.2 U/mL, was 0.8 mM. Influent pH was 7.2-7.3, under the following conditions of $[H_2O_2]$/[aniline]: 1.0, ♦; 1.5, •; 2.0, ▲.
H_2O_2 was fed in steps of two-thirds and one-third in the two CSTRs in series.

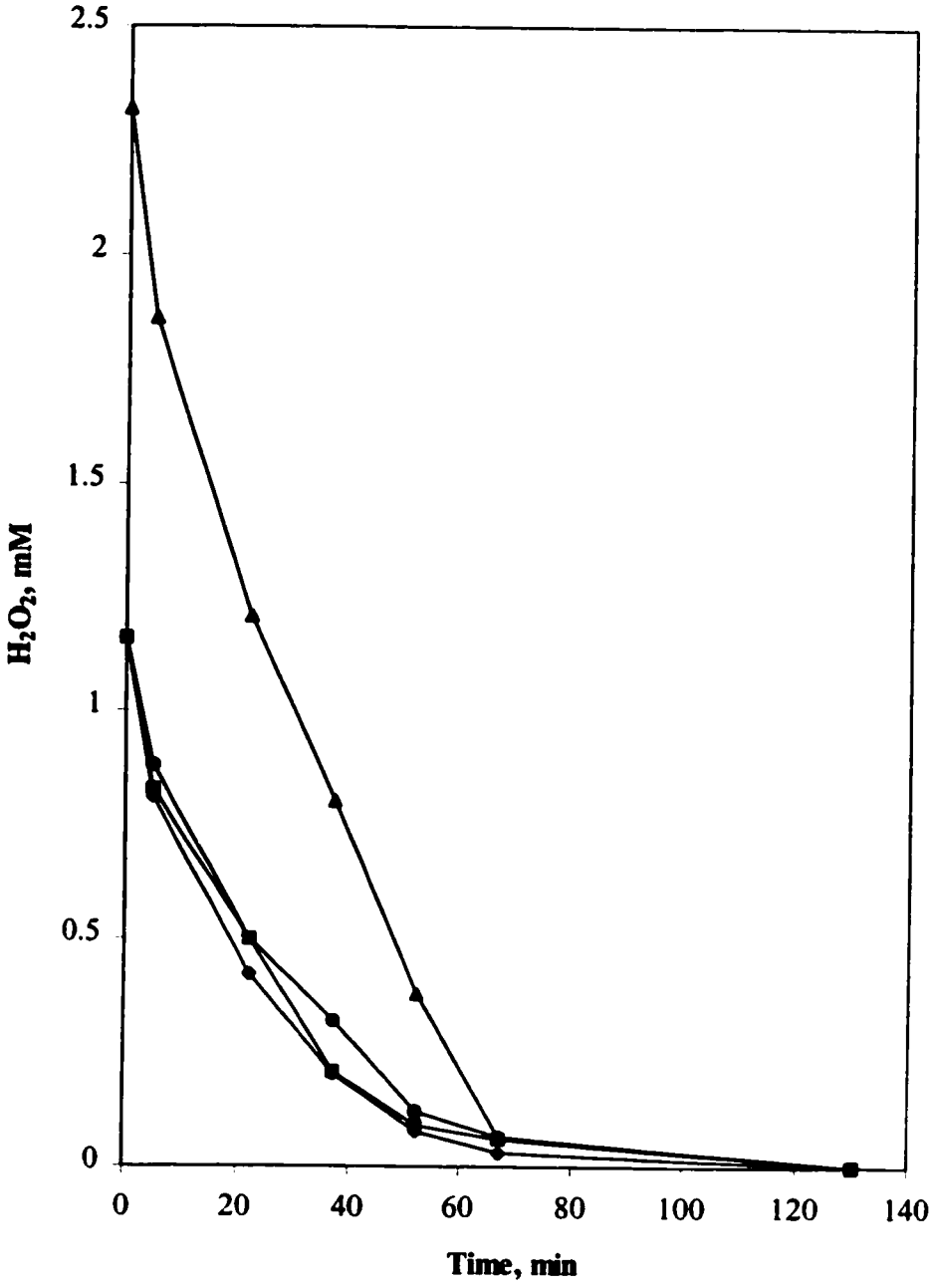

Fig. 4.6.2.7 Change in H_2O_2 concentration with time during removal of aniline in the continuous-flow column

Integrated continuous-flow column studies with initial nitrobenzene, entering the Fe^0 column, of 1 mM. Effective aniline after dilution with peroxide and SBP was 0.8 mM. Influent pH was 7.2-7.3, under the following conditions of SBP, U/mL and initial H_2O_2, mM: 0.15/1.16 •; 0.20/1.16, ■; 0.30/2.32, ♦; 0.30/1.16,▲.

H_2O_2 was added in single step in the CSTR, used as a pre-mixer.

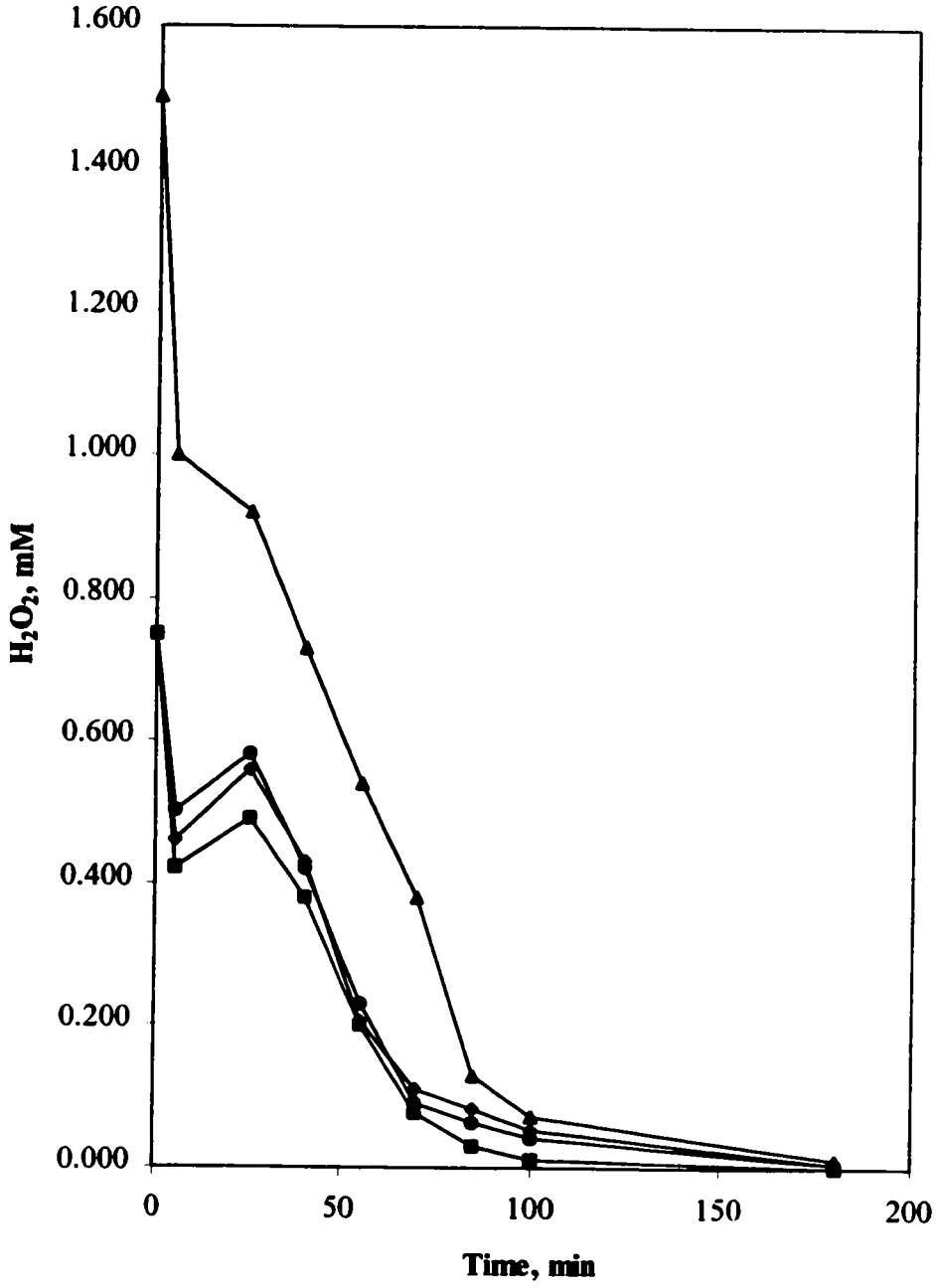

Fig. 4.6.2.8 Change in H_2O_2 concentration, fed in steps of two, with time during removal of aniline in the continuous-flow column

Integrated continuous-flow column studies with initial nitrobenzene, entering the Fe^0 column, of 1 mM. Effective aniline after dilution with peroxide and SBP was 0.8 mM. Influent pH was 7.2-7.3, under the following conditions of SBP, U/mL and initial H_2O_2, mM: 0.15/0.75, •; 0.20/0.75, ■; 0.30/1.5, ♦; 0.30/0.75, ▲.

H_2O_2 was fed in steps of two-thirds and one-third in the two CSTRs in series.

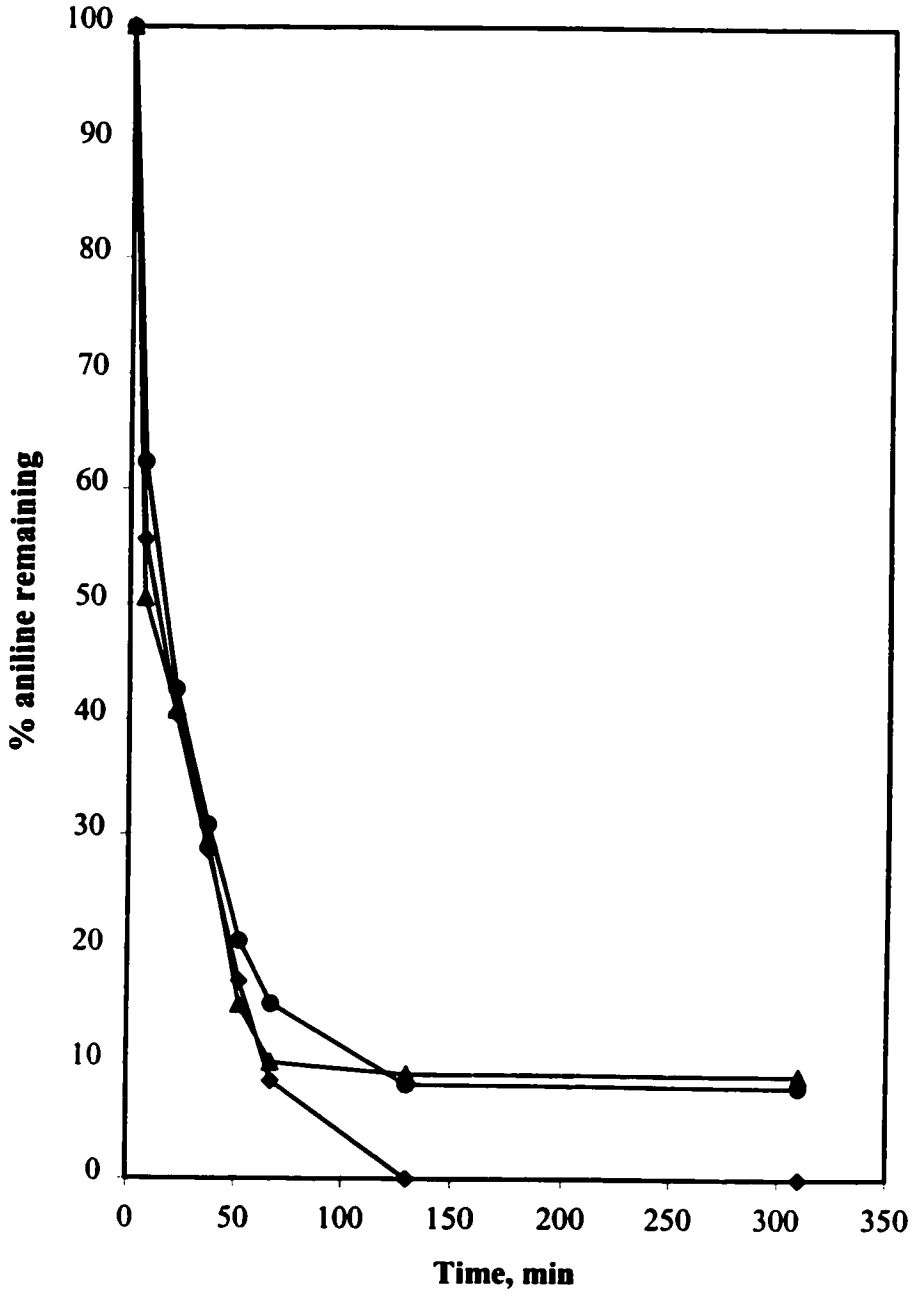

Fig. 4.6.3.1 Optimization of SBP concentration in the continuous-flow column for aniline polymerization

Integrated continuous-flow column studies with initial nitrobenzene, entering the Fe^0 column, of 1 mM. Effective aniline, after dilution with peroxide and SBP, was 0.8 mM. $[H_2O_2]$/[aniline] was 1.5 with influent pH of 7.2-7.3, under the following conditions of SBP concentration, U/mL: 0.15, •; 0.20, ♦; 0.30, ▲.

It is interesting to note that the removal efficiency did not get better with higher enzyme concentration. This was due to the fact that at higher enzyme concentration, 0.30 U/mL, and the same peroxide to substrate ratio of 1.5, the catalase activity of the crude enzyme consumed a greater amount of H_2O_2 than during the reaction when only 0.20 U/mL of enzyme was used. Similar results were obtained for other substrates also, Figures 4.6.3.2-4.6.3.4. However, from Fig. 4.6.3.4 it is seen that enzyme concentration greater than the optimum value does not have a negative effect on the removal efficiency of *p*-toluidine. This could be due to the fact that there is about 15-fold less crude SBP present for *p*-toluidine as there is for aniline and *o*-toluidine. Hence, the catalase action of the enzyme is less significant on *p*-toluidine.

It has been reported that enzyme *turnovers* could be increased by adding enzyme aliquots over a period of time thereby maintaining a low instantaneous active enzyme concentration (Nakamoto and Machida, 1992). It was speculated that a low active enzyme to substrate ratio would reduce the chances of a free radical reaction at the enzyme active site due to a competition for the scant sites. Nicell *et al.* (1993) made a comparison between batch, semi-batch, single CSTR and multiple CSTRs in series. They concluded that the number of reactor turnovers was increased several fold when a low instantaneous enzyme concentration was maintained. They observed that the reaction in a semi-batch mode more than doubled the catalyst turnovers as compared to a batch reactor. To achieve semi-batch/continuous mode of operation in the present study, two CSTRs with detention times of 5 min and 18 min, respectively, were used in series, Figure 4.6.3.5. In the first CSTR with 5 min detention time, 50% of the required amount of SBP was added. The stream after coming out of the first CSTR was directed to the

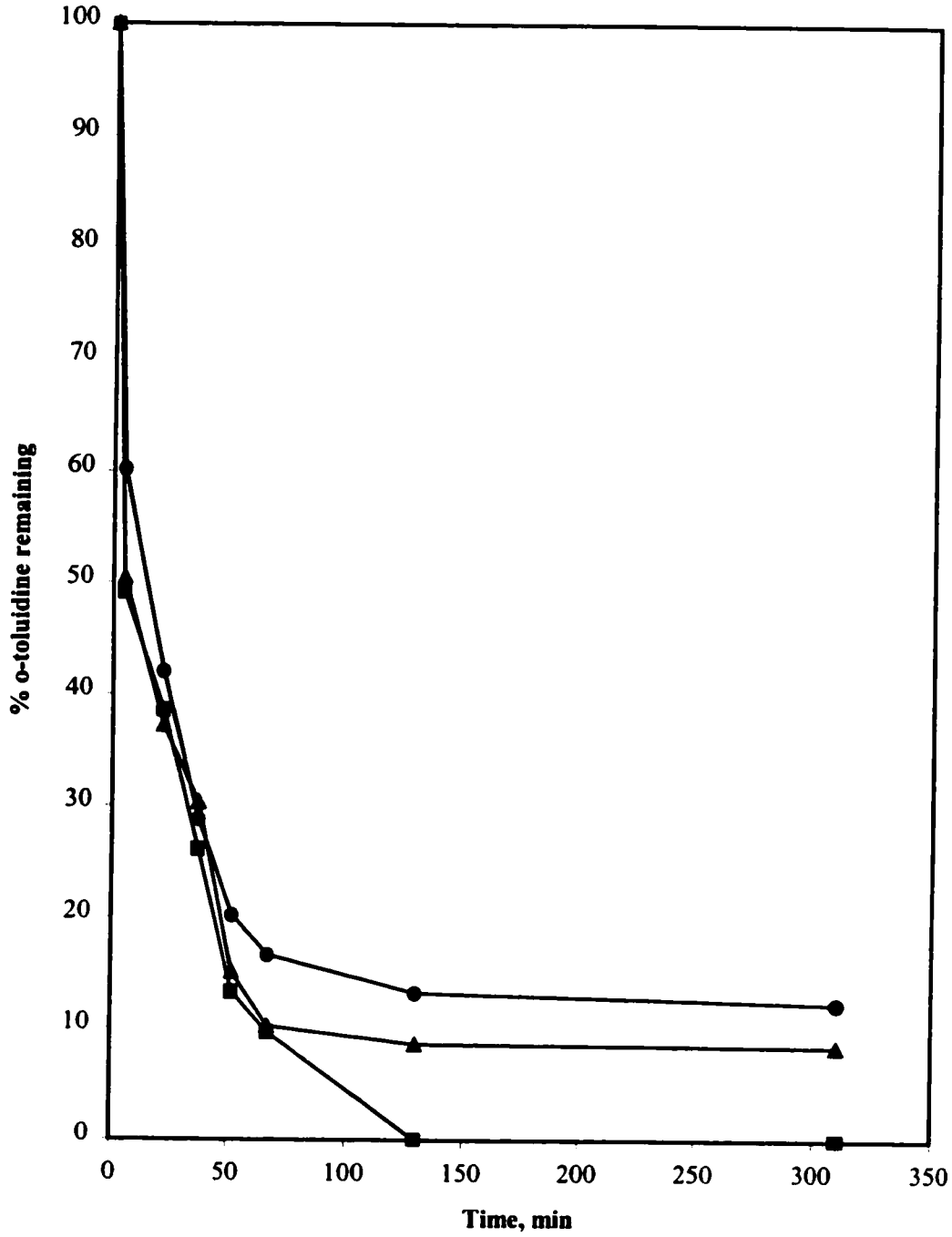

Fig. 4.6.3.2 Optimization of SBP concentration in the continuous-flow column for *o*-toluidine polymerization

Integrated continuous-flow column studies with initial *o*-nitrotoluene, entering the Fe^0 column, of 1 mM. Effective *o*-toluidine, after dilution with peroxide and SBP, was 0.8 mM. $[H_2O_2]/[o\text{-toluidine}]$ was 1.5 with influent pH of 7.4, under the following conditions of SBP concentration, U/mL: 0.20, •; 0.23, ■; 0.26, ▲.

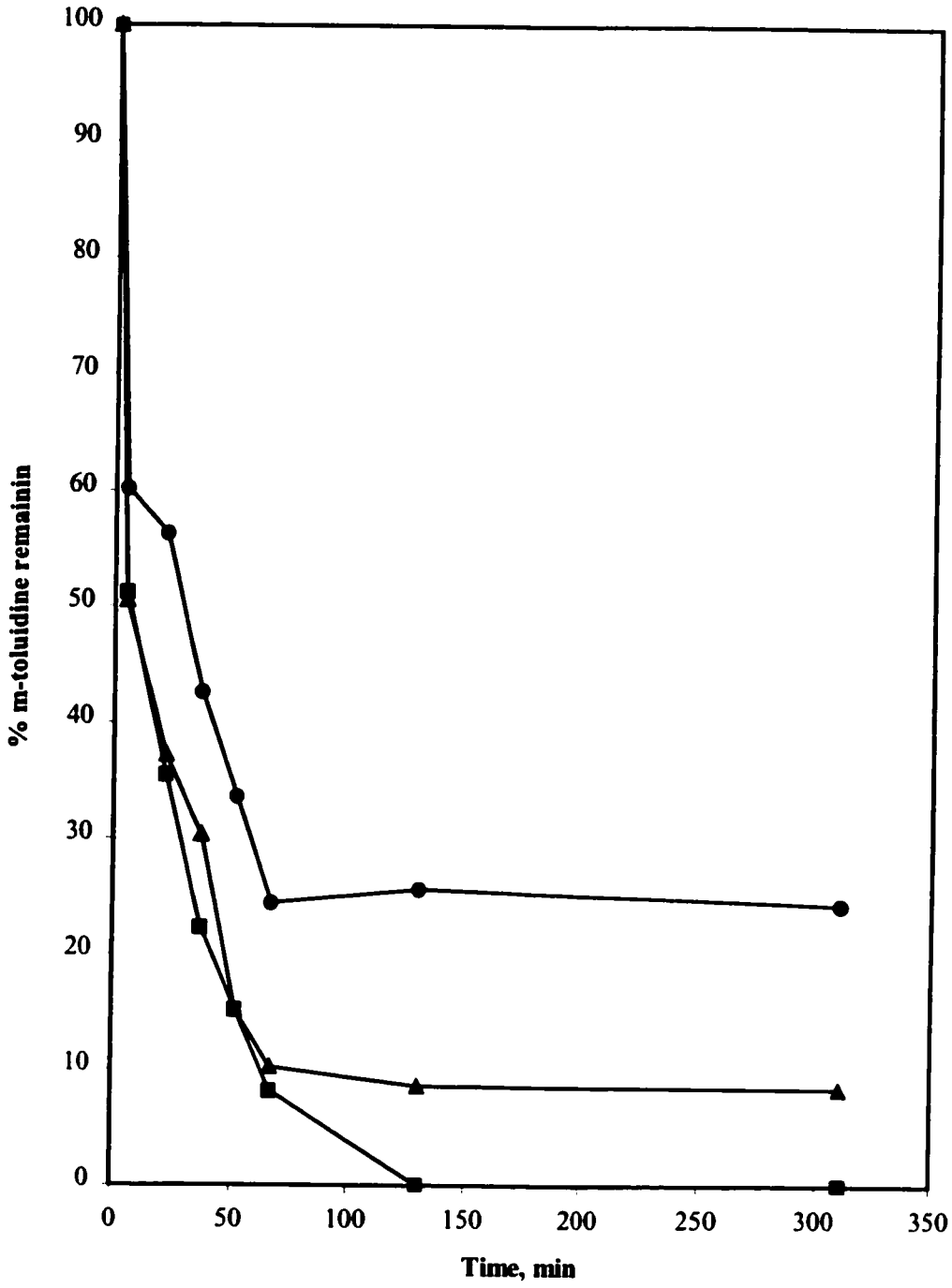

Fig. 4.6.3.3 Optimization of SBP concentration in the continuous-flow column for *m*-toluidine polymerization

Integrated continuous-flow column studies with initial *m*-nitrotoluene, entering the Fe^0 column, of 1 mM. Effective *m*-toluidine, after dilution with peroxide and SBP, was 0.8 mM. $[H_2O_2]$/[*m*-toluidine] was 1.5 with influent pH of 7.4, under the following conditions of SBP concentration, U/mL: 0.07, •; 0.10, ■; 0.15, ▲.

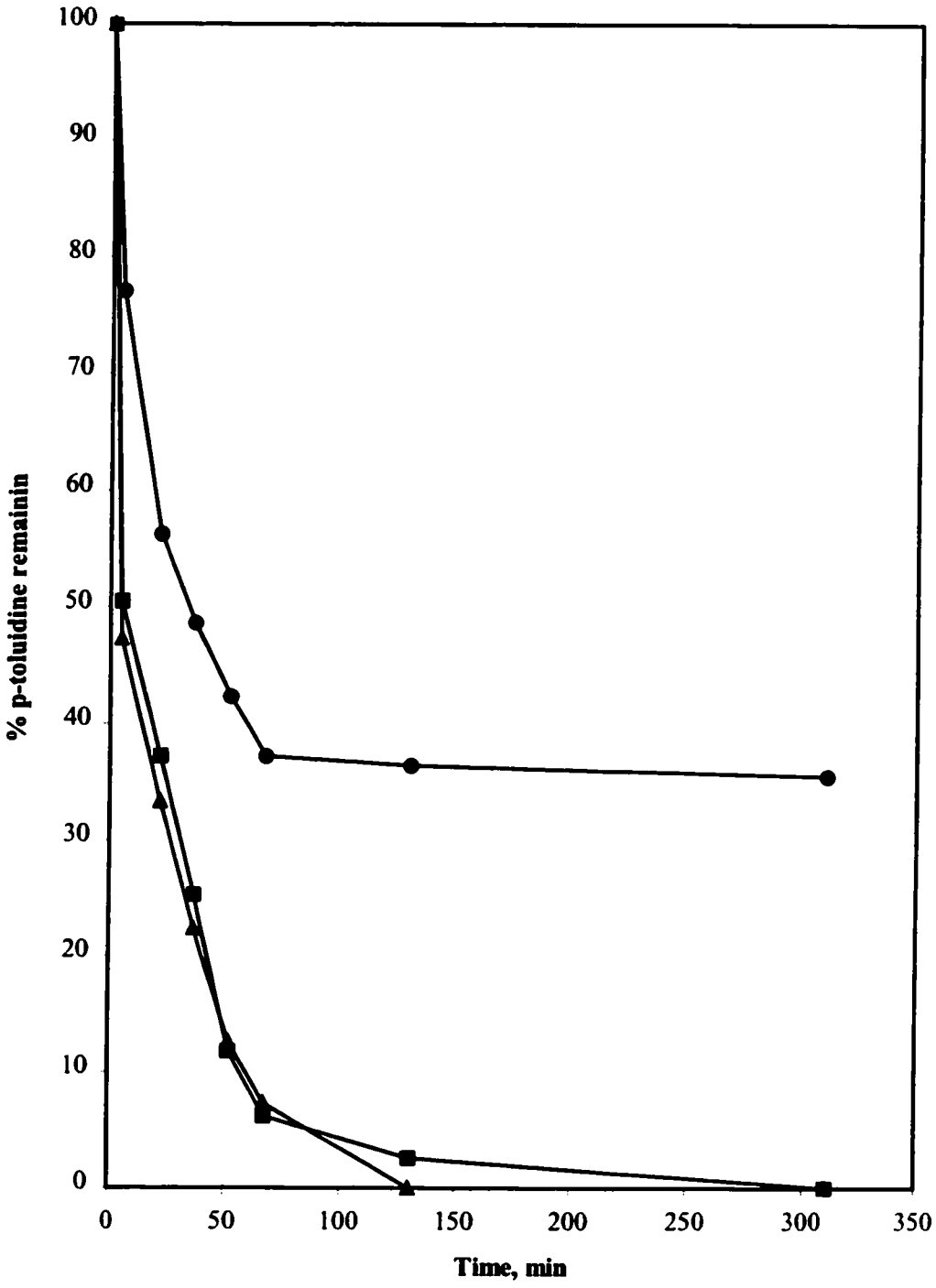

Fig. 4.6.3.4 Optimization of SBP concentration in the continuous-flow column for *p*-toluidine polymerization

Integrated continuous-flow column studies with initial *p*-nitrotoluene, entering the Fe^0 column, of 1 mM. Effective *p*-toluidine, after dilution with peroxide and SBP, was 0.8 mM. $[H_2O_2]/[p\text{-toluidine}]$ was 1.5 with influent pH of 7.4, under the following conditions of SBP concentration, U/mL: 0.005, •; 0.010, ■; 0.015, ▲.

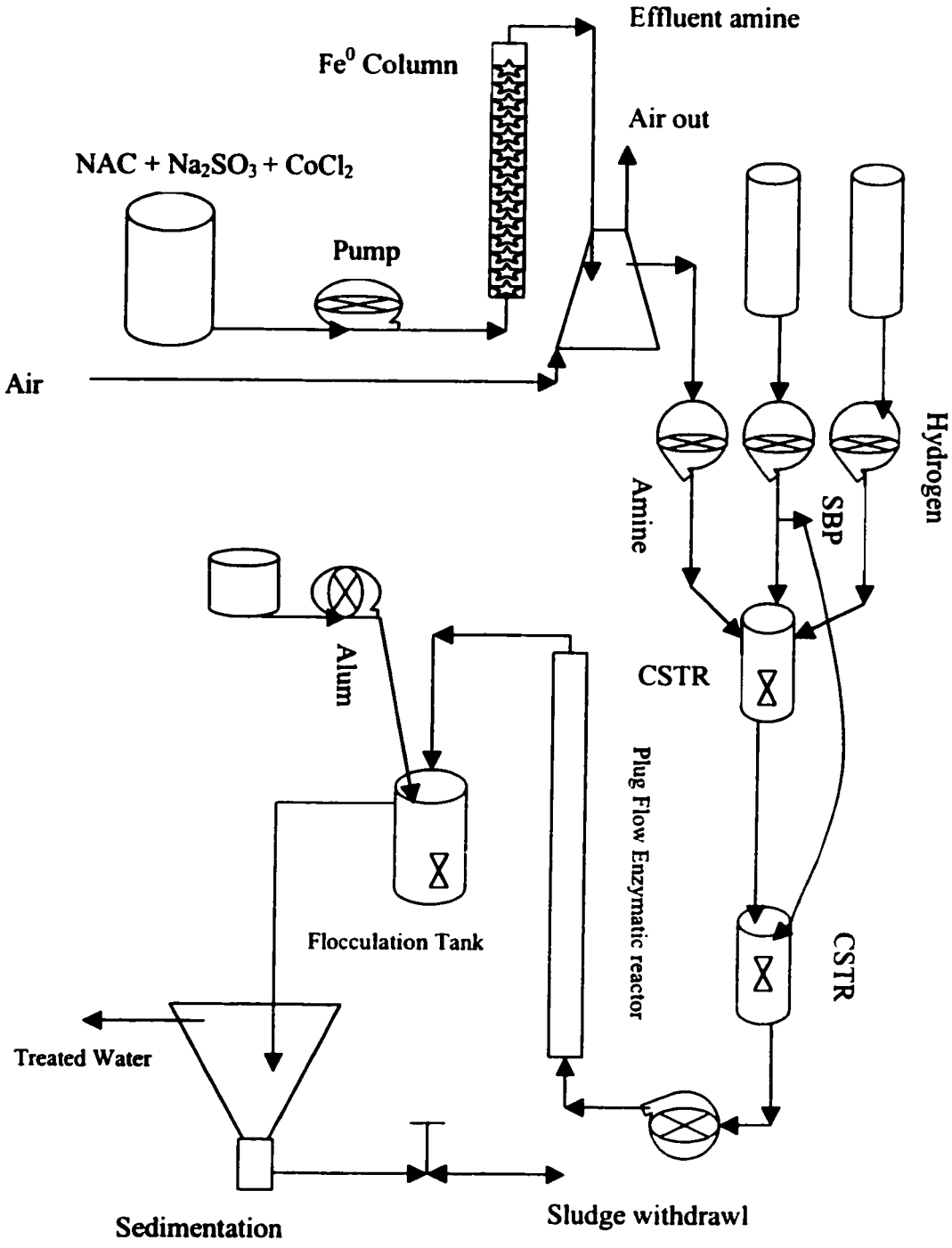

Fig. 4.6.3.5 Schematic of the Continuous-flow system using 2 CSTRs as pre-mixers, where SBP was added in steps

next CSTR with 18 min detention time where the remaining 50% of required total SBP was added to provide the optimum SBP dosage, as found previously. Then the stream entered the PFR. However, in the present study, step-wise feeding of enzyme showed minor improvement in terms of reduced reaction time which may, in effect, be regarded as either reduced enzyme concentration or increased substrate removal, Figure 4.6.3.6. This confirms the findings of other researchers (Al-Kassim *et al.*, 1993). On the contrary, due to the presence of excess instantaneous peroxide, the enzyme tends to get killed and deactivated. In Figures 4.6.3.7 and 4.6.3.8, soybean peroxidase activity is shown as a function of time during the removal of aniline, formed from reduction of NB. It is seen that, either in the presence of excess H_2O_2, as in Fig. 4.6.3.7, or during the step-wise feeding of the enzyme, as in Fig. 4.6.3.8 where the peroxide is present in instantaneous excess, the SBP activity falls quite rapidly due to inactivation by H_2O_2. Hence, there is less than optimum removal of substrate even when there is excess enzyme concentration.

It is possible that step-wise feeding of both H_2O_2 and enzyme at the same time may have had a different effect. However, this was not investigated in the present study.

It is observed that both excess enzyme and excess peroxide are detrimental to the reaction. It is interesting to note that suicide inactivation of peroxidase by H_2O_2 is a known phenomenon (Arnao *et al.*, 1990 and Baynton *et al.*, 1994). However, because of the crude nature of the enzyme SBP, destruction of peroxide by excess enzyme is also seen here. Figure 4.6.3.9 shows the changes in aniline and peroxide concentrations and SBP activity with time and pertains to the situation where only 1 CSTR with 5 min detention time was used as a pre-mixer before the PFR with SBP and hydrogen peroxide being added in single step in the CSTR.

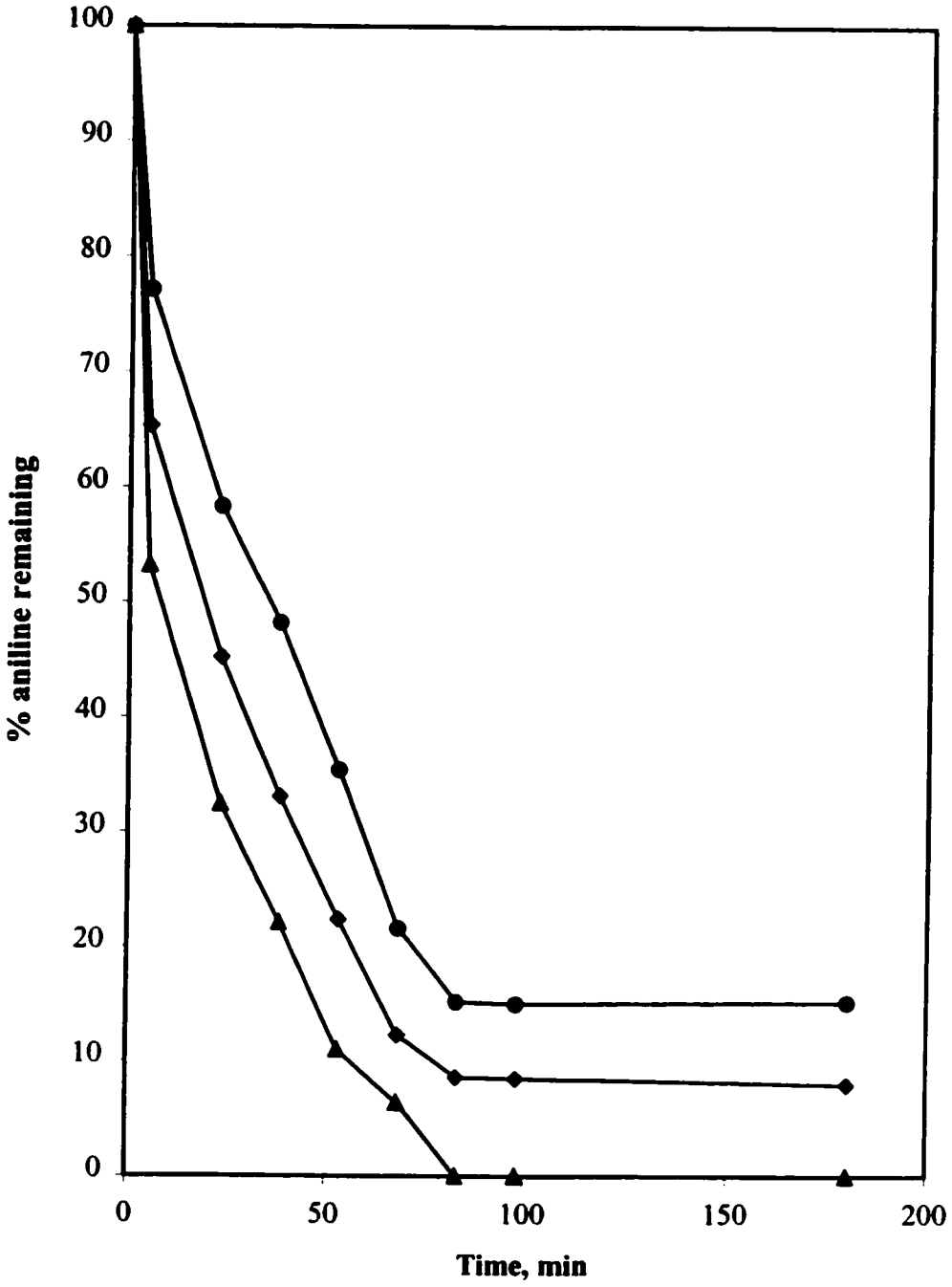

Fig. 4.6.3.6 Step-wise feeding of SBP in the continuous-flow column for aniline polymerization

Integrated continuous-flow column studies with initial nitrobenzene, entering the Fe^0 column, of 1 mM. Effective aniline, after dilution with peroxide and SBP, was 0.8 mM. $[H_2O_2]$/[aniline] was 1.5 with influent pH of 7.2-7.3, under the following conditions of SBP concentration, U/mL: 0.15, •; 0.20, ♦; 0.30, ▲. SBP was fed in steps of half and half in the two CSTRs in series.

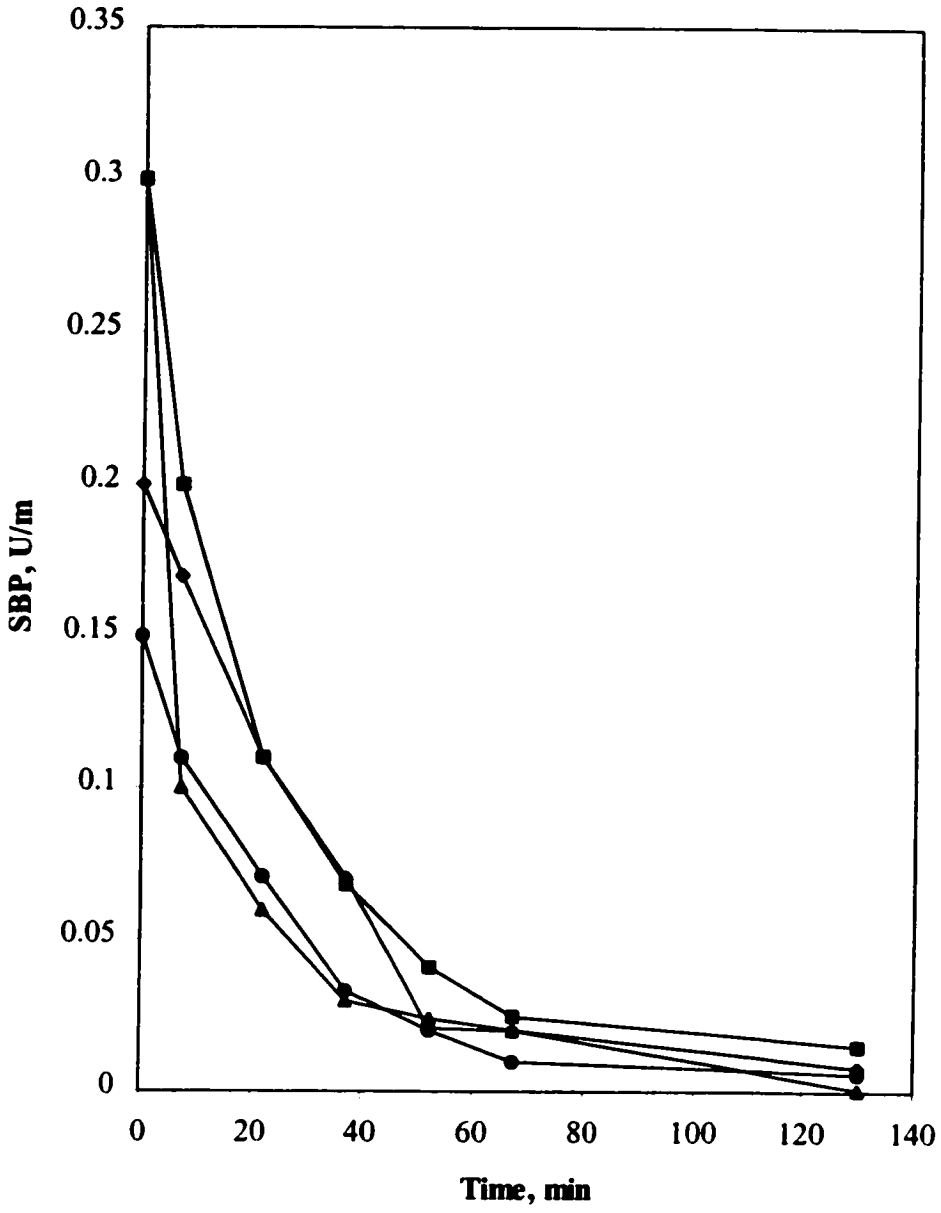

Fig. 4.6.3.7 Change in SBP activity with time during removal of aniline in the continuous-flow column

Integrated continuous-flow column studies with initial nitrobenzene, entering the Fe^0 column, of 1 mM. Effective aniline after dilution with peroxide and SBP was 0.8 mM. Influent pH was 7.2-7.3, under the following conditions of $[H_2O_2]$/[aniline] and initial SBP, U/mL: 1.5/0.15, •; 1.5/0.20, ♦; 3.0/0.30, ▲; 1.5/0.30, ■.

SBP was added in single step in the CSTR, used as a pre-mixer, in different initial concentrations.

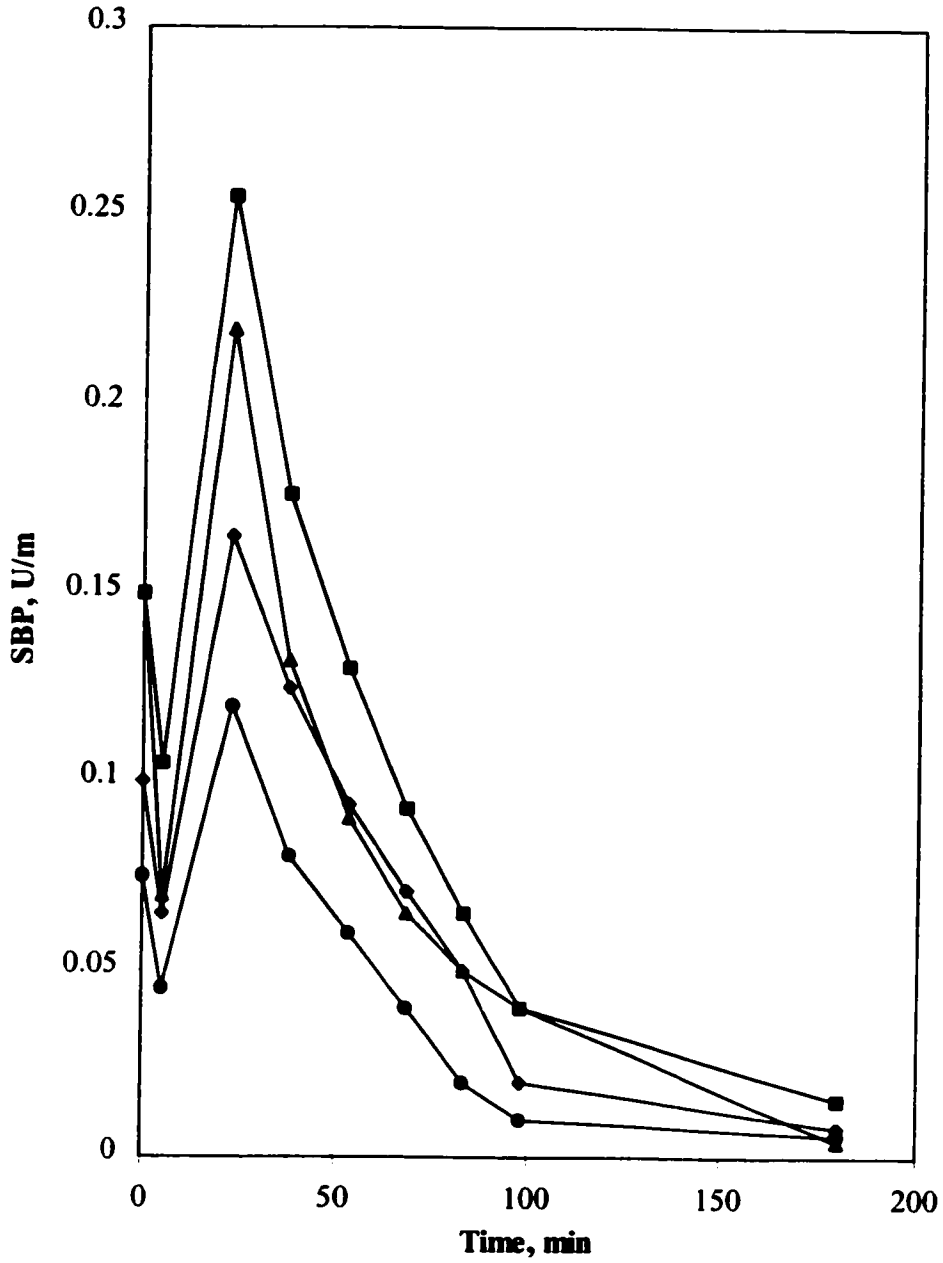

Fig. 4.6.3.8 Change in SBP activity, fed in steps of two, with time during removal of aniline in the continuous-flow column

Integrated continuous-flow column studies with initial nitrobenzene, entering the Fe^0 column, of 1 mM. Effective aniline after dilution with peroxide and SBP was 0.8 mM. Influent pH was 7.2-7.3, under the following conditions of $[H_2O_2]$/[aniline] and initial SBP, U/mL: 1.5/0.08, •; 1.5/0.10, ♦; 3.0/0.15, ▲; 1.5/0.15, ■.

SBP was added in steps of half and half in the two CSTRs in series, used as pre-mixers, in different initial concentrations.

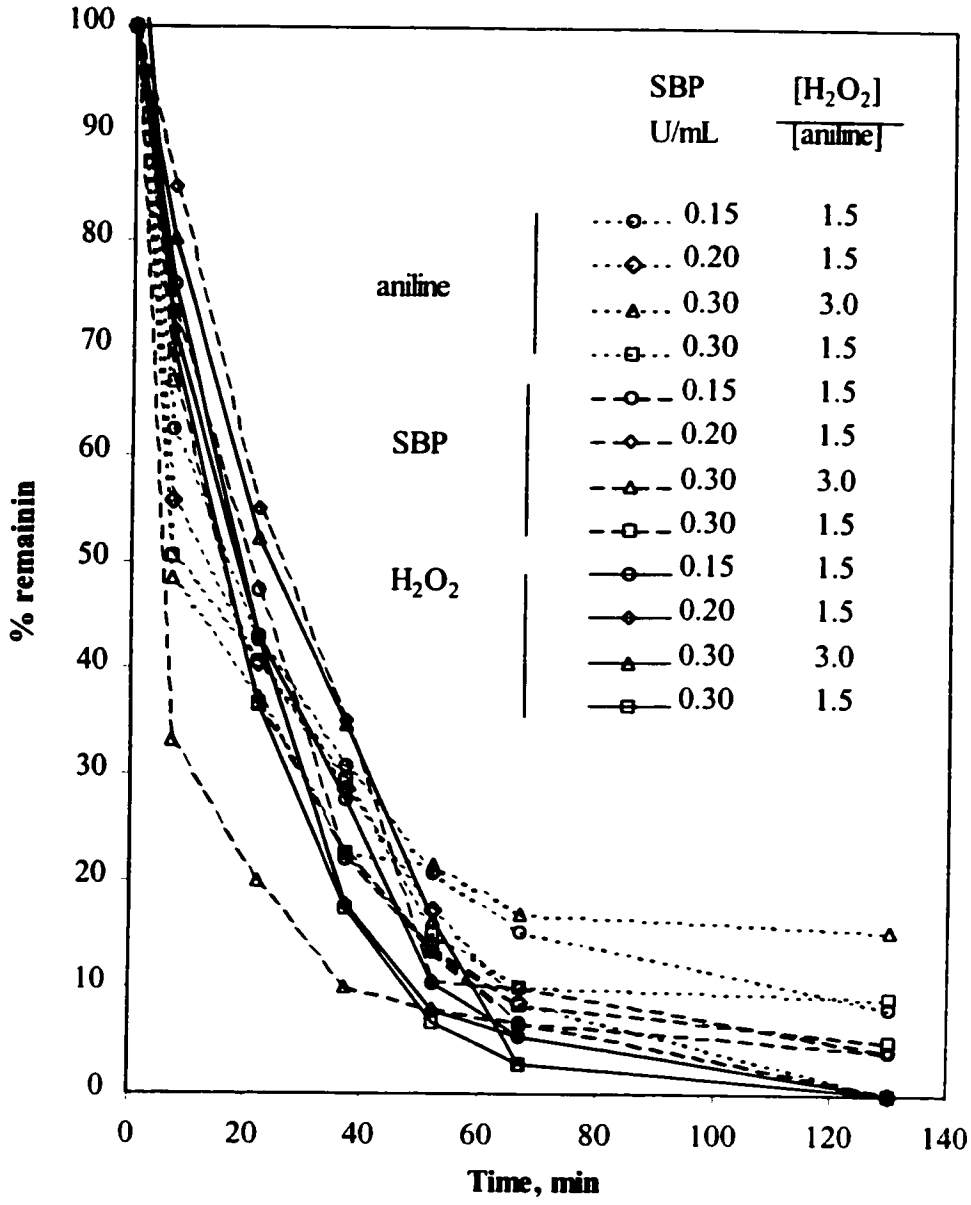

Fig. 4.6.3.9 % change in concentrations of aniline and peroxide and SBP activity with time during removal of aniline in the continuous-flow column

Integrated continuous-flow column studies with initial nitrobenzene, entering the Fe^0 column, of 1 mM. Effective aniline after dilution with peroxide and SBP was 0.8 mM. Influent pH was 7.2-7.3. SBP and H_2O_2 were added in single step in the CSTR, used as a pre-mixer, in different initial concentrations.

4.6.4 Summary of Results

A summary of the optimum reaction parameters, involved in the enzymatic stage of the two-stage continuous-flow operation for the four NACs, is given in the Table 4.6.4.

Detention time in the Fe^0 column, for NAC reduction, was about 8-10 min. An aeration time of 30 min was required for complete conversion of Fe^{2+} to Fe^{3+} and Na_2SO_3 to Na_2SO_4. The reaction time in the second stage, for conversion of anilines to insoluble polymers, was about 1 h, while 3-3½ h were provided for flocculation and sedimentation. Thus the entire process took about 5-5½ h for complete treatment.

Table 4.6.4 Summary of Optimum Reaction Parameters in the enzymatic stage.

Influent NAC at 1 mM was fed through the continuous-flow system (Figure 3.1) as described. The intermediate anilines, after dilution due to addition of peroxide and SBP, were 0.8 mM. All data shown pertain to this final substrate concentration.

NAC	Amine produced	Optimum pH range	Enzyme concentration	$\frac{[H_2O_2]}{[Substrate]}$
nitrobenzene	aniline	5.5-8.0	0.20 U/mL	1.5
o-nitrotoluene	*o*-toluidine	5.5-8.0	0.23 U/mL	1.5
m-nitrotoluene	*m*-toluidine	5.5-8.0	0.10 U/mL	1.5
p-nitrotoluene	*p*-toluidine	5.5-8.0	0.01 U/mL	1.5

CHAPTER 5 MODEL DEVELOPMENT

Kinetic modeling of a reaction is important in developing its reactor system. A kinetic model is a helpful tool to design a reactor system and predict its behavior under different conditions, which in turn helps in optimizing the economics of a process.

5.1 Model Choice

The scope of the present study did not include kinetic model development for the two stages of the operation. However, an attempt has been made to represent the data obtained in the second step of the two-step continuous flow process by a suitable mathematical model.

Soybean peroxidase catalyzed reaction involves two substrates (hydrogen peroxide and aniline). Hence, the enzyme-catalyzed reaction merits treatment as two substrate-two product reaction. This type of reaction is referred to as "bi-bi" reaction (Dunford, 1992). He proposed a modified Ping-Pong Bi-Bi mechanism as shown below:

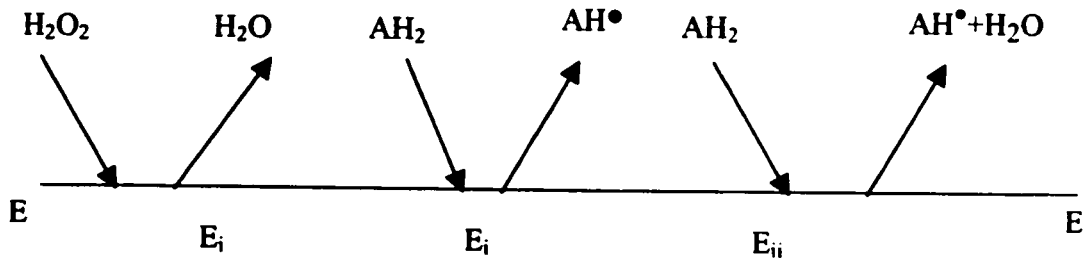

Fig. 5.1.1 Ping-Pong Bi-Bi mechanism for peroxidase

Based on the arguments in Section 2.6, it was conjectured that the most suitable model to represent the present set of data was Model 5 (Ibrahim, 1998) discussed earlier in Section 2.6.2.5:

$$-\frac{d[AH_2]}{dt} = \frac{k_{cat}E_a[AH_2][H_2O_2]}{K_1[AH_2]+K_2[H_2O_2]+[AH_2][H_2O_2]} \qquad (2.6.2.5.1)$$

$$-\frac{dE_a}{dt} = k_r E_a \sqrt{-\frac{d[AH_2]}{dt}} + k_a E_a[H_2O_2] \qquad (2.6.2.5.2)$$

$$[H_2O_2] = [H_2O_2]_0 - \alpha\{[AH_2]_0 - [AH_2]\} \qquad (2.6.2.5.3)$$

where, k_{cat} is the turnover number for the enzyme, E_a represents all forms of the enzyme which have not been permanently inactivated, K_1 is the Michaelis constant of H_2O_2, K_2 is the Michaelis constant of aniline, k_r is the inactivation rate constant of the enzyme arising due to free radicals, k_a is the inactivation rate constant of the enzyme due to H_2O_2 and α is the molar ratio between H_2O_2 and aniline.

Matlab (version 5.3) was employed for analyzing the experimental data obtained in this study. Owing to lack of sufficient initial rate data, K_1 and K_2 were not evaluated independently. Use was made of previous data (Ibrahim, 1998).

The calibration of the model was done with the purpose of estimating k_a, k_r and k_{cat}, since it was known from previous data (Ibrahim, 1998) that K_1, K_2 and α were not significantly different from the initial rate estimation data and stoichiometry respectively. k_r was determined to be 6.21 $M^{-0.5}s^{-0.5}$ in the absence of polyethylene glycol (PEG) (Nicell and Buchanan, 1997). PEG was not used in this study. Initial assumed values for parameters are shown in Table 5.1.1.

The objective function to be minimized in this case was defined as the sum of the squares of the differences between modeled and experimentally obtained substrate concentrations (Ibrahim, 1998). The error function may be represented as:

$$\text{Error} = \sum_{i=1}^{n} \sum_{j=1}^{m_j} \left([AH_2]_{i,j} - [AH_2]_{i,j_{model}} \right)^2 \qquad (5.1.1)$$

where, n represents the number of calibration data sets; m_j represents the number of observations in the i^{th} data set; and $[AH_2]_{i,j}$ and $[AH_2]_{i,jmodel}$ are experimental and calculated (model) substrate concentrations respectively.

The estimated kinetic constants are shown in Table 5.1.2 (Mantha *et al.*, 2001c).

Figures 5.1.2-5.1.4 show the experimental data and the trend predicted by the model. It is observed that the data fit the model reasonably well for H_2O_2 concentration and SBP activity. However, the model under-predicts the removal of aniline at short period of reaction.

Table 5.1.1 Initial assumed values of different parameters (Ibrahim, 1998)

Parameter	Value
k_{cat}	1038 s^{-1}
K_1	0.12 mM
K_2	8.84 mM
k_a	1.676 $M^{-1}s^{-1}$
k_r	6.21 $M^{-0.5}s^{-0.5}$
α	1.5

Table 5.1.2 Calculated parameters from data

Parameter	Value
k_{cat}	1104 s^{-1}
K_1	0.12 mM
K_2	8.84 mM
k_a	1.10 $M^{-1}s^{-1}$
k_r	3.10 $M^{-0.5}s^{-0.5}$
α	1.5

Integrated continuous-flow column studies with initial nitrobenzene, entering the Fe^0 column, of 1 mM. Effective aniline after dilution with peroxide and SBP, 0.2 U/mL, was 0.8 mM. Influent pH was 7.2-7.3 with an optimum $[H_2O_2]/[aniline]$ of 1.5.

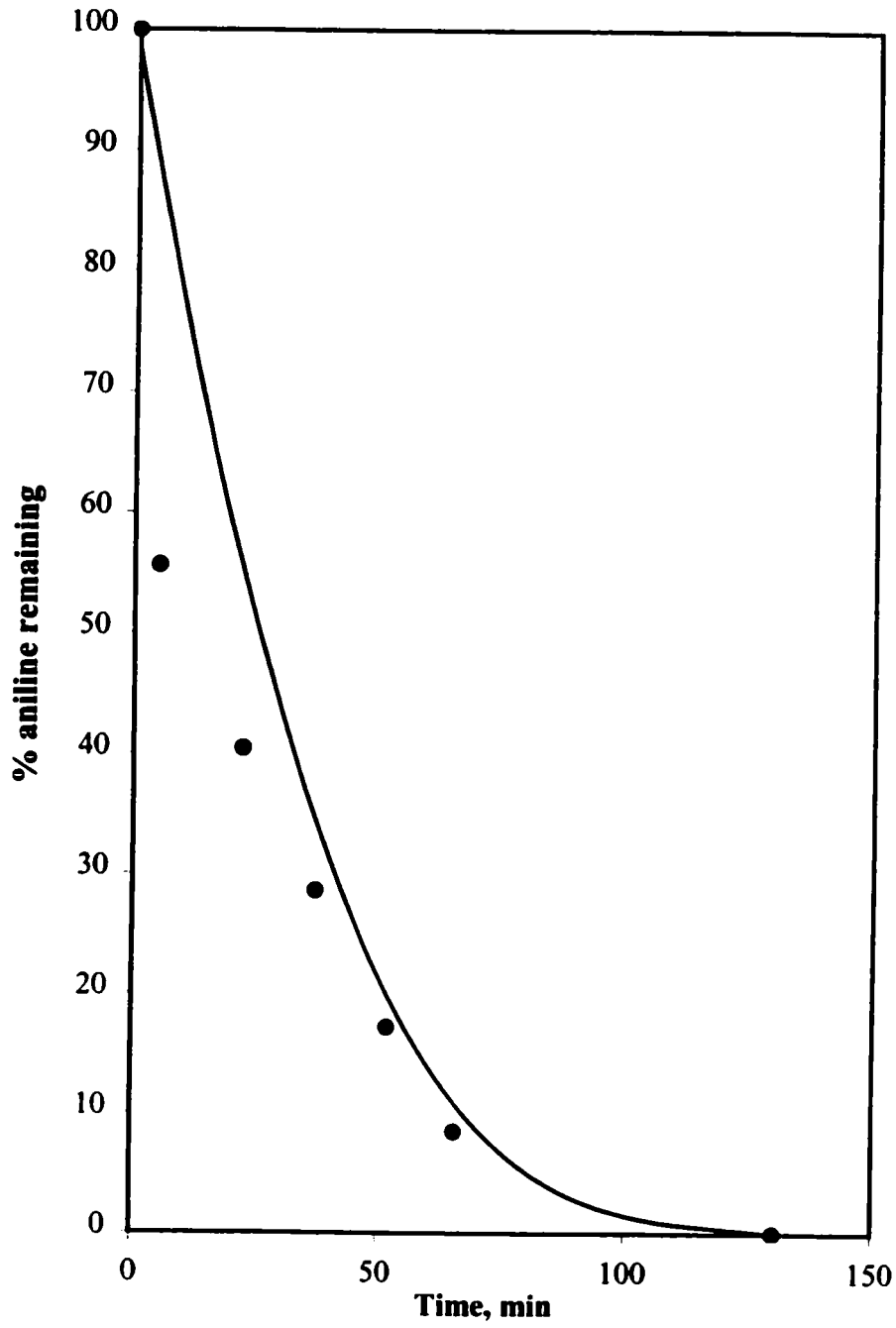

Fig. 5.1.2 Model prediction of aniline polymerization
Integrated continuous-flow column studies with initial nitrobenzene, entering the Fe^0 column, of 1 mM. Effective aniline after dilution with peroxide and SBP, 0.2 U/mL, was 0.8 mM. Influent pH was 7.2-7.3 with an optimum $[H_2O_2]$/[aniline] of 1.5. Experimental data, ●; Model prediction, —.

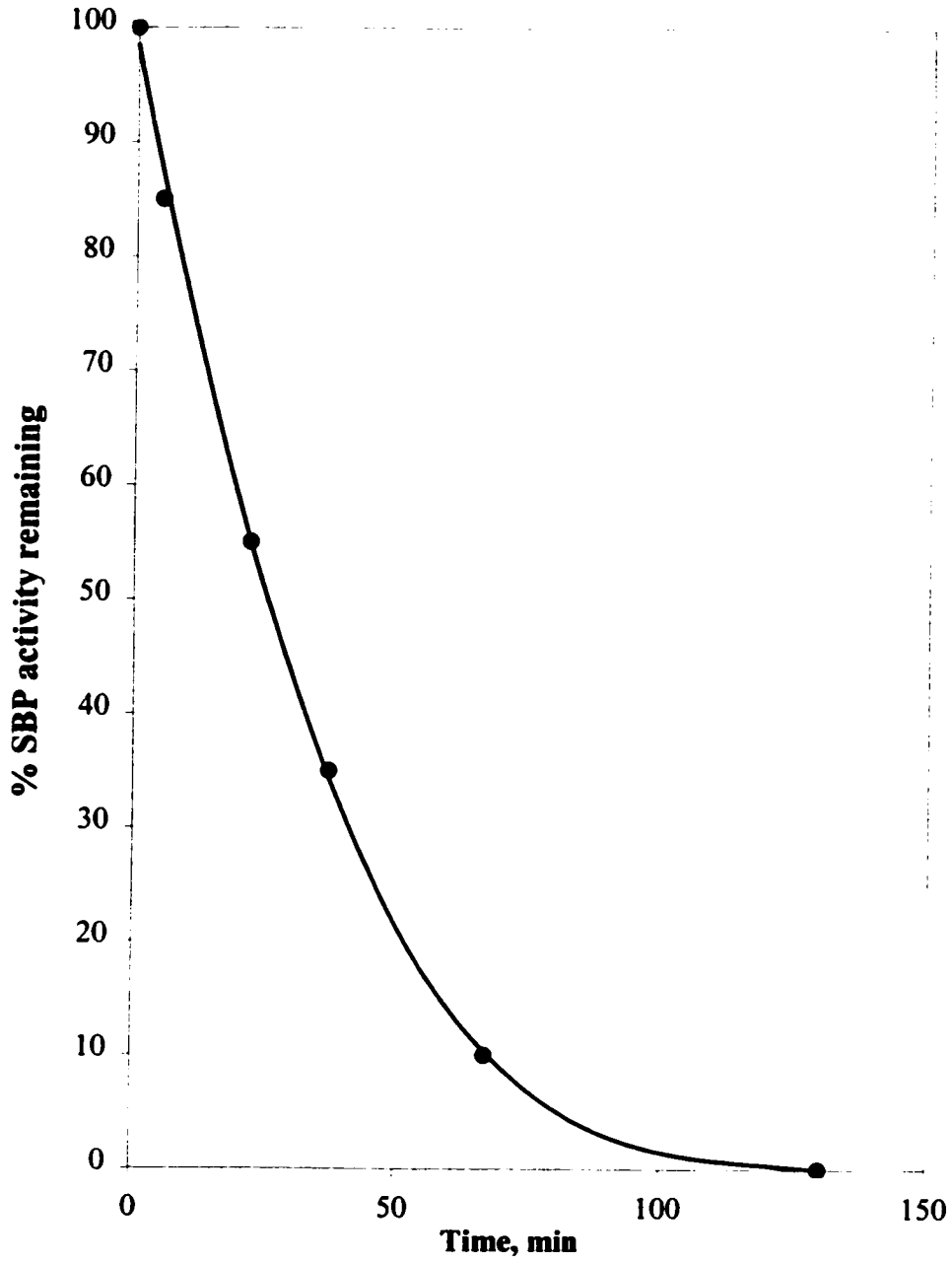

Fig. 5.1.3 Model prediction of SBP activity during aniline polymerization
Integrated continuous-flow column studies with initial nitrobenzene, entering the Fe^0 column, of 1 mM. Effective aniline after dilution with peroxide and SBP, 0.2 U/mL, was 0.8 mM. Influent pH was 7.2-7.3 with an optimum $[H_2O_2]$/[aniline] of 1.5. Experimental data, ●; Model prediction, —.

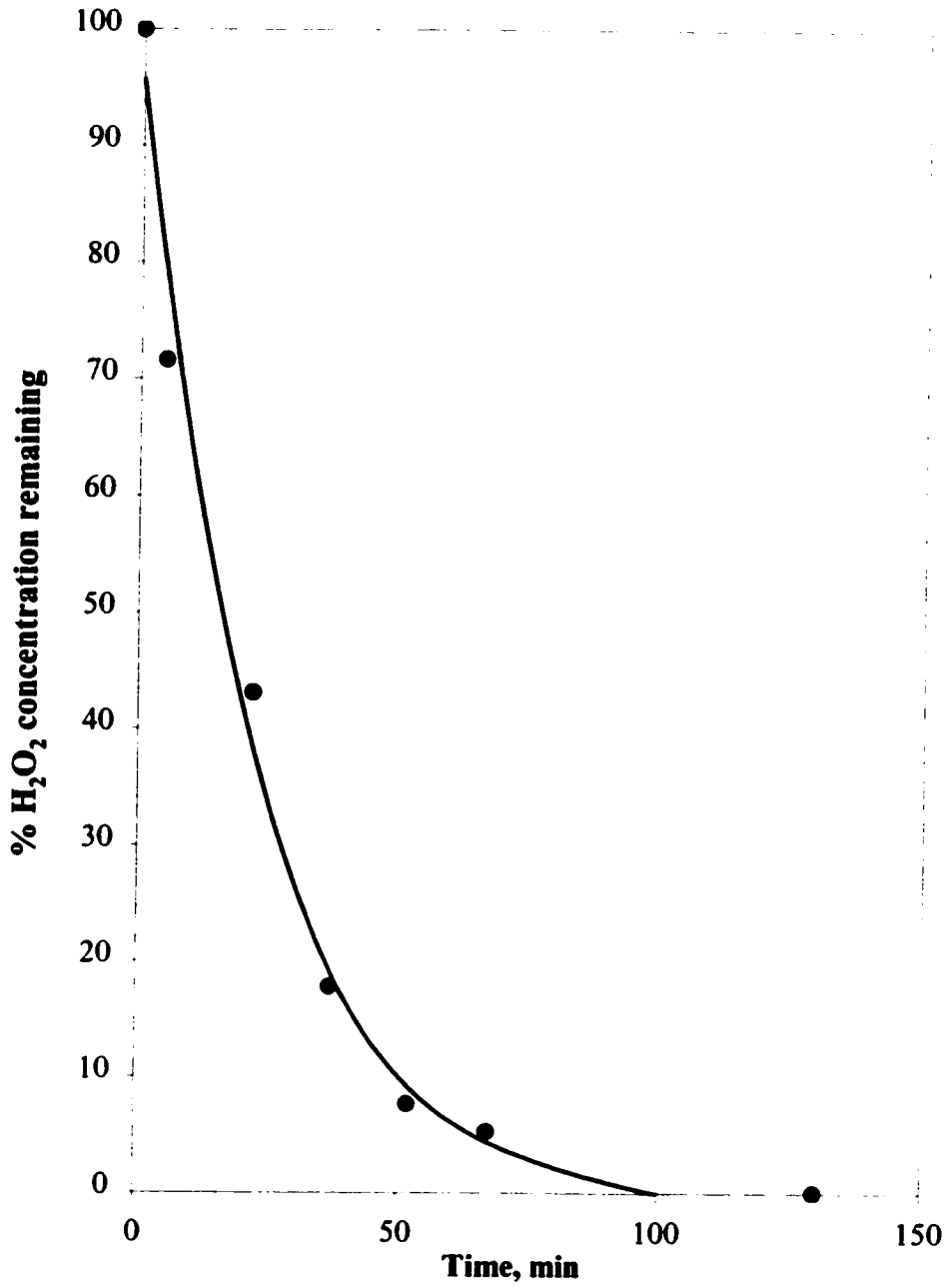

Fig. 5.1.4 Model prediction of H_2O_2 concentration during aniline polymerization
Integrated continuous-flow column studies with initial nitrobenzene, entering the Fe^0 column, of 1 mM. Effective aniline after dilution with peroxide and SBP, 0.2 U/mL, was 0.8 mM. Influent pH was 7.2-7.3 with an optimum $[H_2O_2]$/[aniline] of 1.5. Experimental data, ●; Model prediction, —.

CHAPTER 6 CONCLUSIONS AND RECOMMENDATIONS

6.1 Conclusions

6.1.1 Fe^0 reduction of NACs

- Sodium sulfite in conjunction with cobalt chloride was found to be an efficient oxygen scavenger. Also, it is practical to use chemical scavenging, rather than to use degassed solution.
- Batch reactor data indicated that some amount of the aniline, formed due to reduction of NAC by Fe^0, always remained attached to the iron surface due to adsorption. The adsorption isotherm was well described by a Langmuir isotherm. pH played a major role in the adsorption process, although the conversion itself was independent of the solution pH. In the continuous-flow system, however, the extent of reaction was not affected by sorption.
- NACs investigated in this study were quantitatively reduced by Fe^0 column. Corrosion products formed in the reduction process, caused plugging and porosity reduction and were identified as maghemite by EDS-spectrum and X-ray diffraction analyses. However, once the bed was cleaned *in situ*, it could be used again for the reduction process.

6.1.2 Enzymatic reaction of amines

- Loss of activity of the crude SBP was faster at room temperature than it was when refrigerated.

- PEG had no significant effect either on the removal of anilines or on the savings on enzyme dose.
- Oxidative polymerization of aryl amines exhibited a wide optimum range of pH.
- $[H_2O_2]$/[amine] was similar for all the aryl amines investigated here for both in batch and in continuous-flow systems. A deficiency in peroxide reduced the aniline removal efficiency, while an increase had the effect of inactivating the enzyme, resulting in reduced removal efficiency of the amines. Step-wise feeding of H_2O_2 did not reflect any benefit on savings either on peroxide or on enzyme.
- The optimum enzyme concentration to remove anilines was found to be a fixed value depending on NAC concentration, any deviation from which results in reduced removal efficiency. Step-wise feeding of the enzyme showed no savings in the peroxide or the enzyme. The removal efficiency was also not affected.
- The optimum concentrations of enzyme and H_2O_2 obtained from the batch reactor studies can be applied to the continuous flow reactor to obtain the same removal efficiency of anilines.
- The effluent from the Fe^0 column containing anilines also had Fe^{2+} and Na_2SO_3, which interfered with the enzymatic treatment of the anilines. It was found that unless Fe^{2+} and Na_2SO_3 were removed completely, enzymatic oxidation was not efficient. Thus, pre-aeration was required until Fe^{2+} and Na_2SO_3 were oxidized completely. Once Fe^{2+} and Na_2SO_3 were oxidized completely, the solution behaved as if it contained pure anilines. Therefore, various parameters optimized for pure anilines in batch reactors could be utilized to describe the treatment of anilines formed due to reduction of NACs in the Fe^0 column.

- Use of two CSTRs in series before the PFR did not improve the efficiency of the system in terms of either savings in enzyme or peroxide.
- Addition of alum was necessary to settle the precipitates from the reaction mixture by gravity.

6.2 Recommendations

Further investigations are necessary before the two-step treatment strategy can become a viable alternative to the treatment strategies currently in vogue. The following recommendations are made for further studies:

- The recommended system should be used to test real industrial wastewater. The effect of industrial wastewater matrix on the overall efficiency of the process should be investigated.
- Researchers have previously used bi-metallic beds to reduce various halogenated aliphatic compounds. Further research is required to study the effects of bi-metallic bed and other zero-valent metals on reduction of NACs.
- The present work was only a feasibility study. Detailed kinetic studies need to be done to get insights into the reduction of NACs by zero-valent metals and the subsequent polymerization of anilines formed.
- Step-wise feeding of both H_2O_2 and SBP at the same time needs to be investigated in detail before reaching a concrete conclusion about the step-wise feeding.
- Individual and overall cost analyses of both the stages need to be done to determine the economic viability of the process and its subsequent application for treatment of wastewater on an industrial scale.

- The products of the SBP-based removal of NACs are oligomers. Higher polymers of anilines, e.g. polyaniline (PANI) find important applications as conductors (Liu *et al.*, 1999). Hence, it would be worthwhile to study the properties of the oligomers formed in the enzymatic treatment step. Also, these end products could further be used to produce higher molecular mass polymers that have conducting properties.
- Toxicity studies of the sludge have to be done before it can safely be disposed to landfill sites.

REFERENCES

Agrawal, A. and Tratnyek, P. G. (1996) Reduction of nitro aromatic compounds by zero-valent iron metal. *Environ. Sci. Technol.* **30**, 153–160.

Aitken, M. D. (1993) Waste treatment applications of enzyme: opportunities and obstacles. *Chem. Eng. Journal.* **52**, 1349-1358.

Al-Kassim, L., Taylor, K. E., Bewtra, J. K. and Biswas, N. (1993) Evaluation of the removal of aromatic and halogenated unsaturated hydrocarbons from synthetic wastewater by enzyme catalyzed polymerization. *48th Purdue Industrial Waste Conference Proceedings*, Lewis Publishers, Chelsea, MI, 413-420.

Al-Kassim, L., Taylor, K. E., Bewtra, J. K. and Biswas, N. (1994) Optimization of phenol removal by fungal peroxidase from *Coprinus macrorhizus* using batch, continuous, and discontinuous semi-batch reactors. *Enzyme Microb. Technol.* **16**, 120-124.

Arnao, M. B., Acosta, M., del Rio, J. A., Varon, R. and Garcia-Canovas, F. (1990) A kinetic study on the suicide inactivation of peroxidase by hydrogen peroxide. *Biochem. Biophys. Acta.* **1041**, 43-47.

Arnold, W. A. and Roberts, A. L. (1998) Pathways of chlorinated ethylene and chlorinated acetylene reaction with Zn(0). *Environ. Sci. Technol.* **32**, 3017–3025.

Arnold, W. A. and Roberts, A. L. (2000) Pathways and kinetics of chlorinated ethylene and chlorinated acetylene reaction with Fe(0) particles. *Environ. Sci. Technol.* **34**, 1794–1805.

Atkins, R. C. and Carey, F. A. (1990) Organic chemistry: A brief course. McGraw-Hill publishing company, 175-176.

Babbitt, H. E., Doland, J. J. and Cleasby, J. L. (1975) Water Supply Engineering, sixth edition, McGraw Hill Book Company Inc., 565-567.

Bailey, J. E. and Ollis, D. F. (1986) Biochemical Engineering Fundamentals, 2nd Edition, McGraw Hill Book Company, New York.

Baynton, K. J., Bewtra, J. K., Biswas, N., and Taylor, K. E. (1994) Inactivation of horseradish peroxidase by phenol and hydrogen peroxide: a kinetic investigation. *Biochem. Biophys. Acta.* 1206, 272-278.

Biswas, K. (1999) Removal of cresols from synthetic wastewater using crude soybean peroxidase. *M.A.Sc. Thesis* at University of Windsor, Windsor, ON.

Blowes, D. W., Ptacek, C. J. and Jambor, J. L. (1997) *In situ* remediation of Cr(VI)-contaminated groundwater using permeable reactive walls: laboratory studies. *Environ. Sci. Technol.* 31, 3348-3357.

Boopathy, R. and Manning, J. F. (1996) Characterization of partial anaerobic metabolic pathway for 2,4,6-trinitrotoluene degradation by a sulfate-reducing bacterial consortium. *Can. J. Microbiol.* **42**, 1203-1208.

Brandvold, D. C. (1975) Water treatment: Industrial & Municipal, Vantage Press Inc., NY, 55-57.

Burris, D. R., Campbell, T. J. and Manoranjan, V. S. (1995) Sorption of trichloroethylene and tetrachloroethylene in a batch reactive metallic iron-water system. *Environ. Sci. Technol.* **29**, 2850–2855.

Burris, D. R., Hatfield, K. and Wolfe, N. L. (1996) Laboratory experiments with heterogeneous reactions in mixed porous media. *J. of Environ. Eng.* **122**, 685-691.

Bush, M. T., Touster, O. and Brockman, J. E. (1951) The production of b-nitropropionate by a strain of Aspergillus flavus. *J. Biol. Chem.* **188**, 685-693.

Butler, E. C. and Hayes, K. F. (2000) Effects of solution composition and pH on the reductive dechlorination of hexachloreoethane by iron sulfide. *Environ Sci. Technol.* **32**, 1276-.

Cantrell, K. J., Kaplan, D. I. and Wietsma, T. W. (1995) Zero-valent iron for the *in situ* remediation of selected metals in groundwater. *J. Haz. Materials.* **42**, 201-212.

Caza, N., Bewtra, J. K., Biswas, N. and Taylor, K. E. (1999) Removal of phenolic compounds from synthetic wastewater using soybean peroxidase *Wat. Res.*, **33**, 3012-3018.

Chang, C. W. and Bumpus, J. A. (1993) Oligomers of 4-chloroaniline are intermediates formed during its biodegradation by *Phanerochaete chrysosporium*. *FEMS Microbiology letters*, **107**, 337-342.

Charlet, L., Liger, E. and Gerasimo, P. (1998) Decontamination of TCE- and U-rich waters by granular iron: Role of sorbed Fe (II). *J. Environ. Eng.* **124**, 25-30.

Chem. & Eng. News (1995) **July 3**,19-22.

Chem. & Eng. News (1996) **June 24,** 41.

Cheng, I. F., Fernando, Q. and Kote, N. (1997) Electrochemical dechlorination of 4-chlorophenol to phenol. *Environ. Sci. Technol.* **31**, 1074-1078.

Chew, C. F. and Zhang, T. C. (1998) *In situ* remediation of nitrate-contaminated groundwater by electrokinetics/ iron wall processes. *Wat. Sci. Technol.* **38**, 135-142.

Chuang F. W., Larson, R. A. and Scully, W. M. (1995) Zero-valent iron-promoted dechlorination of polychlorinated biphenyls. *Environ. Sci. Technol.* **29** 2460-2463.

Cornell, R. M. and Schwertmann, U. (1996) The Iron Oxides, VCH Publishers, NY.

Devlin, J. F., Klausen, J. and Schwarzenbach, R. P. (1998). Kinetics of nitroaromatic reduction on granular iron in recirculating batch experiments. *Environ. Sci. Technol.* **32**, 1941-1947.

Farrell, J., Kason, M., Melitas, N. and Li, T. (2000) Investigation of the long-term performance of zero-valent iron for reductive dechlorination of trichloroethylene. *Environ. Sci. Technol.* **34**, 514-521.

Fiedor, J. N., Bostick, W. D., Jarabek, R. J. and Farrel, J. (1998) Understanding the mechanism of uranium removal from groundwater by zero-valent iron using X-ray photoelectron spectroscopy. *Environ. Sci. Technol.* **32**, 1466-1473.

Gillham, R. W. and O'Hannesin, S. F. (1994) Enhanced degradation of halogenated aliphatics by zero-valent iron. *Ground Water* **32**, 958–967.

Gomori, G. (1955) Preparation of buffers for use in enzyme studies. Methods in Enzymology, Vol I, Eds: Colowick, B. D. and Kaplan, N. D., Academic Press Inc., 138-146.

Gotpagar, J., Grulke, E., Tsang, T. and Bhattacharyya, D. (1997) Reductive dehalogenation of trichloroethylene using zero-valent iron. *Environ. Prog.* **16**, 137-143.

Grittini, C., Malcomso, M., Fernando, Q. and Korte, N. (1995) Rapid dechlorination of polychlorinated biphenyls on the surface of a Pd/Fe bimetallic system. *Environ. Sci. Technol.* **29**, 2898-2900.

Gu, B., Liang, L., Dickey, M. J., Yin, X. and Dai, S. (1998) Reductive precipitation of Uranium (VI) by zero-valent iron. *Environ. Sci. Technol.* **32**, 3366-3373.

Gu, B., Phelps, T. J., Liang, L., Dickey, M. J., Roh, Y., Kinsall, B. L., Palumbo, A. V. and Jacobs, G. K. (1999) Biogeochemical dynamics in zero-valent iron columns: implication for permeable reactive barriers. *Environ. Sci. Technol.* **33**, 2170-2177.

Haderlein, S. B. and Schwarzenbach, R. P. (1993) Adsorption of substituted nitrobenzenes and nitrophenols to mineral surfaces. *Environ. Sci. Technol.* **27**, 316-326.

Haderlein, S. B., Hofstetter, T. B. and Schwarzenbach, R. P. (2000) in Biodegradation of nitroaromatic compounds and explosives; Eds: Spain, J. S., Hughes, J. B. and Knackmuss, H. -J, Lewis Publishers, NY, 311-356.

Higson, F. K. (1992) Microbial degradation of nitroaromatic compounds. Adv. Appl. Microbiol; Eds: Neidleman, S. I.; Laskin, A. I. Academic Press Inc., **37**, 1-19.

Howaldt, M., Kulbe, K. D. and Chmiel, H. (1983) Minimizing enzyme requirement by choice of appropriate reactor type. *Ann. N. Y. Acad. Sci.* **413**, 669-675.

Huang, J. and Dunford, H. B. (1990) Oxidation of substituted anilines by horseradish peroxidase compound II. *Can. J. Chem.* **68**, 2159-2163.

Huang, C. P., Wang, H. W. and Chin, P. C. (1998) Nitrate reduction by metallic iron. *Wat. Res.* **32**, 2257-2264.

Hughes, M. F., Smith, B. J. and Eling, T. E. (1992) The oxidation of 4-aminobiphenyl by horseradish peroxidase. *Chem. Res. Toxicol.* **5**, 340-345.

Ibrahim, M. S., Ali, H. I., Taylor, K. E., Biswas, N. and Bewtra, J. K. (1997) Removal of phenol from industrial wastewaters using *Arthromyces ramosus* peroxidase in a continuous flow system. *52nd Purdue Industrial Waste Conference Proceedings*, Ann Arbor Press, MI, 271-277.

Ibrahim, M. S. A. (1998) Development of a continuous flow system for the removal of selected toxic substances from industrial waste streams using various enzymes. *Ph.D dissertation*, Ain Shams University, Cairo, Egypt.

Ibrahim, M. S., Ali, H. I., Taylor, K. E., Biswas, N. and Bewtra, J. K. (2001) Enzyme-catalyzed removal of phenol from refinery wastewater: feasibility studies. *Wat. Environ. Res.* **73**, 165-172.

Ichinohe, D., Muranaka, T., Sasaki, T., Kobayashi, M. and Kise, H. (1998) Oxidative polymerization of phenylenediamines catalyzed by horseradish peroxidase. *J. Poly. Sci.: Part A: Polymer Chemistry* **36**, 2593-2600

Job, D. and Dunford, H. B. (1976) Substituent effect on the oxidation of phenols and aromatic amines by horseradish peroxidase compound. *Eur. J. Biochem.* **66**, 607-614.

Johnson, T. L., Scherer, M. M. and Tratnyek, P. G. (1996) Kinetics of halogenated organic compound degradation by iron metal. *Environ. Sci. Technol.* **30**, 2634-2640.

Kagan, J., Wang, T. P., Benight, A. S., Tuveson, R. W. and Wang, G. R. (1990) The phototoxicity of nitro polycyclic aromatic hydrocarbons of environmental importance. *Chemosphere* **20**, 453-466.

Kim, Y. H. and Carraway, E. R. (2000) Dechlorination of pentachlorophenol by zero valent iron and modified zero valent irons. *Environ. Sci. Technol.* **34**, 2014-2017.

Klibanov, A. M., Alberti, B. N., Morris, E. D. and Felshin, L. M. (1980) Enzymatic removal of toxic phenols and anilines from waste waters. *J. Appl. Biochem.* **2**, 414-421.

Klibanov, A. M., Tu, T. M. and Scott K. P. (1983) Peroxidase catalyzed removal of phenols from coal-conversion wastewater. *Science* **221**, 259-261.

Klausen, J., Trober, S. P., Haderlein, S. B. and Schwarzenbach, R. P. (1995) Reduction of substituted nitrobenzenes by Fe(II) in aqueous mineral suspensions. *Environ. Sci. Technol.* **29**, 2396-2404.

Langmuir, I. (1918) The adsorption of gases on plane surfaces of glass, mica and platinum. *J. Am. Chem. Soc.* **40**, 1361-1403.

Lawniczak, S. L., Refait, P., Ehrhardt, J. J., Lecomte, P. and Genin, J. M. R. (2000) Trapping Cr by formation of ferrihydrate during the reduction of chromate ions by Fe(II)-Fe(III) hydroxysalt green rusts. *Environ. Sci. Technol.* **34**, 438-443.

Liang, L., Korte, N., Goodlaxon, J. D., Clausen, J., Fernando, Q. and Muftikian, R. (1997) Byproduct formation during the reduction of TCE by zero-valence iron and palladized iron. *Ground Water Monitoring and Remediation.* **27**, 122-127.

Liu, W., Kumar, J., Tripathy, S., Senecal, K. J. and Samuelson, L. (1999) Enzymatically synthesized conducting polyaniline. *J. Am. Chem. Soc.* **121**, 71-78.

Mantha, R., Biswas, N., Taylor, K. E., and Bewtra, J. K. (2001a) Removal of nitroaromatics from synthetic wastewater using two step zero-valent iron reduction and peroxidase-catalyzed oxidative polymerization. *Wat. Environ. Res.* (sent).

Mantha, R., Taylor, K. E., Biswas, N. and Bewtra, J. K. (2001b) A continuous system for Fe^0 reduction of nitrobenzene in synthetic wastewater. *Environ. Sci. Technol.* (in press; accepted May 7).

Mantha, R., Biswas, N., Taylor, K. E., and Bewtra, J. K. (2001c) Model for removal of nitrobenzene from synthetic wastewater using 2-step Fe^0 reduction and

peroxidase- catalyzed oxidation. *7th Specialty conference in Environmental Engineering Modeling*, CSCE, Victoria, B.C., Paper No. E16.

Matheson, L. J. and Tratnyek, P. G. (1994) Reductive dehalogenation of chlorinated methanes by iron metal. *Environ. Sci. Technol.* **28**, 2045–2053.

McCoy, E. C., Rosenkranz, H. S. and Mermelstein, R. (1981) Evidence for the existence of a family of bacterial nitroreductases capable of activating nitrated polycyclics to mutagens. *Environ. Mutagen* **3**, 421-427.

McEldoon, J. P., Pokora, A. R. and Dordick, J. S. (1995) Lignin Peroxidase-type of activity of soybean peroxidase. *Enzyme and Micro. Technol.* **17**, 359-365.

McEldoon, J. P. and Dordick, J. S. (1996) Unusual thermal stability of soybean peroxidase. *Biotechnol. Prog.* **12**, 555-8.

Means, G. E., Congdon, W. I. and Bender, M. L. (1972) Reactions of 2,4,6-trinitrobenzenesulfonate ion with amines and hydroxide ion. *Biochemistry* **11**, 3564-3571.

Monsef, H. R., Michels, D. A., Bewtra, J. K., Biswas, N. and Taylor, K. E. (2000) Removal of nitroaromatic compounds from water through combined zero-valent metal reduction and enzyme-based oxidative coupling reactions. In *Emerging Technologies in Hazardous Waste Management 8*; Tedder, D. W.; Pohland, F. G., Eds; Kluwer Academic /Plenum Publishers, New York, 141-152.

Muftikian, R, Fernando, Q. and Korte, N. (1995) A method for the rapid dechlorination of low molecular weight chlorinated hydrocarbons in water. *Wat. Res.* **24**, 2434-2439.

Munnecke, D. M. (1976) Enzymatic hydrolysis of organophosphate insecticides, a possible pesticide disposal method. *Appl. Environ. Microbiol.* **32**, 7-13.

Nakamoto, S. and Machida, N. (1992) Phenol removal from aqueous solutions by peroxidase catalyzed reaction using additives. *Wat. Res.* **26**, 2576-2581.

Nam, S. and Tratnyek, P. G. (2000) Reduction of azo dyes with zero-valent iron. *Wat. Res.* **34**, 1837-1845.

Nicell, J. A. (1991) Enzyme catalyzed polymerization and precipitation of aromatic compounds from wastewater. *Ph.D. Dissertation*, University of Windsor, Windsor, ON.

Nicell, J. A., Bewtra, J. K., Taylor, K. E., Biswas, N. and St. Pierre, C. (1992) Enzyme catalyzed polymerization and precipitation of aromatic compounds from wastewater. *Wat. Sci. Technol.* **25**, 157-164.

Nicell, J. A., Al-Kassim, L., Bewtra, J. K. and Taylor, K. E. (1993a) Treatment of waste waters by enzyme catalyzed polymerization and precipitation. *Biodeterioration Abstracts* **7**, 1-8

Nicell, J. A., Bewtra, J. K., Biswas, N. and Taylor, K. E. (1993b) Reactor development for peroxidase catalyzed polymerization and precipitation of phenols from wastewater. *Wat. Res.* **27**, 1629-1639.

Nicell, J. A. (1994) Kinetics of horseradish peroxidase-catalyzed polymerization and precipitation of aqueous 4-chlorophenol. *J. Chem. Tech. Biotechnol.* **60**, 203-215.

Nicell, J. A. and Buchanan, I. D. (1997) Model development for horseradish peroxidase catalyzed removal of aqueous phenol. *Biotechnol. Bioeng.* **54**, 251-261.

Orth, W. S. and Gillham, R. W. (1996) Dechlorination of trichloroethane in aqueous solution using Fe^0. *Environ. Sci. Technol.* **30**, 66–71.

Peres, C. M., Naveau, H. and Agathos, S. N. (1998) Biodegradation of nitrobenzene by its simultaneous reduction into aniline and mineralization of the aniline formed. *Applied Microbiology and Biotechnology* **49**, 343-349.

Pratt, A. R., Blowes, D. W. and Ptacek, C. J. (1997) Product of chromate reduction on proposed sub-surface remediation material. *Environ. Sci. Technol.* **31**, 2492-.

Ramelmeier, R. A. and Blanch, H. W. (1988) Peroxidase-catalyzed oxidation of *p*-anisidine with H_2O_2 in toluene. *Biotechnol. Bioeng.* **33**, 512-517.

Reynolds, G. W., Hoff, J. T. and Gillham, R. W. (1990) Sampling bias caused by materials used to monitor halocarbons in groundwater. *Environ. Sci. Technol.* **24**, 135-42.

Roberts, A. L., Tottem, L. A., Arnold, W. A., Burris, D. R. and Campbell, T. J. (1996) Reductive elimination of chlorinated ethylene by zero-valent metals. *Environ. Sci. Technol.* **30**, 2654-2659.

Saadi, K. W. (1993) Optimization of the catalytic life of horseradish peroxidase with the aid of an additive. *M. Eng. Project.* McGill University, Montreal, Canada.

Saunders, B. C., Holmes-Siedle, A. G. and Stark, B. P. (1964) Peroxidase, Butterworths, London.

Scherer, M. M., Westall, J. C., Ziomek-Morz, M. and Tratnyek, P.G. (1997) Kinetics of carbon tetrachloride reduction at an oxide-free iron electrode. *Environ. Sci. Technol.* **31**, 2385 – 2391.

Scherer, M. M., Richter, S., Valentine, R. L. and Alvarez, P. J. J. (2000) Chemistry and microbiology of permeable reactive barriers for *in situ* groundwater clean up. *Criti. Rev. in Environ. Sci. and Technol.* **30**, 363-411.

Singh, J., Comfort, S. D. and Shea, P. J. (1998) Remediating RDX-contaminated water and soil using zero-valent iron. *J. Environ. Qual.*, **27**, 1240-1245.

Siddique, M. H. (1992) Heterogeneous reactor system for 4-chlorophenol removal from aqueous streams using horseradish peroxidase. *Ph.D. Dissertation*, University of Windsor, Windsor, Ontario, Canada.

Spectrum Laboratories: chemical fact sheet *ca.* 88722 http:/www.speclab.com/compound/c88722.htm

Sweeny, K. H. and Fischer, J. R. (1972) Reductive degradation of halogenated pesticides. U. S. Patent No. 3,640,821. Feb 8.

Tatsumi, K., Freyer, A., Minard, R. D. and Bollag, J. M. (1994) Enzyme-mediated coupling of 3,4-dichloroaniline and ferulic acid: a model for pollutant binding to humic materials. *Environ. Sci. Technol.* **28**, 210-215.

Thompson, D. C. and Eling, T. E. (1991) Reactive intermediates formed during the peroxidative oxidation of anisidine isomers. *Chem. Res. Toxicol.* **4**, 474-481.

Toxic Release Inventory (TRI) data (1997) web site: http://www.rtk.net

U. S. Department of Health and Human Services, Hazardous Substances Data Bank, 1993 http://www.epa.gov/ttn/uatw/hlthef/nitroben.html

U. S. Environ. Prot. Agency (1980) *Ambient Water Quality Criteria for Nitrobenzene*, EPA 440/5-80-061, **October**.

Vasudevan, D. and Stone, A. T. (1996) Adsorption of catechols, 2-aminophenols, and 1,2-phenylenediamines at the metal (hydr)oxide/water interface: effect of ring substituents on the adsorption onto TiO2 *Environ. Sci. Technol.* **30**, 1604–1613.

Vieth, W. R. and Venkatasubramanian, K. (1973) Enzyme engineering Part I: The utility of supported enzyme systems. *Chemtech.* **November**, 677-684.

Walling, C. (1975) Fenton's reagent revisited. *Acc. Chem. Res.* **8**, 125-131.

Warren, K. D., Arnold, R. G., Bishop, T. L., Lindholm, L. C. and Betterton, E. A. (1995) Kinetics and mechanism of reductive dehalogenation of carbon tetrachloride using zero-valence metals. *J. Haz. Materials.* **41**, 217-227.

Weber, E. J. (1996) Iron-mediated reductive transformations: investigation of reaction mechanism. *Environ. Sci. Technol.* **30**, 716 – 719.

Widrig, D. L., Boopathy, R. and Manning, J. F. (1997) Bioremediation of TNT-contaminated soil: a laboratory study. *Environ. Toxicol. Chem.* **6**, 1141-1148.

Wu, J., Taylor, K. E., Biswas, N. and Bewtra, J. K. (1993) Optimization of the reaction conditions for enzymatic removal of phenol from wastewater in the presence of polyethylene glycol. *Wat. Res.* **27**, 1701-1706.

Wu, Y., Bewtra, J. K., Biswas, N. and Taylor. K. E. (1993) Removal of phenol derivatives from aqueous solution by enzymatic reaction with additives. *Proceedings of the 48th Purdue Industrial Waste Conference*, Lewis Publishers, Chelsea, MI, 421-431.

Wu, Y. (1996) Application of additives in horseradish peroxidase catalyzed removal of phenol derivatives from aqueous solution. *Ph. D. dissertation*, University of Windsor, ON, Canada.

Wu, Y., Taylor, K. E., Biswas, N. and Bewtra, J. K. (1997) Comparison of additives in the removal of phenolic compounds by peroxidase-catalyzed polymerization. *Wat. Res.* **31**, 2699-2704.

Wu, Y., Taylor, K. E., Biswas, N. and Bewtra, J. K. (1999a) Kinetic model for the removal of phenol by horseradish peroxide in the presence of polyethylene glycol. *J. Environ. Eng.* **125**, 451-458.

Wu, Y., Taylor, K. E., Biswas, N. and Bewtra, J. K. (1999b) Kinetic model-aided reactor design for peroxidase-catalyzed removal of phenol in the presence of polyethylene glycol. *J. Chem. Technol. Biotechnol.* **74**, 519-526.

Wust, W. F., Kober, R., Schlicker, O. and Dahmke, A. (1999) Combined zero- and first-order kinetic model of the degradation of TCE and *cis*-DCE with commercial iron. *Environ. Sci. Technol.* **33**, 4304–4309.

Wynn, C. H. (1979) The structure and function of enzyme, Edward Arnold (Publishers) Limited, London 41-53.

Yu, J., Taylor, K. E., Zou, H., Biswas, N. and Bewtra, J. K. (1994) Phenol conversion and dimeric intermediates in horseradish peroxidase-catalyzed phenol removal from water. *Environ. Sci. Technol.* **28**, 2154-2160.

APPENDICES

APPENDIX A

A.1 Calculation of total volume of solution passing through the Fe^0 column by Analytical Integration

The Equation of flow is given by Eq. 4.4.6.2:

$$\text{Flow rate} = -6*10^{-6}*t^3 + 0.0002*t^2 - 0.028*t + 3.1$$

$$\text{Total Flow, mL/min} * \text{h} = \int_0^{72} \left(-6*10^{-6}*t^3 + 0.0002*t^2 - 0.028*t + 3.1\right)dt$$

$$\text{Total Flow, mL/min} * \text{h} = \int_0^{72} \left(-6*10^{-6}*t^3\right)dt + \int_0^{72} \left(0.0002*t^2\right)dt + \int_0^{72} \left(-0.028*t\right)dt + \int_0^{72} 3.1dt$$

Total Flow, mL/min*h = - 40.3 + 24.88 – 72.576 + 223.2

Total Flow, mL/min*h = 135.204

Total Flow, mL = 8112

A.2 Mass balance of Fe^0 dissolved as a result of the reduction reaction

The overall reduction reaction of nitrobenzene can be given as:

$$C_6H_5NO_2 + 3Fe^0 \rightarrow C_6H_5NH_2 + 3Fe^{2+} + 2H_2O$$

Total reaction time: 72 h

NB concentration in the feed = 1 mM

Using Total flow = 8112 mL, as calculated in Appendix A1

Total NB used for reaction = 8.112 mM

Total Fe^0 used up = 3*8.112 mM

Total Fe^0 used up = 3*8.112*55.847/1000 g

Total Fe^0 used up = 1.36 g

DCP Analyses for Total Fe

Effluent Water = 0.667 g

Precipitates = 1.443 g

Total Fe = 2.11 g

APPENDIX B

B.1 SBP Activity Assay

B.1.1 General

The purpose of the assay is to determine the amount of active enzyme that is contained in a sample. The assay uses saturation concentrations of phenol, 4-aminoantipyrine (AAP), and appropriate concentration of hydrogen peroxide such that the initial reaction rate will be proportional to enzyme activity. The initial rate is measured by observing the rate of color formation in a solution in which a reaction between phenol and H_2O_2 is catalyzed by SBP such that the products of reaction react with AAP to form a non-precipitated red colored solution which absorbs light at a peak of 510 nm with a an extinction coefficient of 6000 $M^{-1}.cm^{-1}$.

One unit of activity is defined as the number of micromoles of H_2O_2 utilized in one minute at pH 7.4 and 25 °C in an assay mixture consisting of 10 mM phenol, 2.4 mM AAP and 0.2 mM H_2O_2.

B.1.2 Preparation of reagents

B.1.2.1 Phosphate Buffer (0.5 M, pH 7.4)

In a 1000 mL flask, add the following

13.796 g of monobasic sodium phosphate ($NaH_2PO_4.H_2O$)

56.78 g of dibasic sodium phosphate (Na_2HPO_4)

Add distilled water up to 1 L to make up the solution.

B.1.2.2 Phenol (0.1 M Phenol) in Phosphate Buffer (0.5 M, pH 7.4)

Dissolve 9.411 g of phenol in 1000 mL of 0.5 M Phosphate buffer solution.

B.1.2.3 Hydrogen peroxide (100 mM)

Dilute 567 μL of 30% (w/v) hydrogen peroxide to 50 mL with distilled water. This is to be prepared each time an activity assay is done.

B.1.2.4 Assay Mixture

In a beaker add the following:

25 mg AAP

42.4 mL water

100 μL 100 mM H_2O_2

5 mL 0.1 M Phenol in 0.5 M phosphate buffer

B.1.3 Procedure

The total assay volume is 1 mL, and the assay should be conducted before the substrate depletion becomes significant. Therefore, in a semi-micro cuvette, place solution in following order:

950 μL of assay mixture

50 μL of solution containing SBP

B.1.4 Calculations

One unit of activity is defined as the number of micromoles of hydrogen peroxide utilized in one minute at pH 7.4 and 25 °C in an assay mixture consisting of 10 mM phenol, 2.4 mM AAP, and 0.2 mM H_2O_2. The activity of SBP in the cuvette is obtained from the average slope (absorbance unit per minute) within the linear range. Therefore, the activity within the cuvette, in units of $\mu mol.min^{-1}.mL^{-1}$ (i.e. U/mL) is calculated according to:

$$\text{Activity (U/mL)} = \frac{\text{slope (au/min)}}{6000\ \text{au.L/mol}} \times \frac{10^6 \mu\text{mol}}{\text{mol}} \times \frac{1\text{L}}{1000\ \text{mL}} \qquad \text{(B.1.)}$$

in which au represents absorbance units and 6000 au.L/mol relates color development to peroxide consumption.

Calculate the activity of the sample according to:

$$\text{Sample activity (U/mL)} = \text{Activity U/mL} \times \frac{1000}{\text{sample volume}} \qquad \text{(B.2)}$$

B.2 Hydrogen peroxide assay

B.2.1 General

This end-point colorimetric assay was used to measure the concentration of hydrogen peroxide in a sample. The assay uses *Arthromyces ramosus* peroxidase as a catalyst and 4-aminoantipyrine as a color generating co-substrate in combination with an aromatic substrate, phenol, in the assay mixture. In this assay, the amount of H_2O_2 introduced into the assay sample is the only limiting reactant; therefore, the degree of the color developed in the reaction is proportional to the amount of peroxide in the sample.

Once the maximum amount of color has developed, the absorbance (at 510 nm) is converted to the H_2O_2 concentration in the cuvette by means of a calibration curve. The H_2O_2 concentration in the sample is then calculated according to the dilution the sample had undergone in the cuvette.

B.2.2 Preparation of reagents

B.2.2.1 Phosphate Buffer (0.5 M, pH 7.4)

In a 1000 mL flask, add the following

13.796 g of monobasic sodium phosphate ($NaH_2PO_4.H_2O$)

56.78 g of dibasic sodium phosphate (Na_2HPO_4)

Add distilled water up to 1 L to make up the solution.

B.2.2.2 Phenol (0.1 M Phenol) in Phosphate Buffer (0.5 M, pH 7.4)

Dissolve 9.411 g of phenol in 1000 mL of 0.5 M Phosphate buffer solution.

B.2.2.3 Assay mixture

In a beaker add the following:

41 mg of AAP.

10 mL of 0.1 M phenol in 0.5 M Phosphate buffer pH 7.4

200 µL of ARP stock solution

9.8 mL distilled water

The final total volume of the assay reagent is made up to 20 mL

B.2.3 Calibration Procedure

Make up a stock solution of H_2O_2 with a concentration of 1.0 mM. From this stock solution prepare standards ranging from 0 to 1.0 mM. In a test tube place the following solutions

200 μL of assay reagent

750 μL of distilled water

50 μL of standard sample

The total volume of the assay mixture must be 1 mL and hydrogen peroxide concentration in the assay mixture should be below 50 μM. Immediately after the addition of H_2O_2 standard, shake the tube and then wait until the color is fully developed (usually for 10 min). Put the assay in a semi-micro cuvette and read the peak absorbance at 510 nm. Repeat the procedure for all standards, using triplicate measurements. Make a plot of absorbance *vs.* H_2O_2 concentration in the cuvette, and determine the slope of the trace using linear regression. A typical calibration curve for H_2O_2 is presented in Fig. B.2.3.

B.2.4 Measurement of hydrogen peroxide

In a semi-micro cuvette, place the following reactants in the given order:

200 μL of assay reagent

0-750 μL distilled water

50-800 μL of sample.

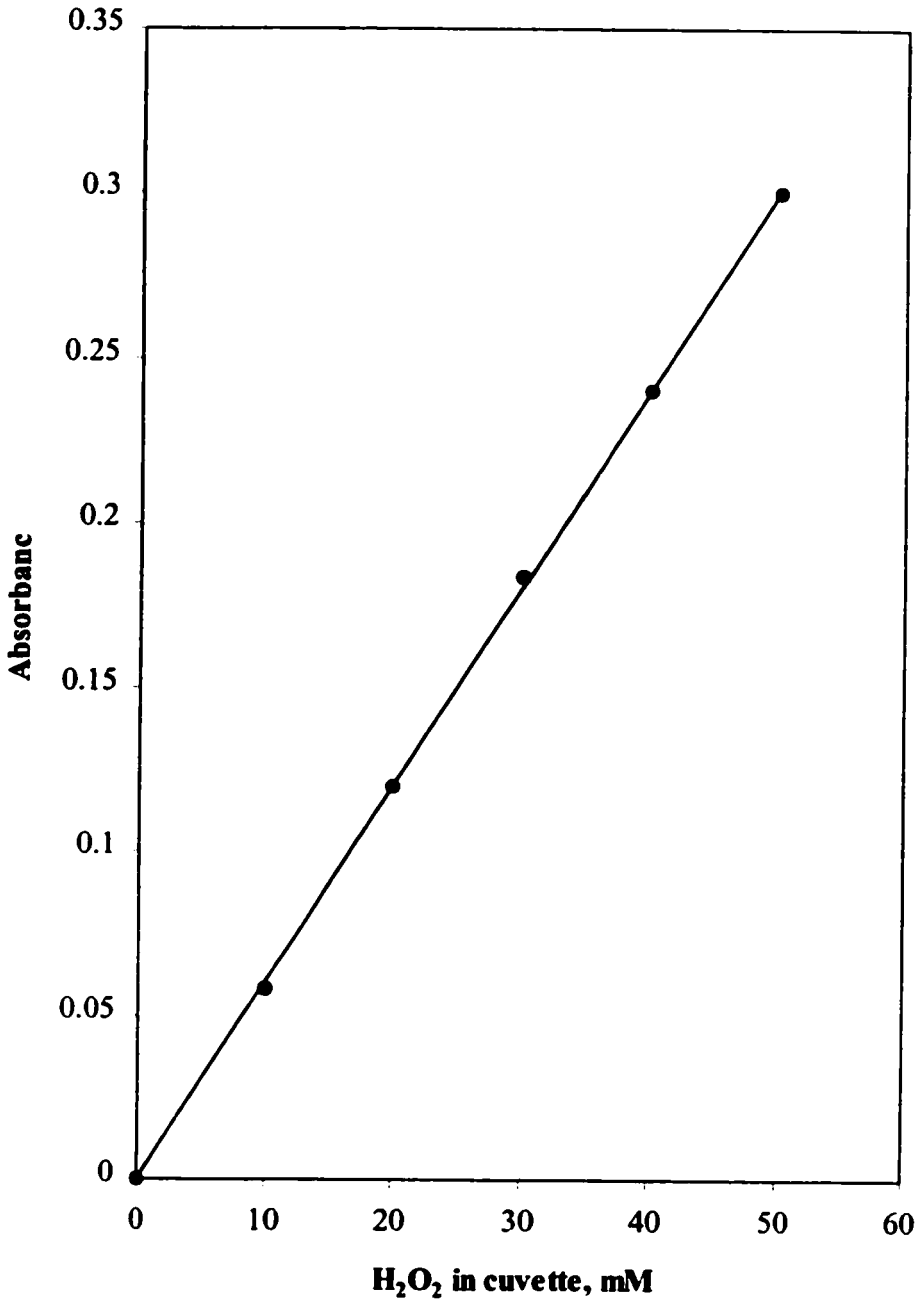

Fig. B.2 Calibration curve for H_2O_2 at 510 nm wave length
In a semi-micro cuvette the following are placed and the measurement taken after the full development of color: 200 µL of assay reagent, 750 µL of distilled water and 50 µL of standard sample.

The total volume in the cuvette must be 1 mL. Immediately after addition of the sample, shake the cuvette and then wait for the full development of the color. Read the maximum amount of absorbance at the peak wavelength of 510nm. Determine the cuvette H_2O_2 concentration from the calibration curve.

B.2.5 Calculations

Determine the sample hydrogen peroxide concentration from:

$$[H_2O_2]_{sample} = [H_2O_2]_{cuvette} \times \frac{1000\,\mu L}{\text{Sample volume}\,\mu L} \qquad \text{(B.2.5)}$$

B.3 TNBS Assay for anilines

B.3.1 General

The purpose of the assay is to determine the concentration of an aromatic amine present in a sample. Anilines fail to respond to the standard color test developed for phenols. The assay employs 2,4,6-trinitrobenzenesulphonic acid (TNBS) to produce color on reacting with amines present in the aqueous solutions; the intensity of color being directly proportional to the amount of amine present in the sample. The sample solutions are buffered at pH 6.4 and the amount of the aromatic amine is the only limiting substance in the solution. Each colored solution of amine absorbs light at a distinct wavelength with a unique extinction coefficient. The reaction mechanism between aniline and TNBS is shown below:

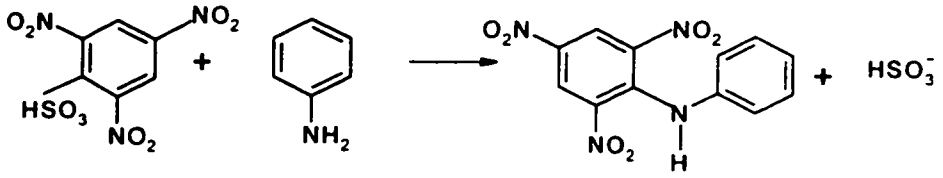

B.3.2 Preparation of reagents

B.3.2.1 Phosphate Buffer (0.5 M, pH 6.4)

In a 1000 mL flask, add the following

51.08 g of monobasic sodium phosphate ($NaH_2PO_4.H_2O$)

35.5 g of dibasic sodium phosphate ($Na_2HPO_4.7H_2O$)

Add distilled water up to 1 L to make up the solution.

B.3.2.2 TNBS solution (10 mM)

In a 10 mL flask, add 29 mg of TNBS

Add distilled water up to 10 mL to make up the solution

Note: Small volumes of TNBS stock solutions are to be prepared since the aqueous solution develops a deep yellow color, which has a large absorbance at the same wave-length as the aromatic amine, thus interfering with the analysis.

B.3.3 Calibration Procedure

Make up a stock solution of aromatic amine with a concentration of 1 mM. From the stock solution, create sub-stock solutions of concentrations ranging from 0-500 μM. In a final volume of 1.0mL, add the solutions in the following order:

100μL of 10mM TNBS

100μL of 0.5 M phosphate buffer of pH 6.4

0-800 μL of sample plus water.

Samples are allowed to stand for specific period of time and then absorbance is measured at the peak wavelength, particular to the aromatic amine, against a reagent blank. Keep the aromatic amine concentration in the cuvette below 50 μM.

B.3.4 Measurement of aromatic amine

In a semi-micro cuvette place in the following order:

100 μL TNBS

100 μL NaPP buffer

50-800 μL sample

0-750 μL water

Shake the cuvette and take the absorbance against the calibrated graph after the specific time period.

B.3.5 Calculations

Calculate the sample amine concentration from:

$$[\text{Amine}]_{\text{in sample}} = [\text{Amine}]_{\text{in cuvette}} \frac{1000\mu\text{L}}{\text{sample volume}, \mu\text{L}}$$

where, $[\text{Amine}]_{\text{in cuvette}}$ is determined from the calibration curves, Fig. B.3.1-B.3.5.

Table B.3 shows all the different parameters for aniline, *o*-, *m*- and *p*-toluidines.

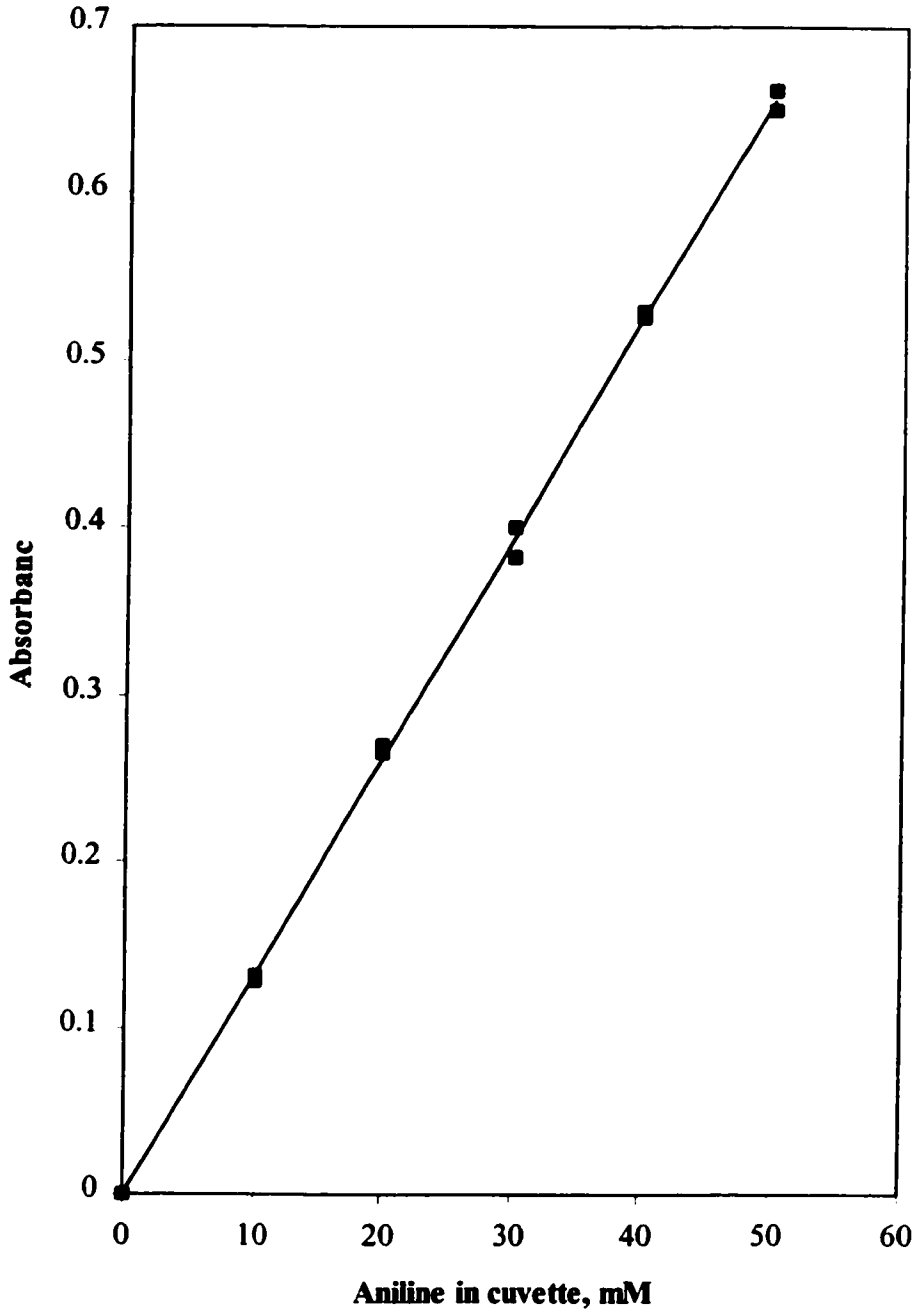

B.3.1 Calibration curve for TNBS test for aniline at 384 nm

The test was done at a pH of 6.4. In a semi-micro cuvette, the following are placed: 100 μL TNBS, 100 μL NaPP buffer, 50-800 μL sample and 0-750 μL water. The time to reach the peak absorbance is 30 min.

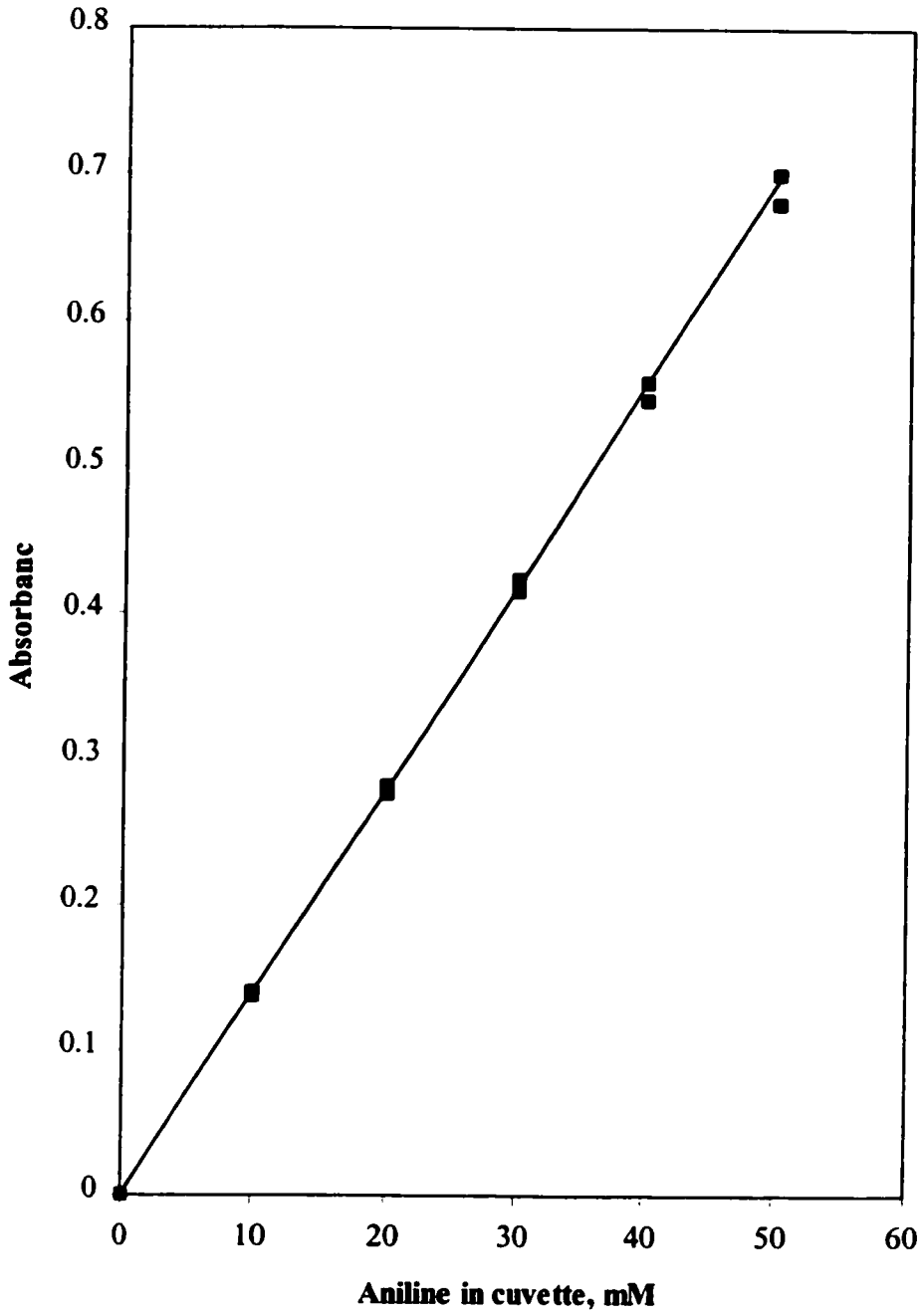

B.3.2 Calibration curve for TNBS test for aniline at 398 nm

The test was done at a pH of 6.4. In a semi-micro cuvette, the following are placed: 100 μL TNBS, 100 μL NaPP buffer, 50-800 μL sample and 0-750 μL water. The time to reach the peak absorbance is 30 min. Na_2SO_3 was added in the test such that the final concentration in the cuvette was 50-250 μM.

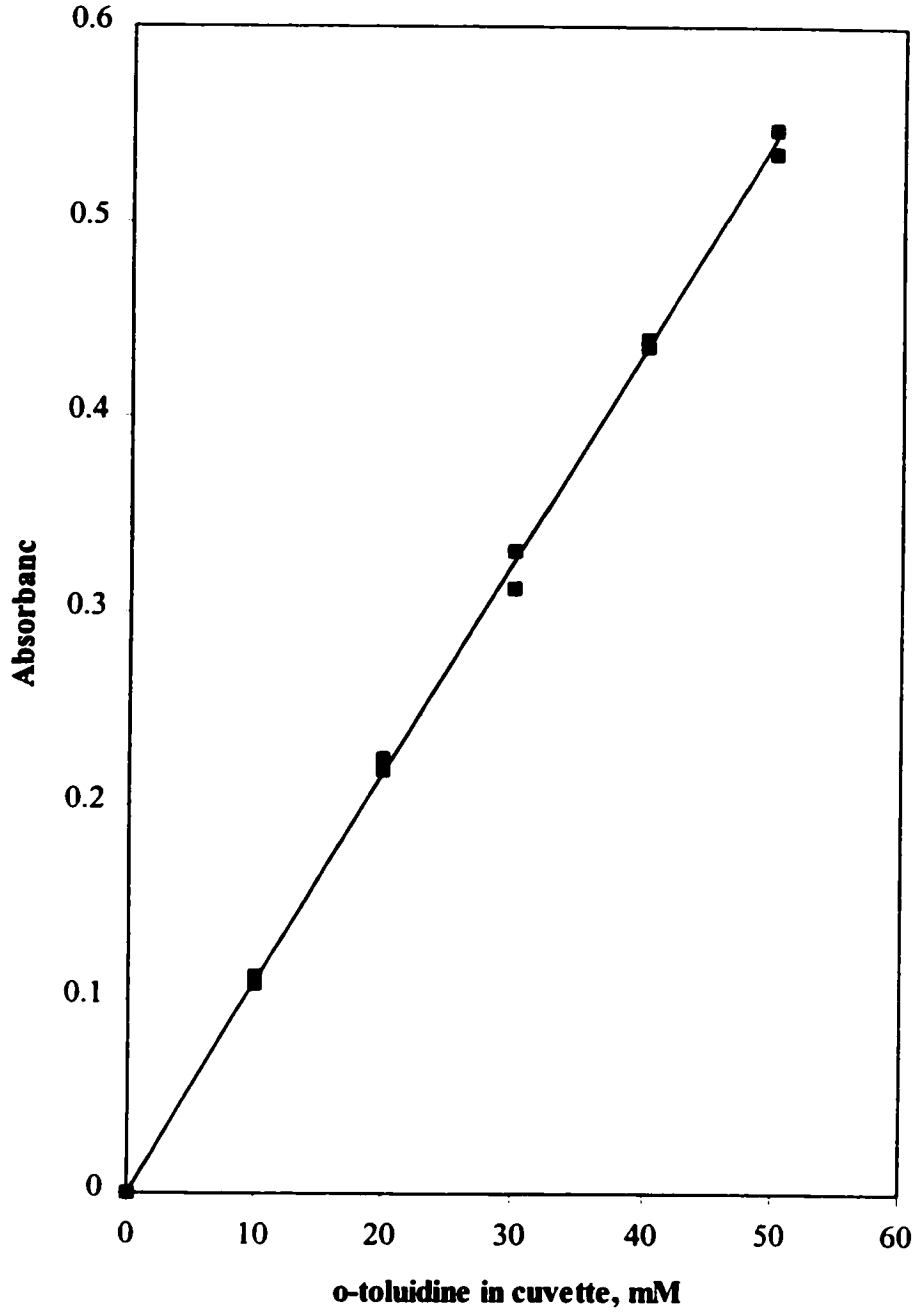

B.3.3 Calibration curve for TNBS test for *o*-toluidine at 376 nm

The test was done at a pH of 7.4. In a semi-micro cuvette, the following are placed: 100 µL TNBS, 100 µL NaPP buffer, 50-800 µL sample and 0-750 µL water. The time to reach the peak absorbance is 30 min. The test was performed at a temperature of 48-50 °C.

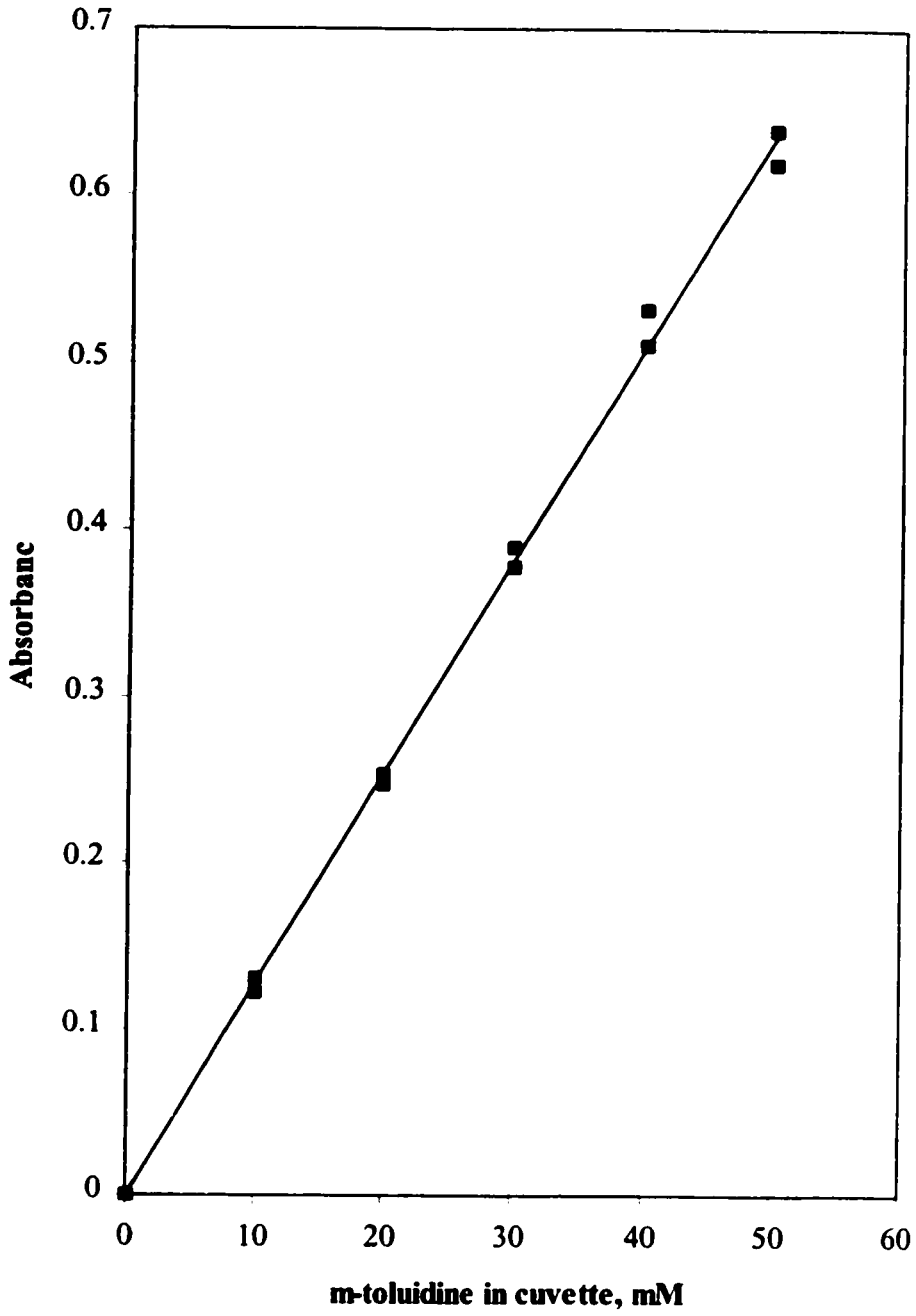

B.3.4 Calibration curve for TNBS test for *m*-toluidine at 390 nm

The test was done at a pH of 6.4. In a semi-micro cuvette, the following are placed: 100 µL TNBS, 100 µL NaPP buffer, 50-800 µL sample and 0-750 µL water. The time to reach the peak absorbance is 25 min. The test was performed at room temperature.

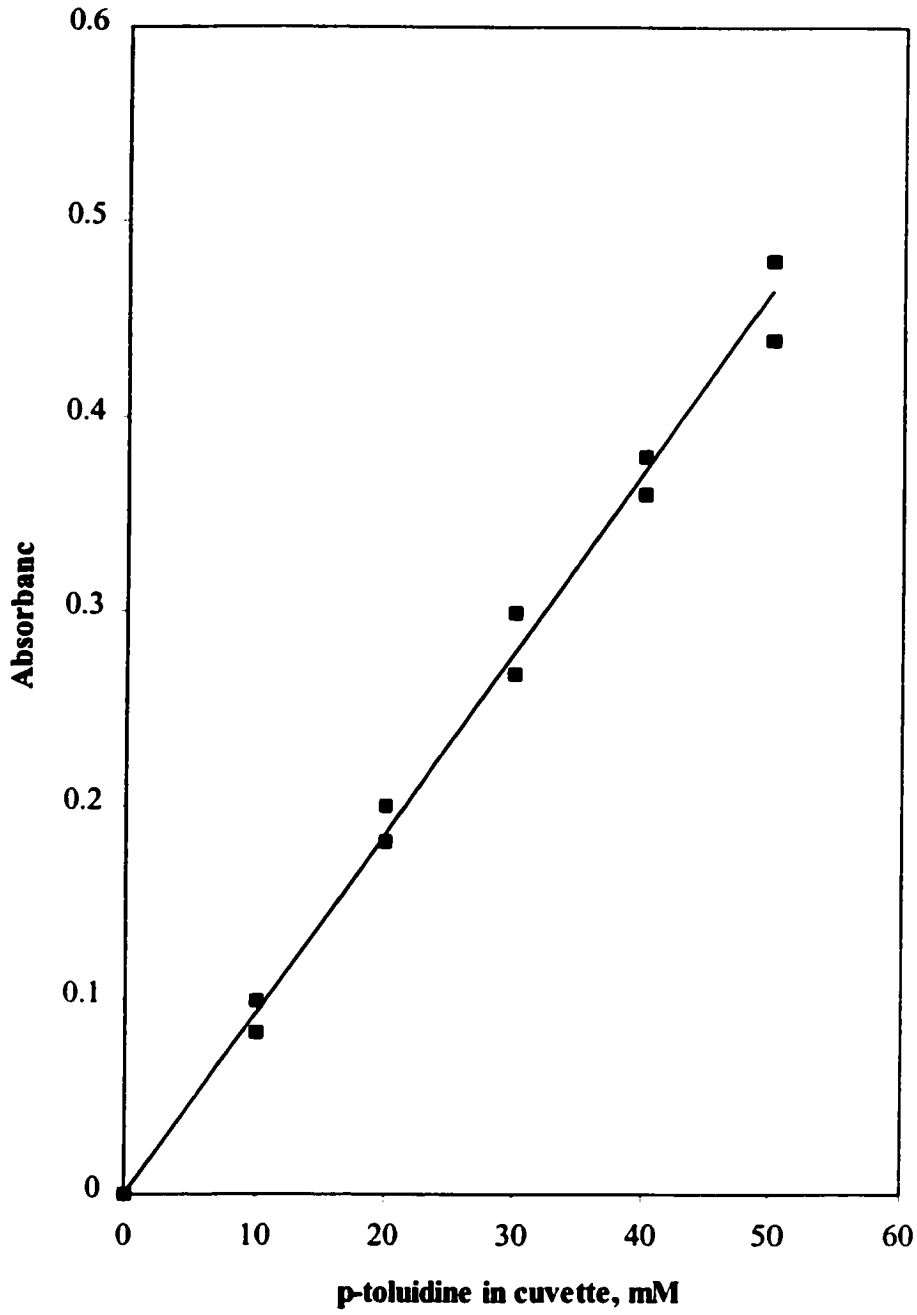

B.3.5 Calibration curve for TNBS test for *p*-toluidine at 400 nm

The test was done at a pH of 7.4. In a semi-micro cuvette, the following are placed: 100 µL TNBS, 100 µL NaPP buffer, 50-800 µL sample and 0-750 µL water. The time to reach the peak absorbance is 15 min. The test was performed at room temperature.

Table B.3 Various parameters involved in the analyses of aromatic amines

Substrate	Peak wavelength, nm	Peak time, min	Temperature	Working pH	Extinction coefficient, $M^{-1}.cm^{-1}$
aniline	384	30	room temp.	6.4	13200
aniline+sulfite	398	30	room temp.	6.4	14000
o-toluidine	376	30	48-50 °C	7.4	10900
m-toluidine	390	25	room temp.	6.4	12800
p-toluidine	400	15	room temp.	7.4	9300

B.4 TNBS Assay for *o*-toluidine

The above discussed method does not generate visible color in reasonable time, when dealing with *o*-toluidine due to its steric factor. The solutions, however, generate color rapidly on heating to a temperature of 48-50°C. The following procedure is followed while dealing with samples of *o*-toluidine.

Prepare samples of various concentrations ranging from 0.01-0.1 mM of *o*-toluidine. Appropriate amounts of TNBS, buffer and water are added to make up the color sample. Larger volumes of sample are prepared in this case, so that even after heating at 48-50°C for 30 min, there is enough solution to be measured in the cuvette. Care is taken to prepare a blank reagent at the same temperature also. The following table is shown hereunder as an illustration:

		o-toluidine, mM					
Contents	Blank	0.01	0.02	0.04	0.06	0.08	0.1
o-toluidine, µL	0	100	200	400	600	800	100
Water, µL	800	700	600	400	200	0	700
Buffer, µL	100	100	100	100	100	100	100
TNBS, µL	100	100	100	100	100	100	100

APPENDIX C

Tables of Experimental Data

Table 3D Error Analysis

TNBS test results for a batch reactors of 30 mL volume that initially contained 1 mM aniline, 1.5 mM H_2O_2 and 0.17 U/mL of SBP at a pH of 7.4. At the end of reaction time of 3 h, catalase, at a final concentration of 125 U/mL, was added to stop the reaction. Alum, at a final concentration of 50 mg/L, was added to help settle the contents by gravity.
Results shown pertain to concentrations in the cuvette

Sample #	Absorbance	Concentration, μM	S.D. (σ)
1	0.4158	31.5	0.125
2	0.4118	31.2	
3	0.4132	31.3	

Batch reactors of 30 mL volume that initially contained 1 mM *p*-toluidine, 0.014 U/mL of SBP and 1.5 mM of H_2O_2 at pH 7.0. At the end of reaction time of 3 h, catalase, at a final concentration of 125 U/mL, was added to stop the reaction. Alum, at a final concentration of 50 mg/L, was added to help settle the contents by gravity.
Results shown pertain to concentrations in the cuvette

Sample #	Absorbance	Concentration, μM	S.D. (σ)
1	0.0446	4.8	0.793
2	0.0567	6.1	
3	0.0391	4.2	

Duplicate batch reactors of 30 mL volume that initially contained 1 mM aniline, 1.0 mM of H_2O_2 and 0.21 U/mL of SBP at pH 7.3. At the end of reaction time of 3 h, catalase, at a final concentration of 125 U/mL, was added to stop the reaction. Alum, at a final concentration of 50 mg/L, was added to help settle the contents by gravity.Results shown pertain to concentrations in the cuvette

Sample #	Absorbance	Concentration, μM	S.D. (σ)
Batch 1			
1	0.6376	48.3	1.003
2	0.6323	47.9	
3	0.6626	50.2	
Batch 2			
1	0.7050	53.4	2.07
2	0.6428	48.7	
3	0.6520	49.4	

Table 4.1.1 Nitrobenzene reduction under different solution conditions
Batch reactions of 30 mL volume, initially contained 1.0 mM of nitrobenzene at pH 8.5 in the presence of 1.0 g Iron-I, under the following conditions: oxygen saturated, degassed, and sodium sulfite present at 5 mM.

Time, min	% aniline formed		
	Solution containing O_2	Previously degassed solution	Solution scavenged with Na_2SO_3
0	0	0	0
10	5.3	40.2	45.3
30	9.2	76.2	72.7
45	12.1	83.4	84.8
60	15.6	84.9	85.1
90	18.4	84.6	85
120	19.5	85	84.9
180	20.1	85.3	85.2

Table 4.1.2 Conversion of nitrobenzene to aniline in a continuous-flow column
Continuous-flow system in a 15x150 mm column with 50 g of Iron-I, influent nitrobenzene concentration of 1 mM at a flow rate of 2.8 mL/min, pH 7.2-7.4 and effluent pH 7.3-7.6. Concentration of Na_2SO_3 in the influent solution was varied.

0 mM		0.5 mM		1 mM		2 mM	
Time h	Aniline % formed	Time h	Aniline % formed	Time h	Aniline % formed	Time h	Aniline % formed
0	0	0	0	0	0	0	0
0.5	18	0.25	25	0.5	36.6	0.5	38.2
1.00	31	1	76	1	76.5	1	78.1
2	52.3	2	80	2	85.4	2	86.2
3	65	3	85	3	91.3	3	90.9
4	64	4	83.2	4	98.3	4	97.8
5	65	5	78.8	6	99.6	6	100
6	63.7	6	75.2	7	100	8	99.7
7	64	7	70.3	9	99.8	10	99.8
8	64.2	9	64.5	10	95.3	13	100
9	64.6	10.5	62.2	14	90.2	14	98.7
10	65	11	60.1	16	85.3	21	97.3
11	63.6	20	54.1	24	75.3	24	95.1
12	63.9	20.5	50.6	25	74.4	26	92.6
13	62	22	48.8	5 mM			
20	52.1	24	47.3	Time h	Aniline % formed		
21	50.6			0	0		
22	50.4			0.5	37.5		
23	51.3			1	77.9		
24	49.8			2	87.2		
				3	89.6		
				4	98.1		
				6	99.8		
				8	100		
				10	99.6		
				11	99.5		
				13	100		
				21	99		
				24	97.4		
				26	95.1		

Table 4.1.3 Amount of O_2 absorbed into the solution

Concentration of oxygen due to re-absorption in the open feed reservoirs, of the type used in continuous column operations under different conditions of sodium sulfite present in the solution initially: 0.5 mM, 1.0 mM, 2.0 mM and 5.0 mM. pH obtained under these conditions was 7.3-8.0.

	Amount of Na_2SO_3 in the solution, mM			
Time, h	0.5	1.0	2.0	5.0
0	1.1	0	0	0
1	2.5	0	0	0
4	4	0	0	0
7	5	0.1	0	0
10.5	6	0.8	0.05	0
17	7.1	3.6	0.1	0.05
24	7.5	5	0.2	0.1

Table 4.3.2.1 Sorption data under different conditions of pH and concentration ranges.

Batch reactors of 30 mL volume contained 5 mM of Na_2SO_3 to make the solutions anoxic. Each batch received 1 g of Iron-I and 0-2 mM authentic aniline. Initial and final concentrations, after 3 h, of aniline were measured in the solution.

pH 7.3		pH 6.8	
C_{aq} mM	C_{ads} mM	C_{aq} mM	C_{ads} mM
0	0	0	0
0.1	0.018	0.1	0.026
0.2	0.04	0.2	0.058
0.5	0.103	0.5	0.16
1	0.171	1	0.322
2	0.198	2	0.444

pH 7.2		pH 8.5	
C_{aq} mM	C_{ads} mM	C_{aq} mM	C_{ads} mM
0	0	0	0
0.1	0.018	0.1	0.012
0.15	0.03	0.2	0.026
0.2	0.046	0.3	0.046
0.3	0.073	0.4	0.063
0.4	0.102	0.5	0.082
0.5	0.112	0.75	0.086

Table 4.4.1 Volatilization data for nitrobenzene

Open fee reservoirs of the type used in continuous operation were set up with different initial nitrobenzene concentration at room temperature. Change in nitrobenzene concentration was noted with time.

Run 1	
Time, h	C, mM
0	2180
2	2165
9	2110
21	2030
24	2010
28	1980
40	1900
49	1840
60	1770
66	1740
73	1700
88	1610

Run 2	
Time, h	C, mM
0	1050
1	1045
10.5	1010
25.3	965
26.5	960
29.5	950
40	915
45	900
50	885
65	840

Run 3	
Time, h	C, mM
0	500
5	490
17.5	470
19	465
22.5	460
67	400

C: Concentration of nitrobenzene in the aqueous solution

Table 4.4.2 Porosity data for Iron-II

Run 1: Volume of column = 6.1 mL

Fe in the column, g	Water added, mL	Porosity
26.5	2.4	0.40
25.3	2.6	0.43
24.7	2.5	0.41
25.6	2.5	0.41

Run 2: Volume of column = 12.3 mL

Fe in the column, g	Water added, mL	Porosity
53.1	5.3	0.43
55.2	5.0	0.41
54.3	5.1	0.41
53.6	5.4	0.44

Run 3: Volume of column = 23.1 mL

Fe in the column, g	Water added, mL	Porosity
100.2	10.1	0.44
99.8	10.3	0.45
100.5	9.7	0.42
101.1	9.6	0.42

Table 4.4.3.2 Reduction of nitrobenzene to aniline at an influent pH of 6.5
Continuous column operations in a 15x300 mm column, with 200 g of Iron-II at a flow rate of 3.1 mL/min. Influent concentration of NB was 1 mM. 1 mM of Na_2SO_3 was included in the solution to make it anoxic. Effluent pH was between 7.4 and 7.6.

Time h	Aniline % formed
0	0
1	34.2
2	81.3
3	90.3
7	98.7
12	99.6
25	100
30	100
36	100
50	100
51	99.6
52	98.7
55	96.8
60	99.6
61	99.8
72	98.7
75	97
80	89.5
82	85.1
83	84.2
84	78.9
92	78
93	80
94	77.9
95	76
96	75

Fig. 4.4.3.3 Reduction of nitrobenzene to aniline at an influent pH of 7.4
Continuous column operations in a 15x300 mm column, with 200 g of Iron-II at a flow rate of 3.1 mL/min. Influent concentration of NB was 1 mM. 1 mM of Na_2SO_3 was included in the solution to make it anoxic. Effluent pH was between 7.4 and 7.6.

Time h	Aniline % formed
0	0
1	36.5
2	82.3
3	92.1
7	100
12	100
25	99.6
30	99.2
36	98.9
50	100
51	98
52	99.5
55	96.7
60	98
61	100
72	100
75	96.5
80	89.5
82	84.6
83	84.1
84	78.8
92	80
93	80
94	77.6
95	75.3
96	72.3

Table 4.4.3.4 Reduction of nitrobenzene to aniline at an influent pH of 8.5
Continuous column operations in a 15x300 mm column, with 200 g of Iron-II at a flow rate of 3.1 mL/min. Influent concentration of NB was 1 mM. 1 mM of Na_2SO_3 was included in the solution to make it anoxic. Effluent pH was between 8.5 and 8.7.

Time h	Aniline % formed
0	0
1	35
2	80
3	91
7	100
12	99
25	98
30	100
36	100
50	97
51	98
52	96
55	99
60	98
61	100
72	100
75	97
80	90
82	85
83	84
84	80
92	80
93	80
94	78
95	76
96	75

Table 4.4.5 Reduction of NAC to the corresponding amine on Fe^0-II bed

Time h	Aniline % formed	*o*-toluidine % formed	*m*-toluidine % formed	*p*-toluidine % formed
0	0	0	0	0
1	35	25	28	30
2	80	75	70	
3		80	78	75
4	93		88	80
5	100	97		90
6	98	100	96	98
7	100	98		99
8			100	
12	99		99	98
13		100		
21		100		99
24				100
25	98	100	98	
29			100	
30	100	99	99	98
35				100
36	100	99	98	
41			98	
50	97	100		100
51	98	99	99	100
55	99	98	100	97
59		99		
60	98		100	100
72	100	100	100	100
75	97	98	96	95
80	90	89	91	88
82	85	85	85	85
84	80	80	80	80
92	80	80	80	80
93	80	80	80	80
94	78	78	78	78
95	76	76	76	76
96	75	75	75	75

Table 4.4.6.1 Change in height of precipitate front from influent end of the column Continuous column operations in a 15x300 mm column, with 200 g of Iron-II at a flow rate of 3.1 mL/min. Influent concentration of NB was 1 mM. 1 mM of Na_2SO_3 was included in the solution to make it anoxic. Influent pH was 7.4 and effluent pH was 7.5-7.6.

Time h	length of precipitate end, mm
0	0
1	0
2	1
3	2
4	3
6	5
10	8
16	11
18	13
25	18
29	23
40	36
42	37
50	45
52	46
61	53
62	54
64	56
68	60
70	61
75	66
83	74
84	76

Table 4.4.6.2 Change in flow-rate due to clogging
Continuous column operations in a 15x300 mm column, with 200 g of Iron-II at a flow rate of 3.1 mL/min. Influent concentration of NB was 1 mM. 1 mM of Na_2SO_3 was included in the solution to make it anoxic. Influent pH was 7.4 and effluent pH was 7.5-7.6.

Time h	Flow rate mL/min
0	3.1
1	3.1
2	3.1
3	3.1
4	3.1
16	3.1
18	3.1
25	3
29	3
40	3
42	2.9
50	2.8
52	2.7
61	2.5
62	2.5
64	2.4
68	2.1
70	1.8
75	1.5

Table 4.5.1 Change in enzyme activity with time
Activity measurements done with crude enzyme SBP stored at two different temperatures: 4°C and 18-20 °C.

Time	activity, U/mL	
day	4°C	18-20°C
0	2.86	2.86
1	2.84	2.2
2	2.8	1.63
3	2.71	1.12
4	2.62	0.75
5	2.51	0.5
6	2.4	0.36
7	2.22	0.32
8	2	0.31
9	1.83	0.3
10	1.75	0.3

Table 4.5.2.2.1 pH optimization for removal of aniline

Batch reactors of 30 mL volume, initially contained 1 mM aniline, 1.5 mM H_2O_2 and 0.17 U/mL of SBP. At the end of reaction time of 3 h, catalase, at a final concentration of 125 U/mL, was added to stop the reaction. Alum, at a final concentration of 50 mg/L, was added to help settle the contents by gravity.

pH	% aniline remaining
4.0	46.7
5.0	31.4
5.5	30.9
6.0	33.0
6.5	31.3
7.0	32.2
7.4	31.5
8.0	34.5
10.0	55.0

Fig. 4.5.2.2.2 pH optimization for removal of *o*-toluidine

Batch reactors of 30 mL volume, initially contained 1 mM *o*-toluidine, 1.5 mM H_2O_2 and 0.20 U/mL of SBP. At the end of reaction time of 3 h, catalase, at a final concentration of 125 U/mL, was added to stop the reaction. Alum, at a final concentration of 50 mg/L, was added to help settle the contents by gravity.

pH	% *o*-toluidine remaining
4.0	54.3
5.0	40.3
5.5	35.3
6.0	33.1
6.5	30.4
7.0	28.3
7.4	29.1
8.0	31.3
10.0	58.3

Fig. 4.5.2.2.3 pH optimization for removal of *m*-toluidine

Batch reactors of 30 mL volume, initially contained 1 mM *m*-toluidine, 1.5 mM H_2O_2 and 0.10 U/mL of SBP. At the end of reaction time of 3 h, catalase, at a final concentration of 125 U/mL, was added to stop the reaction. Alum, at a final concentration of 50 mg/L, was added to help settle the contents by gravity.

pH	% *m*-toluidine remaining
4.0	36.7
5.0	22.3
5.5	23.5
6.0	23.6
6.5	21.1
7.0	21.4
7.4	22.2
8.0	24.4
10.0	48.7

Table 4.5.2.2.4 pH optimization for removal of *p*-toluidine

Batch reactors of 30 mL volume, initially contained 1 mM *p*-toluidine, 1.5 mM H_2O_2 and 0.01 U/mL of SBP. At the end of reaction time of 3 h, catalase, at a final concentration of 125 U/mL, was added to stop the reaction. Alum, at a final concentration of 50 mg/L, was added to help settle the contents by gravity.

pH	% *p*-toluidine remaining
4.0	42.5
5.0	40.3
5.5	21.3
6.0	23.2
6.5	21.5
7.0	20.2
7.4	22.4
8.0	22.6
10.0	63.4

Table 4.5.2.3.1 H_2O_2 optimization for removal of aniline

Batch reactors of 30 mL volume, initially contained 1 mM aniline and 0.20 U/mL of SBP at pH 7.3. At the end of reaction time of 3 h, catalase, at a final concentration of 125 U/mL, was added to stop the reaction. Alum, at a final concentration of 50 mg/L, was added to help settle the contents by gravity.

$[H_2O_2]$/[aniline]	% aniline remaining
1.0	67.1
1.2	40.2
1.5	14.4
1.7	15.7
2.0	20.3

Table 4.5.2.3.2 H_2O_2 optimization for removal of *o*-toluidine
Batch reactors of 30 mL volume, initially contained 1 mM *o*-toluidine and 0.20 U/mL of SBP at pH 7.2. At the end of reaction time of 3 h, catalase, at a final concentration of 125 U/mL, was added to stop the reaction. Alum, at a final concentration of 50 mg/L, was added to help settle the contents by gravity.

$[H_2O_2]$/[aniline]	% *o*-toluidine remaining
1.0	63.4
1.2	45.7
1.5	30.3
1.7	32.6
1.8	38.9
2.0	44.6

Table 4.5.2.3.3 H_2O_2 optimization for removal of *m*-toluidine
Batch reactors of 30 mL volume, initially contained 1 mM *m*-toluidine and 0.07 U/mL of SBP at pH 6.8. At the end of reaction time of 3 h, catalase, at a final concentration of 125 U/mL, was added to stop the reaction. Alum, at a final concentration of 50 mg/L, was added to help settle the contents by gravity.

$[H_2O_2]$/[*m*-toluidine]	% *m*-toluidine remaining
1.0	76.2
1.1	64.4
1.2	55.6
1.3	45.7
1.5	40.3
1.7	45.6
2.0	59.6

Table 4.5.2.3.4 H_2O_2 optimization for removal of *p*-toluidine

Batch reactors of 30 mL volume, initially contained 1 mM *p*-toluidine and 0.008 U/mL of SBP at pH 7.0. At the end of reaction time of 3 h, catalase, at a final concentration of 125 U/mL, was added to stop the reaction. Alum, at a final concentration of 50 mg/L, was added to help settle the contents by gravity.

$[H_2O_2]$/[*p*-toluidine]	% *p*-toluidine remaining
1.0	66.8
1.2	48.8
1.4	33.3
1.5	30.2
1.7	35.6
2.0	53.4

Table 4.5.2.3.5 Step-wise H_2O_2 optimization for removal of aniline

Batch reactors of 30 mL volume, initially contained 1 mM aniline and 0.20 U/mL of SBP at pH 7.3. At the end of reaction time of 3 h, catalase, at a final concentration of 125 U/mL, was added to stop the reaction. Alum, at a final concentration of 50 mg/L, was added to help settle the contents by gravity. H_2O_2 was used in the following ways: single aliquot and in steps of two.

$[H_2O_2]/[aniline]$	% aniline remaining
H_2O_2 in single shot	
1.0	67.1
1.2	40.2
1.5	14.4
1.7	15.7
2.0	20.3
H_2O_2 in steps	
1.0	70.2
1.1	55.5
1.2	38.3
1.3	28.4
1.5	15.6
1.7	14.4
2.0	14.2

Table 4.5.2.3.6 Step-wise H_2O_2 optimization for removal of *o*-toluidine
Batch reactors of 30 mL volume, initially contained 1 mM *o*-toluidine and 0.20 U/mL of SBP at pH 7.2. At the end of reaction time of 3 h, catalase, at a final concentration of 125 U/mL, was added to stop the reaction. Alum, at a final concentration of 50 mg/L, was added to help settle the contents by gravity. H_2O_2 was used in the following ways: single aliquot and in steps of 2.

$[H_2O_2]/[o\text{-toluidine}]$	% *o*-toluidine remaining	
	H_2O_2 in single shot	H_2O_2 in steps
1.0	63.4	75.3
1.2	45.7	52.4
1.5	30.3	29.2
1.7	32.6	28.9
1.8	38.9	27.6
2.0	44.6	31.3

Table 4.5.2.3.7 Step-wise H_2O_2 optimization for removal of *m*-toluidine
Batch reactors of 30 mL volume, initially contained 1 mM *m*-toluidine and 0.07 U/mL of SBP at pH 6.8. At the end of reaction time of 3 h, catalase, at a final concentration of 125 U/mL, was added to stop the reaction. Alum, at a final concentration of 50 mg/L, was added to help settle the contents by gravity. H_2O_2 was used in the following ways: single aliquot and in steps of 2.

$[H_2O_2]/[m\text{-toluidine}]$	% *m*-toluidine remaining	
	H_2O_2 in single shot	H_2O_2 in steps
1.0	76.2	80.3
1.1	64.4	60.2
1.2	55.6	50.4
1.3	45.7	43.3
1.5	40.3	39.8
1.7	45.6	37.7
2.0	59.6	48.6

Table 4.5.2.3.8 Step-wise H_2O_2 optimization for removal of *p*-toluidine
Batch reactors of 30 mL volume, initially contained 1 mM *p*-toluidine and 0.008 U/mL of SBP at pH 7.0. At the end of reaction time of 3 h, catalase, at a final concentration of 125 U/mL, was added to stop the reaction. Alum, at a final concentration of 50 mg/L, was added to help settle the contents by gravity. H_2O_2 was used in the following ways: single aliquot and in steps of 2.

$[H_2O_2]/[p\text{-toluidine}]$	% *p*-toluidine remaining
H_2O_2 in single shot	
1.0	66.8
1.2	48.8
1.4	33.3
1.5	30.2
1.7	35.6
2.0	53.4
H_2O_2 in steps	
1.0	72.3
1.1	65.5
1.2	58.6
1.4	35.2
1.5	31.1
1.7	30.3
1.8	29.6
2.0	35.6

Fig. 4.5.2.4.1 SBP optimization for removal of aniline

Batch reactors of 30 mL volume, initially contained 1 mM aniline and 1.5 mM of H_2O_2 at pH 7.3. At the end of reaction time of 3 h, catalase, at a final concentration of 125 U/mL, was added to stop the reaction. Alum, at a final concentration of 50 mg/L, was added to help settle the contents by gravity.

SBP U/mL	% aniline remaining
0.10	53.8
0.11	50.3
0.17	29.6
0.18	23.7
0.20	20.4
0.25	1.2
0.30	7.5

Table 4.5.2.4.2 SBP optimization for removal of *o*-toluidine

Batch reactors of 30 mL volume, initially contained 1 mM *o*-toluidine and 1.5 mM of H_2O_2 at pH 6.8. At the end of reaction time of 3 h, catalase, at a final concentration of 125 U/mL, was added to stop the reaction. Alum, at a final concentration of 50 mg/L, was added to help settle the contents by gravity.

SBP U/mL	% *o*-toluidine remaining
0.10	61.2
0.20	30.3
0.23	19.6
0.26	0
0.27	1.5
0.30	10.6

Fig. 4.5.2.4.3 SBP optimization for removal of *m*-toluidine

Batch reactors of 30 mL volume, initially contained 1 mM *m*-toluidine and 1.5 mM of H_2O_2 at pH 7.1. At the end of reaction time of 3 h, catalase, at a final concentration of 125 U/mL, was added to stop the reaction. Alum, at a final concentration of 50 mg/L, was added to help settle the contents by gravity.

SBP U/mL	% *m*-toluidine remaining
0.05	49.3
0.07	41.5
0.10	19.4
0.11	8.2
0.12	0
0.15	4.2
0.20	15.6

Fig. 4.5.2.4.4 SBP optimization for removal of *p*-toluidine

Batch reactors of 30 mL volume, initially contained 1 mM *p*-toluidine and 1.5 mM of H_2O_2 at pH 7.0. At the end of reaction time of 3 h, catalase, at a final concentration of 125 U/mL, was added to stop the reaction. Alum, at a final concentration of 50 mg/L, was added to help settle the contents by gravity.

SBP U/mL	% *p*-toluidine remaining
0.001	86.4
0.005	51.7
0.008	29.6
0.010	20.6
0.013	8.3
0.014	4.5
0.015	0
0.018	0
0.020	0

Table 4.5.2.5 Effect of alum on removal of color and time of settling
Batch reactors of 30 mL each were set up, the pH was adjusted to 6.5-8.0 and alum was added in the concentration of 0-300 mg/L. Color absorbance was measured on a spectrophotometer at 500 nm wavelength

Alum concentration, mg/L	Color absorbance	Time of settling, h
0	0.712	>12
50	0.006	1-1.5
100	0	0.67-1
150	0	0.5
200	0	0.5
300	0	0.5

Table 4.6.2.1 Optimization of [H_2O_2]/[aniline] in the continuous-flow column
Integrated continuous-flow column studies with initial nitrobenzene, entering the Fe^0 column, of 1 mM. Effective aniline after dilution with peroxide and SBP, 0.2 U/mL, was 0.8 mM. Influent pH was 7.2-7.3, under the following conditions of [H_2O_2]/[aniline]: 1.0, 1.5 and 2.0

Time min	[H_2O_2]/[aniline]		
	1.0	1.5	2.0
	% aniline remaining		
0	100	100	100
5	58.1	55.6	63.2
22	48.2	40.4	50.3
37	37.6	28.6	42.7
52	28.3	17.2	36.2
67	26.3	8.5	30.5
130	25.1	0	26.2

Table 4.6.2.2 Optimization of [H_2O_2]/[*o*-toluidine] in the continuous-flow column
Integrated continuous-flow column studies with initial *o*-nitrotoluene, entering the Fe^0 column, of 1 mM. Effective *o*-toluidine after dilution with peroxide and SBP, 0.23 U/mL, was 0.8 mM. Influent pH was 7.2-7.3, under the following conditions of [H_2O_2]/[*o*-toluidine]: 1.0, 1.5 and 2.0

Time	[H_2O_2]/[*o*-toluidine]		
min	1.0	1.5	2.0
	% o-toluidine remaining		
0	100	100	100
5	62.3	55.6	58.7
22	51.1	41.2	50.3
37	42.2	27.3	38.3
52	33.6	16.2	29.5
67	28.3	9	25.3
130	25.1	0	20.2

Table 4.6.2.3 Optimization of [H_2O_2]/[*m*-toluidine] in the continuous-flow column
Integrated continuous-flow column studies with initial *m*-nitrotoluene, entering the Fe^0 column, of 1 mM. Effective *m*-toluidine after dilution with peroxide and SBP, 0.10 U/mL, was 0.8 mM. Influent pH was 7.2-7.3, under the following conditions of [H_2O_2]/[*m*-toluidine]: 1.0, 1.5 and 2.0

Time	[H_2O_2]/[*m*-toluidine]		
min	1.0	1.5	2.0
	% *m*-toluidine remaining		
0	100	100	100
5	62.3	55.6	58.7
22	51.1	41.2	50.3
37	42.2	27.3	38.3
52	33.6	16.2	29.5
67	28.3	9	25.3
130	25.1	0	20.2

Table 4.6.2.4 Optimization of [H_2O_2]/[*p*-toluidine] in the continuous-flow column
Integrated continuous-flow column studies with initial *p*-nitrotoluene, entering the Fe^0 column, of 1 mM. Effective *p*-toluidine after dilution with peroxide and SBP, 0.01 U/mL, was 0.8 mM. Influent pH was 7.2-7.3, under the following conditions of [H_2O_2]/[*p*-toluidine]: 1.0, 1.5 and 2.0

Time min	[H_2O_2]/[*p*-toluidine]		
	1.0	1.5	2.0
	% *p*-toluidine remaining		
0	100	100	100
5	58.2	49.1	55.7
22	50.2	38.6	45.3
37	41.7	26.1	33.9
52	32.6	14.3	25.5
67	26.4	6.5	19.3
130	20.3	0	14.2

Table 4.6.2.6 Step-wise feeding of H_2O_2 in the continuous-flow column

Integrated continuous-flow column studies with initial nitrobenzene, entering the Fe^0 column, of 1 mM. Effective aniline after dilution with peroxide and SBP, 0.2 U/mL, was 0.8 mM. Influent pH was 7.2-7.3, under the following conditions of $[H_2O_2]$/[aniline]: 1.0, 1.5 and 2.0

H_2O_2 was fed in steps of two-thirds and one-thirds in the two CSTRs in series.

Time min	$[H_2O_2]$/[aniline]		
	1.0	1.5	2.0
	% aniline remaining		
0	100	100	100
7	85.2	70.3	55.1
25	65.3	35.6	33.3
40	55.4	23.1	20.3
55	54.3	12.5	14.3
70	52.6	8.1	5.4
85	51.3	3.6	0
100	50.6	0	0
180	50.1	0	0

Table 4.6.2.7 Change in H_2O_2 concentration with time during removal of aniline in the continuous-flow column

Integrated continuous-flow column studies with initial nitrobenzene, entering the Fe^0 column, of 1 mM. Effective aniline after dilution with peroxide and SBP was 0.8 mM. Influent pH was 7.2-7.3, under the following conditions of SBP, U/mL: 0.15, 0.20, and 0.30

H_2O_2 was added in single step in the CSTR, used as a pre-mixer.

Time	SBP concentration, U/mL			
min	0.15	0.2	0.3	0.3
	H_2O_2 concentration, mM			
0	1.16	1.16	2.32	1.16
5	0.88	0.83	1.86	0.81
22	0.5	0.5	1.21	0.423
37	0.32	0.206	0.804	0.202
52	0.12	0.089	0.38	0.076
67	0.063	0.061	0.065	0.031
130	0.0004	0.0003	0.0009	0.0006

Table 4.6.2.8 Change in H_2O_2 concentration, fed in steps of two, with time during removal of aniline in the continuous-flow column

Integrated continuous-flow column studies with initial nitrobenzene, entering the Fe^0 column, of 1 mM. Effective aniline after dilution with peroxide and SBP was 0.8 mM. Influent pH was 7.2-7.3, under the following conditions of SBP, U/mL: 0.15, 0.20 and 0.30

H_2O_2 was fed in steps of two-thirds and one-thirds in the two CSTRs in series.

Time, min	SBP concentration in the runs, U/mL			
	0.15	0.20	0.30	0.30
	H_2O_2 concentration, mM			
0	0.750	0.750	1.500	0.750
5	0.500	0.460	1.000	0.420
25	0.580	0.560	0.920	0.490
40	0.420	0.430	0.730	0.380
55	0.230	0.206	0.540	0.200
70	0.090	0.110	0.380	0.076
85	0.063	0.082	0.130	0.031
100	0.042	0.053	0.071	0.010
180	0.005	0.006	0.010	0.001

Table 4.6.3.1 Optimization of SBP concentration in the continuous-flow column for aniline polymerization

Integrated continuous-flow column studies with initial nitrobenzene, entering the Fe^0 column, of 1 mM. Effective aniline, after dilution with peroxide and SBP, was 0.8 mM. $[H_2O_2]$/[aniline] was 1.5 with influent pH of 7.2-7.3, under the following conditions of SBP concentration, U/mL: 0.15, 0.20 and 0.30.

Time	SBP Concentration, U/mL		
min	0.15	0.20	0.30
	% aniline remaining		
0	100	100	100
7	62.3	55.6	50.5
22	42.6	40.4	40.7
37	30.8	28.6	29.5
52	20.7	17.2	15.1
67	15.2	8.5	10.1
130	8.2	0	9.1
310	8	0	9

Table 4.6.3.2 Optimization of SBP concentration in the continuous-flow column for *o*-toluidine polymerization

Integrated continuous-flow column studies with initial *o*-nitrotoluene, entering the Fe^0 column, of 1 mM. Effective *o*-toluidine, after dilution with peroxide and SBP, was 0.8 mM. $[H_2O_2]$/[*o*-toluidine] was 1.5 with influent pH of 7.4, under the following conditions of SBP concentration, U/mL: 0.20, 0.23 and 0.26

Time	SBP concentration, U/mL		
min	0.20	0.23	0.26
	% *o*-toluidine remaining		
0	100	100	100
5	60.2	49.2	50.5
22	42.1	38.6	37.2
37	28.8	26.1	30.3
52	20.2	13.3	15.1
67	16.6	9.7	10.2
130	13.2	0	8.6
310	12.3	0	8.4

Table 4.6.3.3 Optimization of SBP concentration in the continuous-flow column for *m*-toluidine polymerization

Integrated continuous-flow column studies with initial *m*-nitrotoluene, entering the Fe^0 column, of 1 mM. Effective *m*-toluidine, after dilution with peroxide and SBP, was 0.8 mM. $[H_2O_2]/[m\text{-toluidine}]$ was 1.5 with influent pH of 7.4, under the following conditions of SBP concentration, U/mL: 0.07, 0.10 and 0.15.

Time min	SBP concentration, U/mL		
	0.07	0.10	0.15
	% *m*-toluidine remaining		
0	100	100	100
5	60.2	51.2	50.5
22	56.3	35.5	37.2
37	42.6	22.3	30.3
52	33.6	15.2	15.1
67	24.4	8.2	10.2
130	25.6	0	8.6
310	24.3	0	8.4

Table 4.6.3.4 Optimization of SBP concentration in the continuous-flow column for *p*-toluidine polymerization

Integrated continuous-flow column studies with initial *p*-nitrotoluene, entering the Fe^0 column, of 1 mM. Effective *p*-toluidine, after dilution with peroxide and SBP, was 0.8 mM. $[H_2O_2]/[p\text{-toluidine}]$ was 1.5 with influent pH of 7.4, under the following conditions of SBP concentration, U/mL: 0.005, 0.010 and 0.015.

Time	SBP concentration, U/mL		
min	0.005	0.010	0.015
	% *p*-toluidine remaining		
0	100	100	100
5	77.1	50.5	47.3
22	56.3	37.2	33.3
37	48.7	25.3	22.4
52	42.3	11.8	12.6
67	37.2	6.2	7.3
130	36.4	2.6	0
310	35.5	0	0

Table 4.6.3.6 Step-wise feeding of SBP in the continuous-flow column for aniline polymerization

Integrated continuous-flow column studies with initial nitrobenzene, entering the Fe^0 column, of 1 mM. Effective aniline, after dilution with peroxide and SBP, was 0.8 mM. $[H_2O_2]$/[aniline] was 1.5 with influent pH of 7.2-7.3, under the following conditions of SBP concentration, U/mL: 0.15, 0.20 and 0.30. SBP was fed in steps of half and half in the two CSTRs in series.

Time min	SBP concentration, U/mL		
	0.15	0.2	0.3
	% aniline remaining		
0	100	100	100
5	77.1	65.3	53.2
23	58.3	45.2	32.4
38	48.2	33.1	22.1
53	35.4	22.4	11
68	21.6	12.3	6.4
83	15.2	8.6	0
98	15	8.5	0
180	15.2	8	0

Table 4.6.3.7 Change in SBP activity with time during removal of aniline in the continuous-flow column

Integrated continuous-flow column studies with initial nitrobenzene, entering the Fe^0 column, of 1 mM. Effective aniline after dilution with peroxide and SBP was 0.8 mM. Influent pH was 7.2-7.3, under the following conditions of $[H_2O_2]$/[aniline]: 1.5, 1.5, 3.0 and 1.5

SBP was added in single step in the CSTR, used as a pre-mixer, in different initial concentrations.

Time min	$[H_2O_2]$/[aniline]			
	1.5	1.5	3	1.5
	SBP activity, U/mL			
0	0.15	0.2	0.3	0.3
7	0.11	0.17	0.1	0.2
22	0.071	0.11	0.06	0.11
37	0.033	0.07	0.03	0.068
52	0.02	0.021	0.024	0.041
67	0.01	0.02	0.02	0.025
130	0.006	0.008	0.0004	0.015

Table 4.6.3.8 Change in SBP activity, fed in steps of two, with time during removal of aniline in the continuous-flow column

Integrated continuous-flow column studies with initial nitrobenzene, entering the Fe^0 column, of 1 mM. Effective aniline after dilution with peroxide and SBP was 0.8 mM. Influent pH was 7.2-7.3, under the following conditions of $[H_2O_2]$/[aniline]: 1.5, 1.5, 3.0, 1.5.

SBP was added in steps of half and half in the two CSTRs in series, used as pre-mixers, in different initial concentrations.

Time	$[H_2O_2]$/[aniline]			
min	1.5	1.5	3.0	1.5
	SBP concentration remaining, U/mL			
0	0.075	0.1	0.15	0.15
5	0.045	0.065	0.07	0.105
23	0.12	0.165	0.22	0.255
38	0.08	0.125	0.132	0.176
53	0.06	0.094	0.09	0.13
68	0.04	0.071	0.065	0.093
83	0.02	0.05	0.05	0.065
98	0.01	0.02	0.04	0.04
180	0.006	0.008	0.004	0.015

Vita Auctoris

Name: Ramkrishna Mantha

Place of birth: Kolkata, India

Date of Birth: April 29, 1967

Education:

Ph.D., Civil and Environmental Engineering
University of Windsor, ON, Canada
1997-2001

M. Tech., Chemical Engineering
Indian Institute of Technology, Kanpur, India
1988-1990

B.Ch.E., Chemical Engineering
Jadavpur University, India
1984-1988

Work Experience:

Deputy Manager
Steel Authority of India Limited
Bokaro Steel City, India

Awards

Summer Research Scholarship	Summer 2001
OGSST	2000-2001
OGS	1999-2000
U of W Tuition	Winter 1999
Visa Differential	1997-1999
Book Scholarship	1984-1990

Publications

1. Model for removal of nitrobenzene from synthetic wastewater using 2-step Fe^0 reduction and peroxidase-catalyzed oxidation. 7th Environmental Specialty CSCE Conference, Victoria, BC, 2001, Paper No. E16.

2. A continuous system for Fe^0 reduction of nitrobenzene in synthetic wastewater. *Environ. Sci. Technol.* (in press, accepted May 7, 2001).